MULTIDISCIPLINARY CENTER FOR EARTHQUAKE ENGINEERING RESEARCH
A National Center of Excellence in Advanced Technology Applications

ISSN 1520-295X

Seismic Retrofit of End-Sway Frames of Steel Deck-Truss Bridges with a Supplemental Tendon System: Experimental and Analytical Investigation

by

Gokhan Pekcan, John B. Mander and Stuart S. Chen
University at Buffalo, State University of New York
Department of Civil, Structural and Environmental Engineering
Buffalo, New York 14260

Technical Report MCEER-00-0004

July 1, 2000

This research was conducted at the University at Buffalo, State University of New York, and was supported by the Federal Highway Administration under contract number DTFH61-92-C-00106.

NOTICE

This report was prepared by the University at Buffalo, State University of New York, as a result of research sponsored by the Multidisciplinary Center for Earthquake Engineering Research (MCEER) through a contract from the Federal Highway Administration. Neither MCEER, associates of MCEER, its sponsors, the University at Buffalo, State University of New York, nor any person acting on their behalf:

a. makes any warranty, express or implied, with respect to the use of any information, apparatus, method, or process disclosed in this report or that such use may not infringe upon privately owned rights; or

b. assumes any liabilities of whatsoever kind with respect to the use of, or the damage resulting from the use of, any information, apparatus, method, or process disclosed in this report.

Any opinions, findings, and conclusions or recommendations expressed in this publication are those of the author(s) and do not necessarily reflect the views of MCEER or the Federal Highway Administration.

MULTIDISCIPLINARY CENTER FOR EARTHQUAKE ENGINEERING RESEARCH
A National Center of Excellence in Advanced Technology Applications

Seismic Retrofit of End-Sway Frames of Steel Deck-Truss Bridges with a Supplemental Tendon System: Experimental and Analytical Investigation

by

Gokhan Pekcan[1], John B. Mander[2] and Stuart S. Chen[2]

Publication Date: July 1, 2000
Submittal Date: November 18, 1999

Technical Report MCEER-00-0004

Task Number 106-E-7.4

FHWA Contract Number DTFH61-92-C-00106

1 Interim Senior Program Officer for Transportation Research, Multidisciplinary Center for Earthquake Engineering Research, University at Buffalo, State University of New York
2 Associate Professor, Department of Civil, Structural and Environmental Engineering, University at Buffalo, State University of New York

MULTIDISCIPLINARY CENTER FOR EARTHQUAKE ENGINEERING RESEARCH
University at Buffalo, State University of New York
Red Jacket Quadrangle, Buffalo, NY 14261

Preface

The Multidisciplinary Center for Earthquake Engineering Research (MCEER) is a national center of excellence in advanced technology applications that is dedicated to the reduction of earthquake losses nationwide. Headquartered at the University at Buffalo, State University of New York, the Center was originally established by the National Science Foundation in 1986, as the National Center for Earthquake Engineering Research (NCEER).

Comprising a consortium of researchers from numerous disciplines and institutions throughout the United States, the Center's mission is to reduce earthquake losses through research and the application of advanced technologies that improve engineering, pre-earthquake planning and post-earthquake recovery strategies. Toward this end, the Center coordinates a nationwide program of multidisciplinary team research, education and outreach activities.

MCEER's research is conducted under the sponsorship of two major federal agencies, the National Science Foundation (NSF) and the Federal Highway Administration (FHWA), and the State of New York. Significant support is also derived from the Federal Emergency Management Agency (FEMA), other state governments, academic institutions, foreign governments and private industry.

The Center's FHWA-sponsored Highway Project develops retrofit and evaluation methodologies for existing bridges and other highway structures (including tunnels, retaining structures, slopes, culverts, and pavements), and improved seismic design criteria and procedures for bridges and other highway structures. Specifically, tasks are being conducted to:

- assess the vulnerability of highway systems, structures and components;
- develop concepts for retrofitting vulnerable highway structures and components;
- develop improved design and analysis methodologies for bridges, tunnels, and retaining structures, which include consideration of soil-structure interaction mechanisms and their influence on structural response;
- review and recommend improved seismic design and performance criteria for new highway systems and structures.

Highway Project research focuses on two distinct areas: the development of improved design criteria and philosophies for new or future highway construction, and the development of improved analysis and retrofitting methodologies for existing highway systems and structures. The research discussed in this report is a result of work conducted under the existing highway structures project, and was performed within Task 106-E-7.4, "Strength and Ductility of Steel Superstructure Details" of that project as shown in the flowchart on the following page.

The overall objective of this task was to investigate the seismic performance of existing steel superstructure details and to identify details in need of retrofitting. This study investigates an alternative seismic retrofit approach that can be employed in the main sway frames of steel deck-truss bridges. The approach provides various modified bracing configurations that include supplemental damping systems. The effectiveness of the retrofit configurations is demonstrated

experimentally and analytically on the shaking table at the University at Buffalo. The tested configurations include pairs of tendon elements in two directions in the plane of sway-frames with/without supplemental systems. The supplemental system consisted of mechanical fuse-bars and/or elastomeric spring dampers (ESD). Experimental results are presented in comparison with the analytical results using an enhanced version of the nonlinear time history analysis program Drain-2DX.

SEISMIC VULNERABILITY OF EXISTING HIGHWAY CONSTRUCTION
FHWA Contract DTFH61-92-C-00106

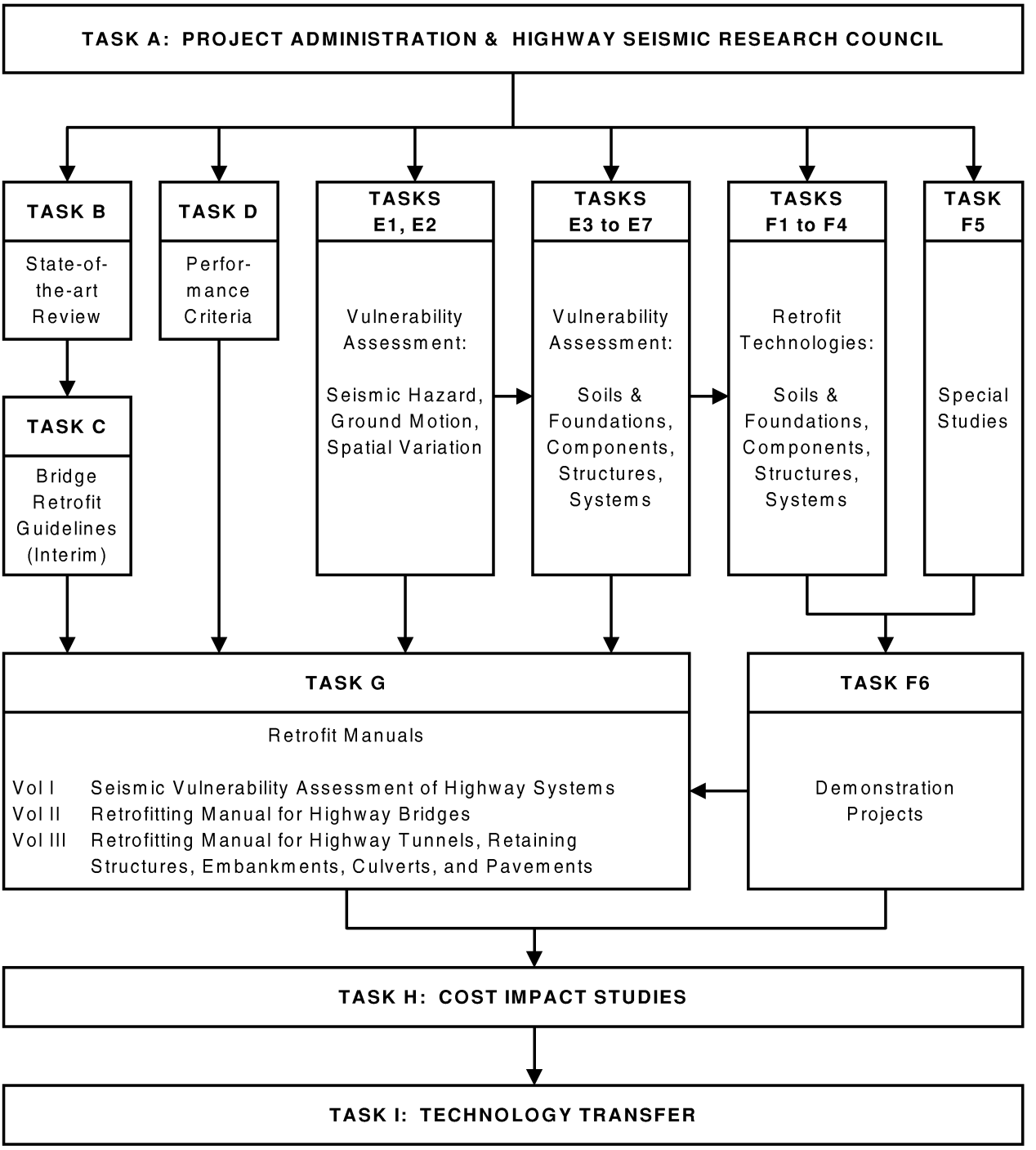

ABSTRACT

Among the various types of steel bridges, deck-truss bridges are particularly vulnerable to seismically induced inertia forces. Under earthquake excitation, high transverse inertia forces that accumulate along the deck are transferred to the end sway frames and bearing supports. Such frames and bearing supports are designed to resist wind loads, but maybe inadequate to resist seismic loading. Moreover, important truss bridges are typically on lifeline routes, therefore it is undesirable to have inelastic behavior in the critical sway frames and bearing elements.

One of the major issues in developing efficient seismic retrofit strategies is to identify the continuous load path traveled by the seismically induced lateral inertial forces from the deck level through lateral load resisting system to the bearings and eventually to the substructure. Hence, this study investigates an alternative seismic retrofit approach that can be employed in main sway frames of steel deck-truss bridges. The proposed approach provides various possible modified bracing configurations that include supplemental damping systems. The effectiveness of the retrofit configurations is demonstrated experimentally and analytically on a one-third scale model of an existing steel end-sway frame structure tested on the shaking table at the State University of New York at Buffalo. The tested configurations include pairs of tendon elements in two directions in the plane of sway-frames with/without supplemental system. The supplemental system consisted of mechanical fuse-bars and/or elastomeric spring dampers (ESD). Experimental results are presented in comparison with the analytical results using an enhanced version of nonlinear time history analysis program Drain-2DX.

ACKNOWLEDGEMENTS

This research was carried out at the Department of Civil, Structural and Environmental Engineering at the State University of New York at Buffalo. The financial support was provided by the Multidisciplinary Center for Earthquake Engineering through a contract by the Federal Highway Administration (FHWA Contract DTFH61-92-C-00106). This support is gratefully acknowledged.

The seismic laboratory technicians, Mark Pitman, assisted with conducting the shaking table tests, Dick Cidziel and Dan Walch, helped during the preparation of the experiments. All are gratefully acknowledged.

TABLE OF CONTENTS

TABLE OF CONTENTS (CONT'D)

LIST OF FIGURES

LIST OF FIGURES - CONT'D

LIST OF TABLES

SECTION 1

INTRODUCTION

1.1 BACKGROUND

The seismic vulnerability of existing bridges remains an important problem, since most of these structures have been built before present seismic design guidelines were established. Seismically induced inertial forces have historically been neglected in the design of bridges until the advent of AASHTO Guide Specifications for the Seismic Design of Highway Bridges (AASHTO, 1983). Recent earthquakes, particularly 1989 Loma Prieta, 1994 Northridge and 1995 Great Hanshin (Kobe) earthquake in Japan, have caused either collapse of, or severe damage to, a considerable number of bridges that were designed for seismic forces. Following the 1971 San Fernando earthquake, much research has been geared toward the development of sound seismic design guidelines for bridges. Retrofit efforts started much later. Although retrofit needs were recognized soon after the 1971 San Fernando earthquake, it was the 1989 Loma Prieta earthquake that spurred the seismic retrofitting efforts after which the California Department of Transportation (CALTRANS) embarked on a retrofitting and research program for highway bridges. Frequent earthquakes around the world (USA, Japan, New Zealand) have led those affected highway departments to focus on similar programs.

Both the seismic design of new and also the retrofitting of existing bridges is based on a philosophy of maintaining life-safety through collapse prevention. Damage, however, may be permitted in the event of large earthquakes. It must be noted that according to the current state-of-the-practice, performance criteria for the bridges are stated by the owners, and may be from *no collapse but extensive damage* to *no damage essentially elastic response*. Consequently, when bridges are subjected to seismic loading, severe damage may be expected, as observe after major earthquakes. Although much attention is given to concrete bridges, steel bridges are also vulnerable to seismic actions. Therefore, economical and effective techniques for retrofitting existing steel bridges are needed. Moreover, retrofitting techniques should go further than preservation of life and limb, ideally a damage avoidance design philosophy should be embraced wherever possible.

Among the various types of steel bridges, deck-truss bridges are particularly vulnerable to seismically induced inertia forces. This class of bridge, which has been constructed for many decades throughout North America, the deck, whose self-weight constitutes most of the dead load of the bridge, is seated on top of the truss structure. Longitudinal lateral bracing is provided in the planes of the top and bottom chords. Under earthquake loading, high transverse inertia forces acting at the deck level are transferred to the end-sway frames and eventually to the bearing supports. Additional sway frames between the top and bottom chords are used to distribute the transverse loads to the lateral system and to keep the system stable during construction.

The transverse lateral load path, whether it is in moment frame or truss action, in these types of bridges, was generally designed only to resist wind forces. Sway bracing is required, usually at each panel, to resist the horizontal forces and to prevent the structure from collapse as shown in figure 1-1. Also shown in the figure are various bracing types used in sway frames/panels. In some structures, it is possible to transfer the forces to the lower lateral bracing by means of the sway bracing at each panel, and then through the lower lateral truss to the supports (Figure 1-1b). It must be noted here that these forces are transferred from their point of application to the supports through those members that are relatively stiffer. In certain designs, an upper lateral bracing consisting of a stiff truss or a continuous rigid deck may carry a large portion of the lateral forces from the deck to the ends of the bridge where these forces are transferred to the supports through a portal bracing or directly to an abutment. Similarly, overturning effects may be mitigated by a continuous deck so that lateral forces are transferred to the main truss supports by means of end-sway frames. Alternatively, when the deck is discontinuous with expansion joints, the transverse forces are transferred to the lower chord by means of sway bracing at each panel and carried through to the end-sway frames.

In general, the structural system (sway frames/bracing) must ensure elastic behavior and safe transfer of seismically induced forces to the supporting substructure (usually piers/abutments) through bearings. However, due to the lack of consideration of seismic forces in the design of older steel truss bridges, the sway frame/bracing is expected to yield and behave in an inelastic fashion. The damage induced in these frames may be, in most cases, irreparable. This poses a dilemma for the owner, especially if the steel bridge in question is a lifeline and/or monumental structure. Therefore, the seismic retrofit of sway frames in steel deck-truss bridges

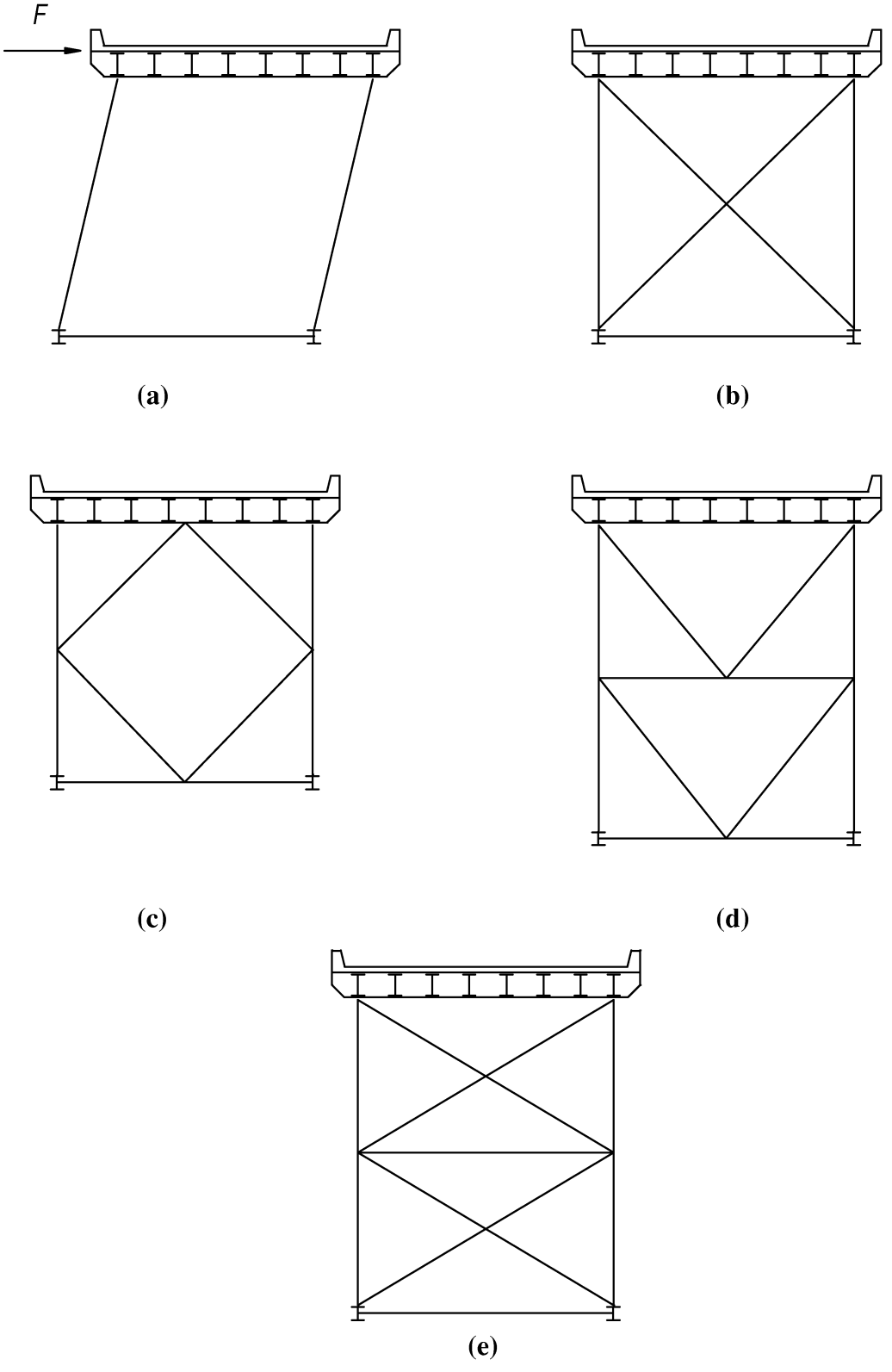

Figure 1-1 Typical Sway Frame and Bracing for Deck-Truss Bridges

by enhancing their lateral load carrying capacities or by reducing seismic demand on the structure must be carefully considered. In fact, various recent experimental and analytical studies, focused on the seismic evaluation of deck-truss bridges, demonstrated the need for extensive retrofit of superstructure members as well as substructure elements (Imbsen and Liu, 1993; Liu et al., 1997; Matson and Buckland, 1995; Imsben, 1995; Shama, 1999).

Among many seismic retrofit alternatives, *strengthening* and *base isolation* are the two most commonly used methods for such bridge structures. Strengthening is the conventional retrofit approach in which the existing weak members that are prone to damage are simply replaced. This approach may also increase the stiffness due to which the seismic force demand on the structural elements may be elevated. Therefore, it is very likely that strengthening of the connections, bearings and/or pier substructure which are typically non-ductile, is required. Although, it is possible to retrofit the bridge structure to behave in essentially an elastic fashion by means of strengthening, the cost of such an approach may be very high and unacceptable to the owner. Moreover, it does not ensure a satisfactory performance in terms of damage avoidance. Sarraf and Bruneau (1998a, b) introduced a ductile retrofit solution in which end-sway frames and lower lateral bracing panels adjacent to the supports are converted into ductile bracing panels. In doing so, based on the damage avoidance philosophy, ductile bracing panels are designed to yield and dissipate energy while preventing damage to the other structural elements.

Well-known principles of isolation may be used as an alternative retrofit strategy. In this approach, existing steel bearings are replaced by energy dissipating bearings, such as sliding bearings, lead-rubber bearings, or other types. Isolation essentially de-couples the structure from potentially damaging earthquake induced ground, or support motions. This de-coupling is achieved by increasing the flexibility of the system, together with appropriate damping (Skinner et al., 1993). The longer the period and the higher the damping provided by the isolation bearings, the lower the seismic demand on the structural elements. Therefore, base isolation may be generally considered as a seismic retrofit strategy for deck-truss bridges. Although, the base isolation approach may generally be a satisfactory method for retrofitting these bridge structures, it can also be expensive, as it sometimes requires extensive pier/abutment modifications and jacking up of the trusses. In some cases, it was shown that base isolation might prove to be more costly than conventional strengthening (Bruneau and Sarraf, 1997). Moreover, due to increased

flexibility, large relative displacements between the superstructure and substructure must be accommodated in the bearings and deck joints. Furthermore, for large (long span) steel truss bridges, the gravity loads in the existing steel bearings are considerable, while the steel bearings themselves are relatively small. As existing steel bearings have not been designed for lateral loads, replacing them with isolation bearings poses a major challenge – it is difficult to provide bearings with a very high vertical load capacity, coupled with large lateral load/movement capability. Ideally, retrofit solutions that permit the existing gravity load bearings to be used and transmit the horizontal shear forces by other means should be sought.

1.2 OBJECTIVES AND SCOPE

Recently, many experimental and analytical studies have been undertaken on the investigation of various methods of *control*, that use either passive, semi-active or active energy dissipation devices. These studies have shown that seismic retrofit of building as well as bridge structures using supplemental energy dissipating systems is a viable alternative to conventional practice of ductility-based toughening/strengthening and base isolation approaches. A comprehensive summary and discussion on the various types of supplemental devices and their applications can be found in Soong and Dargush (1997).

Typically, control methods target reduced seismic demand via increased supplemental damping. This is achieved by dissipating seismic input energy by means of specially designed non-structural elements/devices. The present study provides an alternative and potentially more economical retrofit solution that is based on the principles of passive control. Accordingly, the proposed seismic retrofit approach, suggested by Ye (1998) under the supervision of the second author, is intended to protect both superstructure and substructure of steel deck-truss bridges by introducing replaceable steel fuse-bars and a special type of energy dissipation device on the end-sway frames. The overall supplemental system works only in tension and employs strengthening of the end-sway frame through post-tensioned bracing coupled with supplemental energy dissipation capabilities. A stable energy dissipating mechanism is provided by a supplemental tendon system which consist of rigid tendon elements, fuse elements and a type of re-centering damping device (Elastomeric Spring Damper).

1.3 ORGANIZATION OF THIS REPORT

The primary emphasis is put on the experimental investigation of the proposed supplemental tendon system configuration for the end-sway frames of steel deck-truss bridges. The organization of the report is summarized in what follows.

Section 2 presents the conceptual development of the proposed retrofit strategies and discusses basic design considerations. Section 3 presents the computational modeling and physical properties of the elastomeric spring dampers and fuse elements that was used in this study. Details of the test structure and the test program are also given in Section 3. In Section 4, shaking table experiment results are given in comparison with the analytical predictions for the tested configurations. A discussion of the experimental results and observations are also presented in Section 4, which is followed by a discussion of the subsequent analytical studies. Finally, conclusions are drawn and recommendations are made in Section 5.

SECTION 2

PROPOSED SEISMIC RETROFIT STRATEGIES: CONCEPT DEVELOPMENT

2.1 INTRODUCTION

This section presents alternative seismic retrofit strategies that can be employed in the end-sway frames of steel deck-truss bridges. Firstly, various existing seismic retrofit strategies are discussed, namely; conventional strengthening and base isolation which may be applicable for typical sway frames. Next, a new retrofit method is proposed which utilizes supplemental energy dissipating devices and sacrificial fuse-bars. Various possible configurations for the proposed alternative are introduced. Finally, issues related to preliminary retrofit design of the proposed system are discussed.

2.2 SEISMIC RETROFIT STRATEGIES

As previously mentioned, there has been a number of studies that target improved seismic behavior of various types of bridge structures. These studies were mostly motivated by the observed [sometimes] catastrophic failures of bridge structures during recent earthquakes. Numerous types of steel bridge component as well as bearing failures were recorded, such as; severe buckling of steel verticals, brittle steel bracing failures, etc. Observed damage and failures in past earthquakes clearly demonstrate the need to design and detail steel bridge components for improved ductile seismic response.

Under one category of steel bridges, existing deck-truss bridges are generally vulnerable to seismically induced damage. These structures seem to be particularly vulnerable to moderate to high seismic ground motions. Therefore, effective and economical seismic rehabilitation alternatives for such bridges are needed. As many steel bridges are supported by seismically vulnerable substructures, and that substructure retrofit/rehabilitation in most cases is very costly, it is advantageous to develop a practical strategy to limit or reduce the seismically induced lateral inertial loads transferred to these non-ductile existing piers, abutments and bearings. Some of the existing retrofit approaches are discussed previously in Section 1. A simple analysis is presented to highlight the vulnerability of end-sway frames to seismically induced lateral forces and deformations in what follows.

2.2.1 Assessment of Drift Capacity of Sway Frames

A simple analysis based on the principle of virtual work can be used to evaluate the deformation capacity of typical end-sway frames. The key assumptions that allow such a simplified evaluation procedure are i) X-braces yield in tension and compression before the yielding of the sway frame verticals, and ii) composite action of the deck and the top beam results in a rigid element with high axial stiffness (figure (2-1)).

As can be seen in figure (2-1), sway frame system can be treated as a truss assembly and top-lateral drift, Δ is calculated using the unit load method. It can be shown that

$$\theta = \frac{\Delta}{H} = \frac{F_t}{EA_t}\left[\frac{1}{\sin\alpha\cos\alpha} + \rho\tan\alpha\sin\alpha\right] \qquad \textbf{(2-1)}$$

in which θ = drift angle, H = height of the sway frame, B = width of the sway frame, $F_t = 1/2P\sqrt{1+(H/B)^2}$, is the axial force in brace elements, α = $\tan^{-1}(H/B)$, E = Young's Modulus, and $\rho = A_t / A_c$, is the ratio of cross-sectional area of the brace element to that of the vertical. Note that second term in parenthesis on the right-hand side of equation (2-1) may be negligible if $A_c >> A_t$, hence $\rho \to 0$ whereas the upper bound value of ρ = 1.0.

Assuming that at the onset of *yield* drift, one brace buckles in compression and the other yields in tension, and braces have identical tension and compression properties, the yield drift of the sway frame can be calculated using equation (2-1) as,

$$\theta_y = \varepsilon_y\left[\frac{1}{\sin\alpha\cos\alpha} + \rho\tan\alpha\sin\alpha\right] \qquad \textbf{(2-2)}$$

in which ε_y = is the yield strain of the material used in braces.

Equation (2-2) is plotted in figure (2-2) for a typical value of ε_y = 0.0012 for various aspect ratios, H/B and for extreme values of ρ = 0 and 1.0. As can be seen in this figure, yield drifts in the order of 0.3% may be expected for typical H/B values (0.75 ~ 1.5). This observation suggests that end-sway frame braces, which are generally designed to resist wind forces, are

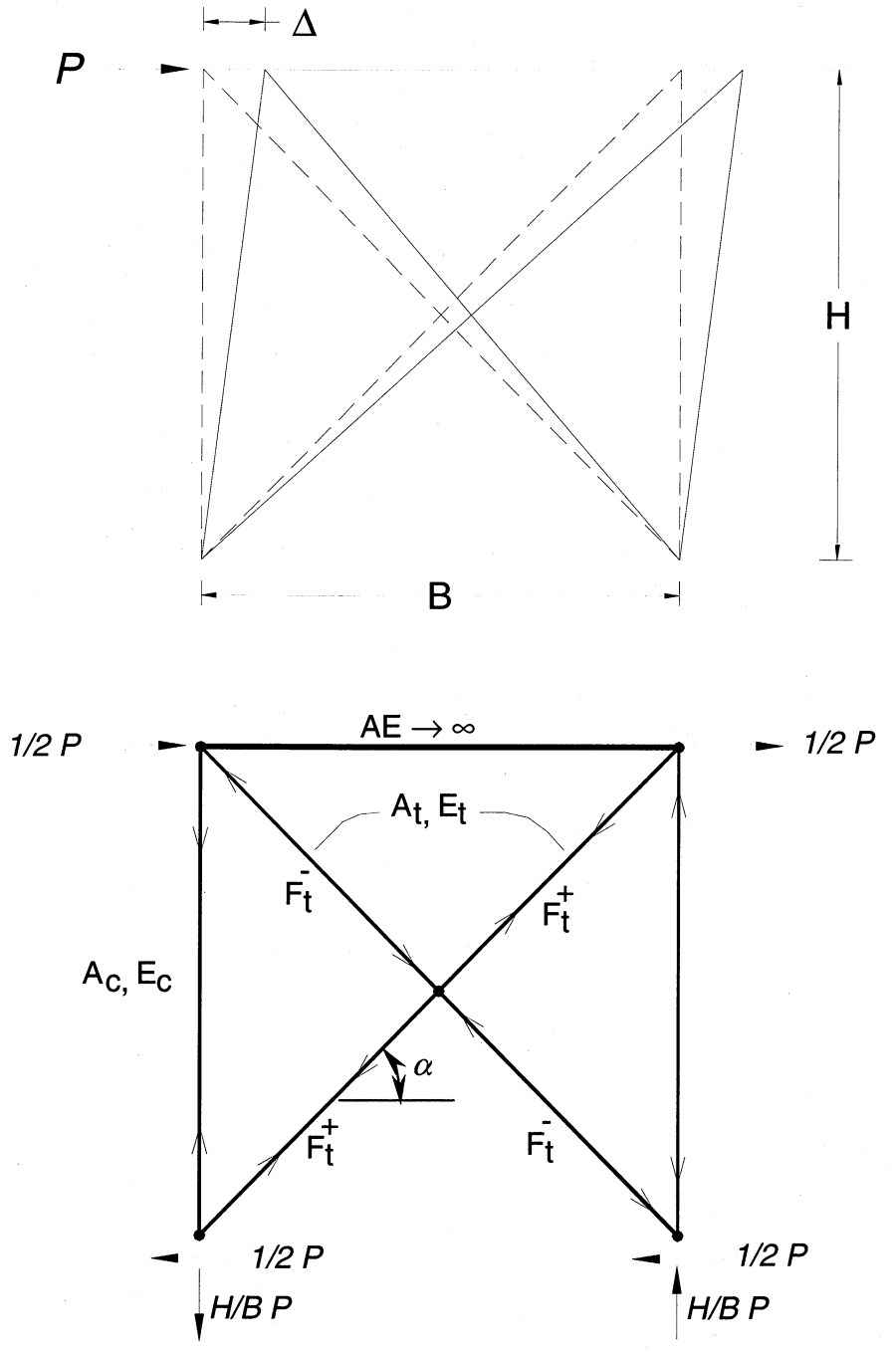

Figure 2-1 Evaluation of Drift Capacity of End-Sway Frames

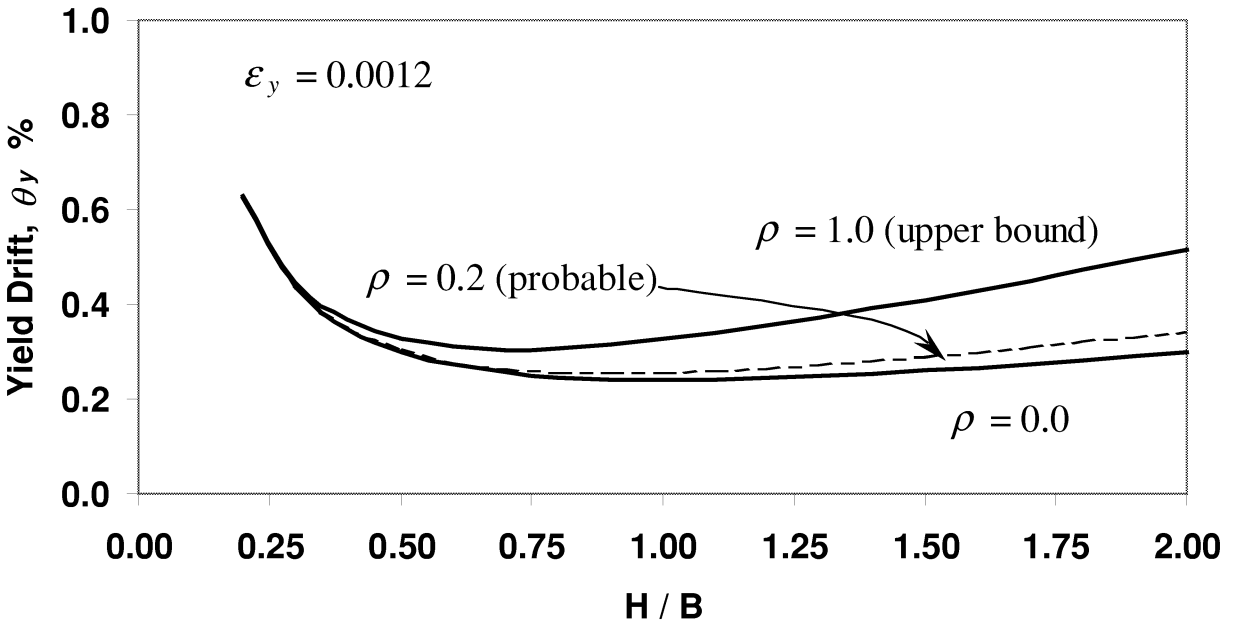

Figure 2-2 Yield-Drift Capacity of End-Sway Frames Based on Truss Analysis

prone to buckling at very small drift angles. It is well known that due to its nonductile nature and limited energy dissipation, buckling of these elements must be avoided. One seismic retrofit strategy to achieve this objective is to strengthen these elements. However, it can be seen from figure 2-2 that strengthening of the braces (i.e. increasing ρ) for a given aspect ratio provides only marginal improvement in the yield drift capacity and furthermore braces do still buckle. Moreover, as mentioned previously, strengthening usually increases overall stiffness hence elevates the seismic force demand on the braces as well as on the supporting steel bearings. As a result, strengthening of the braces should generally be accompanied by the strengthening of the verticals, brace connections and steel bearings as well.

Following above discussion, three alternative retrofit strategies for the end-sway frames are introduced in what follows.

2.3 PROPOSED SUPPLEMENTAL TENDON SYSTEM

One of the major issues in developing efficient seismic retrofit strategies is to identify the continuous load path traveled by the seismically induced lateral inertial forces from the deck

level through lateral load resisting system to the bearings and eventually to the substructure. Furthermore, necessary considerations must be given to ensure a certain degree of redundancy which is required to avoid structural collapse upon failure of the load bearing elements. As was discussed previously in Section 1, the load transfer within steel deck-truss bridges is usually provided by bracing elements in the sway frames. These loads must then be safely transferred to the pier by the bearings which are typically non-ductile hence vulnerable to seismically induced damages. Therefore, it is believed that a system which radically modifies the existing load path and that reduces seismic demand on the truss elements and bearings would be a viable strategy for retrofitting steel deck-truss bridges.

2.3.1 Tendon Only (TO) System

In its most basic form, existing braces are simply replaced by post-tensioned tendons. In this tendon only (*TO*) configuration (figure 2-3a), tendons can be designed to provide comparable (or better) lateral capacity as the *unretrofitted structure*. In fact, this configuration used as the basis of comparison in the experimental study (Section 3 and 4).

This configuration can be improved to achieve the objective mentioned above (Section 2.3) by means of post-tensioned tendons that replace the existing bracing elements and bypass the steel bearings. The tendons can be attached to the sway frame at the deck level and anchored to the pier as schematically shown in figure 2-3b. Post-tensioned tendon elements can be designed to provide the same stiffness to the sway frame as the original bracing. The prestress level in the tendons can be accurately determined and adjusted to avoid the system becoming slack under expected seismic loading conditions.

This tendon only seismic retrofit strategy merely modifies the lateral force load path. The intent is neither to reduce the seismic demand nor to increase the capacity of the existing truss elements. It does however indirectly improve the seismic capacity by transferring less force to the critical members of the structure – the bearings and sway bracing (which may fail by buckling). Being a tension-only system, failures associated with the buckling of bracing elements are avoided. Moreover, tendon elements may be designed to behave inelastically, i.e. to yield, under severe ground shaking. This can still be achieved without increasing the seismic demand on the structural elements. As the overall stiffness of the existing sway frame members can be kept unchanged.

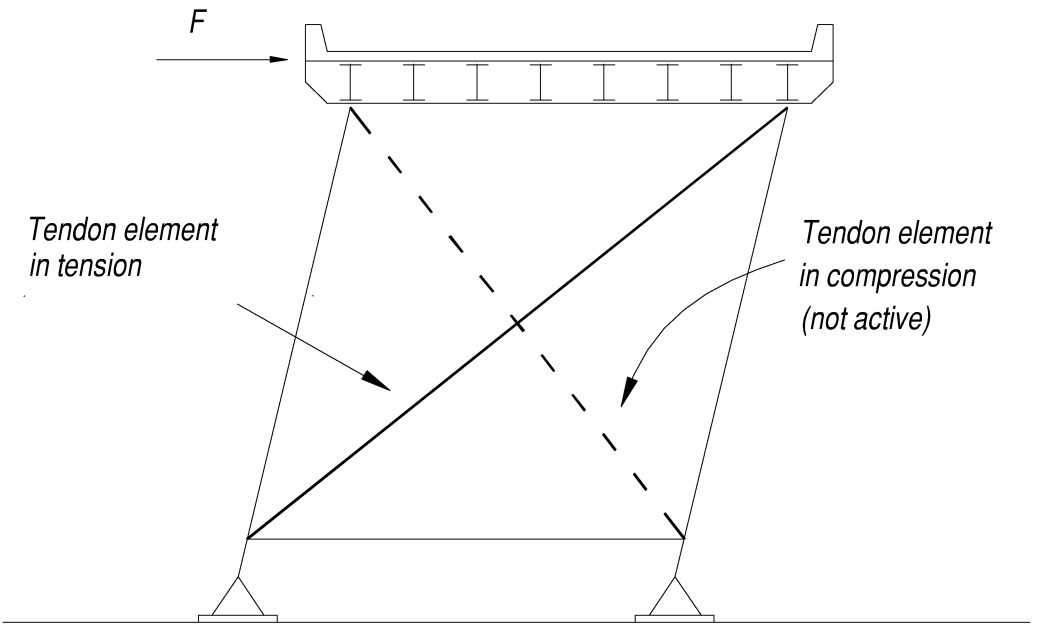

** Tendon elements are simply used to replace the existing braces*

Figure 2-3a Post-Tensioned Tendon Elements Replacing Existing Braces (TO)

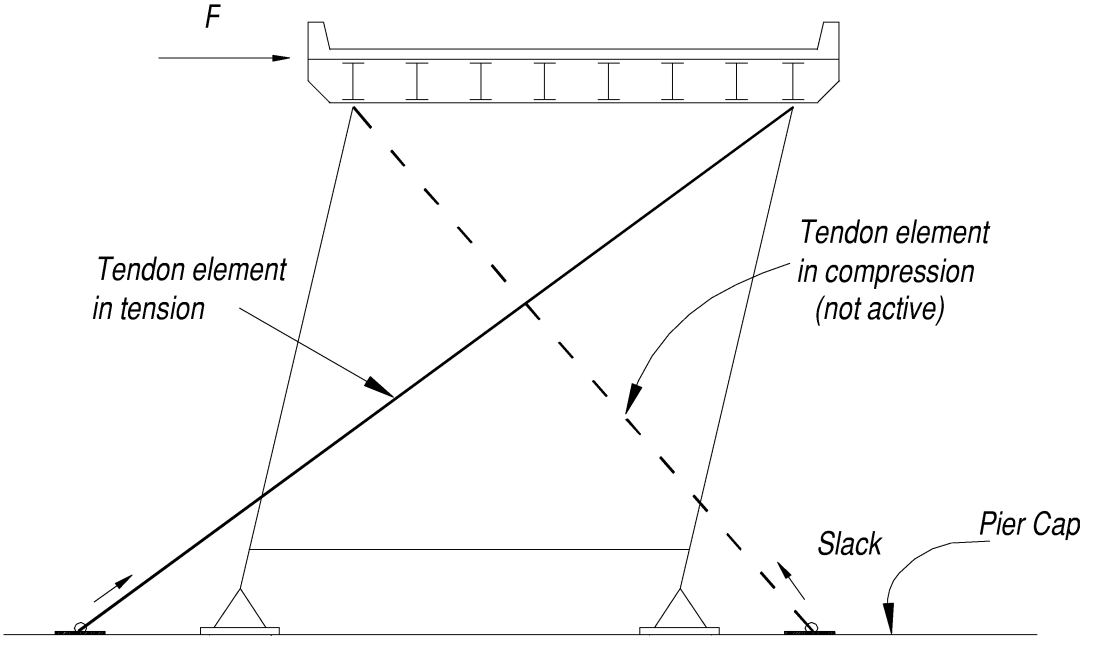

Figure 2-3b Modifying the Load Path by means of Post-Tensioned Tendon Elements (TO)

The effect of prestressing the tendon elements is in fact to produce a shift in the axis of the axial load-elongation relationship. The shift results in an apparent compressive strength equal to the prestressing level as shown in figure 2-4. Therefore, the level of prestress can be determined so that the tendon elements start to yield at pre-defined deformation levels. As the yielding of these elements takes place, hysteretic energy will be dissipated contributing to the damping of the overall structural system. It should be noted that after first yield, a certain amount of initial prestress may be lost, and permanent elongation of the tendon element occurs. Initially, both tendon elements will continue to work together in each cycle until the tendon on the compression side (anchored on the leeward side) becomes slack due to yielding in the previous cycle of response. This relaxes the structure which increases the apparent natural period of vibration and as this composite system is more flexible, the seismic demand is reduced.

Although the retrofit approach described above provides a more desirable load path for improved seismic response compared to that in the original system, the retrofitted system obviously does not have necessary redundancy. In other words, when/if one of the tendon elements fails upon excessive yielding, the structural system may entirely lose its lateral capacity which may lead to catastrophic failure of the entire or part of a bridge. This issue is further discussed and remedies are presented later in this section.

2.3.2 Tendon – Fuse (TF) System

By introducing fuses in series with the tendons, a tendon-fuse (TF) system is formed. This is an improved alternative to the tendon-only system described in the previous section. The overall configuration is the same as the tendon-only system (figure 2-3) in which the rigid tendon elements are attached to the sway frame at the deck level. Fuse-bar(s) are connected to the tendon element by couplers and then to the pier bypassing the existing steel bearings as shown in figure 2-5. As the TF configuration is also a tension-only system, tendons and fuse-bar(s) should be prestressed to avoid the overall system becoming slack under loading conditions arising from wind and live load effects.

Fuse bars, as the name implies, are manufactured devices designed to yield at pre-defined load levels. This can be achieved by using high strength steel bars specially machined to

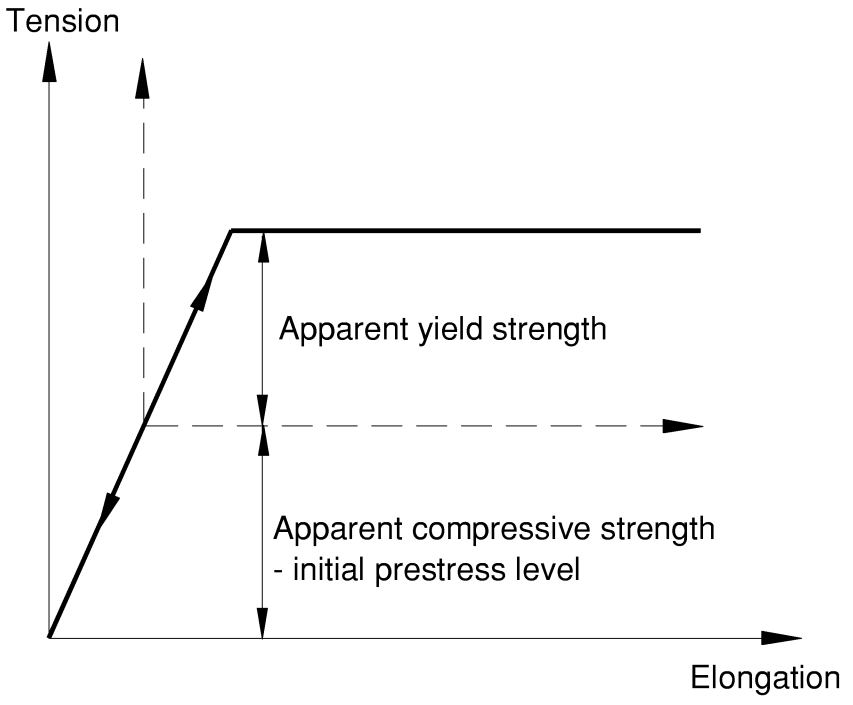

Figure 2-4 Effect of Prestress on the Behavior of Tendons and Fuse Elements

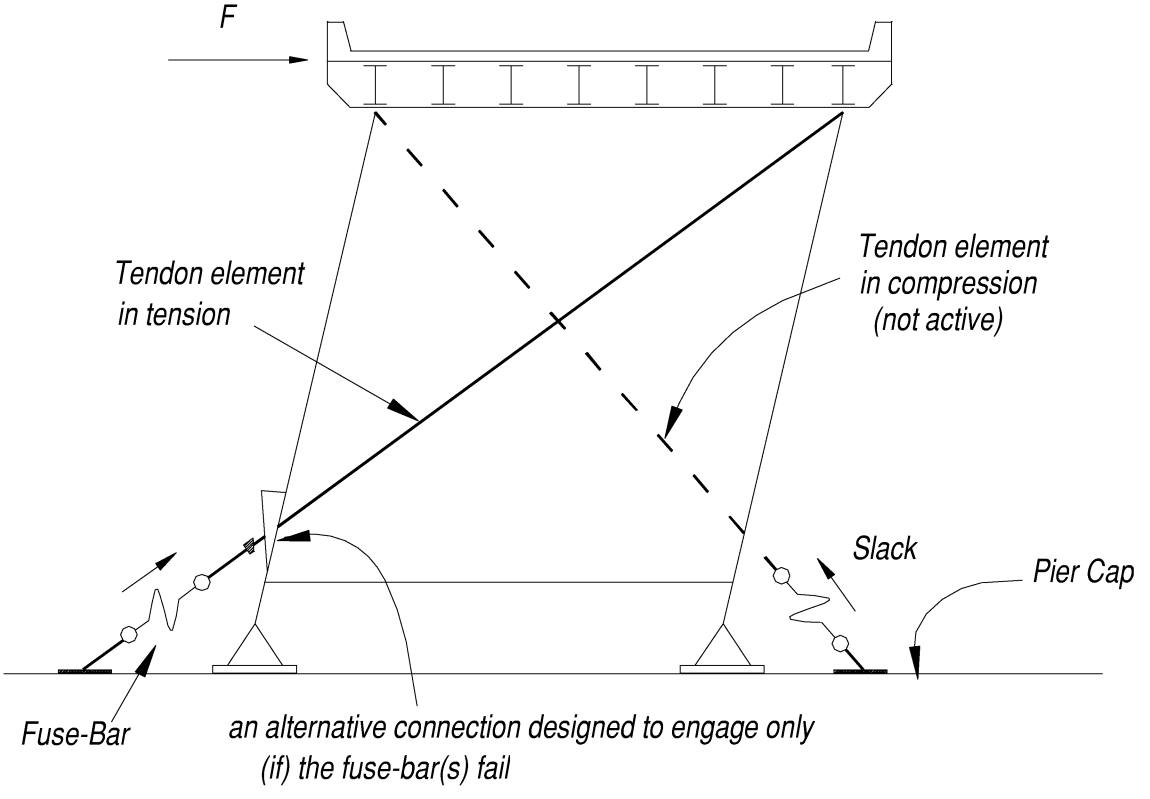

Figure 2-5 Tendon-Fuse (TF) Retrofit Alternative

have a specified cross-sectional area and fuse length. If the fuse-bars are prestressed to a pre-determined level, such that they start yielding at the onset of maximum response, they also contribute to the energy dissipation. This approach therefore follows the principle of ductile design in which the specially detailed critical regions of lateral force resisting systems undergo inelastic action (plastic hinges). Consequently, damage to existing structural members can be avoided. The TF approach is superior to the TO system mainly because the stiffness and strength of the retrofitted structure can be more accurately controlled by proper fuse-bar design. Moreover, following a major event, fuse-bar(s) can be very easily and quickly replaced and the system can be re-tensioned which would restore the structure to its pre-event state.

2.3.3 Tendon – Fuse + Damper (TFD) System

Neither tendon-only (if allowed to yield) nor the TF system described above can reduce the seismic demand on the bridge structure as their contributions to the overall damping is marginal. As a result, forces in the structural elements are at the same (if not higher) level as in the original (unretrofitted) structure. Moreover, both systems lack redundancy, therefore they are not desirable from the seismic response/performance stand point. Consequently, a second enhancement over the tendon-only system that provides redundancy as well as reduces seismic demand is described in what follows.

In this alternative configuration, fuse-bars are designed to resist static, low level, seismic or wind loads and connected to rigid tendon elements as in the TF system. However, supplemental energy dissipation devices (dampers) are used in parallel to the fuse-bars to introduce damping hence to reduce the seismic demand. Moreover, the damper elements provide the required redundancy to the overall structural system, as they can still be functional after the fuse-bars fail as shown in figure 2-6. The TFD system should also be prestressed, mainly to avoid the tendons becoming slack during loading cycles. Therefore, it is recommended that spring dampers which can be preloaded be used in this retrofit configuration. Typically, such devices can be designed to have re-centering capabilities. In fact, this is a very desirable feature especially when applied to flexible-yielding structures or systems (such as TF system) as the permanent deformation due to yielding can be effectively reduced (if not eliminated).

In general, retrofit design of combined TFD system requires several recursive steps utilizing capacity-demand spectral design approach (Pekcan, 1998, 2000b).

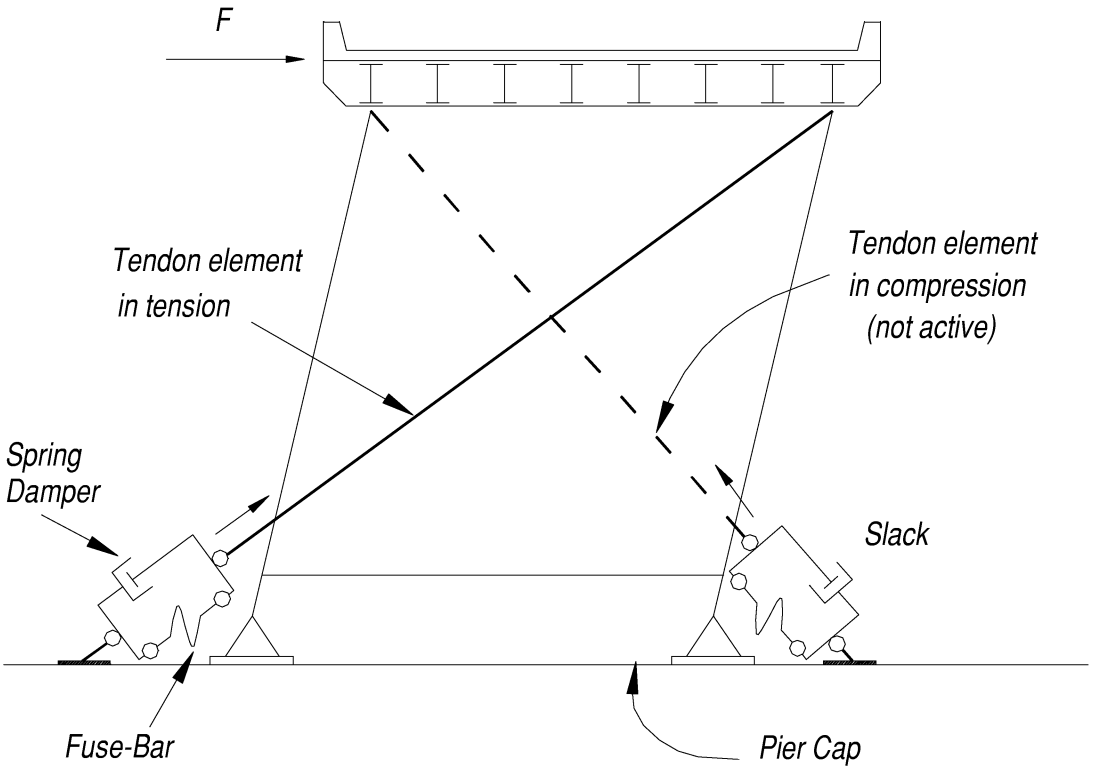

Figure 2-6 Tendon-Fuse+Damper (TFD) Retrofit Alternative

In principle, any type of ductile energy dissipation system can be implemented in sway frames as long as its stiffness and strength characteristics satisfy appropriate stiffness and strength requirements (Bruneau and Sarraf, 1997). Therefore, the following typical strength requirements must be adopted:

i) Strength of the retrofitted sway frames must be selected to limit the horizontal shear response to protect the steel bearings from damage, and also to prevent the verticals from buckling. It must also be noted that an increase in the overall structural system stiffness would attract higher forces which in turn must be reacted by the FT system. Therefore, higher axial forces on the sway frame verticals may be expected.

ii) The over-strength capacity provided by the retrofitted sway frame system must not exceed the dependable horizontal force capacity that would cause any failure elsewhere in the substructure, such as piers and/or foundations, existing bearings.

iii) The dependable elastic base shear capacity provided by the retrofit sway frames must be greater than the strength needed to resist wind loads.

Similarly, typical stiffness requirements are:

i) the stiffness of the retrofitted sway frames must be chosen to be as small as possible to limit seismic demand.

ii) the stiffness of the retrofitted sway frames must be chosen to keep the displacement demands within reasonable limits and to ensure that the fuse-bars have enough deformation capacities.

iii) overall stiffness distribution within the bridge structure should be altered, if possible, to make sure that the stiffness of the bracing in the plane of the top chord allows less forces to be transferred to the intermediate cross frames. Therefore, forces are directly transferred to the end sway frame, thus enhancing the effect of the tendon, TF or TFD system, which will be introduced later in this section.

Based on the discussion above, certain limits on the cross-sectional area of the fuse-bar(s) as well as on the fuse-length must be provided as described in what follows.

2.3.4 Minimum and Maximum Design Cross-Sectional Area of the Fuse-Bar

The diameter of the fuse-bar is determined based on the maximum expected horizontal load acting at the deck level as shown in figure 2-7. In the figure, F represents the maximum

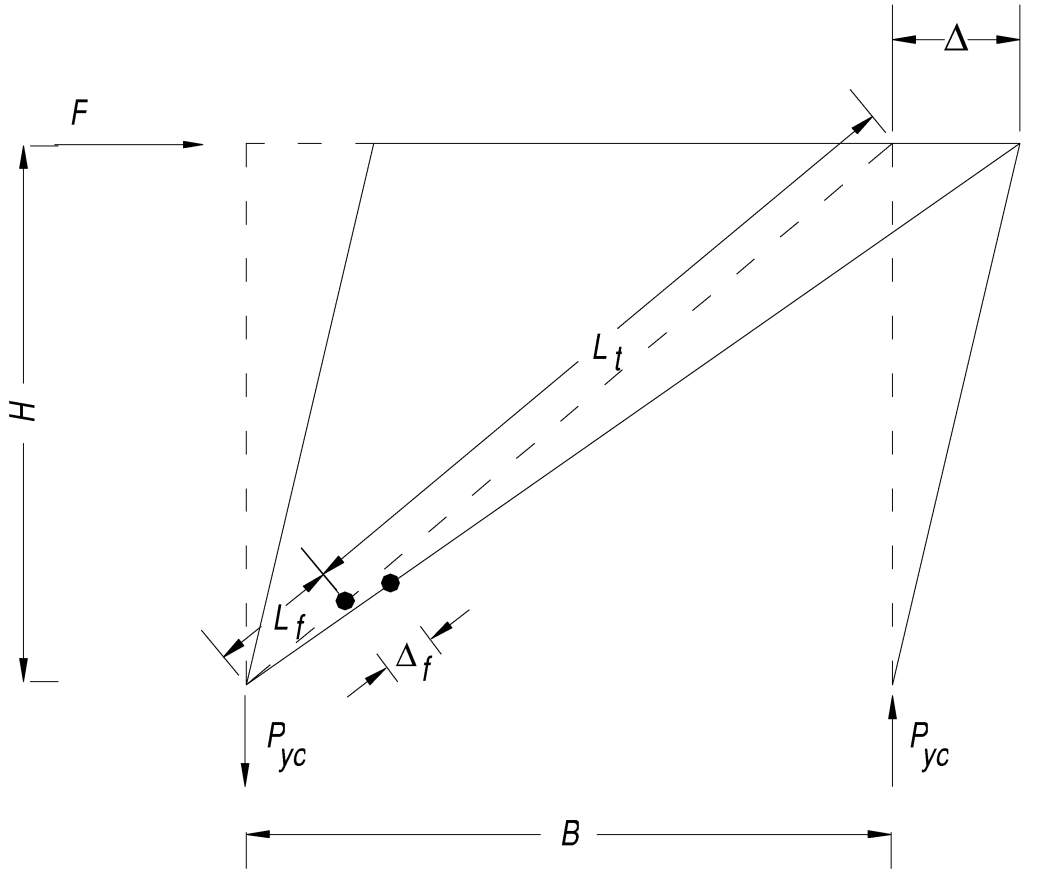

Figure 2-7 Idealized Retrofitted Sway Frame Deformation

horizontal load, H represents the height and B is the width of the sway frame. Since the supplemental tendons are designed to work in tension only, it will be assumed that only one tendon works at a given time as shown in the deflected shape of the sway frame in figure 2-7. Therefore, the force in the fuse-bar (or tendon) can be expressed as

$$F_f^{min} = \frac{F}{cos\,\alpha} - F_D \qquad \textbf{(2-3)}$$

in which F_D = force in the damper devices (if any) which may be a function of displacement and velocity, and F_f^{min} = the maximum force in the fuse-bars. It must be noted that superscript "min" is used to designate the maximum fuse-bar force that is used to calculate the "minimum"

cross-sectional area. Therefore, the minimum required cross-sectional area of the fuse-bar can be determined as:

$$A_{f,min} = \frac{\lambda F_f^{min}}{f_y} \tag{2-4}$$

in which $\lambda =$ a safety factor whose value should be specified by the design engineer, and $f_y =$ yield stress of the fuse-bar.

Similarly, an upper limit to the cross-sectional area of the fuse-bars must be specified to prevent sway frame verticals from buckling. If P_{yc} is the axial force capacity of the verticals (figure 2-7), they will either buckle or yield, assuming the same capacity in both tension and compression, when the axial force exceeds P_{yc}. Let the axial force in the vertical due to gravity loads be P_{dc}, and the maximum force in the damper device be F_D therefore the maximum allowable additional force P_{uc} due to the lateral force F is given by

$$P_{uc} = P_{yc} - P_{dc} \tag{2-5}$$

The lateral force F that would produce this axial force, P_{uc} can be determined based on the geometry as:

$$F = \frac{P_{uc}}{\tan\alpha} \tag{2-6}$$

Therefore, the maximum force in the fuse-bars can be calculated using equation (2-3) as:

$$F_f^{max} = \frac{F}{\cos\alpha} - F_D \tag{2-7}$$

where $F_f^{max} =$ the maximum fuse-bar force and F = calculated using equation (2-6). Similarly, superscript "max" is used to designate the maximum fuse-bar force that is used to calculate the "maximum" cross-sectional area. Finally, the maximum allowable cross-sectional area can be determined as:

$$A_{f,max} = \frac{\lambda F_f^{max}}{f_y} \tag{2-8}$$

2.3.5 Minimum and Maximum Design Length of the Fuse-Bar

A minimum fuse-length requirement should be specified in order to prevent fuse-bars from failing prematurely by tensile fracture. This requirement can be easily quantified by considering the total tendon and supplemental system elongation and, stress-strain properties of the material used for the fuse-bar element. For this purpose, let Δ be the maximum allowable deck drift during a major event, therefore total elongation of the fuse element can be written as follows:

$$\Delta_f + \Delta_t = \Delta \cos\alpha \tag{2-9}$$

in which Δ_f and Δ_t are the fuse-bar and tendon elongations, respectively. Note that in case of TFD system damper and fuse elongation is the same as they are in parallel. Equation (2-9) can be solved for Δ_f using the following relationships:

$$k_t \Delta_t = k_f \Delta_f \quad and \quad k_t = \frac{EA_t}{L_t}, k_f = \frac{EA_f}{L_f} \tag{2-10}$$

in which k_t, k_f = axial stiffness, L_t, L_f = length, A_t, A_f = cross-sectional area of the tendon and fuse-bar, respectively. Therefore, equation (2-9) becomes:

$$\Delta_f = \frac{\Delta \cos\alpha + F_D L_t / EA_t}{(1 + \frac{A_f}{A_t}\frac{L_t}{L_f})} \tag{2-11}$$

The strain within the fuse-bar, ε_f, must be limited by the ultimate strain of the material used as the fuse-bar;

$$\varepsilon_f = \frac{\Delta_f}{L_f} = \frac{\Delta \cos\alpha + F_D L_t / EA_t}{(L_f + \frac{A_f}{A_t} L_t)} \leq \phi \varepsilon_u \qquad \textbf{(2-12)}$$

in which ε_u = ultimate strain, ϕ = an under-capacity factor which is less than 1.0 $(\phi < 1.0)$. Therefore, the minimum fuse-length, L_f^{min} must satisfy the above inequality.

A maximum fuse-length should be specified in order to limit deck drift within a reasonable range under near static conditions or wind loading. If the service drift is designated by Δ_s and the combined equivalent stiffness of the system as k^*:

$$k^* = \frac{k_t k_f}{k_t + k_f} = \frac{EA_f A_t}{A_f L_t + A_t L_f} \qquad \textbf{(2-13)}$$

the following inequality must be satisfied:

$$k^* \Delta_s \cos\alpha \geq \lambda F \qquad \textbf{(2-14)}$$

in which λ = a load factor which is greater than 1.0 $(\lambda > 1.0)$, and F is the lateral force that can be considered as static loading. Note that in equation (2-13) any possible stiffness contribution from the dampers devices is neglected for the near static condition. Finally, the maximum fuse-length, L_f^{max} must satisfy the inequality given by equations (2-13) and (2-14).

As previously noted, the TF system can be more efficiently designed and employed in the retrofit of end-sway frames. However, once the fuse-bars yield or fail after a major event, the TF system must be quickly restored to its pre-event condition. Since the entire load resistance is provided by the TF system, it is clear that the overall structural system lacks redundancy. One way to avoid what might be the reason of a catastrophic failure of the bridge structure is to provide redundancy by carefully detailing an alternative secondary connection at the lower end of the tendon element (figure 2-5). The gap between the angled-washer plate and the outer face of the sway frame vertical can be determined so as to allow the fuse-bars to operate within their design (elongated) length. Therefore, the washer plate engages the secondary connection after the fuse-bars can no longer provide resistance under subsequent lateral loading cycles. This

detailing can be considered as analogous to hinge restrainers used in between discontinuous deck connections in highway bridges.

2.4 BENEFITS OF PROPOSED RETROFIT ALTERNATIVES

The overall benefits of the proposed retrofit alternatives can be summarized as follows:

1) The magnitude of the support reaction transferred to the existing cap beam and pier is limited by the maximum design capacity of the fuse-bars.
2) The sway frame can be designed to be more flexible which in turn will reduce the base shear response and also protect the substructure and foundation.
3) By anchoring the fuses and dampers directly to the cap beam, horizontal forces transferred to the bearing can be generally reduced which may eliminate the need for retrofitting the existing steel bearings.
4) Since the fuse-bars can be easily replaced after a major event, the bridge can be opened to traffic in a very short time.
5) Especially when dampers are used, the axial forces in the verticals may be reduced due to reduced seismic demand. Therefore, buckling of the sway frame verticals can be avoided.

2.5 SUMMARY

The primary purpose of this section was to propose a new retrofit concept for mitigating seismically induced lateral loads on the end-sway frames of steel deck-truss bridges and their supports. Three alternative retrofit configurations were introduced. The proposed systems consist of a post-tensioned tension element with or without supplemental – nonstructural elements. First, fuse-bars alone were considered as the supplemental elements which are connected in series to the tendon elements (TF system). Next, an improved system was introduced in which damper elements are designed to provide damping for reducing the seismic demand (TFD system). Finally, the benefits of the proposed retrofit strategies are given.

SECTION 3

MODEL STRUCTURE AND TEST PROGRAM

3.1 INTRODUCTION

This section first presents details of the supplemental system elements used in the experimental study. A prototype sway frame structure is introduced and the one-third scale physical model of the prototype structure is described. Next, details of the experimental setup and the shaking table test program are presented. Finally, relevant analytical modeling assumptions adopted in a modified version of DRAIN-2DX (Prakash et al., 1992) are discussed.

3.2 ELASTOMERIC SPRING DAMPERS (ESD)

The ESDs used in the experimental study were off-the-shelf devices. Single-acting (compression only) dampers were modified to enable the application as energy dissipating systems in building structures, by building a housing around the damper to give similar tension and compression attributes as shown in figure 3-1. These *re-centering* devices were previously used to retrofit a 1:3 scale reinforced concrete and 1:4 scale steel model structure at the State University of New York at Buffalo (Pekcan et al., 1995, 1999 and 2000a). ESDs contain a silicone-based elastomer whose consistency gives both compressibility and viscous attributes. Thus, dampers can be designed to give both spring and hysteretic behavior.

The devices were tested under displacement-controlled sinusoidal motions at various frequencies and amplitudes. Some selected force-displacement plots are shown in figure 3-2. These specimen tests were used to identify the parameters in the computational model that was previously proposed by Pekcan et al. (1995) and later advanced to improve the numerical stability of the solution of the equations of motion by Pekcan et al. (1999). The two-component velocity-dependent model is given as follows:

$$F_D = K_2 x + \frac{(K_1 - K_2)x}{\sqrt{1 + \left(\frac{K_1 x}{P_y}\right)^2}} + C_D \, \mathrm{sgn}(\dot{x}) \left| \dot{x} \frac{x}{x_{\max}} \right|^{\alpha} \qquad \textbf{(3-1)}$$

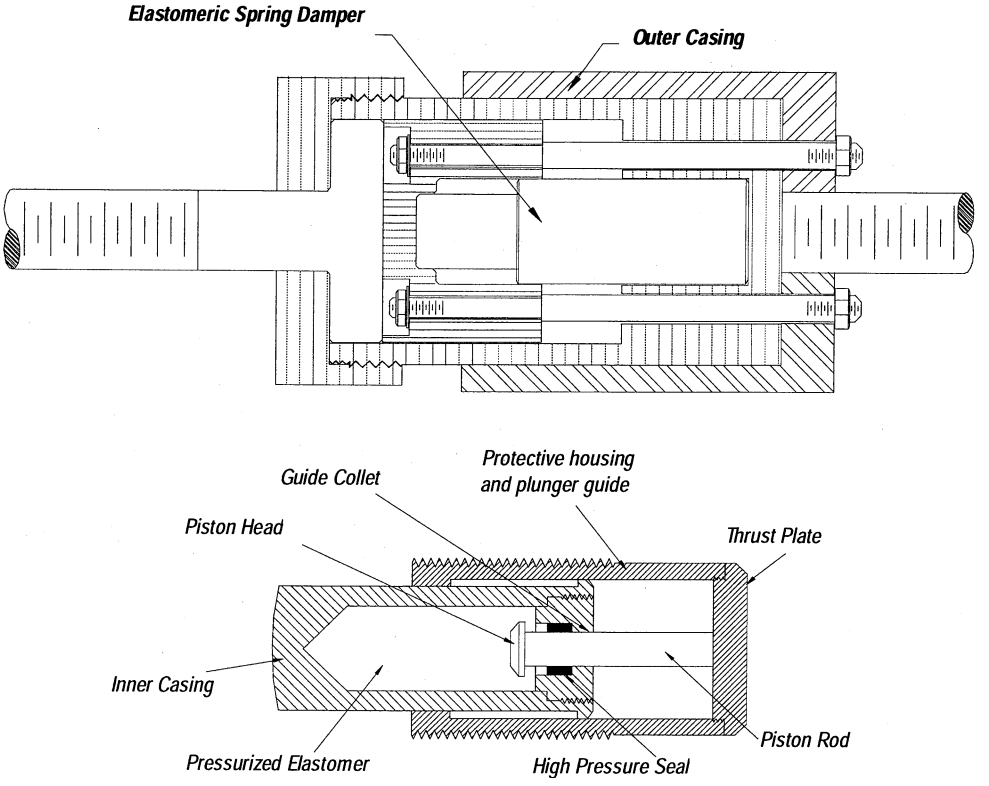

Figure 3-1 Elastomeric Spring Damper

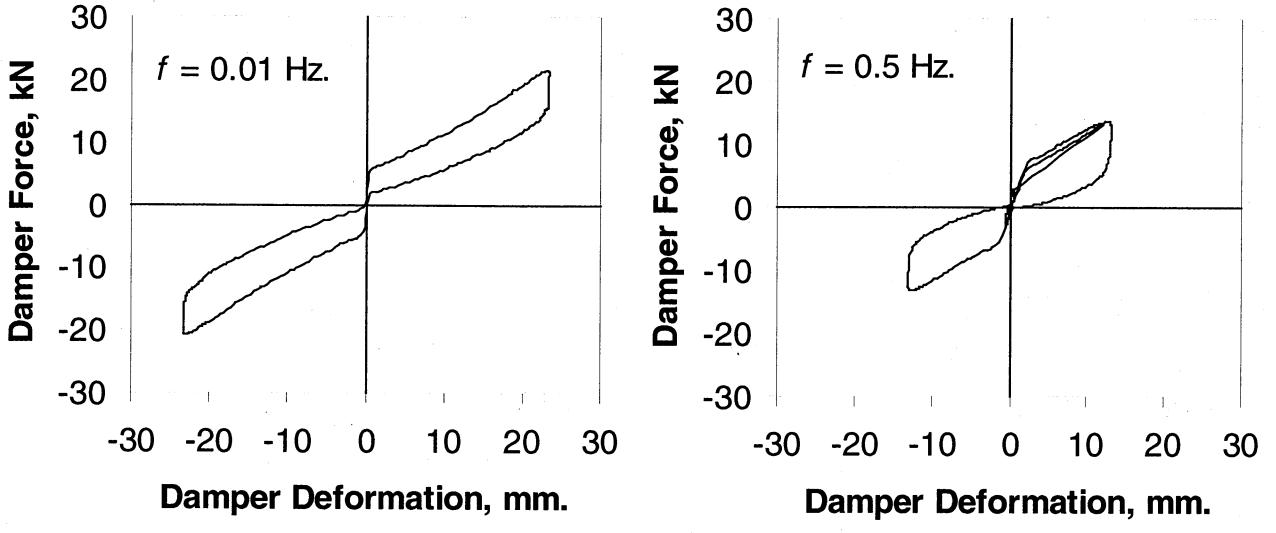

Figure 3-2 ESD Force-Displacement Relationship

Table 3-1 Properties of the Fuse-Bars

Type	Diameter (mm)	Fuse Length (mm)	Yield Force (kN)	Ultimate Force (kN)	Designation
I	7	150	36.6	41.1	F*I*1
I	4	230	11.9	13.4	F*I*2
II	5	230	14.9	17.7	F*II*1

in which x = the damper displacement, K_1 = the initial stiffness, K_2 = elastomeric stiffness after the pre-stress has been overcome, P_y = damper static pre-stress force (preload), C_D = the damper constant, $\dot{x}$ = the damper velocity, $x_{\max}$ = the damper stroke capacity, and α is a positive real exponent.

For the devices used in this study the following average values were identified from individual tests and used in subsequent analytical modeling:

K_1 = 25.0 kN/mm, K_2 = 0.6 kN/mm, P_y = 2.78 kN, x_{max} = 25.4 mm,

C_D = 1.09 kN/(mm/sec)$^{0.35}$, and α = 0.35, giving

$$F_D = 0.6x + \frac{(25.0-0.6)x}{\sqrt{1+\left(\frac{25.0x}{2.78}\right)^2}} + 1.09\,\mathrm{sgn}(\dot{x})\left|\dot{x}\frac{x}{25.4}\right|^{0.35} \qquad \textbf{(3-2)}$$

3.3 FUSE-BARS

Replaceable high strength, ϕ12 mm threaded rods were machined to specified diameter over a specified fuse length. Stress-strain curves of the fuse-bars used in the experimental study are shown in figure 3-3. Fuse-bar *type-I* had an average yield strength of f_y=950 MPa, and ultimate strength of f_{su}=1069 MPa where corresponding values for *type-II* were 760 MPa and 900 MPa, respectively. The strain at the onset of strain hardening was ε_{sh}=0.021 and that of at the ultimate stress was (approximately) ε_{su}=0.06 for both types. Young Modulus was found to be E=200 GPa and post yield modulus E_{sh}=2600 MPa. Details of the fuse-bar dimensions and the type of fuse-bar are given in table 3-1 with reference to figure 3-3.

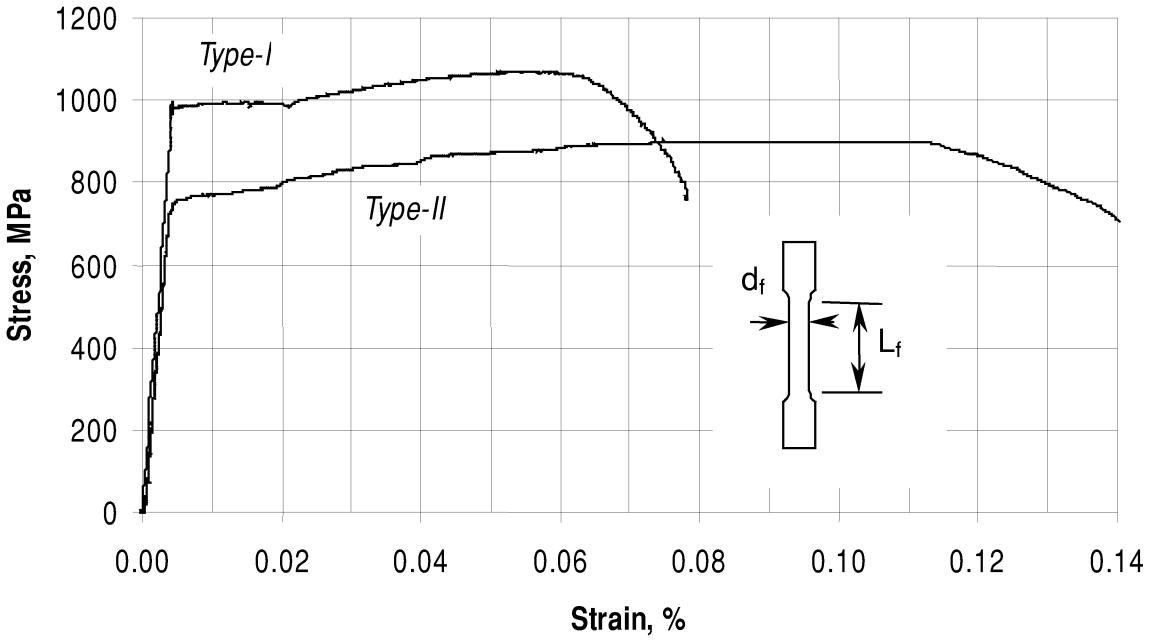

Figure 3-3 Average Stress-Strain Relationship of Fuse-Bars

Figure 3-4 Photograph of Prototype North Grand Island Bridge

3.4 PROTOTYPE END-SWAY FRAME AND SCALED MODEL STRUCTURE

The prototype structure is an existing toll bridge on I190 located near Niagara Falls, New York – North Grand Island Bridge. A photograph of the deck-truss bridge is shown in figure 3-4a. A prototype end-sway frame considered herein is taken from one of the end-sway frames at one of the piers which connects a 61 m simple span and a 76 m simple span. Front and side elevations of the 1:3 scaled model are shown in figure 3-5a. It must be noted here that the experimental model consists of two identical frames. Each frame was supported by pin connections under the verticals (columns).

The cross-beam (W8x21)-column (W8x24) connections were top-and-seat angle connections which had a minimal moment capacity to simulate the actual truss connections on the prototype frame. Eight #9 (28 mm diameter) bars were provided to act as rigid tendons which had a nominal cross sectional area of 645 mm^2 and weight per unit length of 0.05 kN/m. Two tendons (one on each side of each frame) were used as shown in the photograph of figure 3-6a. The tendon elements were connected to the columns at their lower and upper ends at the centerline of cross beams. Specially machined angled-washers were used only on one side of the lower end connections to allow the tendons to work only in tensions. This configuration was used to represent the original end-sway frame. For the retrofitted configuration, the lower ends of the tendon elements were directly connected [in series] to the supplemental system which were fixed to the shaking table (by a pull-plate) as shown in figure 3-6b. The fuse-bars were attached to the tendons at one end. A special type of turn-buckle was used at the other end which engaged the system only in tension (figure 3-6c).

In the first part of the experimental study, the proposed retrofit strategy was tested on the scaled model which had a tributary weight of 54 kN/per frame. The tributary weight was then increased to 76 kN which had an effect of increasing the natural period of vibration by a factor of (approximately) 1.41. In fact, in the latter case displacement demand on the structure was increased to study of the effectiveness of the supplemental system under such conditions.

3.5 INSTRUMENTATION

A total of 44 data channels were used to monitor the model structure response. A complete list of these channels and corresponding descriptions is given in table 3-2. A schematic view of the instrumentation on the structure is shown in figure 3-7.

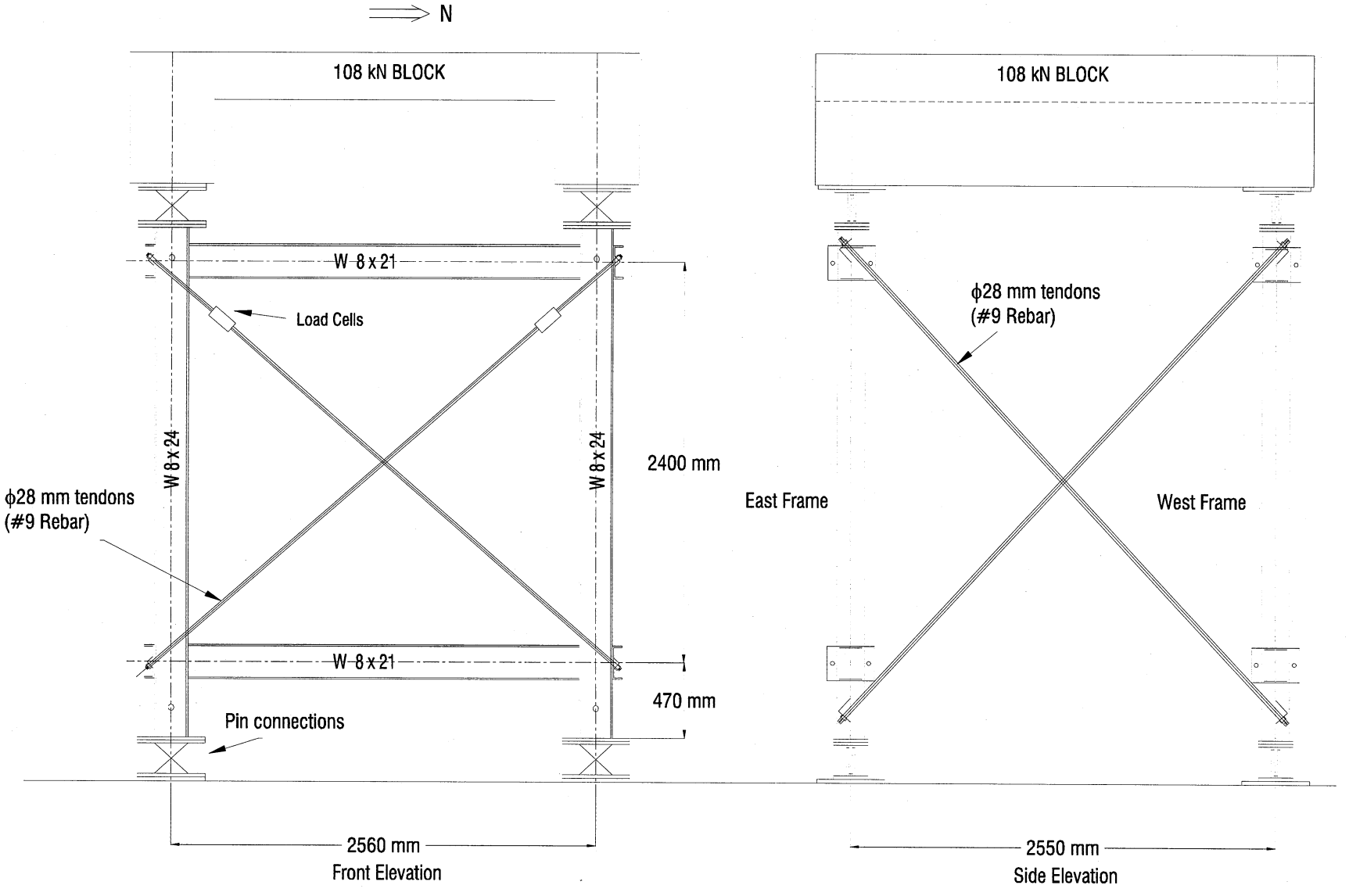

Figure 3-5a Front and Side Elevation View of the Experimental Model with Tendons Only

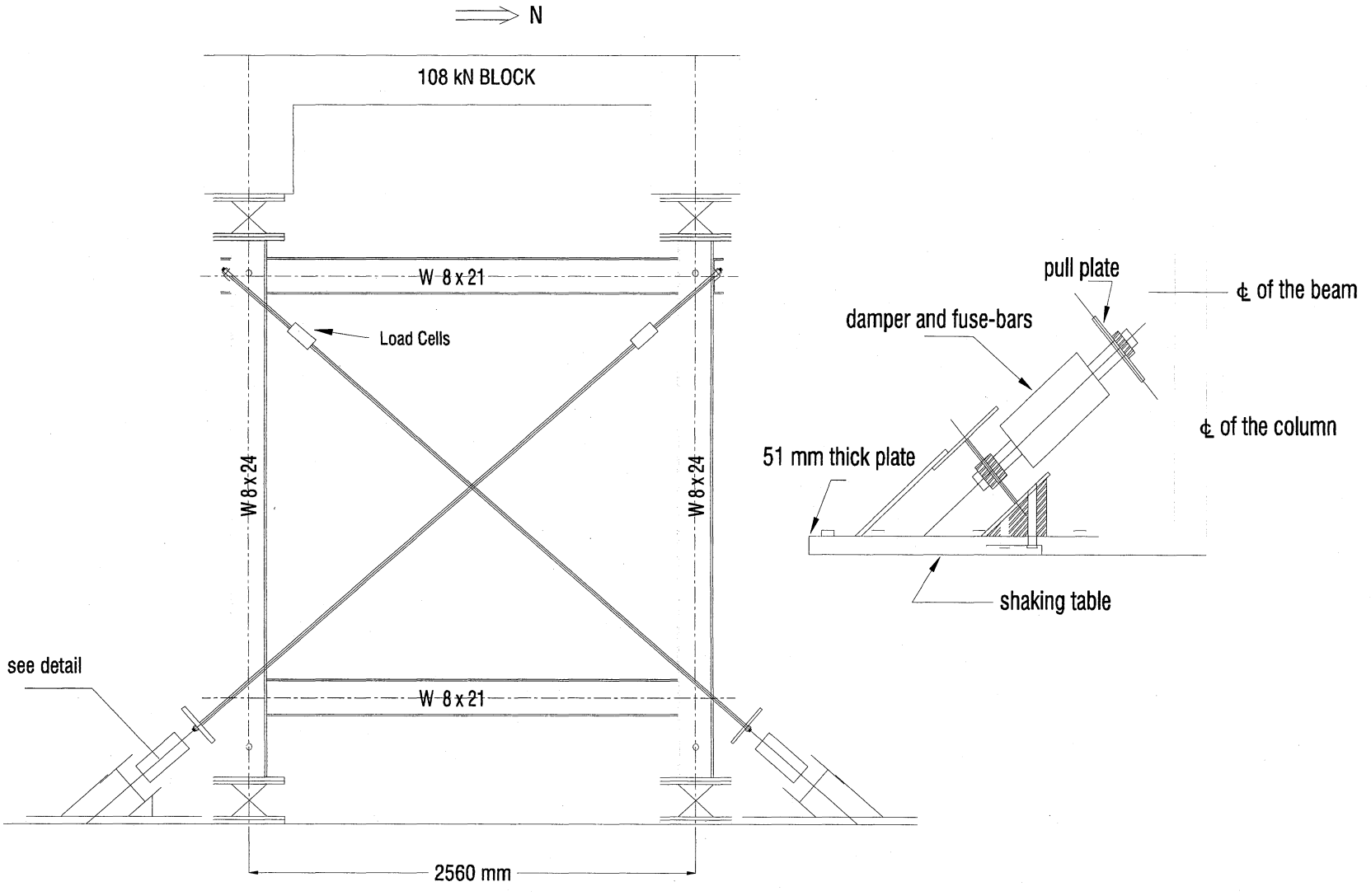

Figure 3-5b Front Elevation of the Experimental Model with Supplemental System

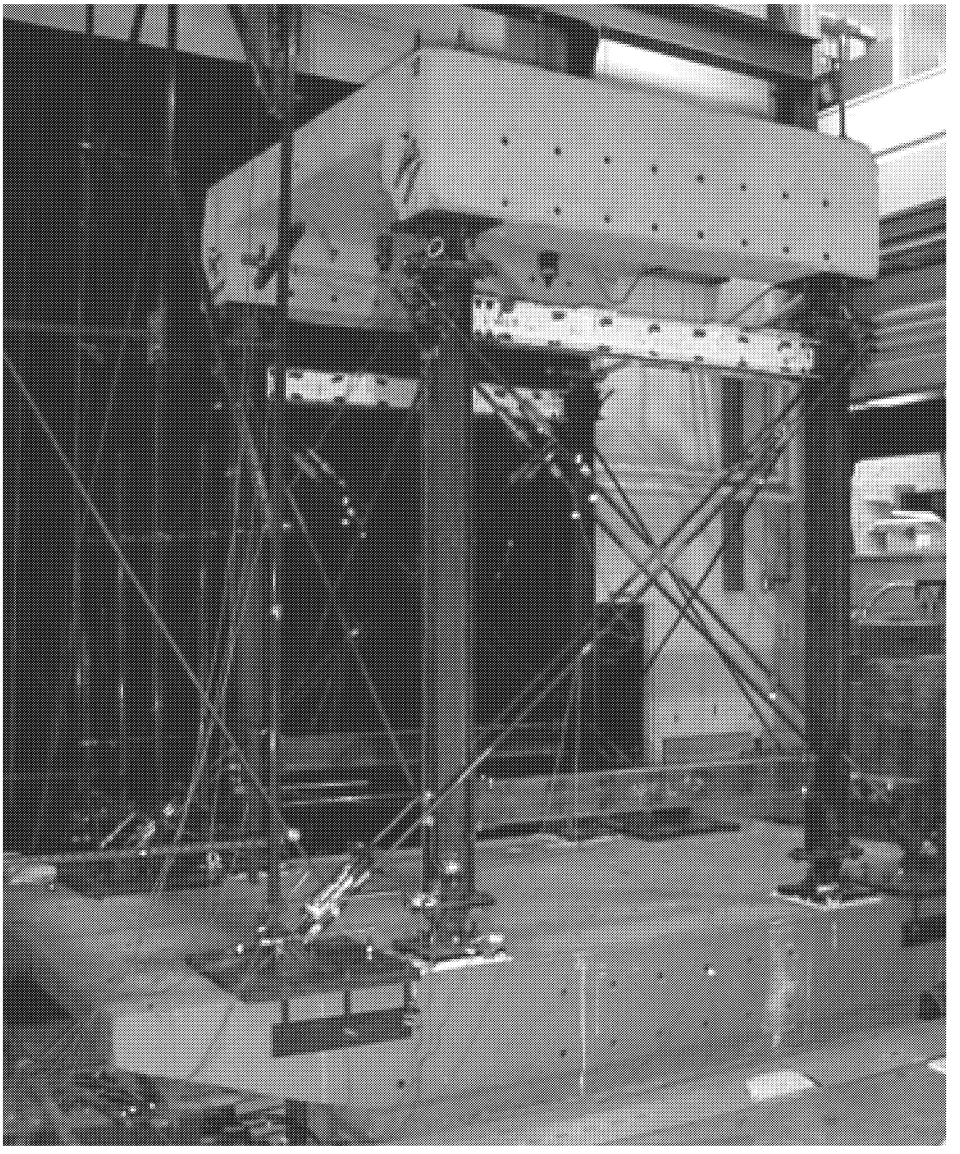

Figure 3-6a Photograph of the 1/3 Scale Model Test Structure on the Shaking Table

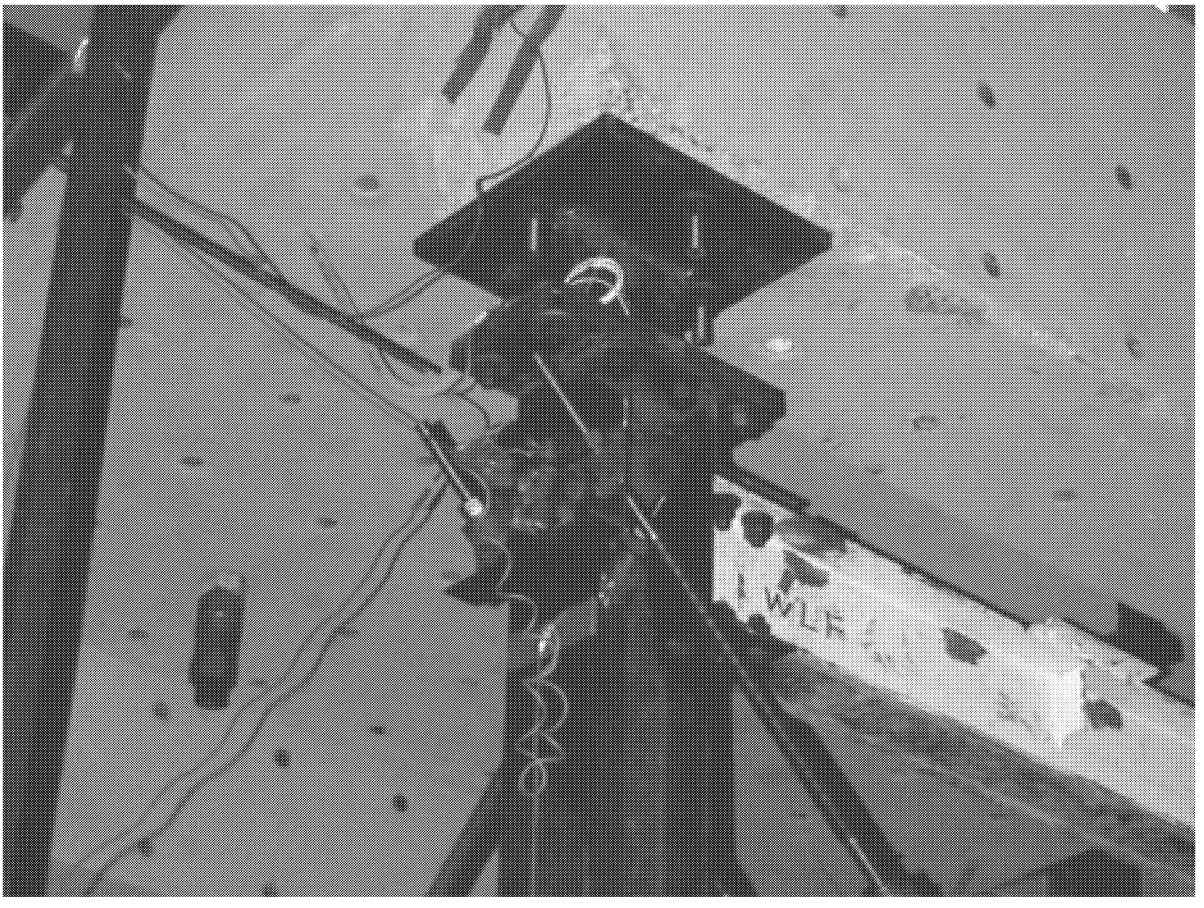

Figure 3-6b Photograph of the Tendon Connection at the Deck Level: Load cells with a capacity of 130 kN were installed in series with the tendon in order to record the supplementary system forces at this level.

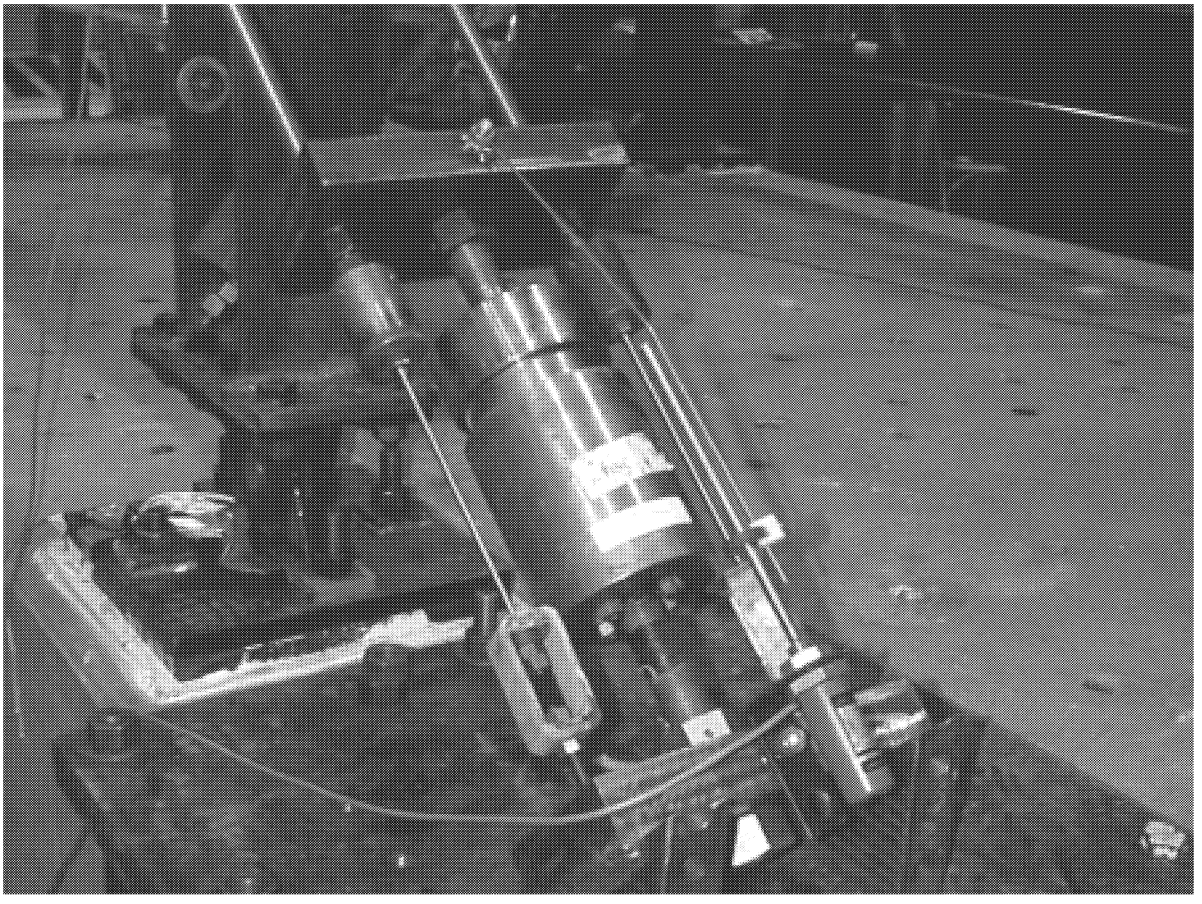

Figure 3-6c Photograph of the Details of the Supplemental System and its Tendon Connections: Note that the special turn-buckles were used which allowed the fuse-bars (directly in series with the tendons) to work in tension only

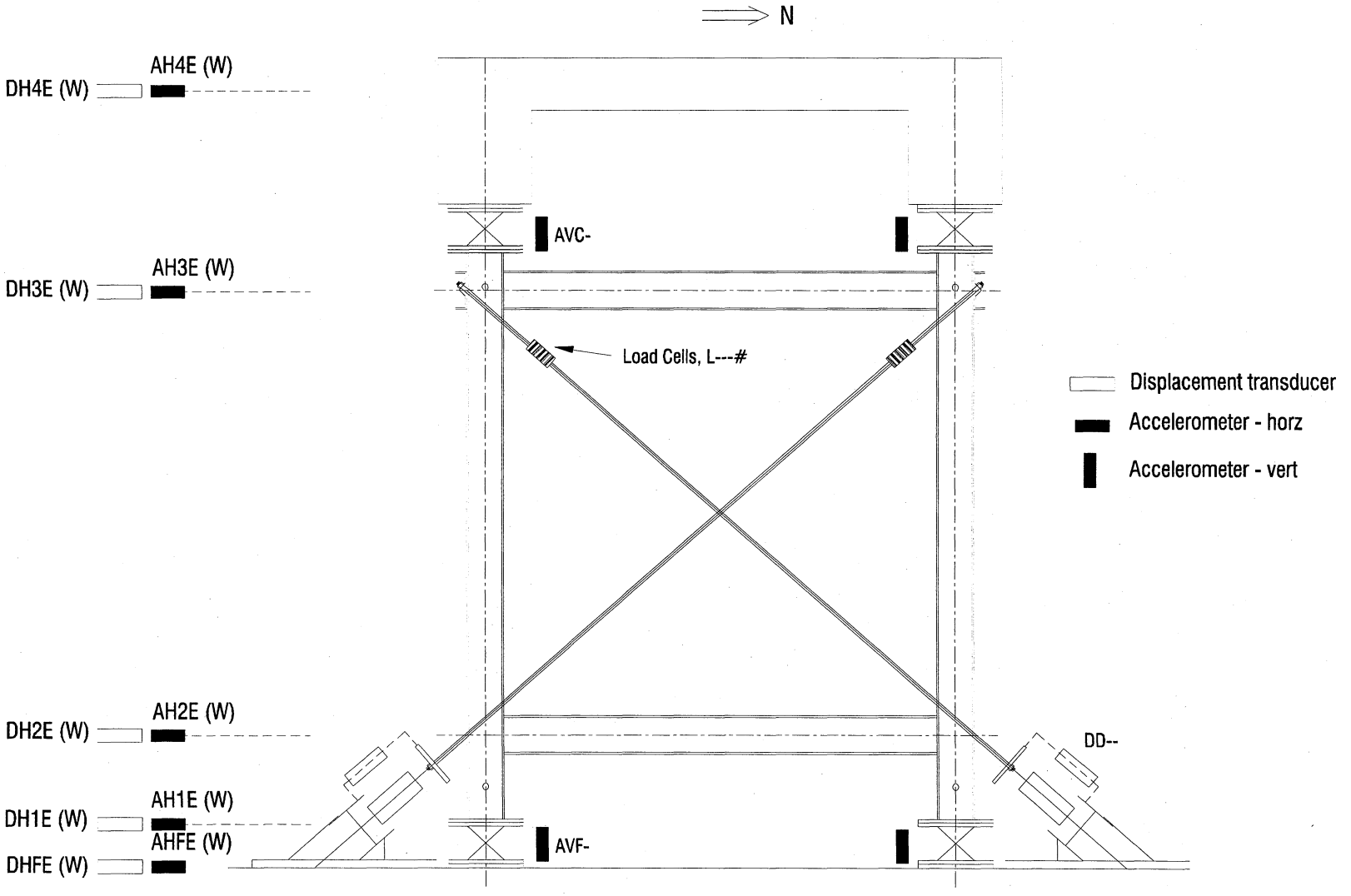

Figure 3-7 Schematic View of the Instrumentation

Table 3-2 List of Instrumentation

Channel Name	Units	Description/Remarks
AHFE	G's	Horizontal acceleration at the base level – east sway frame
AH#E	G's	Horizontal acceleration at levels 1 through 4 – east sway frame
AHFW	G's	Horizontal acceleration at the base level – west sway frame
AH#W	G's	Horizontal acceleration at levels 1 through 4 – west sway frame
AVF-	G's	Vertical acceleration at the base level – SE, SW, NE and NW
AVC-	G's	Vertical acceleration at the deck level – SE, SW, NE and NW
DHFE	mm.	Horizontal (in the direction of shaking) displacement at the base - east sway frame
DH#E	mm.	Horizontal (in the direction of shaking) displacement at levels 1 through 4– east sway frame
DHFW	mm.	Horizontal (in the direction of shaking) displacement at the base - west sway frame
DH#W	mm.	Horizontal (in the direction of shaking) displacement at levels 1 through 4– west sway frame
DD--	mm.	Fuse+damper system deformation – SE, SW, NE and NW
L---#	kN	Tendon force (load cell) – SE-SEE, SW-SWW, NE-NEE, NW-NWW ends of the tendons
DLAT	mm.	Shaking table horizontal displacement
ALAT	G's	Shaking table horizontal acceleration
DVRT	mm.	Shaking table vertical displacement
AVRT	G's	Shaking table vertical acceleration

A set of displacement transducers as well as horizontal and vertical accelerometers were installed on each frame. Linear displacement transducers were used to measure the absolute displacement response at below and above the pin support, at the lower and upper end of the tendon, and at the center of concrete weight, all in the longitudinal (horizontal N-S) direction. Four additional displacement transducers were installed to monitor the relative translation between the shaking table and the pull-plate (hence, average damper/fuse deformation, figures 3-6c and 3-7) at the tendon's lower end. Horizontal accelerometers were installed on each level where the displacement measurements were taken.

Tendon forces were recorded using eight identical load cells, connected in series to the tendon elements at their upper end.

3.6 TEST PROGRAM AND TESTED CONFIGURATIONS

In the experimental study, numerous shaking table experiments were performed using five different ground motions at various peak ground accelerations (PGA) levels with various configurations:

i) 1952 Kern County – Taft N21E,

ii) 1940 Imperial Valley – El Centro NS,

iii) 1971 San Fernando – Pacoima Dam S16E,

iv) 1994 Northridge – Sylmar County 90°,

v) 1995 Great Hanshin – Kobe NS.

Ground motions were time scaled (by a factor of $1/\sqrt{3}$) in order to meet the similitude requirements. Time scaled acceleration-time histories of the ground motions are shown in figure 3-8. A wide-band (0 to 50 Hz) white noise base excitation (0.05 g) was used before and after each configuration change to determine the dynamic characteristics of the test structure.

As previously mentioned in section 3.4, model frame systems were tested with different tributary weights of 54 kN and 76 kN per frame. These are referred to as *SF1* and *SF2*, respectively. *SF1* was first tested with tendons only in X-braced configuration in which the lower ends of the tendon elements were connected to the frame columns at the lower cross-beam level. This configuration was considered to be the case where existing truss braces were replaced with post-tensioned tendon elements on a prototype structure. This typical retrofit alternative will be referred to as *tendon only* (*TO*). Next, the configuration which had the damper

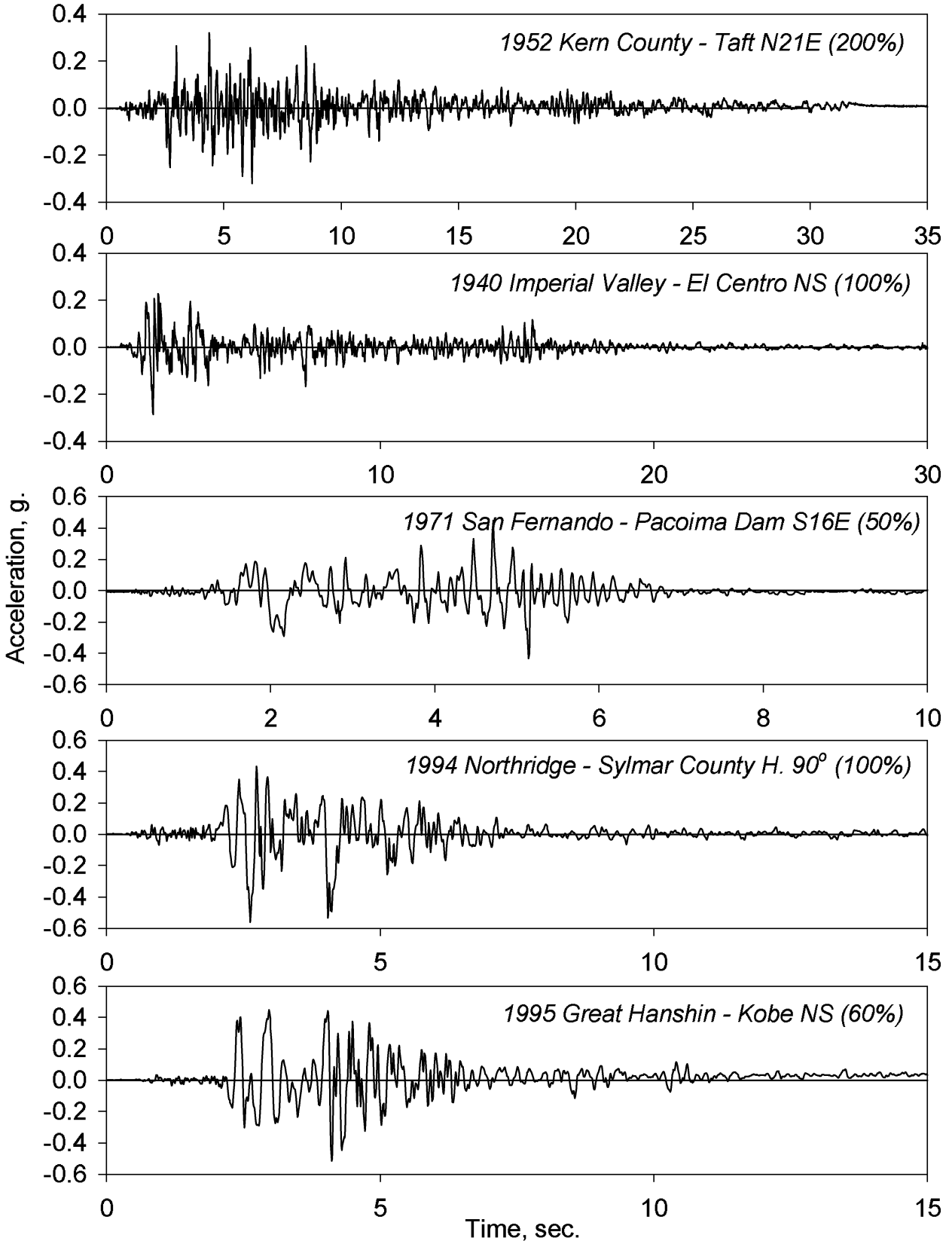

Figure 3-8 Sample Acceleration-Time Histories as Obtained from the Experiments (time scaled)

Table 3-3 Tested Configurations

Configuration Id.	Description
SF1	Base model frame with a tributary weight of 54 kN
SF2	Base model frame with a tributary weight of 76 kN
SF1-TO *SF2-TO*	Sway frame models with tendons only.
SF1-TD *SF2-TD*	Sway frame models with dampers in series with tendons.
SF1-TF *SF2-TF*	Sway frame models with fuse-bars in series with tendons.
SF1-TFD *SF2-TFD*	Sway frame models with both fuse-bars and dampers in series with tendons.

Table 3-4 Shaking Table Test Program – *SF1*

Test	Group Id.	Gr Motion	Table Acc. (g)	Case	Filename	Remarks
1	SF1 – G1	White Noise 0-50 Hz.	0.050	TO	WNPRWB.001	w/o prestress
2		El Centro S00E (60%)	0.205	"	ELPRWB.001	"
3		Taft N21E (100%)	0.158	"	TAPRWB.001	"
4	SF1 – G2	White Noise 0-50 Hz.	0.050	"	WNPRWB.002	w/ prestress
5		El Centro S00E (75%)	0.265	"	ELPRWB.002	"
6		White Noise 0-50 Hz.	0.050	"	W3PRWB.001	As is
7		Pac. Dam S16E (25%)	0.252	"	PAPRWB.001	w/ prestress
8		Sylmar 90 deg (40%)	0.243	"	SYPRWB.001	"
9		Kobe NS (45%)	0.272	"	KOPRWB.001	"
10		White Noise 0-50 Hz.	0.050	"	W4PRWB.001	As is
11		White Noise 0-50 Hz.	0.050	"	W5PRWB.001	As is
12	SF1 – G3	White Noise 0-50 Hz.	0.050	TD	WAPRDA.001	w/ prestress at ~P_y
13		Pac. Dam S16E (20%)	0.230	"	PAPRDA.001	"
14		Sylmar 90 deg (50%)	0.281	"	SYPRDA.001	"
15		Kobe NS (30%)	0.270	"	KOPRDA.001	"
16		El Centro S00E (70%)	0.241	"	ELPRDA.001	"
17		Taft N21E (100%)	0.146	"	TAPRDA.001	"
18		White Noise 0-50 Hz.	0.050	"	WBPRDA.001	As is
19	SF1 – G4	White Noise 0-50 Hz.	0.050	TD	WCPRDA.001	w/ prestress at ~$0.75P_y$
20		El Centro S00E (80%)	0.285	"	ELPRDB.001	"
21		Pac. Dam S16E (40%)	0.455	"	PAPRDB.001	"
22		Sylmar 90 deg (80%)	0.503	"	SYPRDB.001	"
23		Kobe NS (45%)	0.371	"	KOPRDB.001	"
24		Taft N21E (280%)	0.433	"	TAPRDB.001	"
25		White Noise 0-50 Hz.	0.050	"	WDPRDA.001	As is
26	SF1 – G5	White Noise 0-50 Hz.	0.050	TF – F*I*1	WENSFA.001	w/o prestress
27		El Centro S00E (55%)	0.193	"	ELNSFA.001	"
28		Taft N21E (110%)	0.172	"	TANSFA.001	"
29		Pac. Dam S16E (15%)	0.174	"	PANSFA.001	"
30		White Noise 0-50 Hz.	0.050	"	WFNSFA.001	As is
31	SF1 – G6	White Noise 0-50 Hz.	0.050	TFD – F*I*2	WGNDFA.001	w/ prestress at ~ $0.25P_y+0.25F_y$
32		El Centro S00E (55%)	0.190	"	ELNDFA.001	"
33		Pac. Dam S16E (15%)	0.161	"	PANDFA.001	"
34		Sylmar 90 deg (45%)	0.274	"	SYNDFA.001	"
35		Kobe NS (35%)	0.277	"	KONDFA.001	SE, SEE, NEE and SWW fuse-bars broken
36		White Noise 0-50 Hz.	0.050	"	WHNDFA.001	As is

Table 3-4 Shaking Table Test Program – *SF1* (cont'd)

Test	Group Id.	Gr Motion	Table Acc. (g)	Case	Filename	Remarks
37	SF1 – G7	White Noise 0-50 Hz.	0.050	TFD – F*II*1	WIPDFA.001	w/ prestress at ~ 0.25 P_y+0.25F_y
38		El Centro S00E (60%)	0.213	"	ELPDFA.001	"
39		Pac. Dam S16E (20%)	0.213	"	PAPDFA.001	"
40		Sylmar 90 deg (55%)	0.330	"	SYPDFA.001	"
41		Kobe NS (40%)	0.348	"	KOPDFA.001	"
42		Taft N21E (200%)	0.298	"	TAPDFA.001	"
43	SF1 – G8	Pac. Dam S16E (50%)	0.491	TFD – F*II*1	PAPDFB.001	w/ prestress at ~ P_y+0.25F_y
44		Kobe NS (50%)	0.404	"	KOPDFB.001	w/ prestress at ~ P_y+0.50F_y SE, NE, SW, and NW fuse-bars broken
45		White Noise 0-50 Hz.	0.050	"	WJPDFA.001	As is
46	SF1 – G9	White Noise 0-50 Hz.	0.050	TFD – F*II*1	WKPDFC.001	w/ prestress at ~ P_y+0.75F_y
47		El Centro S00E (75%)	0.260	"	ELPDFC.001	"
48		Pac. Dam S16E (20%)	0.198	"	PAPDFC.001	"
49		Sylmar 90 deg (50%)	0.300	"	SYPDFC.001	"
50		Kobe NS (40%)	0.310	"	KOPDFC.001	"
51		Taft N21E (300%)	0.452	"	TAPDFC.001	"
52	SF1 – G10	White Noise 0-50 Hz.	0.050	TFD – F*II*1	WLPDFD.000	w/ prestress at ~ P_y+F_y
53		Pac. Dam S16E (40%)	0.421	"	PAPDFD.000	"
54		Sylmar 90 deg (100%)	0.578	"	SYPDFD.001	"
55		Kobe NS (60%)	0.521	"	KOPDFD.001	SE, SEE, SW, and SWW fuse-bars broken

Table 3-5 Shaking Table Test Program – *SF2*

Test	Group Id.	Gr Motion	Table Acc. (g)	Case	Filename	Remarks
56	SF2 – G1	White Noise 0-50 Hz.	0.050	TD	WMNPDA.001	w/o prestress
57		White Noise 0-50 Hz.	0.050	"	WNPRDA.001	w/ prestress at ~P_y
58		El Centro S00E (55%)	0.187	"	E2PRDA.001	"
59		Taft N21E (100%)	0.151	"	T2PRDA.001	"
60		Pac. Dam S16E (15%)	0.164	"	P2PRDA.001	"
61		Sylmar 90 deg (40%)	0.255	"	S2PRDA.001	"
62		Kobe NS (30%)	0.258	"	K2PRDA.000	"
63		White Noise 0-50 Hz.	0.050	"	WOPRDA.001	As is
64	SF2 – G2	White Noise 0-50 Hz.	0.050	TFD – F*II*1	WPPDFA.000	w/ prestress at ~ P_y+F_y
65		El Centro S00E (55%)	0.193	"	E2PDFA.000	"
66		Taft N21E (100%)	0.160	"	T2PDFA.000	"
67		Pac. Dam S16E (20%)	0.190	"	P2PDFA.000	"
68		Sylmar 90 deg (40%)	0.253	"	S2PDFA.000	"
69		Kobe NS (40%)	0.336	"	K2PDFA.000	"
70		White Noise 0-50 Hz.	0.050	"	WQPDFA.000	As is
71	SF2 – G3	White Noise 0-50 Hz.	0.050	TFD – F*II*1	WRPDFA.000	w/ prestress at ~ P_y+F_y
72		Pac. Dam S16E (40%)	0.478	"	P2PDFB.000	SE and SW fuse-bars broken
73		White Noise 0-50 Hz.	0.050	"	WSPDFA.000	As is
74	SF2 – G4	White Noise 0-50 Hz.	0.050	TFD – F*II*1	WTPDFB.001	w/ prestress at ~ P_y+F_y
75		Sylmar 90 deg (75%)	0.439	"	S2PDFB.001	"
76		Kobe NS (60%)	0.499	"	K2PDFB.001	NE, NEE, NW and NWW fuse-bars broken
77		White Noise 0-50 Hz.	0.050	"	WUPDFB.001	As is
78	SF2 – G5	White Noise 0-50 Hz.	0.050	TO	WWPRWB.000	w/ prestress
79		White Noise 0-50 Hz.	0.050	"	WXPRWB.001	"
80		Pac. Dam S16E (20%)	0.247	"	P2PRWB.001	"
81		Sylmar 90 deg (40%)	0.226	"	S2PRWB.001	"
82		Kobe NS (35%)	0.291	"	K2PRWB.001	"
83		El Centro S00E (80%)	0.286	"	E2PRWB.001	"
84		Taft N21E (100%)	0.169	"	T2PRWB.001	"
85		White Noise 0-50 Hz.	0.050	"	WYPRWB.001	As is
86	SF2 – G6	White Noise 0-50 Hz.	0.050	SF2	W1NBXM.001	Bare frame – SF2
87		Taft N21E (50%)	0.077	SF2	TANBXM.001	"
88	SF1 – G11	White Noise 0-50 Hz.	0.050	SF1	W1NBNM.001	Bare frame – SF1
89		Taft N21E (50%)	0.079	SF1	TANBNM.001	"

and tendon elements in series bypassing the pin supports was tested with varying levels of prestress. This will be referred to as *tendon damper* (*TD*) alternative. And finally, one pair of fuse-bars were connected (parallel to the dampers) in series with the tendon elements on both sides of damper elements. Similarly, this retrofit alternative is referred to as the *tendon-fuse+damper* (*TFD*) alternative. A number of experiments were also conducted by deactivating the damper elements which will be referred to as *tendon fuse* (*TF*) alternative. After the first part of the experiments conducted on *SF1* frame, an additional concrete block was placed on the structure. Similar experiments were conducted on the *SF2* frame system. Tested configurations are listed in table 3-3 for reference. A complete list of shaking table test program is given in tables 3-4 and 3-5.

3.7 COMPUTATIONAL MODELING

The experimental structure was model in the enhanced version of DRAIN-2DX (Pekcan et al., 1995). The main assumptions considered in the model are as follows:

i) Main gravity load carrying elements were modeled using beam-column elements with a specified P-M interaction,

ii) Stiffness coefficients for the cross-beams (W8x21) were input assuming a 30% connectivity due to top-and-seat angle connections,

iii) Tributary weight of the structure, hence masses are assumed to be lumped at the nodes,

iv) Earthquake excitation is defined in the horizontal direction and all support points are assumed to move in-phase,

v) Viscous damping of the structure is considered using a Rayleigh damping model – that is a linear combination of the mass and the stiffness matrices. Damping values from the experiments were used as input for the analytical predictions.

The tendon-supplemental system was modeled using four different elements in series/parallel arrangement as shown in figure 3-9. These elements were used to model:

i) tendons (two #9 bars combined) that transfer the supplemental system's force to the upper joints, K_T, (low (EI) – realistic (EA) beam-column elements).

ii) tension only ESD devices and fuse-bars, K_{ESD}, C_{ESD} and K_f,

iii) dummy element with high axial stiffness (EA), K_d.

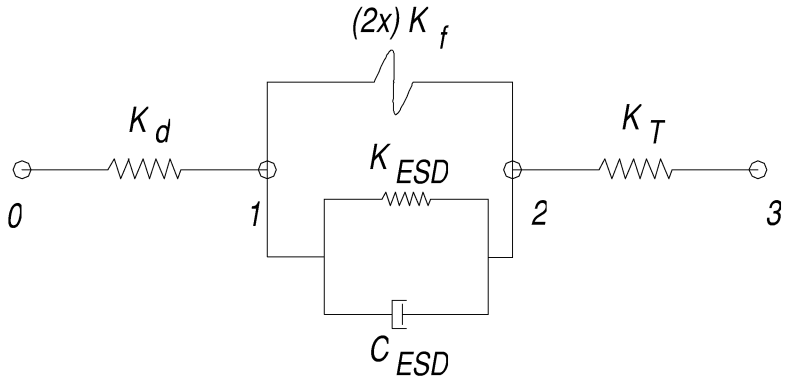

Figure 3-9 Modeling of the Supplemental Tendon System

Each analysis requires two steps: a) nonlinear static analysis, b) nonlinear dynamic time-history analysis. In the static analysis part, a set of nodal loads are applied at joint 1 (figure 3-9) with controlled loading steps until the desired (experimental) initial prestress level is achieved in the tendon elements. The dynamic time-history analysis then commences with the initial conditions attained at the end of the previous static analysis. Hence, the dummy beam-column element with high axial rigidity (EA) serves to "lock-in" the initial prestress level.

SECTION 4

EXPERIMENTAL RESULTS AND ANALYTICAL STUDY

4.1 INTRODUCTION

This section presents the experimental and analytical results that demonstrate the effectiveness of the retrofit configurations. The tested configurations include pairs of tendon elements in two directions in the plane of frames with/without supplemental system that consists of mechanical fuse-bars and/or elastomeric spring dampers (ESD). In this study, well-known ground motions were used to investigate the performance of a one-third scale model steel end-sway frame structure. Two "different" structural configurations that had different tributary weights were tested. Experimental results are presented in comparison with the analytical predictions. The analytical part of this study was performed using an enhanced version of the nonlinear time history analysis program Drain-2DX (Pekcan et al., 1999)

4.2 CHARACTERISTICS OF TESTED CONFIGURATIONS

This subsection summarizes the structural dynamic properties of various tested configurations with and without the supplemental tendon system. One pair of white noise test was conducted on the model structure for each configuration tested in order to identify the dominant natural periods of vibration and corresponding equivalent viscous damping ratios. Modal properties were then determined from the deck level transfer functions calculated as the ratio of the Fourier Transform of the deck acceleration to that of input acceleration at the pin supports. The Hanning windowing technique was employed with a 50% overlap (total of seven averages over 4,096 data points) along the time axis of the acceleration time histories. Approximate viscous damping ratios were calculated using the Half Power Method (Clough and Penzien, 1993).

It must be noted here that the model structure was ideally considered to be a single-degree-of-freedom (SDOF) system. However, due to the nature of the supplemental system and to the fact that it operates only in tension, more than one predominate frequency was observed. These corresponded to the cases when i) the tendons in both directions were active, ii) one of the tendons was slack, and/or iii) fuse-bars yielded or were broken. These cases were obviously

more apparent during moderate to high level ground excitations. Therefore corresponding modal properties were also identified from the ground motion experiments using the procedure described in the previous paragraph. Table 4-1 summarizes range of the identified natural periods of vibrations, viscous damping ratios for the configurations tested with reference to the assigned group identifications in tables 3-4 and 3-5. Selected transfer functions are plotted in figure 4-1 and 4-2 for the *SF1* and *SF2* frames, respectively.

In table 4-1, the two parent bare frames (SF1-G11 and SF2-G6) had natural period of vibrations of 0.44 sec. and 0.54 sec., respectively. A general comparison of dominant periods obtained from the white noise and the ground motion experiments reveals that in the latter case, when the supplemental tendon system was activated, dominant period of vibration lengthens due to the inherent characteristics of the supplemental system. TFD (SF1 – G6 through – G10 and SF2 – G2 through – G4) configurations had their shorter periods close to that of corresponding TO configurations. The longer period was due to either fuse-bar yielding or to the activation of the dampers' elastomeric stiffness (K_2). The calculated equivalent viscous damping ratios were typically higher for the TD configurations compared to that of TFD configurations. As summarized in table 4-1, equivalent viscous damping ratio was in excess of 30% in TD configuration (SF1-G4) as observed during high intensity ground motion excitations (tables 3-4, 3-5 and 4-2). For the TFD configurations, equivalent viscous damping ratios ranged between 2% to 9% when there was not significant yielding of the fuse elements. However, yielding (and eventually failure) of the fuse elements allowed dampers to operate at higher amplitudes which resulted in higher damping ratios of up to 18% to 23% in SF1-G7 and SF2-G4 configurations.

Finally, the scatter in the identified period of vibrations and damping ratios can also be attributed to the unequal prestress levels in the tendon elements from one experiment to another.

4.3 SHAKING TABLE EXPERIMENTS

A combined total of 58 simulated ground motion experiments were conducted on SF1 and SF2 frame systems using five ground motions at various PGA levels. Both frame systems were tested with TO, TD, TF and TFD supplemental system with varying prestress levels. It must be noted here that the TO configuration must be viewed as the unretrofitted case. Also

Table 4-1 Summary of the Characteristics of the Test Structure

Sway Fr.	Group Id.	Configuration - prestress level	East Frame				West Frame			
			White Noise		Ground Motion		White Noise		Ground Motion	
			Period sec.	ξ %	Period sec.	ξ %	Period sec.	ξ %	Period sec.	ξ %
SF1	G1	TO	0.19~0.28	15~38	0.18~0.34	7~25	0.15~0.28	14	0.16~0.34	8
	G2	TO	0.17~0.28	7~33	0.18~0.22	5~6	0.13~0.28	7	0.18~0.23	5~7
	G3	TD - ~P_y	0.15~0.24	14~23	0.32~0.38	12~24	0.23~0.24	19~21	0.32~0.38	11~24
	G4	TD - ~0.75P_y	0.14~0.28	14~27	0.19~0.44	6~32	0.13~0.28	17~28	0.33~0.44	5~12
	G5	TF	0.34~0.35	13~15	0.21~0.39	8~20	0.35	15	0.25~0.34	4~10
	G6	TFD- 0.25P_y+0.25F_y	0.14~0.23	13~19	0.16~0.34	13~29	0.23	24	0.27~0.33	9~15
	G7	TFD- 0.25P_y+0.25F_y	0.14~0.23	15~17	0.16~0.27	5~18	0.23	15	0.15~0.27	6~17
	G8	TFD- P_y+0.50F_y	0.15~0.25	9~14	0.24	5	0.25	16	0.24	6
	G9	TFD- P_y+0.75F_y	0.15	8	0.16~0.25	3~9	0.15	8	0.16~0.25	2~9
	G10	TFD- P_y+F_y	0.15	9	0.19~0.26	6	0.14	6	0.19	7
	G11	Bare Frame	0.44	7	0.49	5	0.44	7	0.49	5
SF2	G1	TD - ~P_y	0.17~0.26	15~25	0.34~0.47	9~23	0.25	15~18	0.34~0.47	9~24
	G2	TFD- P_y+F_y	0.17~0.23	8~18	0.19~0.23	5~9	0.14~0.22	6	0.19~0.23	6~9
	G3	TFD- P_y+F_y	0.16~0.25	7~19	0.19~0.22	8~9	0.17~0.24	6	0.19~0.22	9
	G4	TFD- P_y+F_y	0.18	9	0.17~0.25	20~23	0.18	6	0.24	12
	G5	TO	0.21	5	0.22~0.27	4~7	0.21	5	0.22~0.24	5~6
	G6	Bare Frame	0.54	7	0.57	9	0.54	7	0.63	6

SF1 – Sway Frame 1, Structural Weight = 54 kN
SF2 – Sway Frame 1, Structural Weight = 76 kN

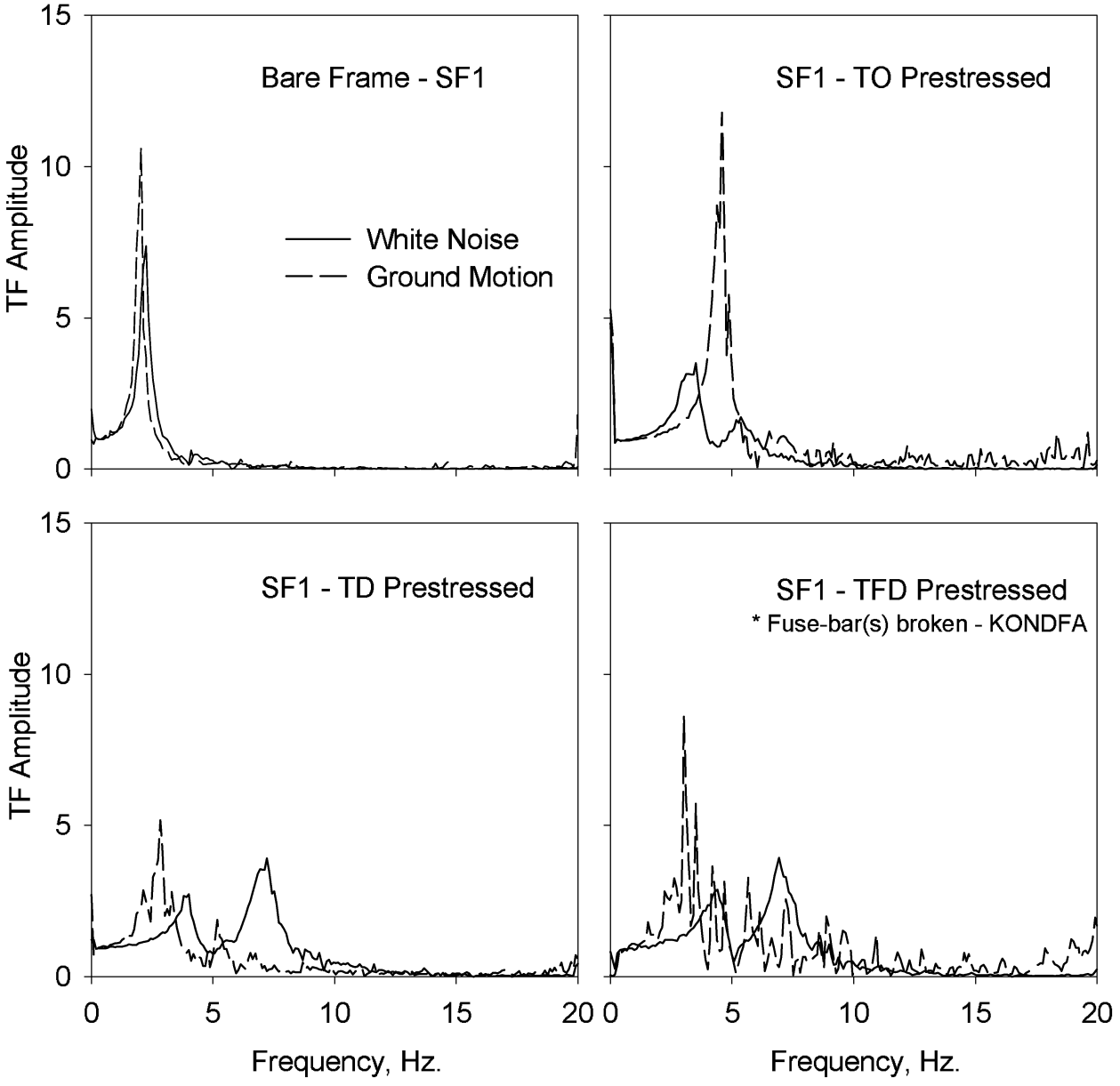

Figure 4-1 Sample Transfer Functions obtained from White Noise and Ground Motion Experiments - SF1 Frame

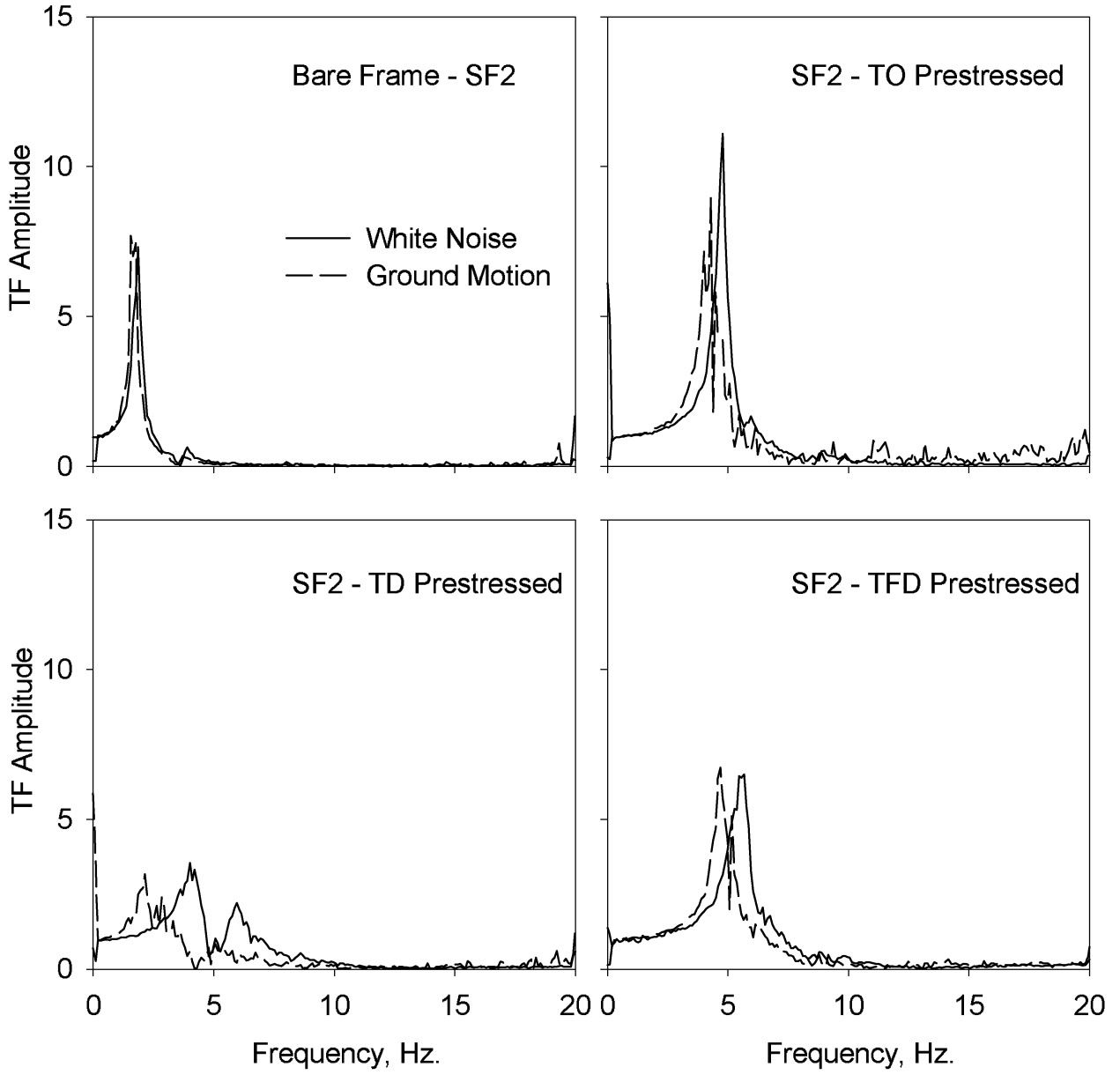

Figure 4-2 Sample Transfer Functions obtained from White Noise and Ground Motion Experiments - SF2 Frame

Table 4-2 Summary of Maximum Responses – SF1 System

Test Id.	Peak Table Acc. (g)	East Frame								West Frame								Configuration/Remarks
		Drift (mm)	Accel. (g)	Device South			Device North			Drift (mm)	Accel. (g)	Device South			Device North			
				Def. (mm)	Force (kN)	Pres. (kN)	Def. (mm)	Force (kN)	Pres. (kN)			Def. (mm)	Force (kN)	Pres. (kN)	Def. (mm)	Force (kN)	Pres. (kN)	
ELPRWA	0.205	7	0.385	-	29.7	-	-	27.6	-	7	0.366	-	26.4	-	-	38.6	-	TO – no prestr.
TAPRWB	0.158	6	0.344	-	26.7	12.3	-	22.5	12.0	5	0.320	-	20.9	13.0	-	31.0	12.6	TO
ELPRWB	0.265	6	0.563	-	33.5	11.9	-	40.2	12.2	6	0.499	-	29.1	12.5	-	41.9	12.1	TO
PAPRWB	0.252	7	0.710	-	61.7	13.1	-	65.3	12.8	7	0.679	-	57.3	14.0	-	71.9	14.5	TO
SYPRWB	0.243	4	0.354	-	35.8	13.7	-	36.4	13.8	4	0.346	-	33.8	14.3	-	41.9	13.7	TO
KOPRWB	0.272	7	0.673	-	60.1	13.5	-	62.2	13.6	7	0.636	-	59.5	13.9	-	67.5	12.8	TO
PAPRDA	0.230	5	0.180	3	7.0	4.5	2	7.5	4.7	4	0.171	3	7.3	4.4	2	7.0	4.5	TD – prestr. at ~P_y
SYPRDA	0.281	11	0.314	8	10.8	4.4	5	10.0	4.7	10	0.328	7	11.4	4.4	5	9.6	4.4	"
KOPRDA	0.270	11	0.323	7	11.1	4.5	7	11.0	4.6	12	0.321	7	11.3	4.4	7	11.3	4.5	"
ELPRDA	0.241	13	0.355	9	12.9	4.6	7	11.5	4.4	12	0.370	9	12.8	4.4	7	11.8	5.0	"
TAPRDA	0.146	4	0.165	3	8.2	5.2	2	8.1	5.0	4	0.151	3	8.6	5.0	2	8.6	5.6	"
ELPRDB	0.285	16	0.420	10	12.2	2.6	10	12.4	2.9	15	0.410	10	12.5	3.0	9	12.3	2.8	TD – prestr. at ~0.75P_y
PAPRDB	0.455	12	0.311	8	9.2	3.2	6	9.4	3.3	12	0.304	7	9.4	3.0	6	9.5	3.2	"
SYPRDB	0.503	26	0.607	17	19.4	2.4	14	16.6	2.9	24	0.626	17	19.1	2.6	14	17.8	2.6	"
KOPRDB	0.371	31	0.709	20	23.3	2.8	19	20.4	2.6	32	0.733	20	22.4	2.6	19	22.5	2.5	"
TAPRDB	0.433	28	0.623	18	20.4	3.2	15	17.1	2.9	26	0.644	18	19.7	2.9	15	18.9	3.2	"
ELNSFA	0.193	6	0.463	2	28.4	-	3	33.4	-	6	0.431	3	25.5	-	2	37.2	-	TF – F*I*1 – no prestr.
TANSFA	0.172	5	0.305	3	21.0	-	3	16.1	-	4	0.239	2	15.9	-	2	18.1	-	"
PANSFA	0.174	3	0.133	3	8.6	-	2	9.4	-	3	0.115	1	6.3	-	1	8.8	-	"
ELNDFA	0.190	4	0.306	1	18.0	3.1	1	21.7	3.7	3	0.295	1	13.9	2.8	1	25.3	4.4	TFD – F*I*2 – prestr. at ~ 0.25P_y+0.25F_y
PANDFA	0.161	3	0.248	1	20.6	2.8	1	17.4	3.7	3	0.279	1	16.6	3.1	1	24.2	3.9	"
SYNDFA	0.274	5	0.393	2	28.1	2.8	2	26.4	3.6	5	0.365	1	25.3	2.9	2	29.9	3.6	"
KONDFA	0.277	11	0.486	4	29.5	3.0	8	28.2	3.7	8	0.479	2	27.7	2.7	4	33.7	3.0	SE, SEE, NEE and SWW fuse-bars broken
ELPDFA	0.213	3	0.320	1	*	4.0	1	24.8	4.3	4	0.305	1	15.6	3.6	1	26.5	4.4	TFD – F*II*1 – prestr. at ~ 0.25 P_y+0.25F_y
PAPDFA	0.213	4	0.337	2	*	3.1	1	26.2	4.1	4	0.373	1	25.6	3.3	1	30.1	3.3	"
SYPDFA	0.330	6	0.580	2	*	4.2	1	47.2	4.4	7	0.616	2	45.1	3.6	2	56.8	3.6	"
KOPDFA	0.348	7	0.679	2	51.2	5.5	2	52.6	4.8	8	0.727	2	50.1	4.5	3	62.2	5.0	"
TAPDFA	0.298	5	0.506	2	43.9	4.2	1	38.0	4.3	5	0.483	2	36.2	4.2	2	40.8	4.4	"

* Load cell malfunction

Table 4-2 Summary of Maximum Responses – SF1 System (cont'd)

Test Id.	Peak Table Acc. (g)	East Frame								West Frame								Configuration/Remarks
		Drift (mm)	Accel. (g)	Device South			Device North			Drift (mm)	Accel. (g)	Device South			Device North			
				Def. (mm)	Force (kN)	Pres. (kN)	Def. (mm)	Force (kN)	Pres. (kN)			Def. (mm)	Force (kN)	Pres. (kN)	Def. (mm)	Force (kN)	Pres. (kN)	
PAPDFB	0.491	8	0.829	2	60.7	9.5	3	64.1	10.4	9	0.814	2	58.8	9.2	3	67.5	10.6	TFD – F*II*1 – prestr. at ~ P_y+0.25F_y
KOPDFB	0.404	10	0.883	6	66.3	18.7	4	66.7	18.1	10	0.900	5	65.4	17.5	4	70.7	17.8	TFD – F*II*1 – prestr. at ~ P_y+0.50F_y SE, NE, SW, and NW fuse-bars broken
ELPDFC	0.260	4	0.526	1	51.3	24.3	1	45.4	20.5	4	0.535	1	45.5	21.7	1	54.2	25.4	TFD – F*II*1 – prestr. at ~ P_y+0.75F_y
PAPDFC	0.198	3	0.405	0	44.8	23.5	1	38.2	19.4	4	0.423	0	39.8	20.5	1	46.5	24.9	"
SYPDFC	0.300	4	0.615	1	54.9	23.4	1	50.4	19.9	6	0.622	1	48.6	20.3	1	60.1	24.8	"
KOPDFC	0.310	7	0.781	2	60.8	22.5	1	60.0	18.9	6	0.735	2	57.7	19.4	2	64.4	23.6	"
TAPDFC	0.452	11	0.831	5	65.5	10.9	2	63.1	9.3	9	0.868	4	62.7	12.5	2	64.8	14.2	"
PAPDFD	0.421	5	0.697	2	64.1	36.2	1	63.6	34.3	7	0.739	2	61.9	33.9	1	64.7	35.3	TFD – F*II*1 – prestr. at ~ P_y+F_y
SYPDFD	0.578	10	0.885	4	66.9	30.5	5	69.6	29.1	12	0.927	4	65.7	29.2	5	72.3	31.3	"
KOPDFD	0.521	15	1.569	11	69.3	29.5	5	71.2	30.0	12	1.007	7	69.1	33.6	3	70.7	29.4	SE, SEE, SW and SWW fuse-bars broken

Table 4-3 Summary of Maximum Responses – SF2 System

Test Id.	Peak Table Acc. (g)	East Frame								West Frame								Configuration/Remarks
		Drift (mm)	Accel. (g)	Device South			Device North			Drift (mm)	Accel. (g)	Device South			Device North			
				Def. (mm)	Force (kN)	Pres. (kN)	Def. (mm)	Force (kN)	Pres. (kN)			Def. (mm)	Force (kN)	Pres. (kN)	Def. (mm)	Force (kN)	Pres. (kN)	
E2PRDA	0.187	10	0.182	6	10.2	4.2	7	9.5	3.6	9	0.201	6	10.2	4.0	7	12.0	4.3	TD – prestr. at ~P_y
T2PRDA	0.151	8	0.144	6	9.0	4.2	4	7.7	3.7	7	0.173	5	9.5	3.9	4	9.6	4.3	"
P2PRDA	0.164	5	0.115	3	7.9	5.0	2	6.9	4.4	4	0.117	3	8.1	4.7	2	7.8	5.0	"
S2PRDA	0.255	15	0.293	11	13.8	4.5	9	12.1	3.9	15	0.273	10	13.7	4.2	10	14.2	4.3	"
K2PRDA	0.258	23	0.427	14	17.9	4.5	17	18.2	3.9	23	0.392	15	18.5	4.3	16	22.4	4.3	"
E2PDFA	0.193	4	0.437	1	58.8	30.6	1	53.6	27.0	5	0.443	1	52.2	27.2	1	61.4	31.0	TFD – F*II*1 – prestr. at ~ P_y+F_y
T2PDFA	0.160	4	0.405	1	60.4	29.0	1	53.2	25.4	4	0.430	1	54.7	25.2	1	62.0	29.5	"
P2PDFA	0.190	5	0.517	1	64.1	28.7	2	61.6	25.2	6	0.522	1	59.0	24.7	2	67.4	28.4	"
S2PDFA	0.253	5	0.434	1	58.6	28.6	1	57.7	27.5	5	0.454	1	56.4	27.5	1	62.0	27.7	"
K2PDFA	0.336	7	0.555	3	66.6	28.1	3	66.6	27.0	8	0.623	3	63.8	26.7	3	70.7	26.7	"
P2PDFB	0.478	13	1.401	9	66.8	38.1	3	67.5	38.6	15	1.274	10	63.8	40.9	3	71.6	39.3	TFD – F*II*1 – prestr. at ~ P_y+F_y SE and SW fuse-bars broken
S2PDFB	0.439	10	0.602	3	65.2	35.2	2	62.1	30.8	10	0.577	2	62.3	31.9	1	68.0	34.0	TFD – F*II*1 – prestr. at ~ P_y+F_y
K2PDFB	0.499	21	0.830	7	73.2	33.2	16	66.3	33.0	14	0.672	4	67.6	32.9	12	76.0	33.0	NE, NEE, NW and NWW fuse-bars broken
P2PRWB	0.247	7	0.448	-	67.0	17.8	-	59.8	19.6	7	0.473	-	70.5	18.6	-	69.8	16.6	TO
S2PRWB	0.226	6	0.416	-	60.3	18.9	-	60.9	19.5	7	0.431	-	64.0	18.8	-	67.7	17.5	TO
K2PRWB	0.291	9	0.642	-	73.5	18.4	-	88.1	18.7	9	0.653	-	76.9	19.4	-	97.7	19.8	TO
E2PRWB	0.286	7	0.528	-	65.6	19.1	-	75.0	19.1	7	0.551	-	67.6	18.2	-	84.5	17.4	TO
T2PRWB	0.169	6	0.409	-	59.5	18.8	-	59.8	18.8	5	0.437	-	61.5	18.5	-	68.5	18.7	TO
TANBXM	0.077	7	0.084	-	-	-	-	-	-	7	0.082	-	-	-	-	-	-	Bare frame – SF2
TANBNM	0.079	9	0.141	-	-	-	-	-	-	8	0.135	-	-	-	-	-	-	Bare frame – SF1

tested were the bare frames (without tendons) in order to check the accuracy of the Drain-2DX computational model. Experimental results are summarized in tables 4-2 and 4-3 for SF1 and SF2 systems respectively. Each table lists the peak table accelerations, deck drift and acceleration, maximum device deformations and forces, and initial prestress levels for both east and west frames. It should be noted that one pair of tendons was used on both east and west frames (i.e. one on either side of the columns). Therefore, the maximum tendon force listed in tables are in fact the sum of the maxima in two tendon elements (see figure 3-6). Overall experimental results are also presented in Appendix A for the relative deck displacement and support-shear time histories, base shear versus deck drift and recorded supplemental system force-deformation. In these plots, experimental responses for east and west frames are overplotted for comparison. In general, both frames' responses were identical except for the TFD configurations in which fuse-bar(s) either yielded or failed. Therefore, the discussion of the experimental results will be focused only on the east frame response in the following sections.

Experimental results and observations are briefly discussed in subsections for the tested configurations in what follows. Analytical and experimental results of selected experiments are compared in terms of the recorded deck drift, bearing and total base shear time histories, and supplemental system deformation versus force response (TD and TFD configuration). Note that the experimental results of different configurations for a given ground motion are not directly comparable as the input acceleration histories differed in both amplitude and frequency content. The main reason for this was the interaction between table and the model structure, and continuous change in the structural system characteristics (due to yielding of fuse-bar(s), etc.) during the experiments. In general, the higher the ratio of model weight to payload limit (for the desired input acceleration levels) of the shaking table, and the higher the uncertainties in the model characteristics, the harder it is to control the input acceleration without distortion.

Finally, it should be kept in mind that the analytical model is a two-dimensional model. Therefore, it was not possible to model all of the tendon elements and fuse-bars as in the model structure. However, both pairs of tendons and fuse-bars were modeled as one element with combined properties. As can be seen from the results given in tables 4-2 and 4-3, the response was not symmetric even in the two tendons (or fuse-bars) on either side of the columns (note that in most of the cases only one of the two fuse-bars failed or yielded, e.g. KONDFA, KOPDFB,

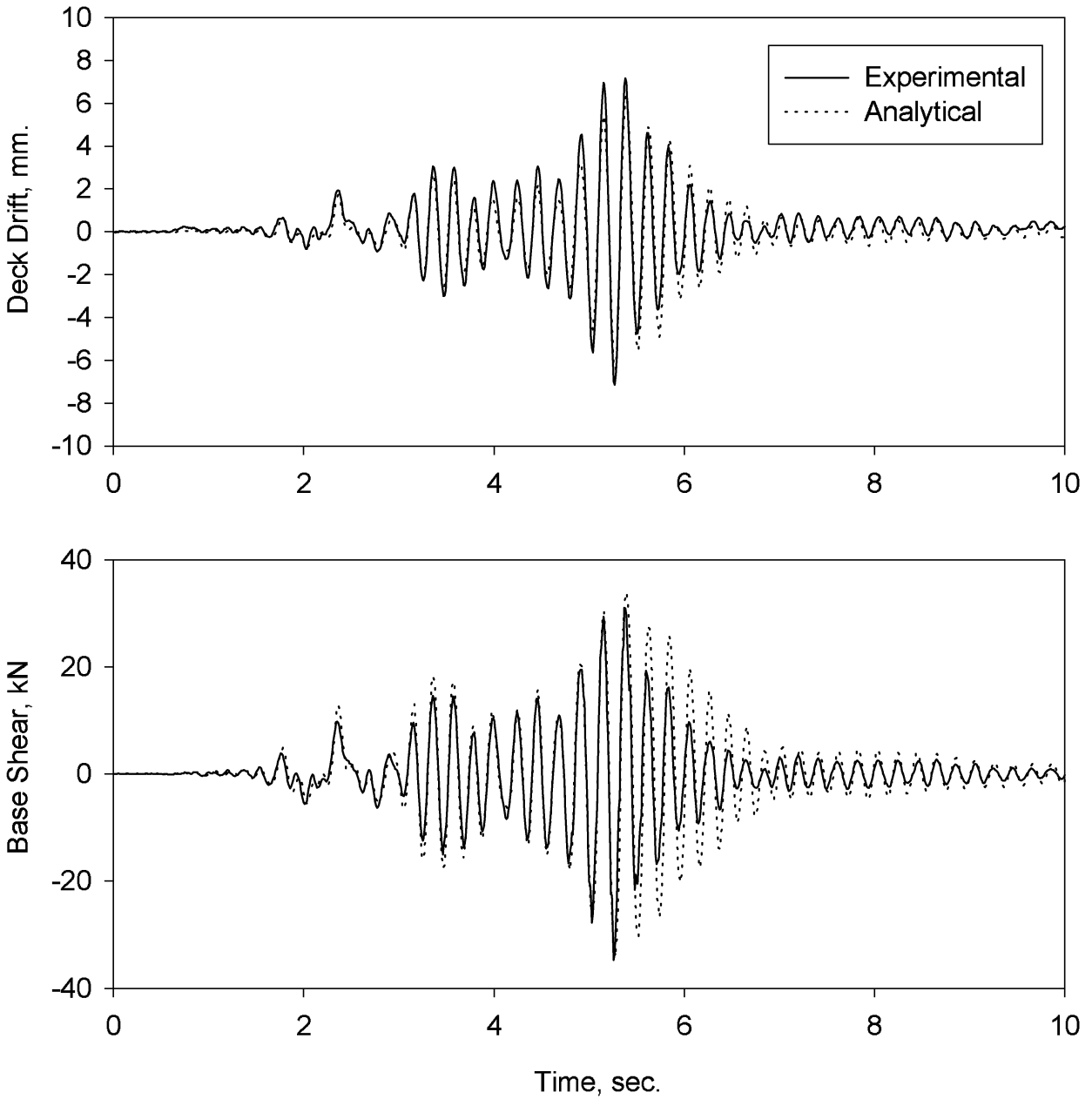

Figure 4-3 Comparison of Experimental and Analytical Results - PARPWB
Ground Motion: Pacoima Dam - PGA=0.252 g
Configuration: SF1 - TO

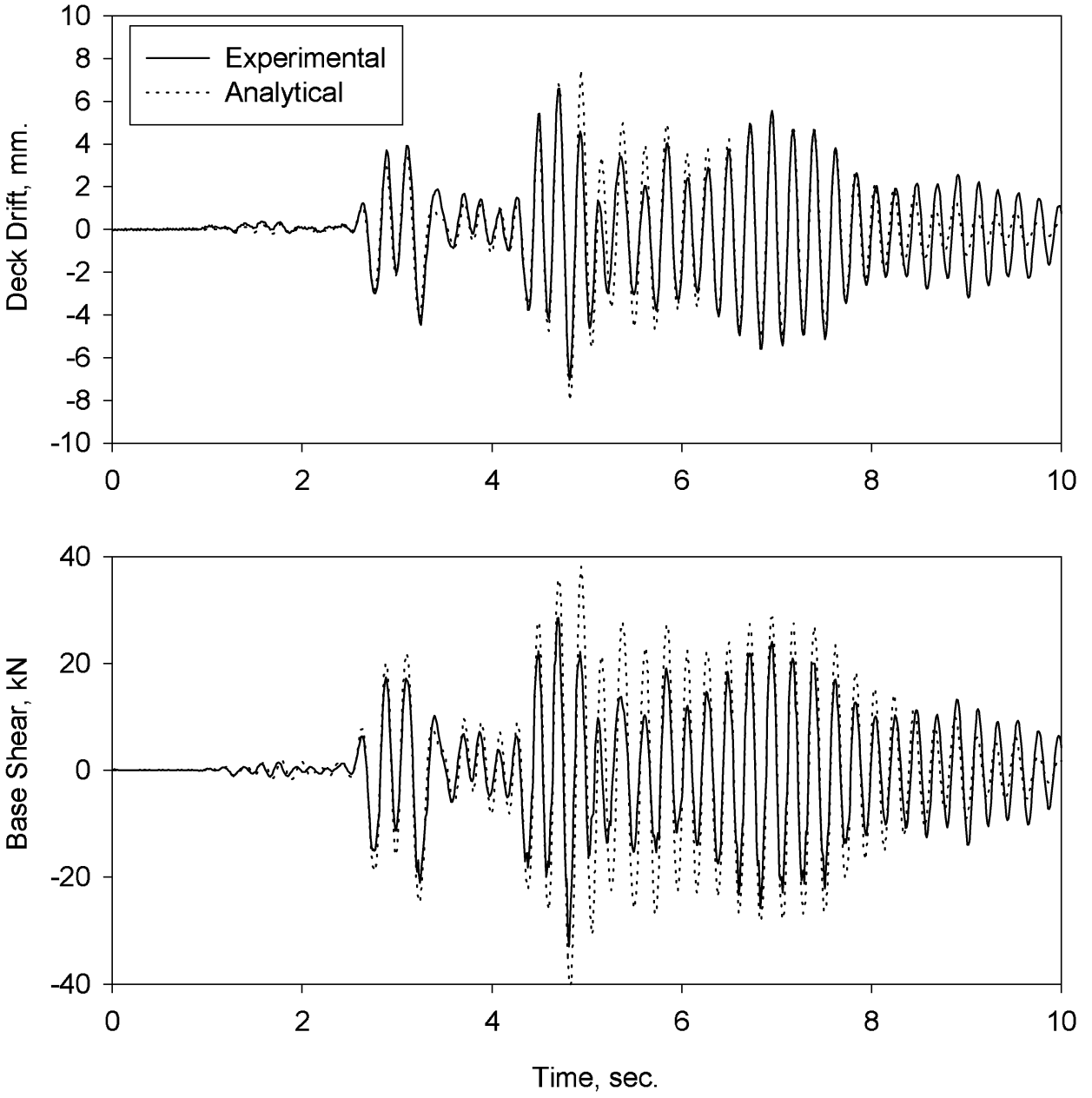

Figure 4-4 Comparison of Experimental and Analytical Results - KOPRWB
Ground Motion: Kobe - PGA=0.272 g
Configuration: SF1 - TO

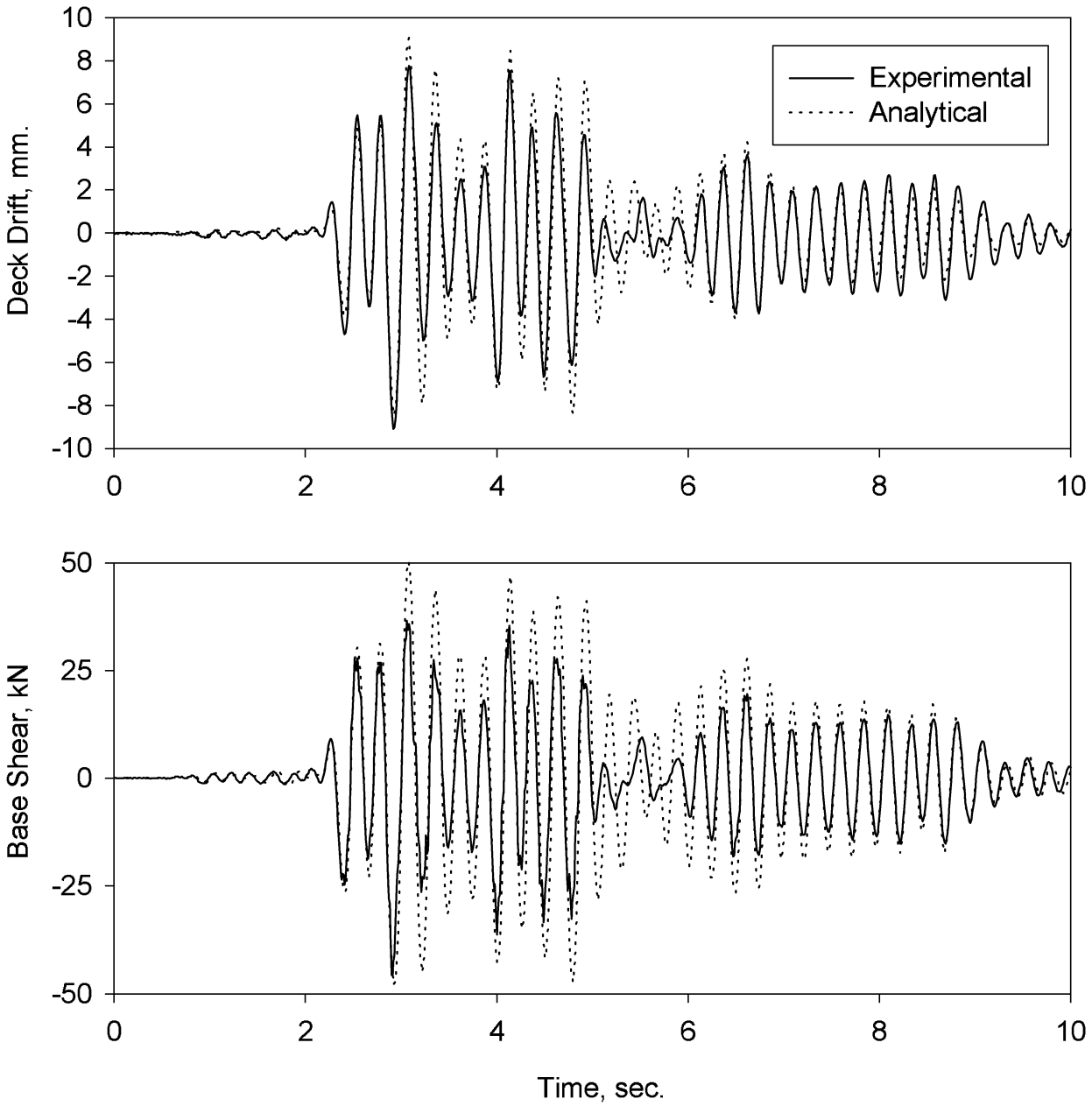

Figure 4-5 Comparison of Experimental and Analytical Results - K2PRWB
Ground Motion: Kobe - PGA=0.291 g
Configuration: SF2 - TO

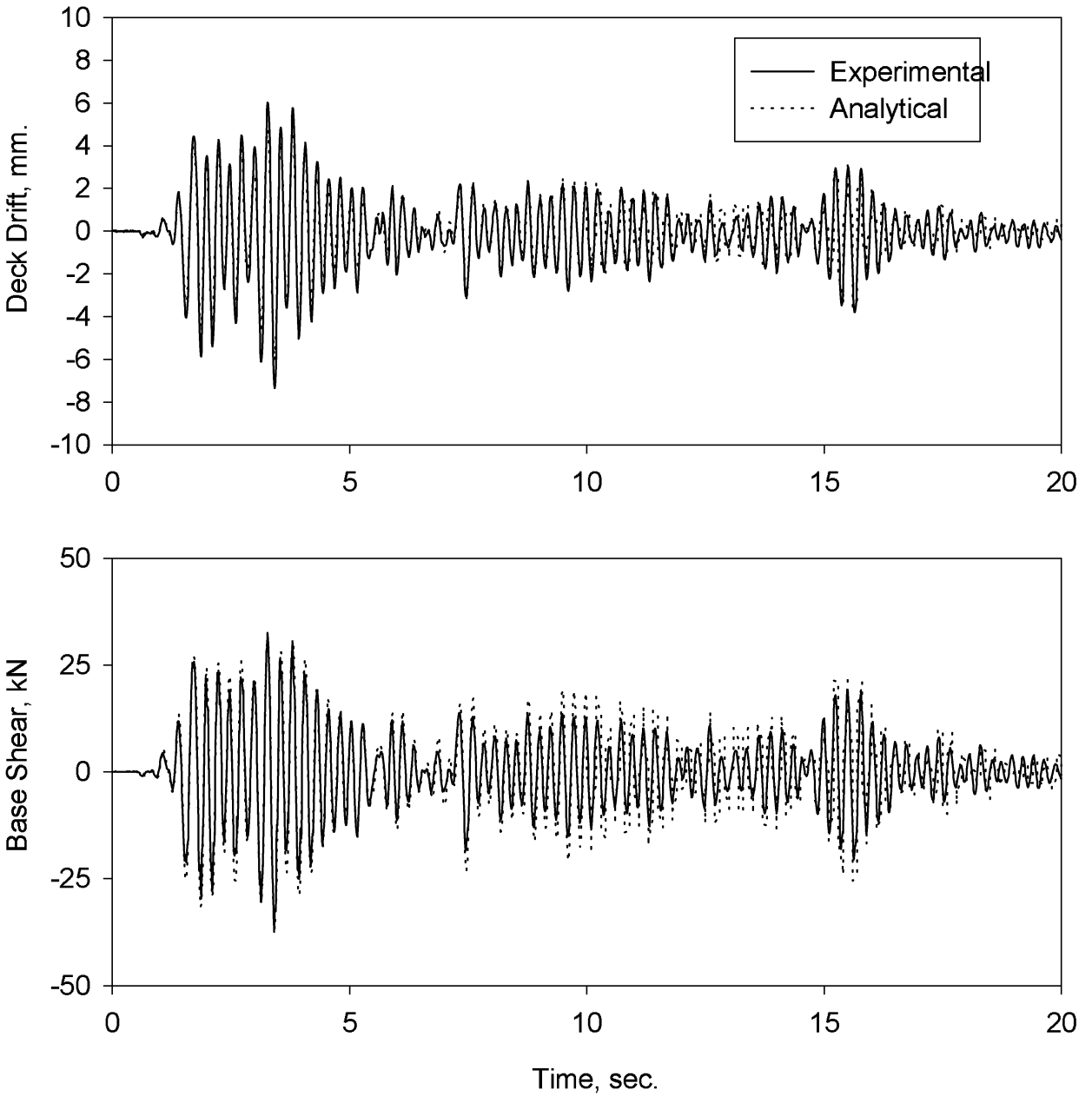

Figure 4-6 Comparison of Experimental and Analytical Results - E2PRWB
Ground Motion: El Centro - PGA=0.286
Configuration: SF2 - TO

etc.). Consequently, analytical predictions presented in the following pages represent the response when/if ideally identical fuse-bars and tendons were used.

4.3.1 Experiments with TO Configuration

A total of ten simulated ground motion experiments were conducted on SF1 and SF2 systems (five on each) with the tendon-only (TO) configuration at moderate levels of acceleration (~0.25 g). The tendons were initially prestressed to approximately 25% of the total structural weight in each direction. No prestress loss was observed during consecutive experiments. Experimentally observed and analytically obtained deck drift and base shear are compared for selected experiments in figures 4-3 through 4-6. Good agreement between the experimental and analytical results can be observed.

The TO configuration in this form (figure 2-3a) was intended to represent the conventional end-sway frame with the exception that the diagonal truss (tendon) members are not allowed to buckle. As can be seen in tables 4-2 and 4-3, the accelerations were amplified by a factor of 2 to 2.5 at the deck level. Therefore, high inertia forces were transferred to the supporting bearings by the tendon elements. The peak relative deck displacements were kept below 10 mm in all cases.

4.3.2 Experiments with TD Configuration

A total of 10 simulated ground motion experiments were conducted on SF1 system retrofitted with the damper-tendon (TD) configuration. The tendons were initially prestressed approximately to the preload level (P_y) of the dampers in each direction. After the first five experiments which were conducted at moderate levels of accelerations, the prestress level was reduced approximately to 75% of the damper preload. Five experiments were then conducted using the same set of ground motions at slightly higher acceleration levels. Similar experiments (total of five) were also conducted on SF2 system in which the tendons were prestressed to P_y. No prestress loss was observed during the consecutive experiments. The level of initial prestress did not have an apparent effect on the overall structural response. As can be seen in table 4-2, El Centro experiments had comparable peak ground accelerations (ELPRDA – 0.241 g and ELPRDB – 0.285 g) for which the maximum responses were also comparable.

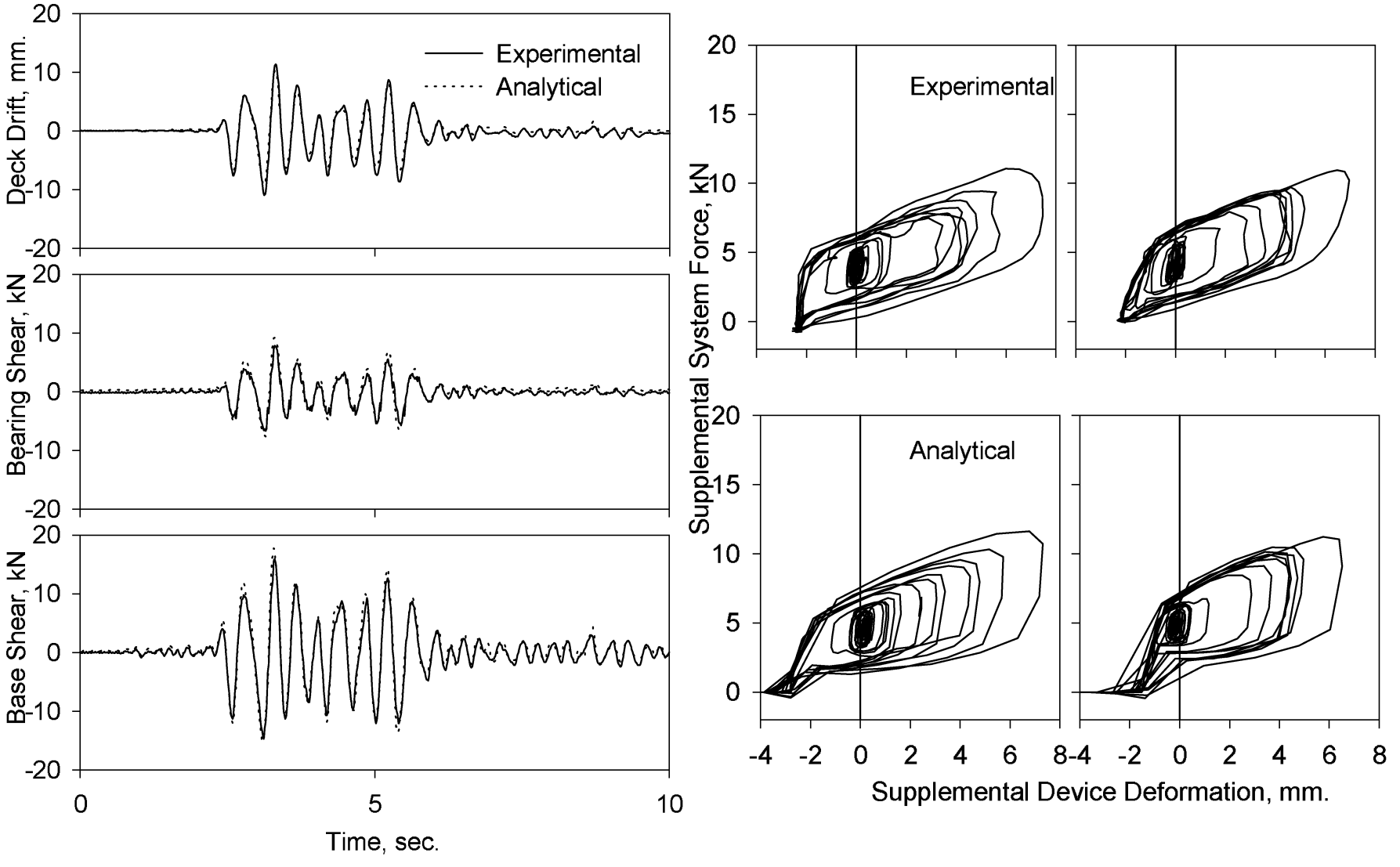

Figure 4-7 Comparison of Experimental and Analytical Results - KOPRDA
Ground Motion: Kobe - PGA=0.270 g
Configuration: SF1 - TD

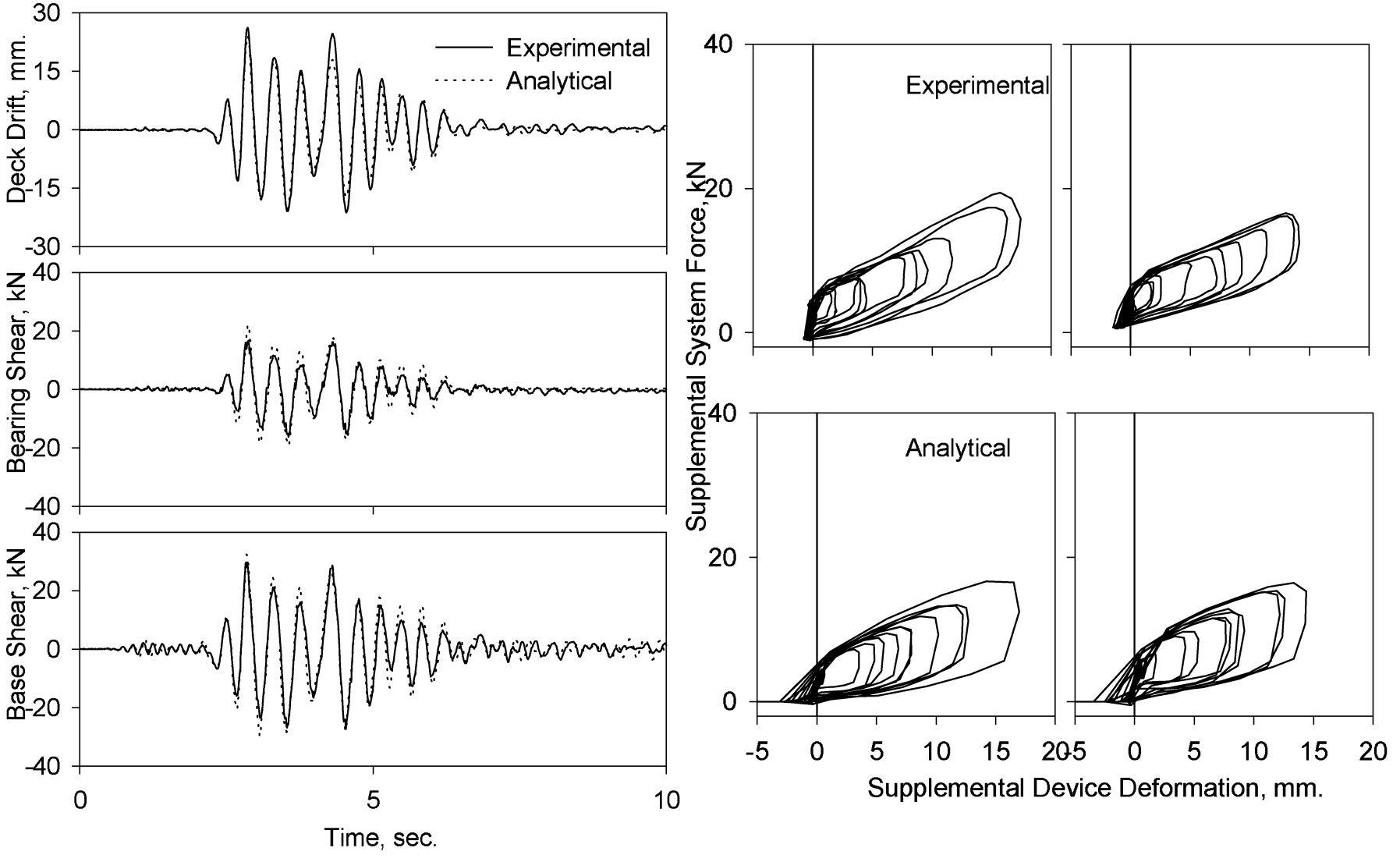

Figure 4-8 Comparison of Experimental and Analytical Results - SYPRDB
Ground Motion: Sylmar - PGA=0.503 g
Configuration: SF1 - TD

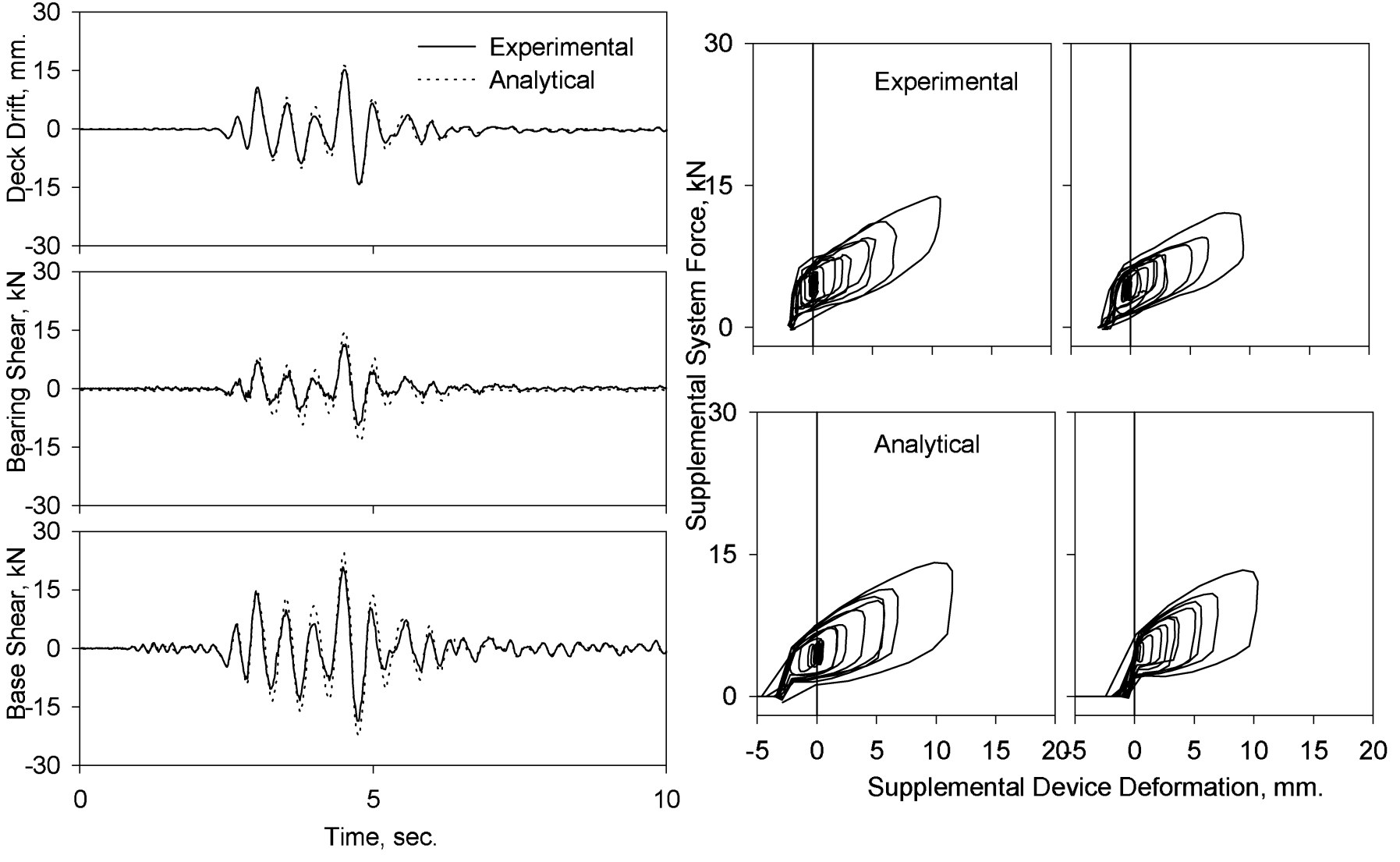

Figure 4-9 Comparison of Experimental and Analytical Results - S2PRDA
Ground Motion: Sylmar - PGA=0.255 g
Configuration: SF2 - TD

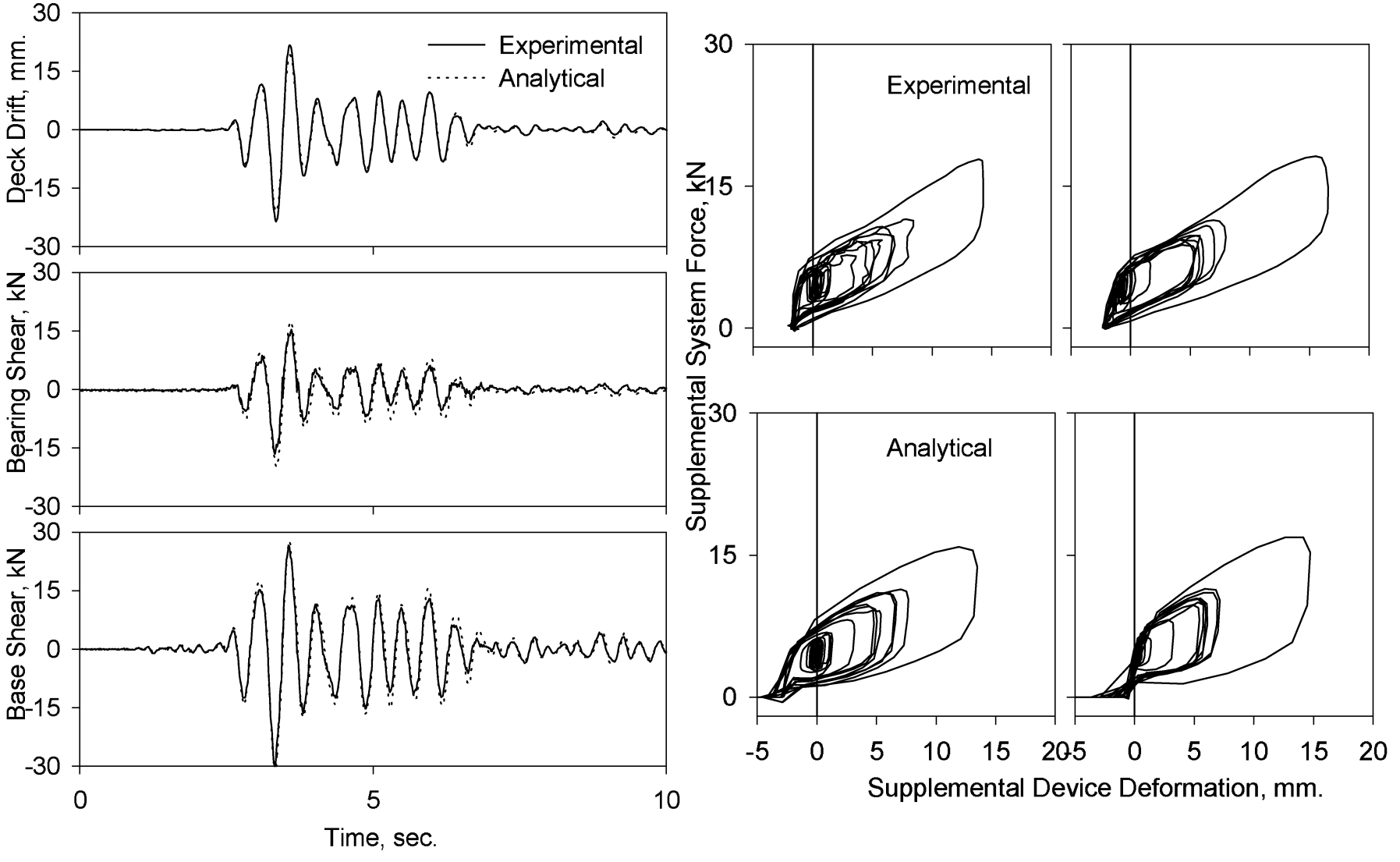

Figure 4-10 Comparison of Experimental and Analytical Results - K2PRDA
Ground Motion: Kobe - PGA=0.258
Configuration: SF2 - TD

As was mentioned previously, both SF1 and SF2 systems were more flexible when retrofitted with the TD configurations, compared to TO and TFD configurations. Hence, higher displacement demands were obtained as can be seen in tables 4-2 and 4-3. However, maximum ground accelerations were amplified (in some cases de-amplified; Pacoima Dam and Sylmar) only by a factor of 1.5. Moreover, it can be concluded from the figures of Appendix A that inertia forces were ideally transferred to the table platform by-passing the supporting bearings. Experimentally observed and analytically obtained deck drift, total base shear and bearing shear as well as supplemental system response are compared in figures 4-7 through 4-10 for selected experiments. Note that in general, good agreement between the experimental and analytical results is evident.

4.3.3 Experiments with TFD Configuration

A combined total of 27 experiments were conducted on both SF1 and SF2 systems retrofitted with TFD configuration at various ground acceleration levels. Overall results are given in tables 4-2 and 4-3. Experimentally observed and analytically obtained deck drift, total base shear and bearing shear as well as supplemental system response are compared in figures 4-11 through 4-14 for selected experiments. In general, good agreement can be observed in these figures. The reason for the discrepancy between the analytical predictions and the experimental response was noted in the previous paragraphs.

First, SF1 system was retrofitted with relatively weak fuse-bars (F*I*1) installed in parallel to the dampers. Tendons and the supplemental system were initially prestressed such that both dampers and the fuse-bars were stressed up to 25% of their yield capacity (i.e. $0.25P_y$+$0.25F_y$). The structural system was subjected to moderate levels of ground acceleration (ELNDFA … KONDFA). There was no significant prestress loss in the tendon elements. However, the prestress level was restored to desired level after each experiment, when especially one or more fuse-bars yielded. Maximum deck drift was typically kept below 5 mm. during El Centro, Pacoima Dam and Sylmar ground motions. Finally, three fuse-bars on the east frame and only one fuse-bar on the west frame failed during Kobe ground motion. As can be seen in table 4-2 (and also figure A-23 in Appendix A), base shear demand on the supporting bearings was remarkably reduced while keeping the maximum deck drift at 11 mm and 8 mm on the east and west frames, respectively.

A second set of fuse-bars with slightly higher yield force capacity (F*II*1) was installed and the tendons were again prestressed up to 20% of damper preload and fuse-bar yield force combined. Experiments were repeated using the same ground motions at higher acceleration levels (ELPDFA … TAPDFA). It is evident from table 4-2 that maximum deck drift was better controlled at the expense of higher inertia forces compared to the previous experiments. However, the supplemental tendons virtually transferring the inertia forces directly to the table platform, drastically reduced base shear demand on the bearings. Since none of the fuse-bars failed, the same set was used for the two consecutive experiments (PAPDFB and KOPDFB). However, the tendon system was initially prestressed to give P_y+0.25F_y and P_y+0.5F_y conditions, respectively. As can be seen in table 4-2 and in figures A-29 and A-30, maximum deck drift was kept below 10 mm. High inertia forces are evident as the maximum accelerations at the deck level were 0.829 g and 0.883 g for Pacoima Dam and Kobe experiments, respectively. However, base shear demand on the bearings was again markedly reduced. It must be noted that only one of the fuse-bars at each corner of the model failed during KOPDFB experiment. Therefore, deck drift response was still controlled by the stiffness contribution of one fuse-bar.

Next, a new set of fuse-bars (F*II*1) was installed to further investigate the response with different initial prestress levels. Hence, the tendon system was prestressed to give a total force of P_y+0.75F_y. Five experiments were conducted at moderate levels of ground acceleration (except for Taft – TAPDFC, figure 4-13). Recorded maximum responses under comparable levels of ground excitation were also comparable for the TFD configurations tested (table 4-2). Finally, initial prestress level was increased up to P_y+F_y and the system was tested under high acceleration levels. As can be seen in table 4-2 and in figures A-36 through A-38, the performance of the model structure was superior to that for the previous cases tested. The fuse-bars efficiently reduced the deck drift response while the dampers controlled the response after the fuse-bars failed (KOPDFD). Although the inertia forces were high, the base shear demands on the bearings were still remarkably small.

An overview of the experimental response suggests that when the initial prestress level was equal to P_y+0.5F_y or higher, the maximum response was controlled better. This was expected as when the fuse-bars are prestressed close to their yield force capacity, they yield earlier contributing to the energy dissipation. Experiments were conducted on SF2 system and similar observations are made (table 4-3).

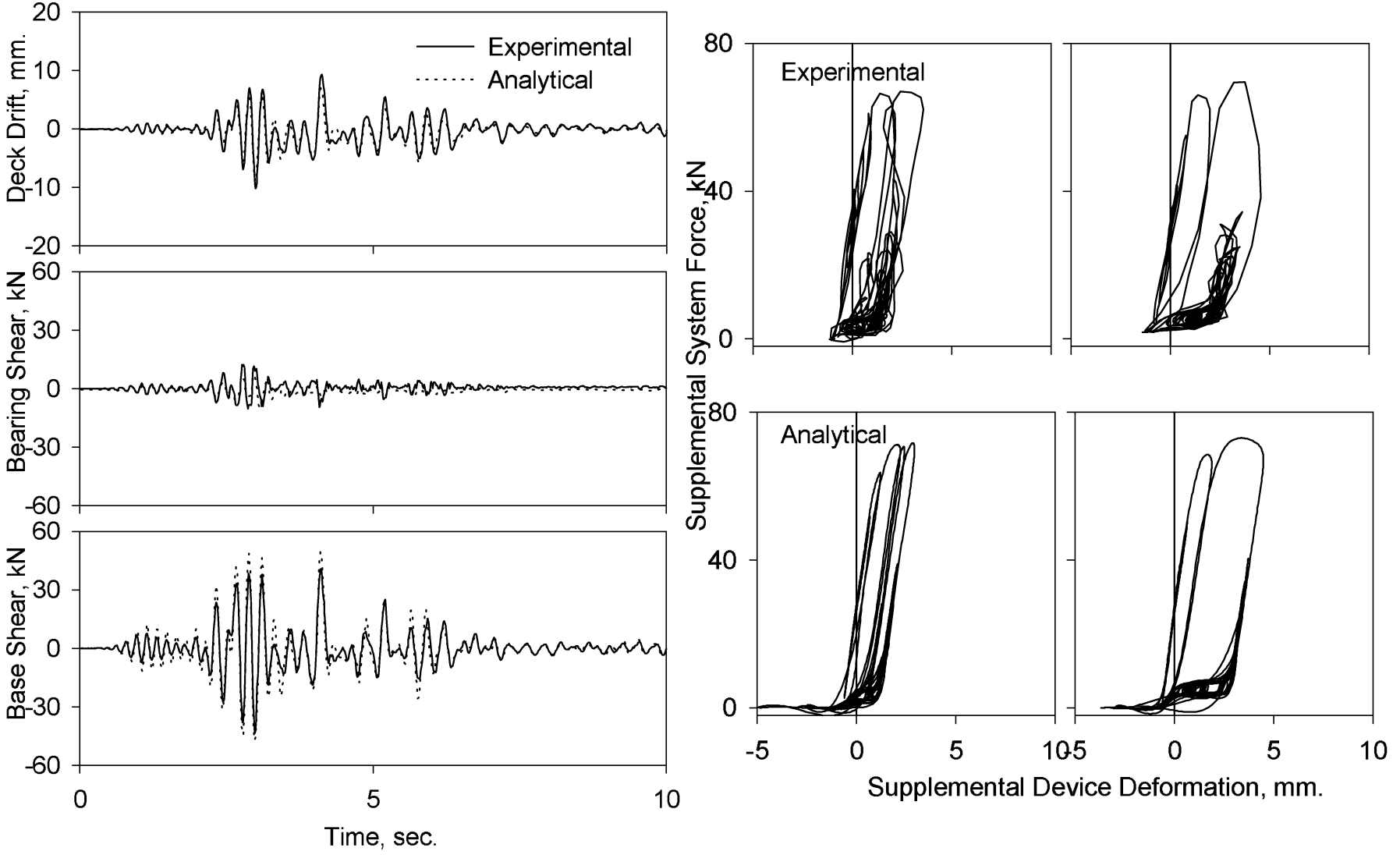

Figure 4-11 Comparison of Experimental and Analytical Results - SYPDFD
Ground Motion: Sylmar - PGA=0.578 g
Configuration: SF1 - TFD

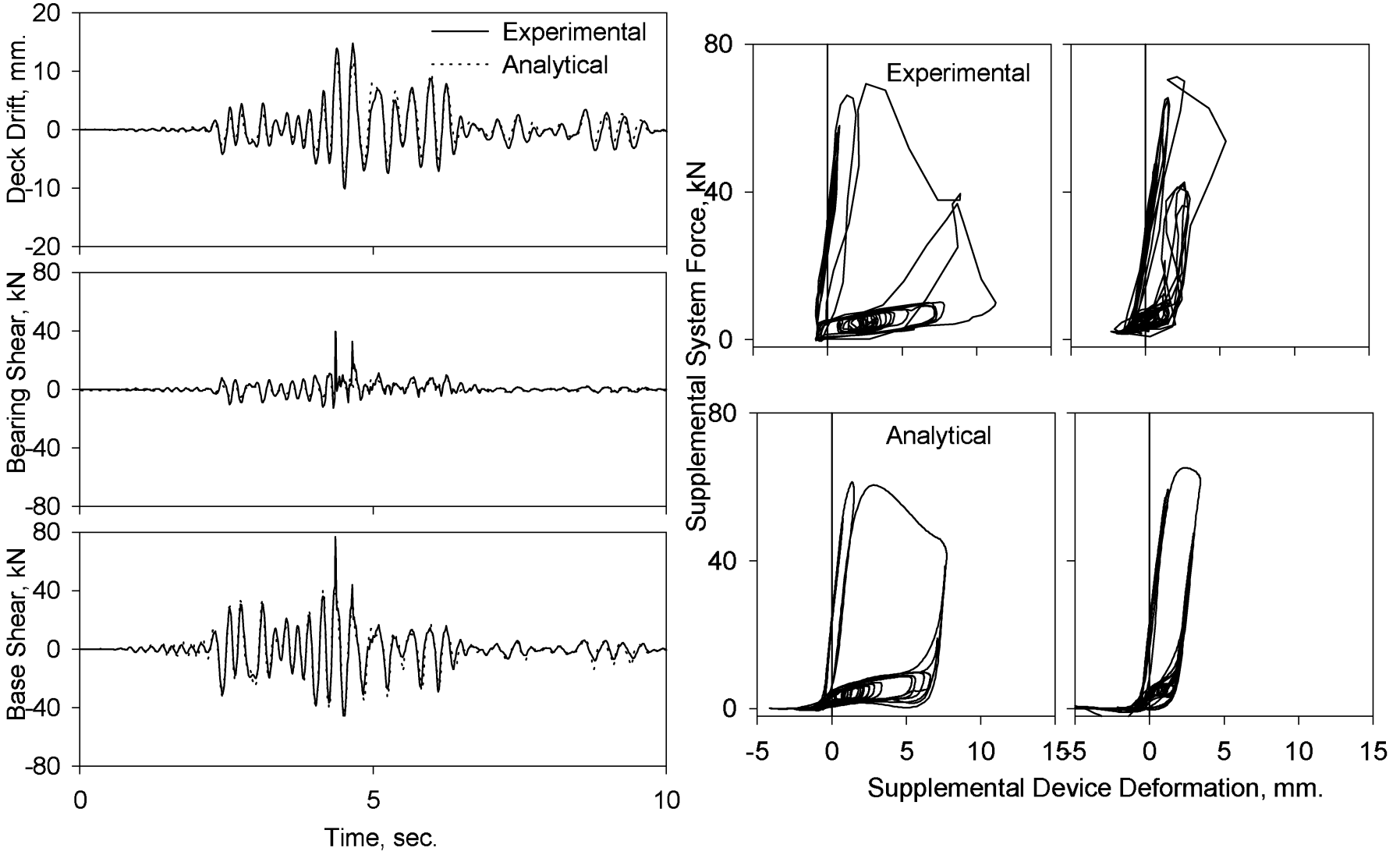

Figure 4-12 Comparison of Experimental and Analytical Results - KOPDFD
Ground Motion: Kobe - PGA=0.521 g
Configuration: SF1 - TFD

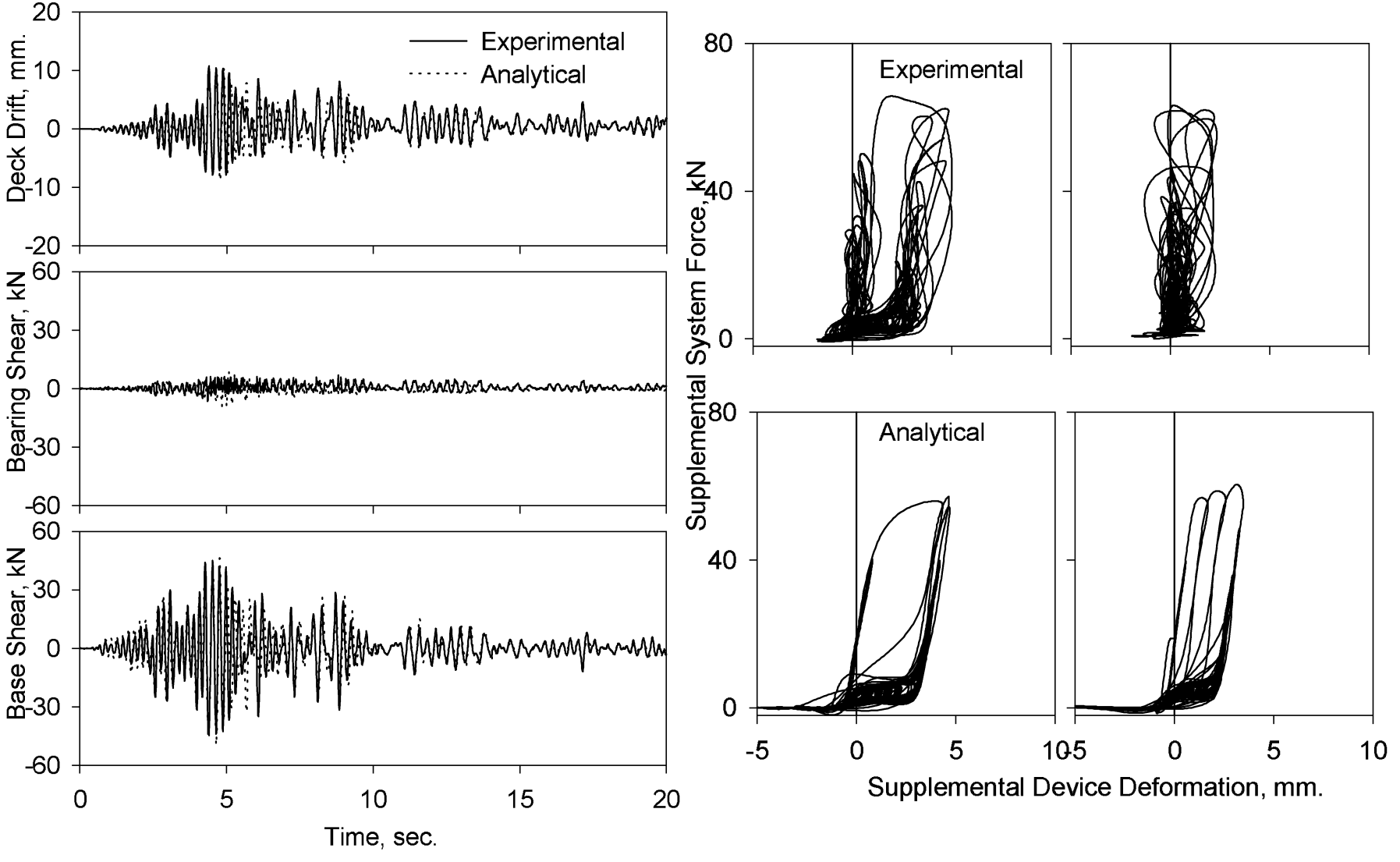

Figure 4-13 Comparison of Experimental and Analytical Results - TAPDFC
Ground Motion: Taft - PGA=0.452 g
Configuration: SF1 - TFD

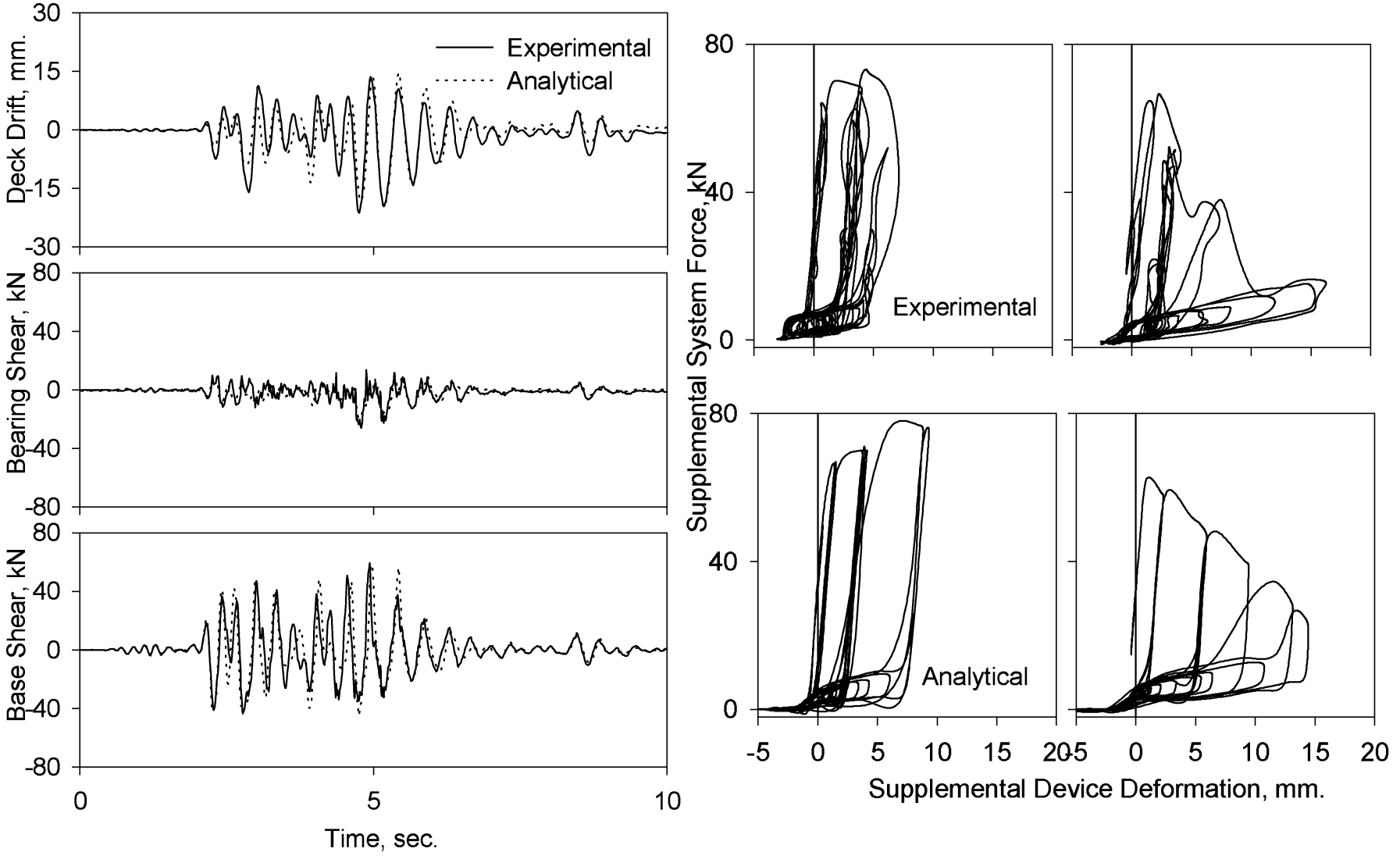

Figure 4-14 Comparison of Experimental and Analytical Results - K2PDFB
Ground Motion: Kobe - PGA=0.499 g
Configuration: SF2 - TFD

4.4 DISCUSSION OF THE EXPERIMENTAL RESULTS AND GENERAL OBSERVATIONS

This subsection provides an overall discussion on the seismic response of the model end-sway frame retrofitted with one of the alternatives introduced in section 2. The effect of various configurations on the behavior of the model structure is discussed with reference to key response parameters; deck drift, base shear, bearing shear, etc. As previously stated, different configurations could not be subjected to identical ground accelerations. Therefore, analytical predictions are used to demonstrate the response behavior of various configurations in comparison, under the same ground motions input. For this purpose, experimental response of the end-sway frame with TFD configuration is taken as basis for the purpose of comparative study. Hence, analytical predictions of TO, TD and TF configurations subjected to Taft (TAPDFC, 0.452 g), Sylmar (SYPDFD, 0.578 g), and Kobe (KOPDFD, 0.521 g) are compared with the corresponding experimental response in TFD configuration.

As was mentioned in section 2, one of the most desirable features of the proposed retrofit alternatives is that the shear demand on the non-ductile steel bearings is reduced very effectively. This was experimentally observed as shown in the figures of Appendix A. Accordingly, recorded maximum shear force on the supporting bearings was only 40 to 80% of the total base shear as the tendons transferred the inertia forces directly to the shaking table platform (pier or abutment in the prototype) through supplemental devices. However, due to the inherent nature of the TO configuration, inertia forces were resisted and transferred by the bearings. It should be noted here that an efficient retrofit should require minimal substructure modifications. It is experimentally shown that this can be achieved by a careful design of TFD system with which the base shear demand on the pier (or abutment) is not increased for the same level of ground motion compared to unretrofitted case (TO). As can be seen in figure A-54 and A-48, recorded maximum base shear for both K2PRWB (TO, PGA=0.291 g) and K2PDFA (TFD, PGA=0.336 g) is about 50 kN. Therefore, no pier or abutment modifications/retrofit will be necessary, as the base shear demand on the substructure does not change (if already not deficient). Moreover, it is clear from the figures that in the former case base shear demand on the bearings is 50 kN whereas this value is only 15 kN in TFD configuration.

In general, maximum deck drift was better controlled by the TFD configuration compared to TD and TO configurations. Evidently, fuse-bars improved the lateral stiffness of

the model structure and arrested excessive deck displacements during the ground excitations. However, accelerations at the deck level (hence inertia forces) were higher compared to that in the TD configurations. This was mainly due to higher lateral stiffness of the model structure with the fuse-bars and lower equivalent viscous damping ratio in the system in TFD configuration (note that supplemental device deformations are much smaller in TFD configuration).

Deck displacement time histories of four different configurations (TFD, TF, TD, and TO) are compared in figures 4-15 through 4-17, and maximum response quantities are summarized in table 4-4. Seismic responses of the model end-sway frame in TF, TD, and TO configurations subjected to experimentally recorded [time-scaled] Taft, Sylmar and Kobe ground motions are analytically determined using the enhanced version of Drain-2DX (Pekcan et al., 1995). Each case is compared with the corresponding experimental response in TFD configuration. Accordingly, prestress levels in TFD configurations in terms of the preload of the damper P_y, and the yield force capacity of the fuse-bars F_y, were P_y+0.75F_y for Taft and P_y+F_y for Sylmar and Kobe ground motion experiments. For the analytical predictions of the system in TD configuration, tendon elements were prestressed up to the preload level of the dampers (P_y = 4.5 kN). Corresponding prestress levels in the tendon elements were 30 kN (15kN+15kN, i.e. two fuse-bars both at their F_y) and 14 kN for TF and TO configurations, respectively. It should be noted here that in modeling the fuse-bars it was assumed that they had enough fuse-length to accommodate the imposed deformation with yielding (hence lengthening) but without fracture.

As can be seen in figures 4-15-4-17 and table 4-4, overall seismic response in terms of both deck displacement and shear forces is controlled very effectively by the TFD configuration. Apparently, the improved lateral stiffness of the frame system due to fuse-bars coupled with the added damping due to dampers is the most desired configuration among various alternatives presented. Although due to higher flexibility of the TD configuration, deck displacements may be higher compared to other cases, base shear demand on the substructure can be considerably less. However, it should be noted that this statement is true only for this specific case as the damper size used in the simulations (as well as in the experiments) was not chosen based on a target response in TD configuration. It is evident that damper devices can be designed and sized to provide the desirable damping, hence desirable performance.

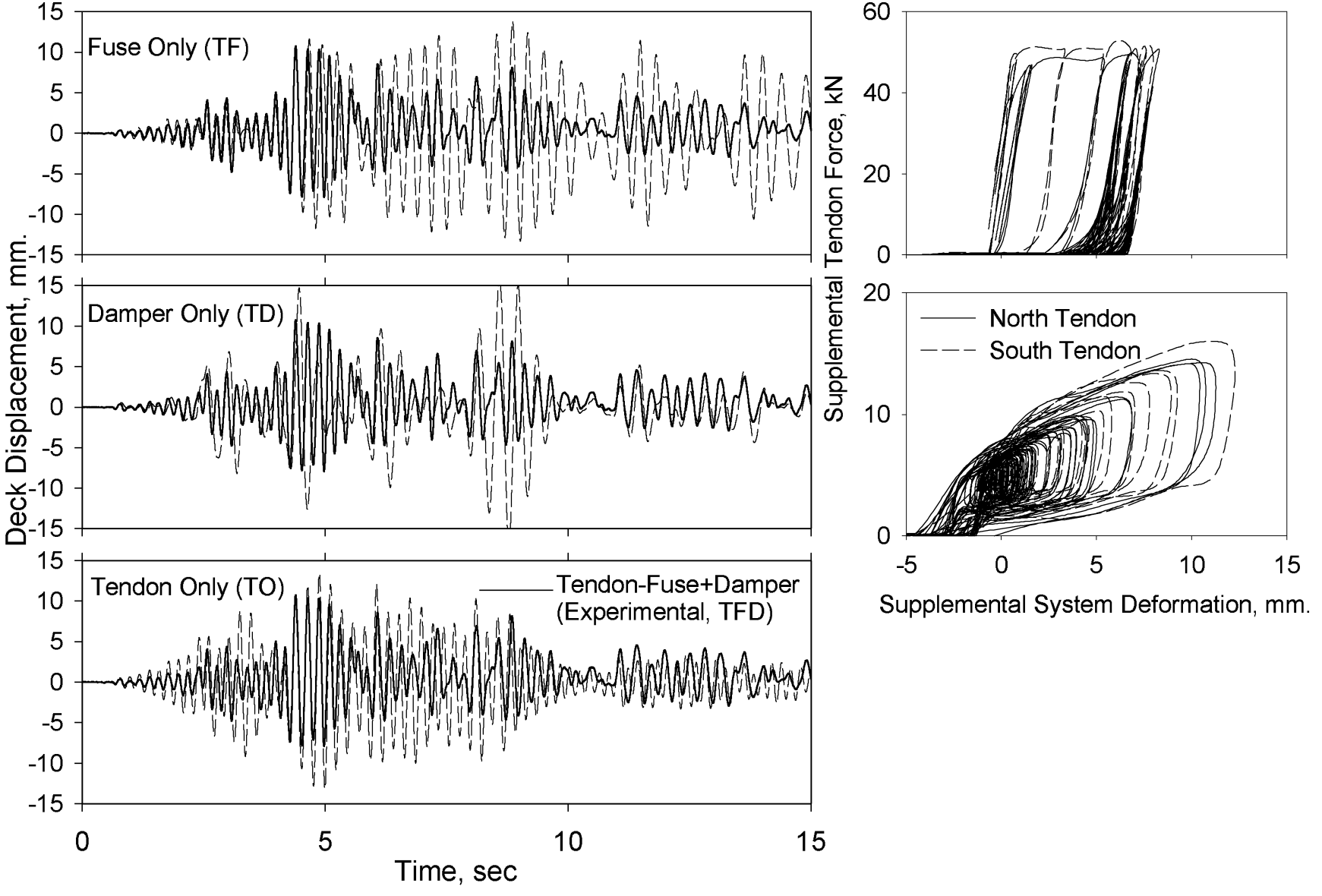

Figure 4-15 Response Comparison of Various Configurations - Taft - PGA = 0.452 g

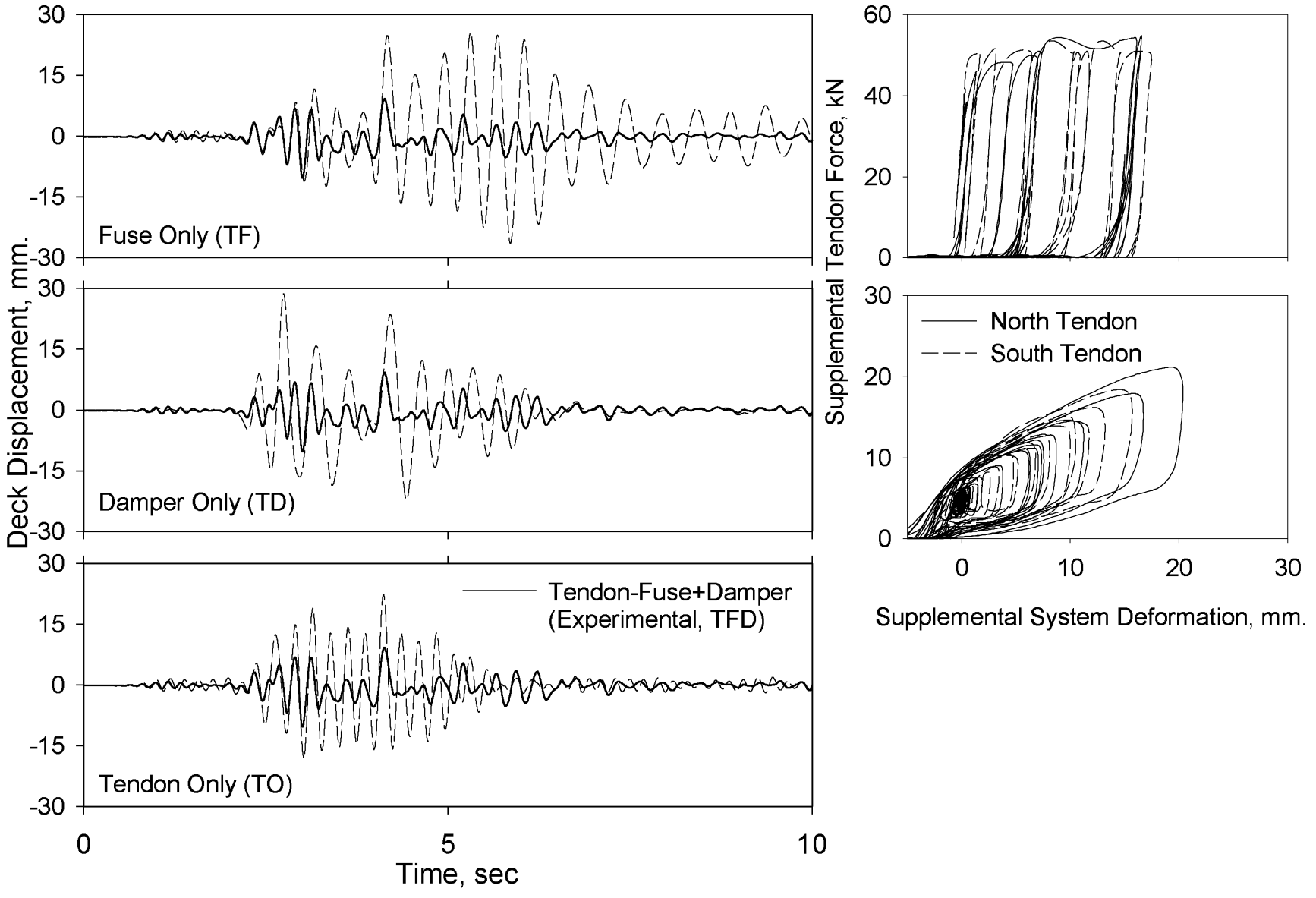

Figure 4-16 Response Comparison of Various Configurations - Sylmar - PGA = 0.578 g

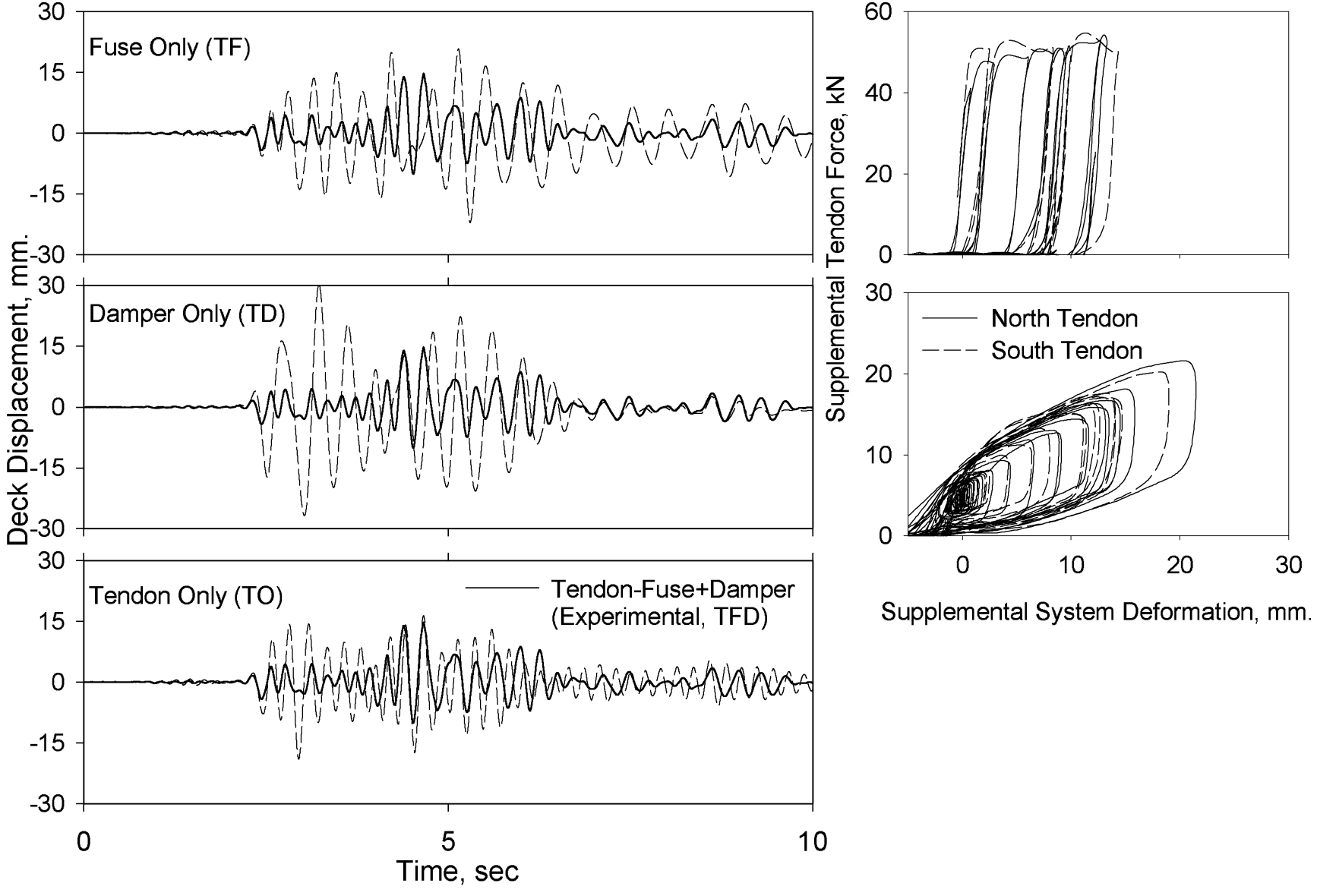

Figure 4-17 Response Comparison of Various Configurations - Kobe - PGA = 0.521 g

Table 4- 4 Maximum Response Comparison of Various Configurations[1]

Ground Motion	Config.	Prestress (kN)	Deck Displ. (mm)	Base Shear (kN)	Bearing Shear (kN)
Taft PGA = 0.452 g	**TFD**	P_y+0.75F_y	11	45.0	7.0
	TF	F_y	14	46.6	12.8
	TD	P_y	20	29.2	20.4
	TO	14.0	14	64.9	64.9
Sylmar PGA = 0.578 g	**TFD**	P_y+F_y	10	45.0	11.0
	TF	F_y	26	60.7	24.3
	TD	P_y	30	40.9	27.6
	TO	14.0	18	83.1	83.1
Kobe PGA = 0.521 g	**TFD**	P_y+F_y	15	74.0	38.0
	TF	F_y	22	53.4	19.1
	TD	P_y	31	43.2	29.4
	TO	14.0	24	109.2	109.2

[1] Experimental results for TFD configurations and corresponding analytical results for TF, TD and TO configurations are reported

4.5 SUMMARY AND CONCLUSIONS

Shaking table tests were conducted on a 1/3 scale model of a steel sway frame of a prototype deck-truss bridge with and without supplemental devices. An enhanced version of the non-linear time history analysis program DRAIN-2DX was used to analytically compare the predicted response with the experimental behavior of the structure. The analytical predictions compared well with the experimental results. The efficacy of a practical and accurate analytical tool is thought to be encouraging for future analytical-parametric studies as well as for design verification studies.

One of the major objectives of performing this experimental study was to investigate the effectiveness of an innovative supplemental *tendon-fuse+damper* system in reducing the seismic response of deck-truss bridge structures under recorded ground motion excitations. The computational model was used to predict the response of the model structure at PGA levels to which the structure could not be subjected to in following configurations; damper devices only (TD), fuse-bars only (TF) and tendon only (TO). These predictions were compared to experimental response of the structure with the *tendon-fuse+damper* (TFD) system.

Among the parameters investigated that have primary effect on the overall response are: a) bracings, b) elastomeric spring damper devices alone (TD), c) *fuse+damper* system (TFD), d) tension only system (TO) and, e) prestress level in the supplemental tendons.

Based on the experimental and analytical results reported in the previous sections, the following conclusions are drawn:

1. *Tendon-fuse+damper* (TFD) system reduced the overall seismic response of the model structure to a lower value than the other two systems.
2. Added damping by the supplemental system in the TFD system was small mainly because of the relatively small deformations in the supplemental system. However, it is well known that high damping does not always mean improved response. In fact, for flexible structures even small amounts of added damping can reduce the structural response to acceptable limits.
3. Tension-only working tendon systems may be criticized as follows. When the tension is applied in later loading cycles (when the tendons are slack due to fuse yielding) the loading may be applied abruptly and may cause high accelerations through the height of the structure. A further concern is that the structure lacks redundancy. These drawbacks of tension-only systems can be overcome by prestressing the supplemental system together with the steel tendon. Depending on the initial prestress level, prestress helps delay, if not outright prevent, the systems' becoming slack. Thus, initial prestressing would eliminate, or at least significantly reduce the problems associated with the sudden loading of the supplemental system, as long as there is no appreciable creep or relaxation in the system.
4. Fuse-bars were very effective in reducing the peak response at least to a level where the unretrofitted structure responded at 2-3 times lower PGA inputs. As can be seen from the experimental results, fuse-bars yielded at high deformations reducing the amount of [initial] prestress in the system. However, it does not necessarily lead to the total loss of the prestress. Therefore, fuse-bars can be allowed to yield without completely losing the prestress force. In such cases, ESD devices (with preload) act as a backup system and lock the prestress. This is consistent with the experimental observations as no prestress losses were recorded during the shaking table experiments. No apparent effect of initial prestress level on the overall response was observed.

5. It was experimentally and analytically shown that the supplemental system can be designed to provide comparable or higher lateral stiffness than the unretrofitted structure. The desired effects could be observed in term of reduced deck drift and base shear response due to added damping and remarkably reduced bearing shear response mainly due to altered load path.
6. Unequal prestress in the tendons on either side of the sway frame structure resulted in negligible torsional response of the structure.

SECTION 5

SUMMARY, CONCLUSIONS AND FUTURE RESEARCH RECOMMENDATIONS

5.1 SUMMARY

A new and efficient retrofit alternative for reducing the effects of seismically induced lateral loads on the end-sway frames of steel deck-truss bridges and their supporting non-ductile steel bearings was proposed. The proposed system consists of post-tensioned tension elements - referred to as *tendon* - with or without supplemental devices that are connected in series to the tendon. The supplemental system consists of energy dissipators (dampers, preferably with a preload capability) and sacrificial fuse elements (fuse-bars) with a prescribed initial stiffness and displacement ductility. This supplemental system is designed and detailed to work only in tension and is connected to the deck at the upper end and anchored to the pier cap or abutment at the lower end. The main load path within the end-sway frame is therefore altered to bypass the seismically vulnerable, non-ductile steel bearings. Therefore, it is believed that expensive bearing retrofit can be avoided by the installation of the proposed alternatives.

In its most basic form, tendon elements are designed to replace the existing braces to provide either comparable or improved lateral stiffness and strength. This is referred to as *tendon-only (TO) system*. In the experimental study, this configuration is used to form the basis for comparison with the other two configurations. To achieve a desired load path, however, it is proposed that the tendons be used to replace the existing braces and anchored to the pier/abutment bypassing the seismically vulnerable – nonductile steel bearings. The main advantage of TO alternative in this form is that i) consequence of buckling of the brace elements are avoided using a tension-only system, and ii) inertia forces are directly transferred to the substructure bypassing the existing steel bearings.

Several improved configurations were then introduced with the addition of sacrificial fuse elements (*tendon-fuse system, TF*). It was shown that the fuse elements could be designed to accommodate desired levels of deformation and forces and to improve the overall response characteristics of the end-sway frames provided that certain strength and stiffness characteristics are met. Therefore certain limits on the cross-sectional area of the sacrificial fuse elements as well as fuse length were specified. Finally, another enhancement over the TO and TF systems

was introduced in which supplemental energy dissipation devices were used in parallel to the fuse elements in TF configuration to provide damping hence to reduce the seismic demand (*tendon-fuse-damper system, TFD*).

It was noted that the supplemental tendon system would ideally be initially prestressed up to a prescribed level to avoid the system becoming slack and to provide a better energy dissipation mechanism in case of TF alternative. Therefore, an important parameter involved in the design of the proposed systems is the level of prestressing force initially applied to the tendon system with or without the supplemental elements. When dampers are used in TFD alternative, it is required that these devices are preloaded in order to accommodate the applied prestressing forces.

All of the above mentioned alternatives were experimentally investigated on a one-third scale model of a prototype end-sway frame of an existing deck-truss bridge. Several types of fuse elements with different stress-strain properties and one type of elastomeric spring damper (ESD) were tested with different prestress levels. The test structure with various configurations was subjected to five different ground motions at various peak ground acceleration (PGA) levels. These included i) 1952 Kern County - Taft N21E, ii) 1940 Imperial Valley - El Centro NS, iii) 1971 San Fernando - Pacoima S16E, iv) 1994 Northridge - Sylmar County 90°, and v) 1995 Great Hanshin - Kobe NS.

5.2 CONCLUSIONS

Based on the experimental and analytical results, following conclusions are drawn:

1. *Tendon-fuse+damper* (TFD) system reduced the overall seismic response of the model structure. High initial stiffness is also considered beneficial under low levels of ground motions as well as wind loading. In fact, stiffening of the sway frame leads to further reduction of deformations but at the expense of increased acceleration response. Improved response due to presence of sacrificial fuse-bars was evident compared to damper-only tendon system. High initial stiffness of the fuse-bars provided increased capacity while at larger deformations damping due to yielding was supplemented by the dampers hence reduced the response.
2. Added damping by the supplemental system in the TFD system was small mainly because of the relatively small deformations in the supplemental system. However, it is well known that

high damping does not always mean improved response. In fact, for flexible structures even small amounts of added damping can reduce the structural response to acceptable limits.

3. Tension-only working tendon systems may be criticized as follows. When the tension is applied in later loading cycles (when the tendons are slack due to fuse yielding) the loading may be applied abruptly and may cause high accelerations through the height of the structure. A further concern is that the structure lacks redundancy. These drawbacks of tension-only systems can be overcome by prestressing the supplemental system together with the steel tendon. Depending on the initial prestress level, prestress helps delay, if not outright prevent, the systems' becoming slack. Thus, initial prestressing would eliminate, or at least significantly reduce the problems associated with the sudden loading of the supplemental system, as long as there is no appreciable creep or relaxation in the system. No apparent effect of initial prestress level was observed.
4. Fuse-bars were very effective in reducing the peak response at least to a level where the original structure responded at 2-3 times lower PGA inputs. As can be seen from the experimental results, fuse-bars yielded at high deformations. It is a common understanding that yielding in tension reduces the amount of initial prestress in the system. However, it does not necessarily lead to the total loss of the prestress. Therefore, fuse-bars can be allowed to yield without completely losing the prestress force. In such cases, ESD devices act as a backup system and lock the prestress. This is consistent with the experimental observations as no prestress losses were recorded during the shaking table experiments.
5. It was experimentally and analytically shown that the supplemental system can be designed to provide comparable or better lateral stiffness as the unretrofitted structure. The desired effects could be observed in term of reduced deck drift and base shear response due to added damping and remarkably reduced bearing shear response mainly due to altered load path.
6. Flexibility of the prestressed tendon and its anchorages should be carefully considered in the design of such systems since it has a direct effect on the effectiveness of the supplemental system.
7. Unequal prestress in the tendons on either side of the sway frame structure must be kept at minimum since this may cause undesirable torsional response of the structure.

5.3 RECOMMENDATIONS FOR FUTURE RESEARCH

1. Both the experimental and the analytical studies reported herein suggest that the tension only tendon system is a promising and potentially more economical retrofit and design alternative in reducing the seismic response of deck-truss bridges (compared to other available alternatives). However, it must be noted that overall seismic retrofit strategy deals with the retrofit of end-sway frames, hence it is assumed that necessary precautions are taken with respect to other critical details and members such as truss connections, critical truss members on the intermediate sway frames, and top and bottom lateral bracings. Therefore, more comprehensive analytical models; three-dimensional or simplified two-dimensional that can capture the lateral transverse response of the actual structure, should be developed. These models may be utilized with simplified design procedures and allow detailed evaluation of deck-truss bridges and its structural elements.

2. Linear elastic analysis and design methods are in general not permitted nor appropriate for inelastic structures with or without supplemental damping systems. A significant departure from linear elastic analysis has been the adoption of nonlinear methods of analysis over the last decade. Dramatic advancements in the development of computational tools have made nonlinear time history analysis methods easily accessible to the practicing engineers. This took place almost concurrently with the establishment of the capacity design principles as the preferred design methodology.

   The capacity spectrum method has been becoming the preferred method used for the design and retrofit of structures. It estimates the peak response by expressing both the structural capacity and seismic demand in terms of spectral accelerations and displacements. The response of a nonlinear structure can be estimated graphically as the point where the capacity curve of the structure intersects the elastic demand curve that corresponds to the available damping in the structural system. Hence, one of the steps in capacity spectrum method is the determination of the pushover capacity of the structural system via pushover analysis.

   Due to its simplicity and ability to represent response beyond elastic limits, it is believed that capacity spectrum method is most suitable for design and retrofit methodologies with especially supplemental damping systems. Therefore, further experimental and analytical

studies are necessary in order to establish dependable guidelines for the application of this method by practicing engineers to the design and retrofit of deck-truss bridges.

3. Deck-truss bridges are generally long-span bridges which are characterized as being important structures on long established roadways that have become vital links as part of the Nations' lifelines. As previously mentioned, these bridges are considered to be seismically vulnerable and require some type of retrofit for their continuing function after an earthquake. Since very limited information is available concerning evaluating the seismic vulnerability or retrofitting of these bridges, they are evaluated on a case-by-case basis. It is therefore recognized that unified seismic evaluation and retrofit guidelines as well as cost-effective retrofit measures are needed for long span bridges in general. For this purpose, one should consider all available retrofit alternatives including conventional, protective systems, etc., and categorize them with respect to their key functions.

SECTION 6

REFERENCES

Bruneau, M., and Sarraf, M., (1997), "Ductile Seismic Retrofit Solution for Deck Trusses," *Proceedings of the 2nd National Seismic Conference on Bridges and Highways,* CALTRANS and FHWA, Sacramento, California.

Clough, R.W., Penzien, J., (1993), "Dynamics of Structures," McGraw-Hill, Inc., 2nd Edition, New York, USA.

Imbsen, R., and Liu, W. (1993), "Seismic Evaluation of Benicia-Martinez Bridge," *Proceedings of 1st U.S. Seminar on Seismic Evaluation and Retrofit of Steel Bridges*, University of California at Berkeley.

Imbsen, R., Schamer, R., and Davis, G., (1995), "Seismic Retrofit of the North Approach Viaduct of the Golden Gate Bridge," *Proceedings of the 1st National Seismic Conference on Bridges and Highways,* CALTRANS and FHWA, San Diego, California.

Liu, W., Nobari, F., Schamber, A. , and Imbsen, R., (1997), "Performance Based Seismic Retrofit of Benicia-Martinez Bridge," *Proceedings of the 2nd National Seismic Conference on Bridges and Highways,* CALTRANS and FHWA, Sacramento, California.

Matson, D.D., and Buckland, P.G., (1995), "Experience with Seismic Retrofit of Major Bridges," *Proceedings of the 1st National Seismic Conference on Bridges and Highways,* CALTRANS and FHWA, San Diego, California.

Pekcan, G., Mander, J.B., and Chen, S.S., (1995a), " The Seismic Response of a 1:3 Scale R.C. Structure with Elastomeric Spring Dampers," *Earthquake Spectra*, Vol. 11, No.2, pp. 249-267.

Pekcan, G., Mander, J.B., and Chen, S.S., (1995b), " Experimental Performance and Analytical Study of a Non-Ductile Reinforced Concrete Frame Structure Retrofitted with Elastomeric Spring Dampers,". *Technical Report NCEER-95-0010*, National Center for Earthquake Engineering Research, SUNY at Buffalo, July.

Pekcan G., (1998), "Design of Seismic Energy Dissipation Systems for Reinforced Concrete and Steel Structures," *Ph.D. Dissertation*, State University of New York at Buffalo

Pekcan, G., Mander, J.B., and Chen, S.S., (1999), "Experimental Investigation and Computational Modeling of Seismic Response of a 1:4 Scale Model Steel Structure with a Load Balancing Supplemental Damping System," *Technical Report MCEER-99-0006*, Multidisciplinary Center for Earthquake Engineering Research, Buffalo, N.Y.

Pekcan G., Mander, J.B., and Chen, S.S., (2000a), "Experiments on a Steel MRF Building with a Supplemental Tendon System." *Journal of Structural Engineering*, ASCE, Vol. 126, No.4, 437-444.

Pekcan G., Mander, J.B., and Chen, S.S., (2000b), "Balancing Lateral Loads Using Tendon-Based Supplemental Damping System." *Journal of Structural Engineering*, ASCE, Vol. 126, No.8.

Prakash, V., Powell, G.H., and Filippou, F.C., (1992), "Drain-2DX: Base Program User Guide," *Report No. UCB/SEMM-92/29*, University of California at Berkeley, December.

Sarraf, M., and Bruneau, M., (1998a), "Ductile Seismic Retrofit of Steel Deck-Truss Bridges. I: Strategy and Modeling," *Journal of Structural Engineering, ASCE,* Vol. 124, No. 11, pp. 1253-1262.

Sarraf, M., and Bruneau, M., (1998b), "Ductile Seismic Retrofit of Steel Deck-Truss Bridges. II: Design Applications," *Journal of Structural Engineering, ASCE,* Vol. 124, No. 11, pp. 1263-1271.

Shama, A., (1999), "Seismic Evaluation Of A Cantilever Truss Bridge," *Master Thesis*, State University of New York at Buffalo.

Skinner, R.I., Robinson, W.H., and McVerry, G.H., (1993), "An Introduction To Seismic Isolation," Wiley, New York.

Soong, T.T., and Dargush, G.F., (1993), "Passive Energy Dissipation Systems In Structural Engineering," Wiley, New York, USA.

Ye, Q., (1998), "Computational Modeling Of Spring Dampers And The Seismic Retrofit Of Sway Frames," *Master Thesis*, State University of New York at Buffalo.

APPENDIX

DETAILED EXPERIMENTAL RESULTS

This appendix presents the experimental results that are listed in tables 4-2 and 4-3. The appendix contains one page of graphs; for each of the tests following graphs are presented:

1. Time history of displacement at the deck level relative to shaking table for the east and west frames.
2. Time history of bearing shear for the east and west frames.
3. Base shear vs. Deck drift plots for the east and west frames.
4. Tendon force vs. Supplemental system deformation plots for east and west frames.

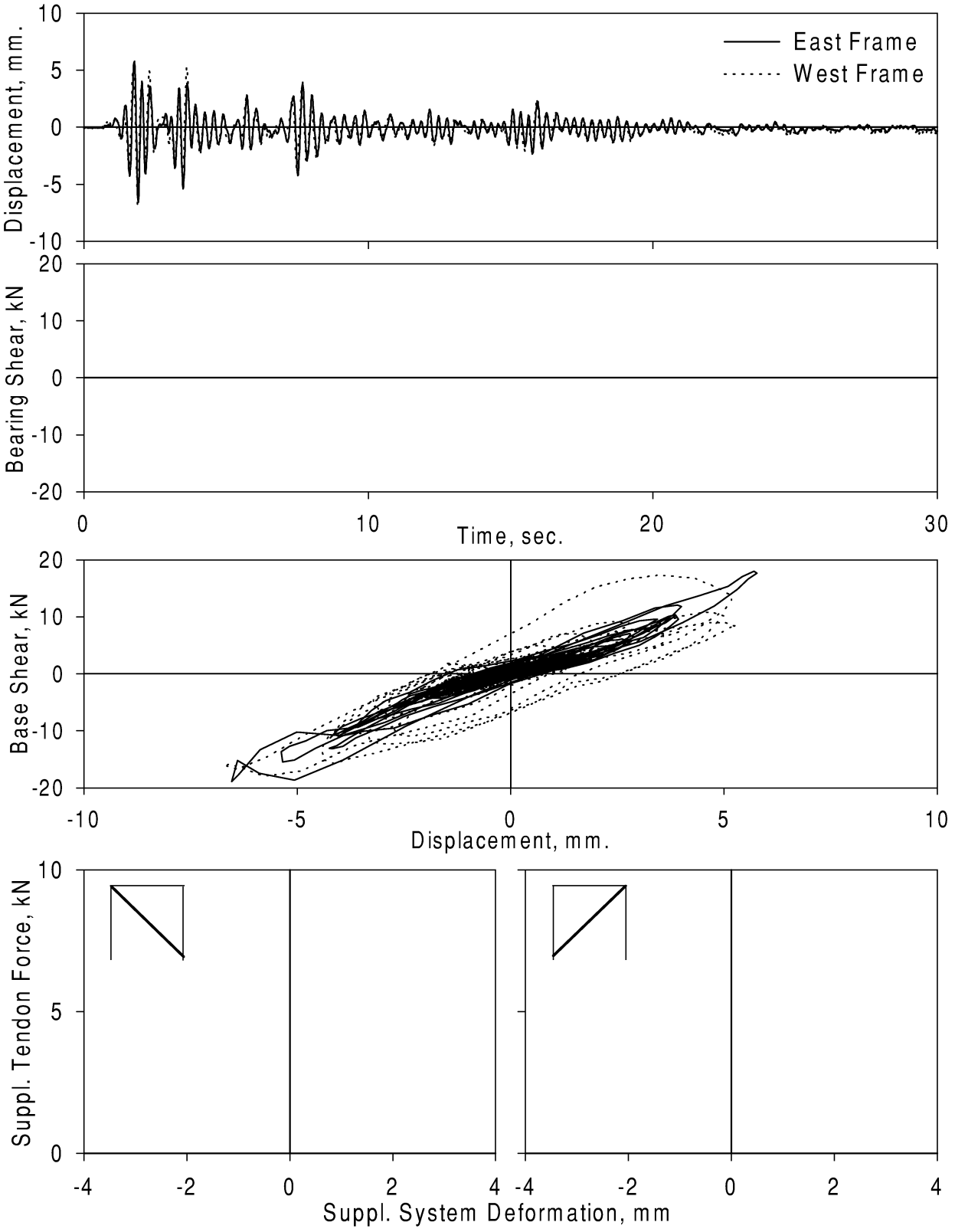

Figure A-1. Experimental Results - ELPRWA
Ground Motion: El Centro (PGA=0.205 g)
Configuration: w/Tendons (Bracing)

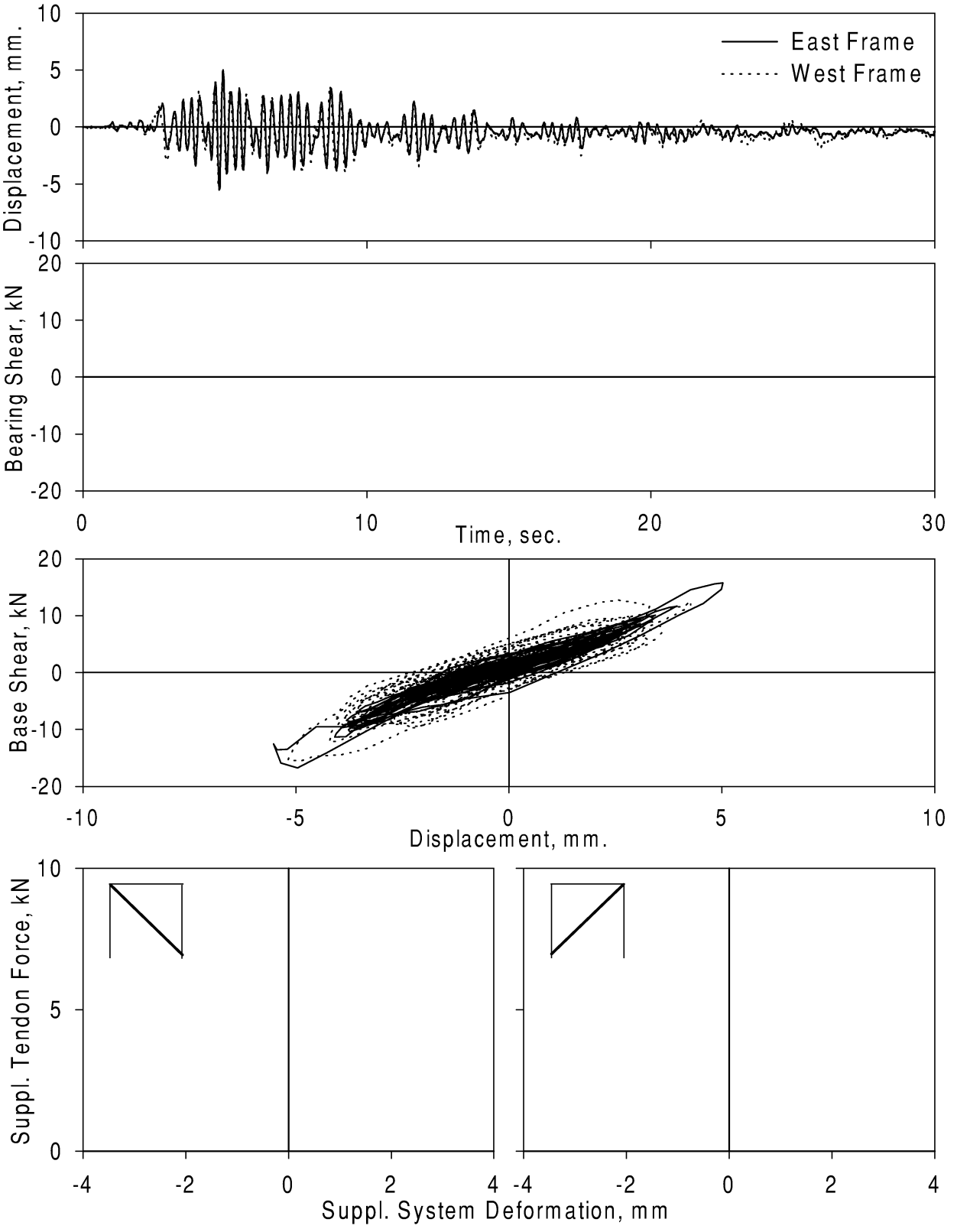

Figure A-2. Experimental Results - TAPRWB
Ground Motion: Taft (PGA=0.158 g)
Configuration: w/Tendons (Bracing)

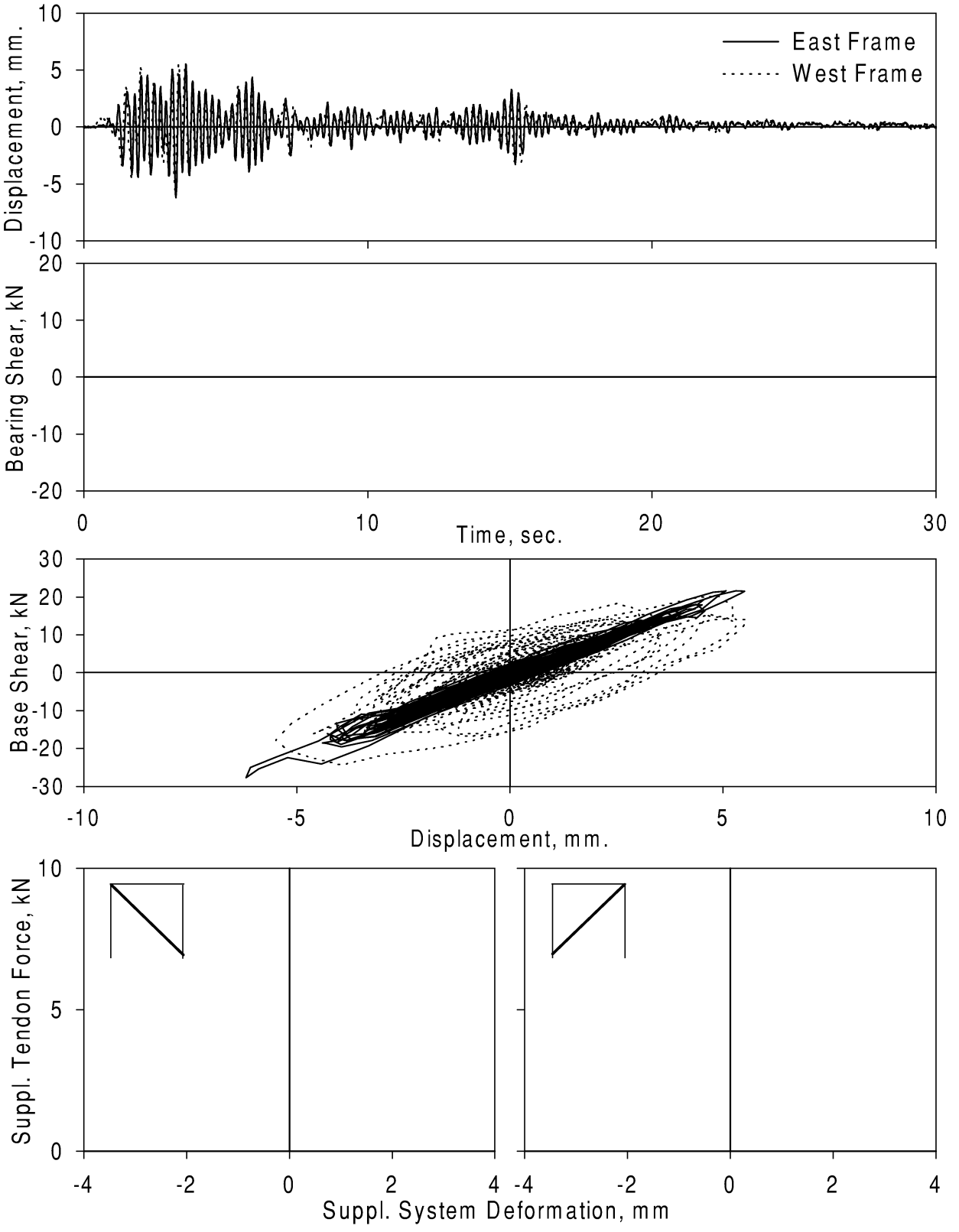

Figure A-3. Experimental Results - ELPRWB
Ground Motion: El Centro (PGA=0.265 g)
Configuration: w/Tendons (Bracing)

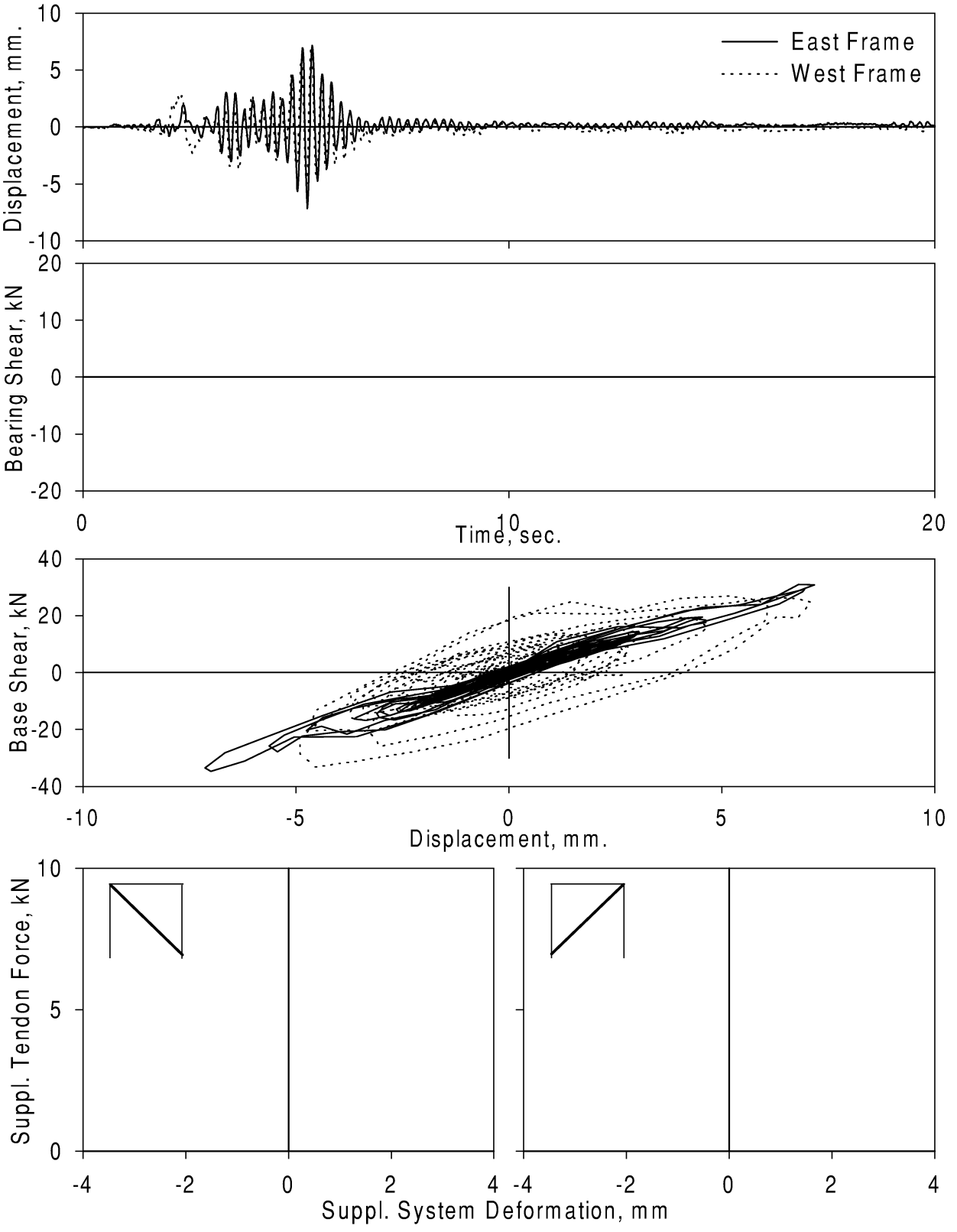

Figure A-4. Experimental Results - PAPRWB
Ground Motion: Pacoima Dam (PGA=0.252 g)
Configuration: w/Tendons (Bracing)

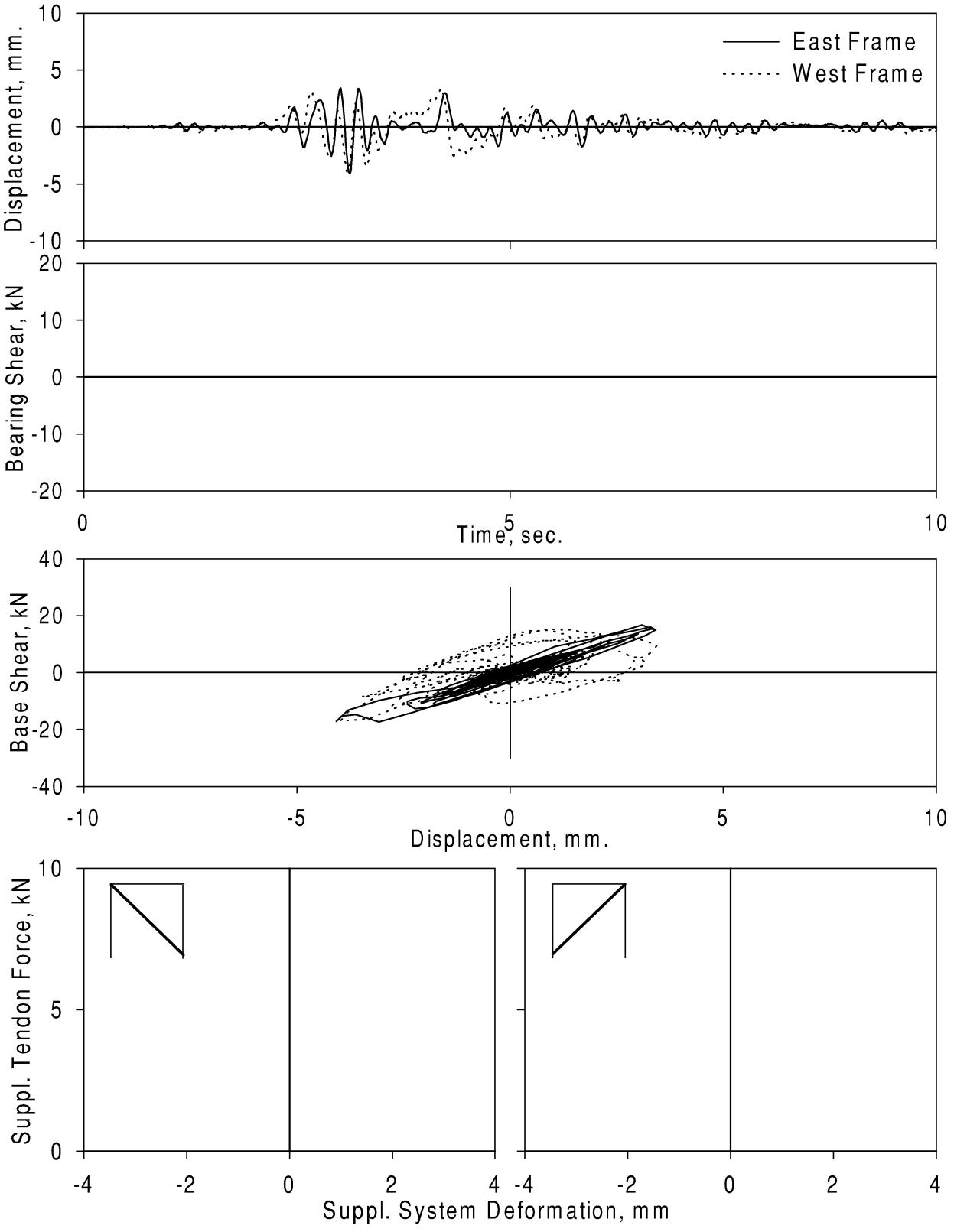

Figure A-5. Experimental Results - SYPRWB
Ground Motion: Sylmar (PGA=0.243 g)
Configuration: w/Tendons (Bracing)

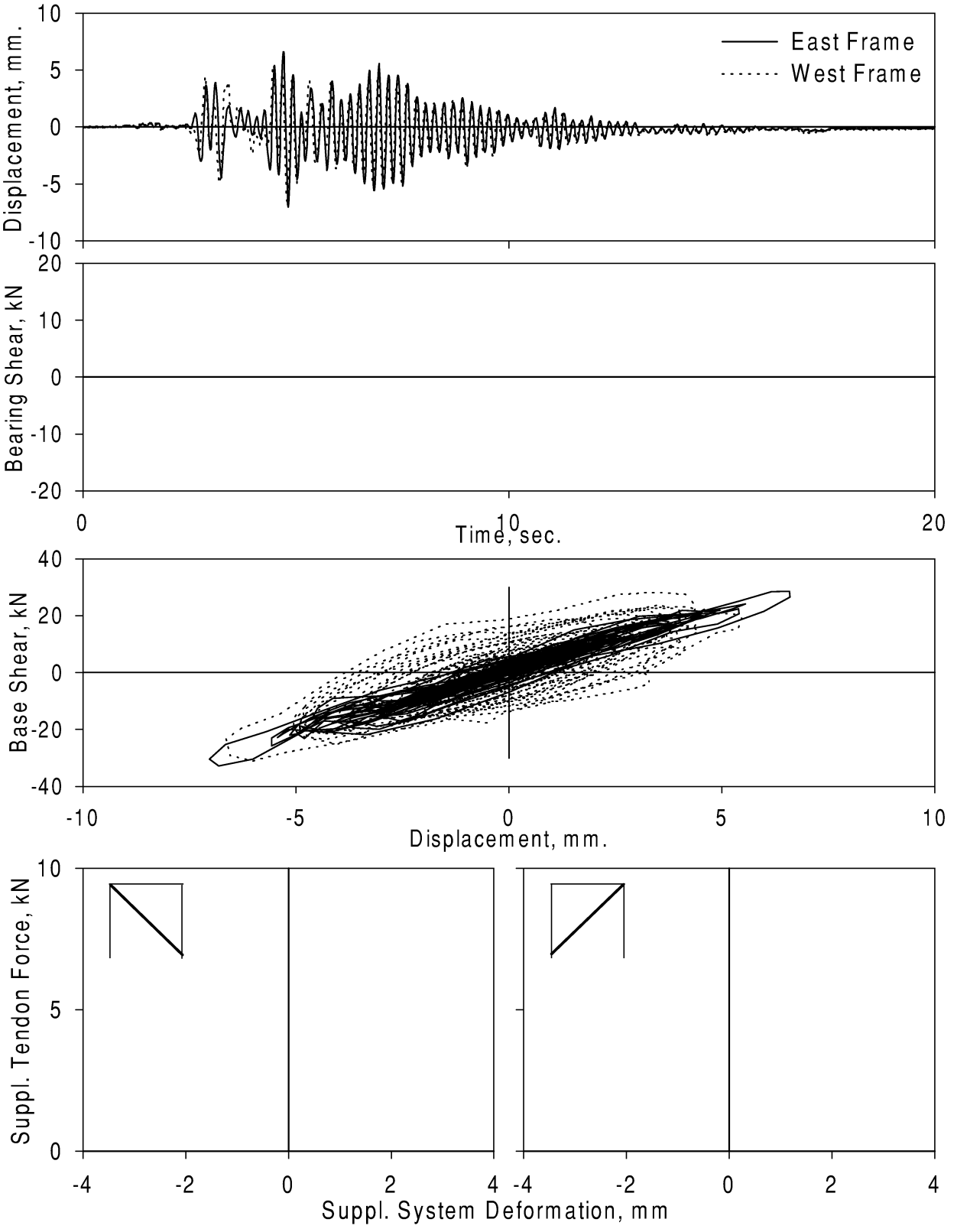

Figure A-6. Experimental Results - KOPRWB
Ground Motion: Kobe (PGA=0.272 g)
Configuration: w/Tendons (Bracing)

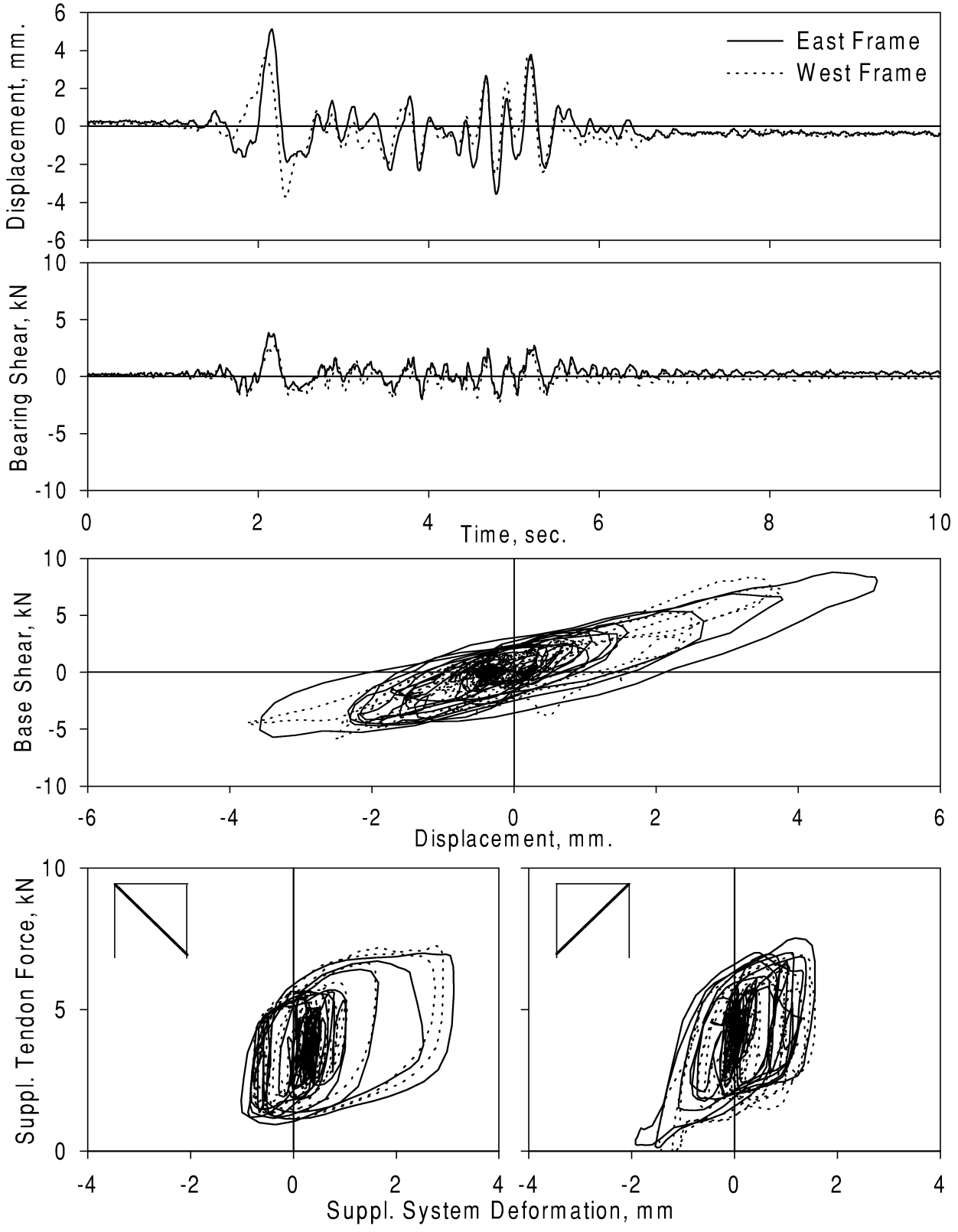

Figure A-7. Experimental Results - PAPRDA
Ground Motion: Pacoima Dam (PGA=0.224 g)
Configuration: Retrofitted/Dampers only

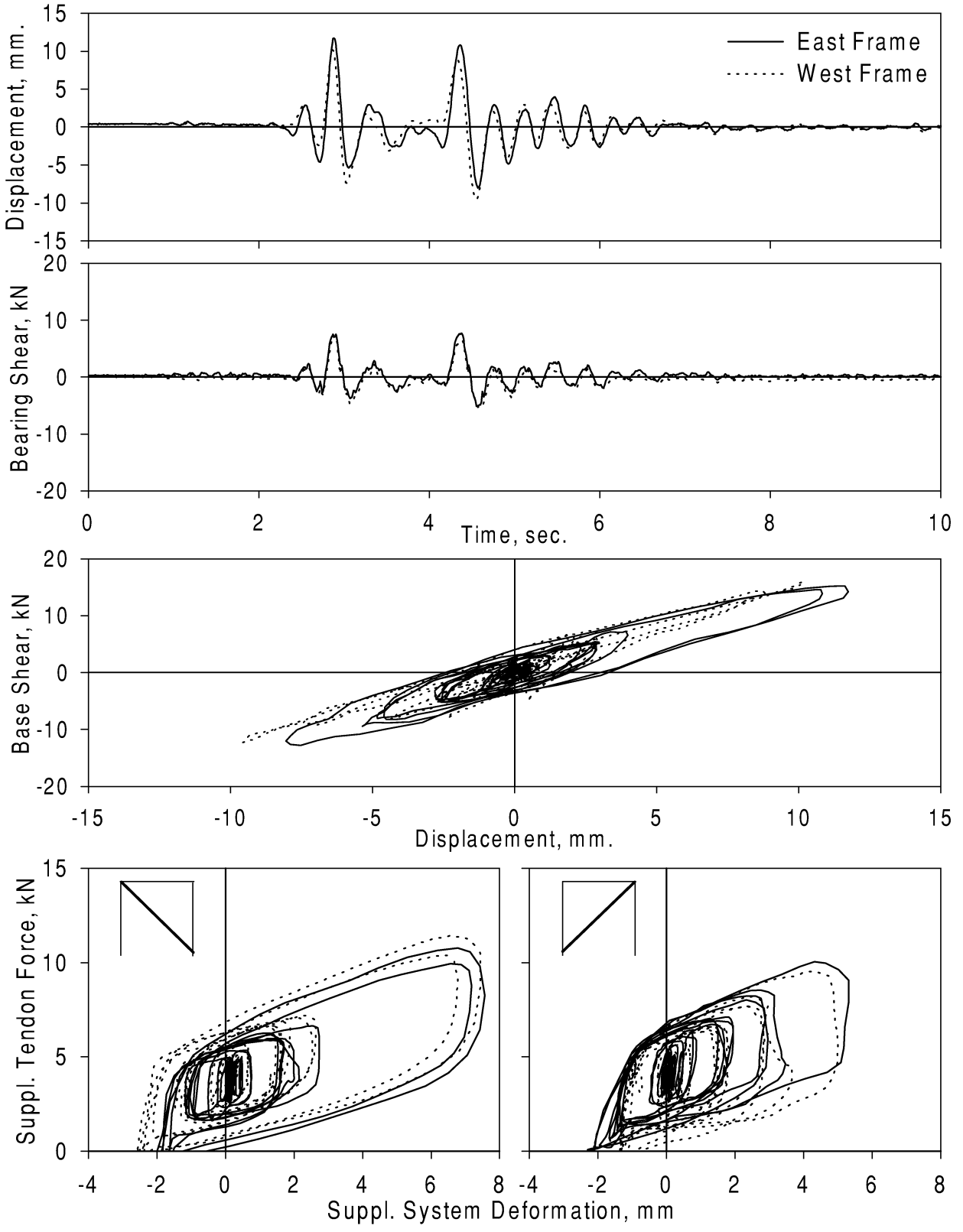

Figure A-8. Experimental Results - SYPRDA
Ground Motion: Sylmar (PGA=0.287 g)
Configuration: Retrofitted/Dampers only

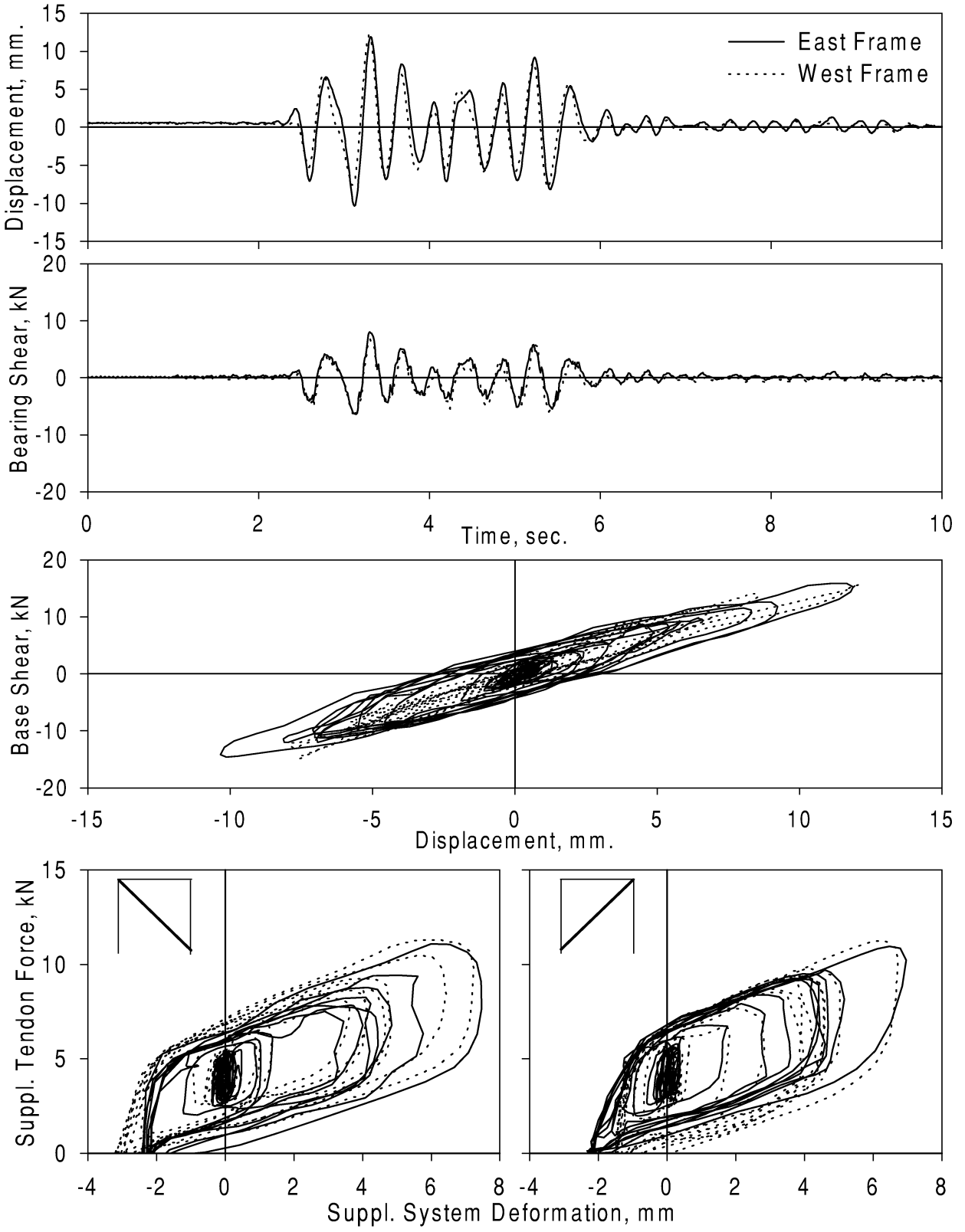

Figure A-9. Experimental Results - KOPRDA
Ground Motion: Kobe (PGA=0.264 g)
Configuration: Retrofitted/Dampers only

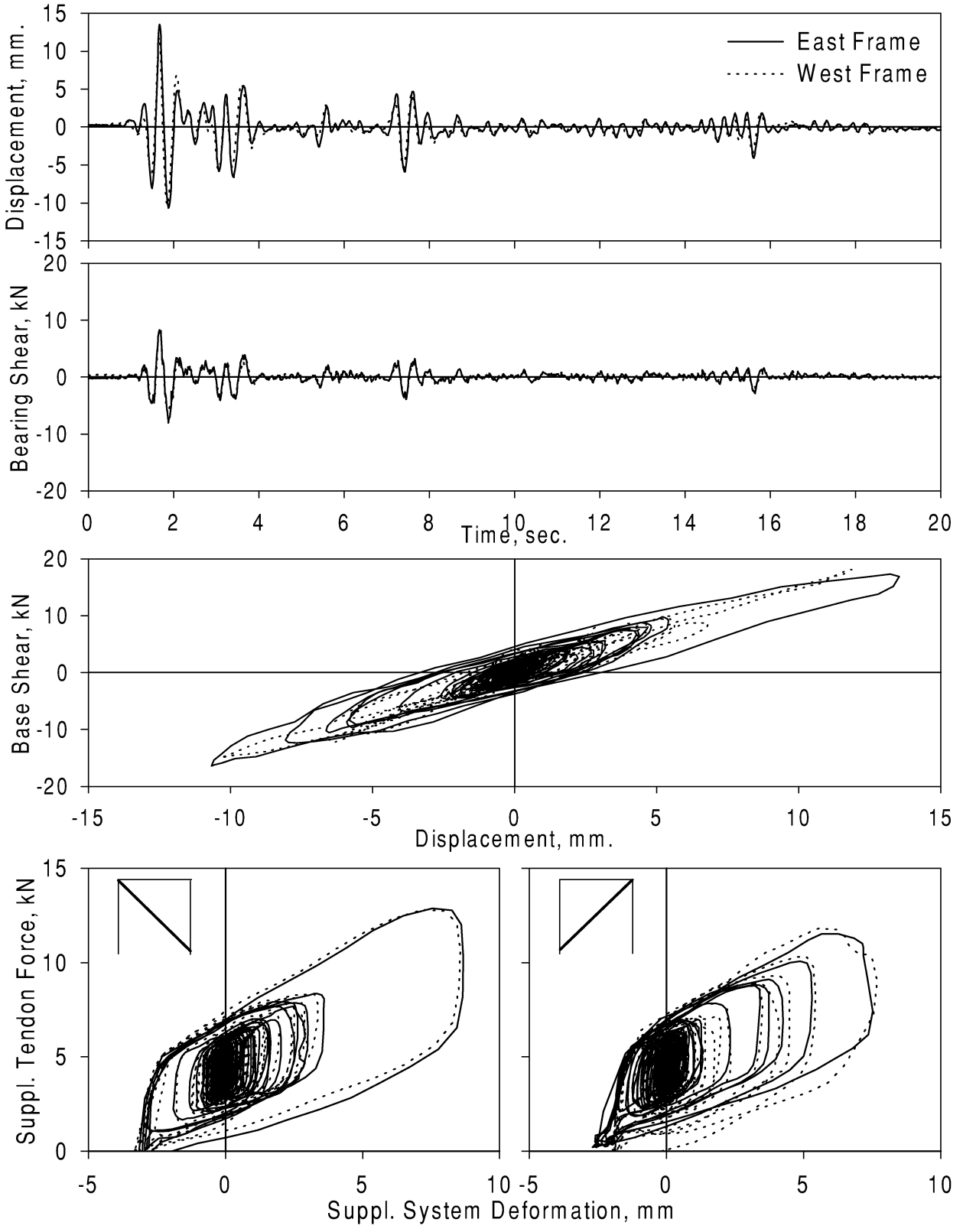

Figure A-10. Experimental Results - ELPRDA
Ground Motion: El Centro (PGA=0.243 g)
Configuration: Retrofitted/Dampers only

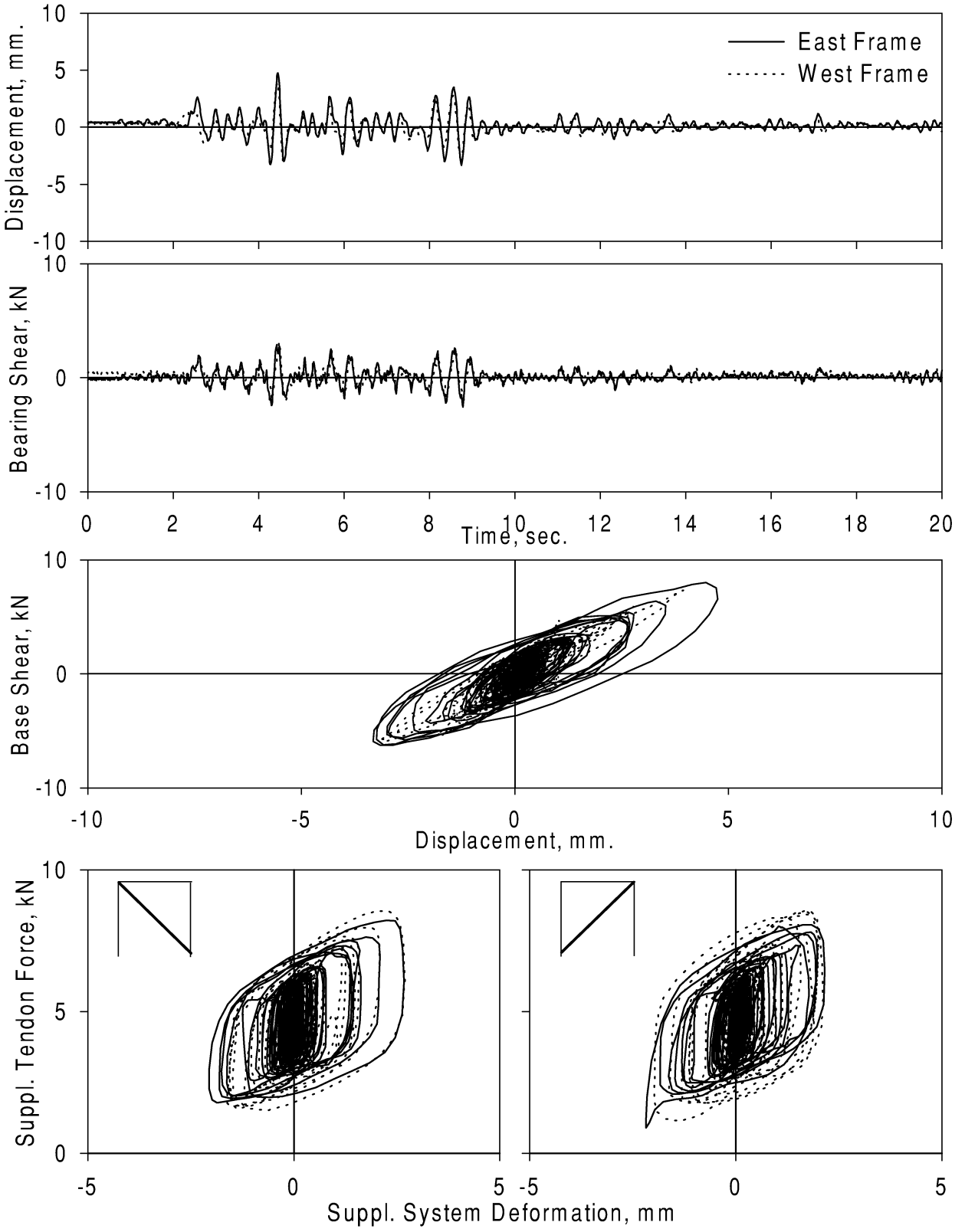

Figure A-11. Experimental Results - TAPRDA
Ground Motion: Taft (PGA=0.144 g)
Configuration: Retrofitted/Dampers only

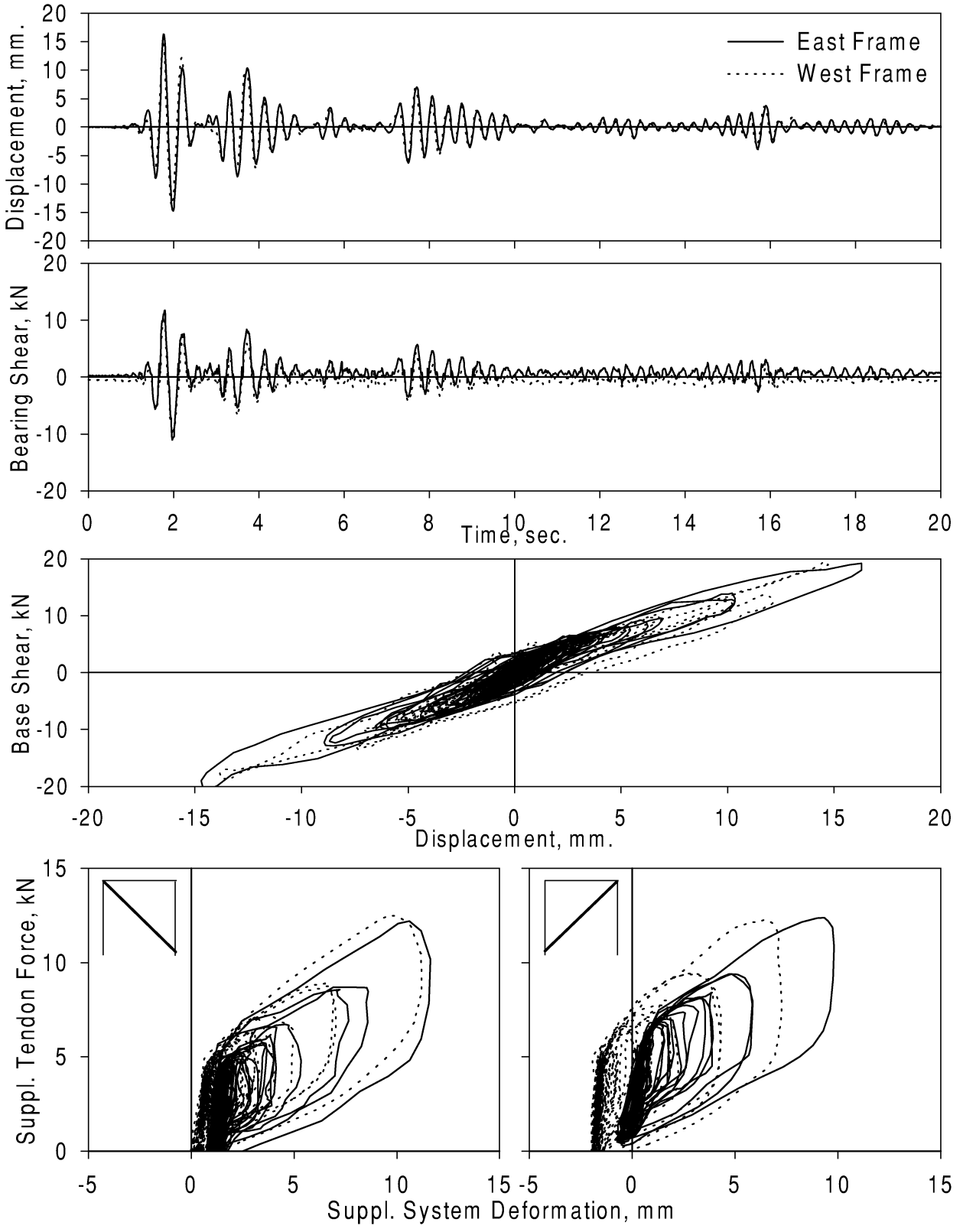

Figure A-12. Experimental Results - ELPRDB
Ground Motion: El Centro (PGA=0.293 g)
Configuration: Retrofitted/Dampers only

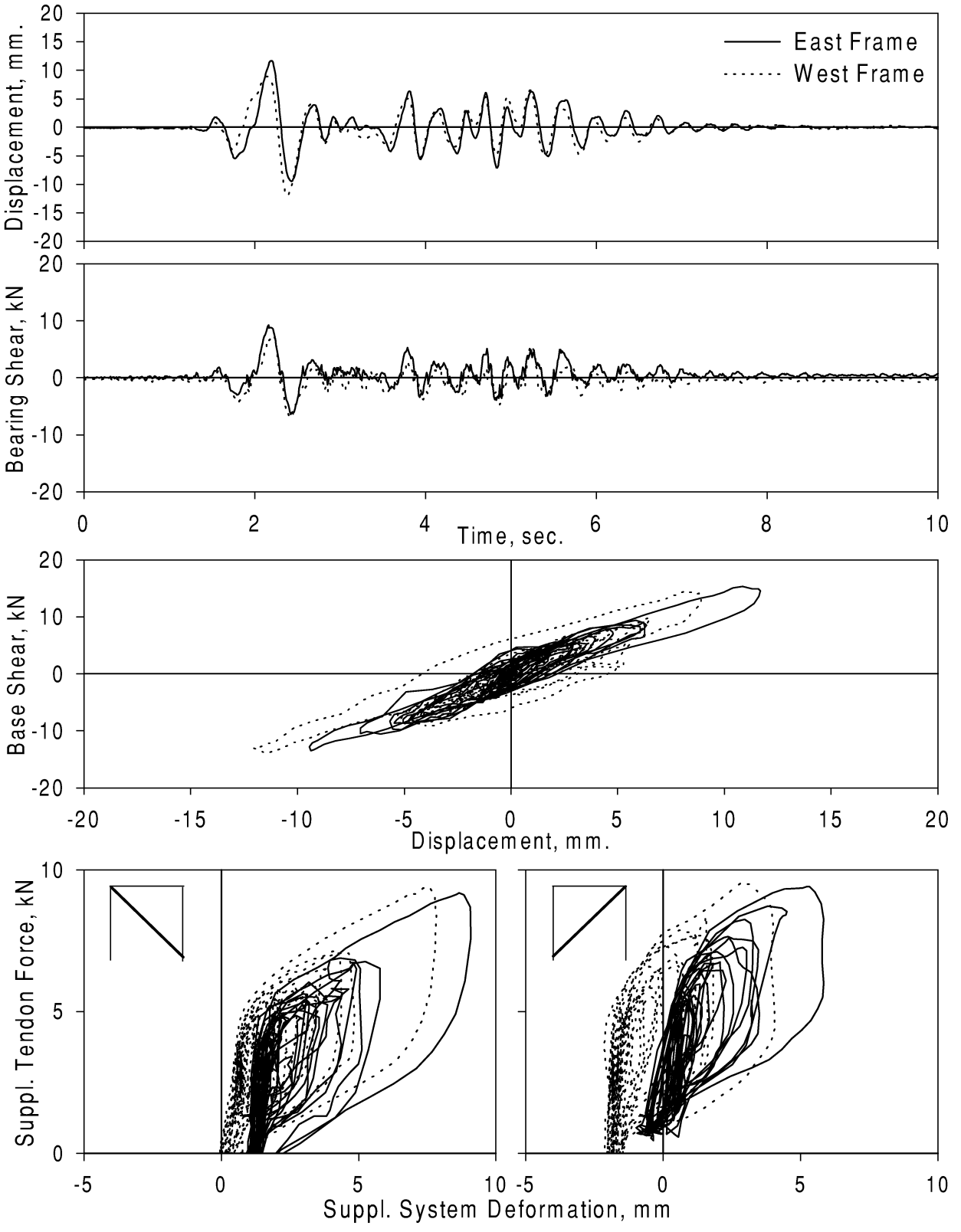

Figure A-13. Experimental Results - PAPRDB
Ground Motion: Pacoima Dam (PGA=0.448 g)
Configuration: Retrofitted/Dampers only

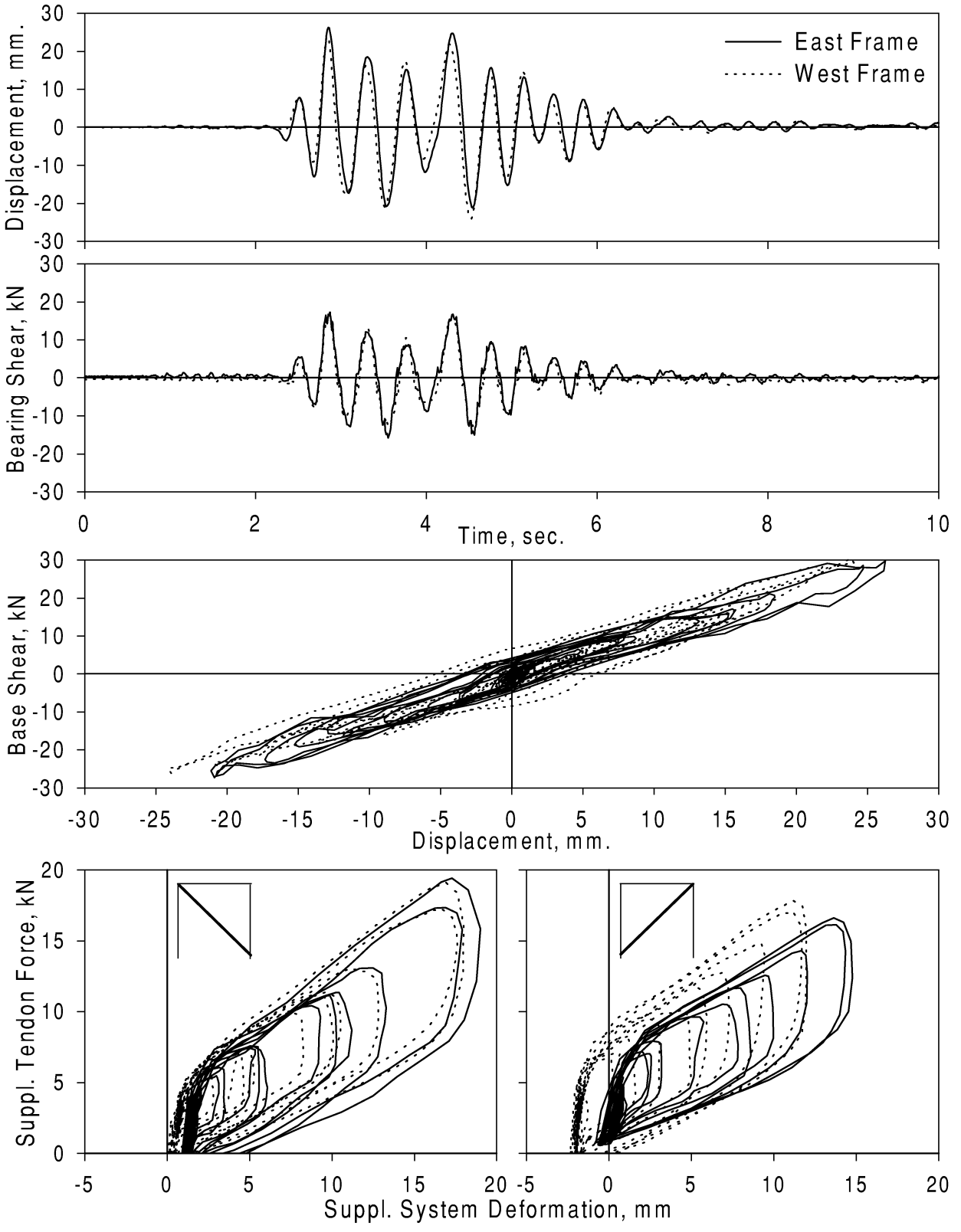

Figure A-14. Experimental Results - SYPRDB
Ground Motion: Sylmar (PGA=0.510 g)
Configuration: Retrofitted/Dampers only

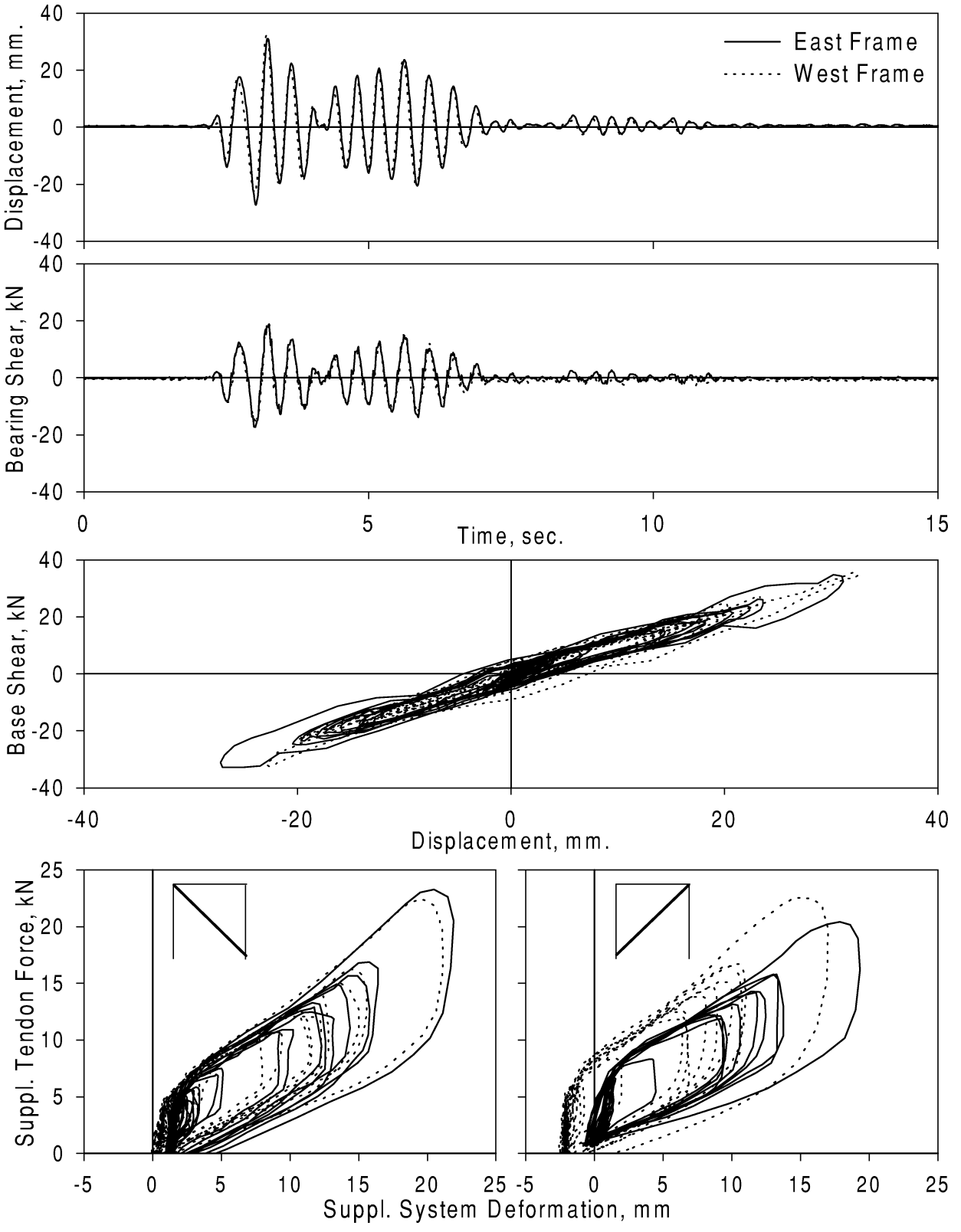

Figure A-15. Experimental Results - KOPRDB
Ground Motion: Kobe (PGA=0.365 g)
Configuration: Retrofitted/Dampers only

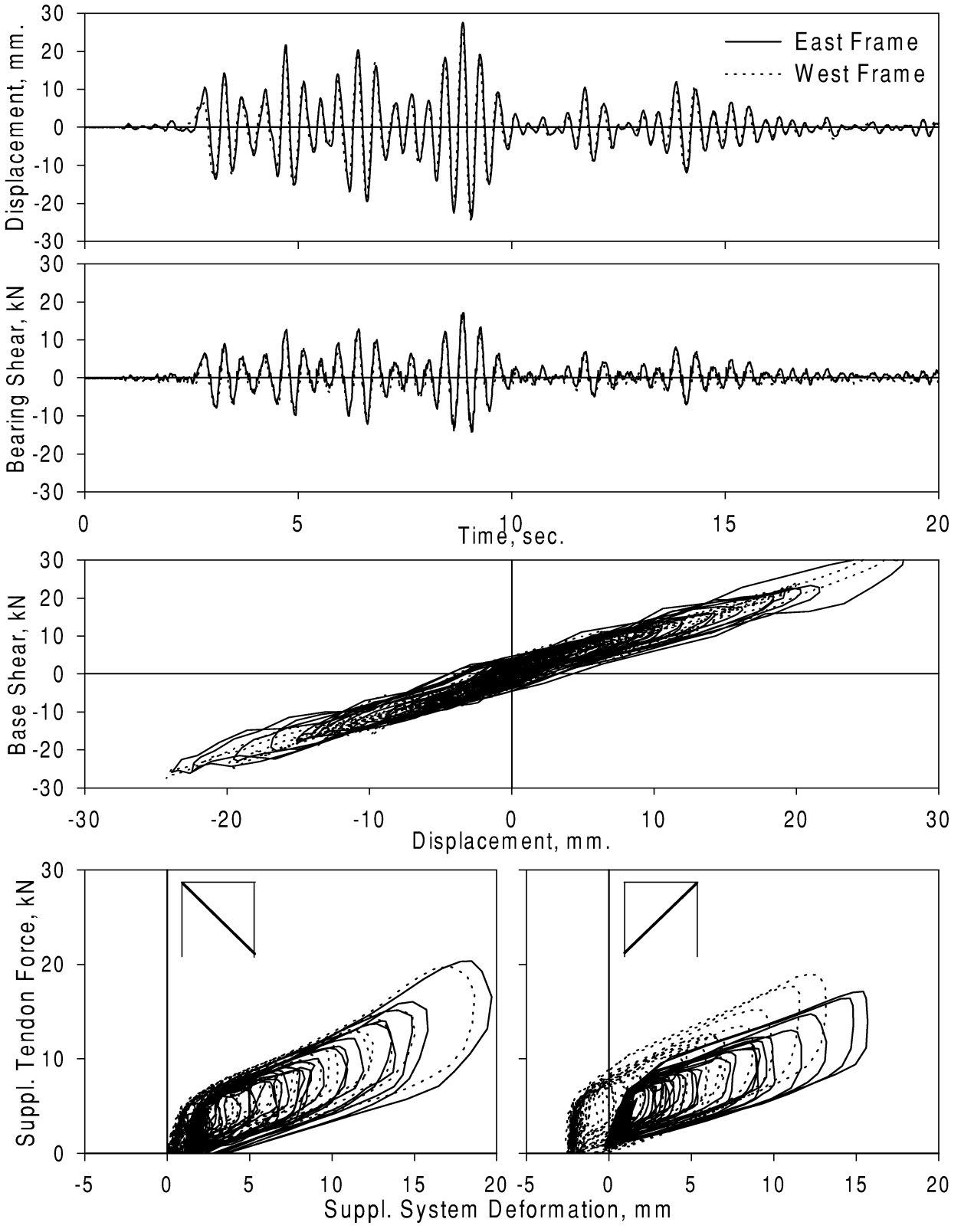

Figure A-16. Experimental Results - TAPRDB
Ground Motion: Taft (PGA=0.440 g)
Configuration: Retrofitted/Dampers only

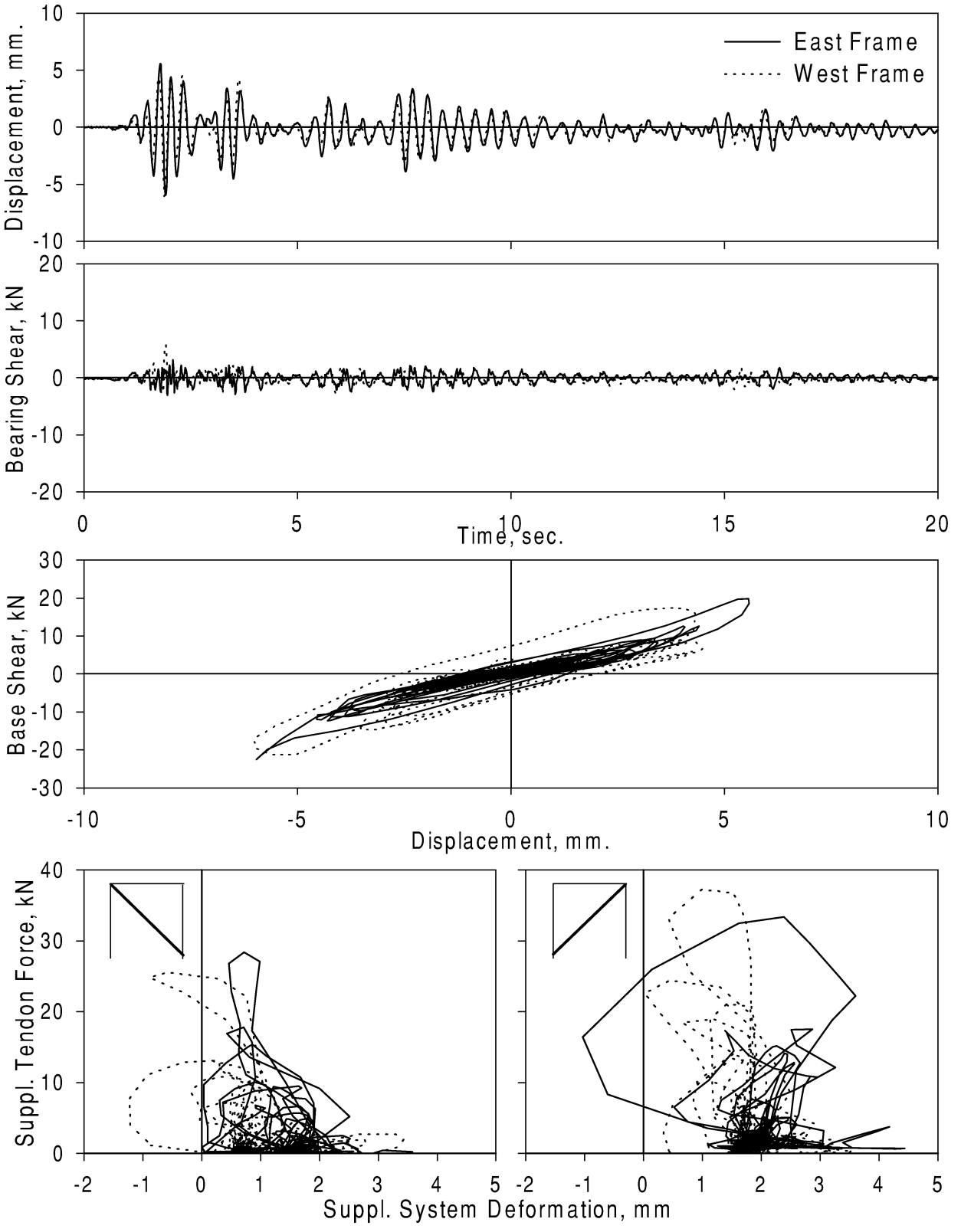

Figure A-17. Experimental Results - ELNSFA
Ground Motion: El Centro (PGA=0.188 g)
Configuration: Retrofitted/Fuse-bars only/Snug

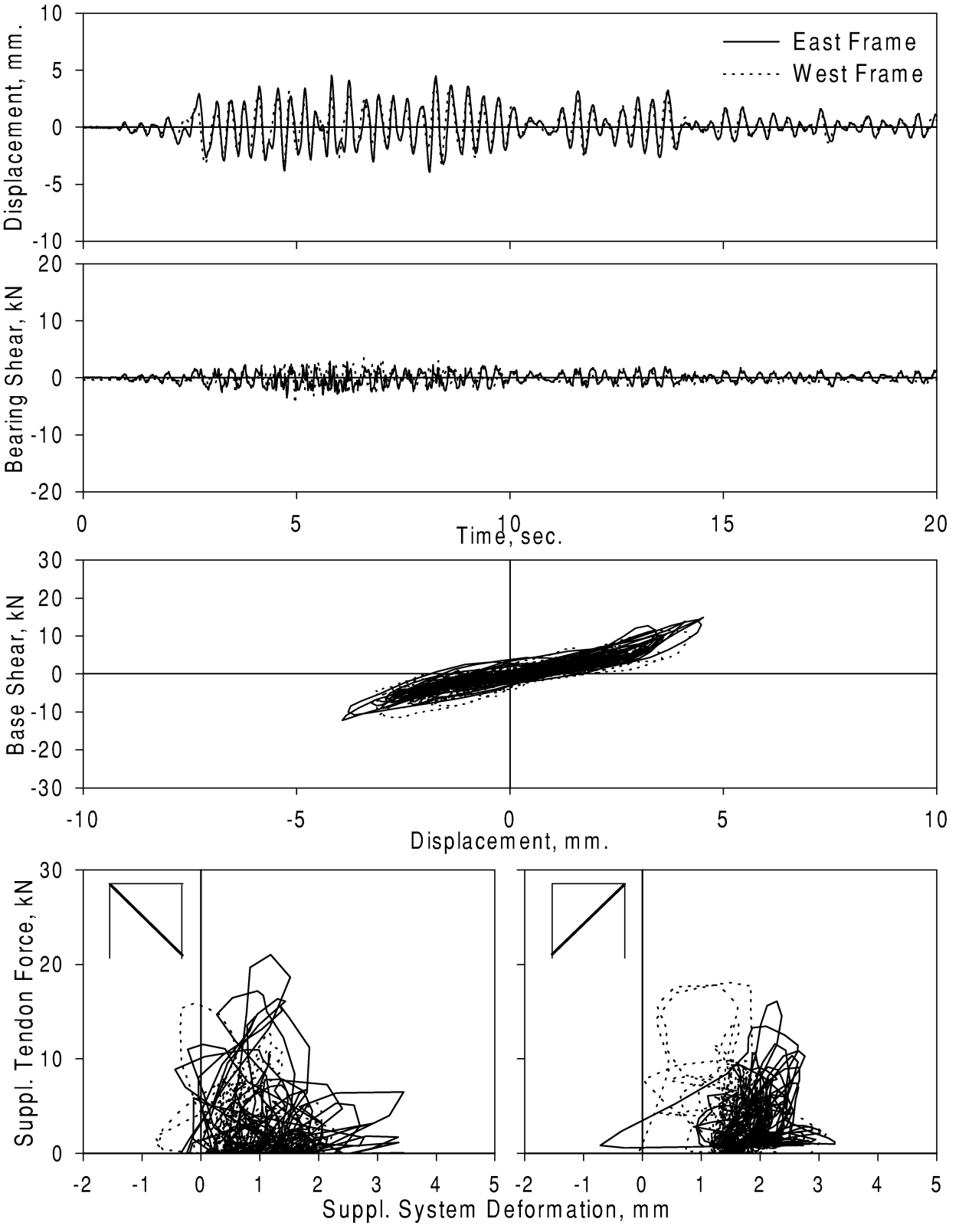

Figure A-18. Experimental Results - TANSFA
Ground Motion: Taft (PGA=0.153 g)
Configuration: Retrofitted/Fuse-bars only/Snug

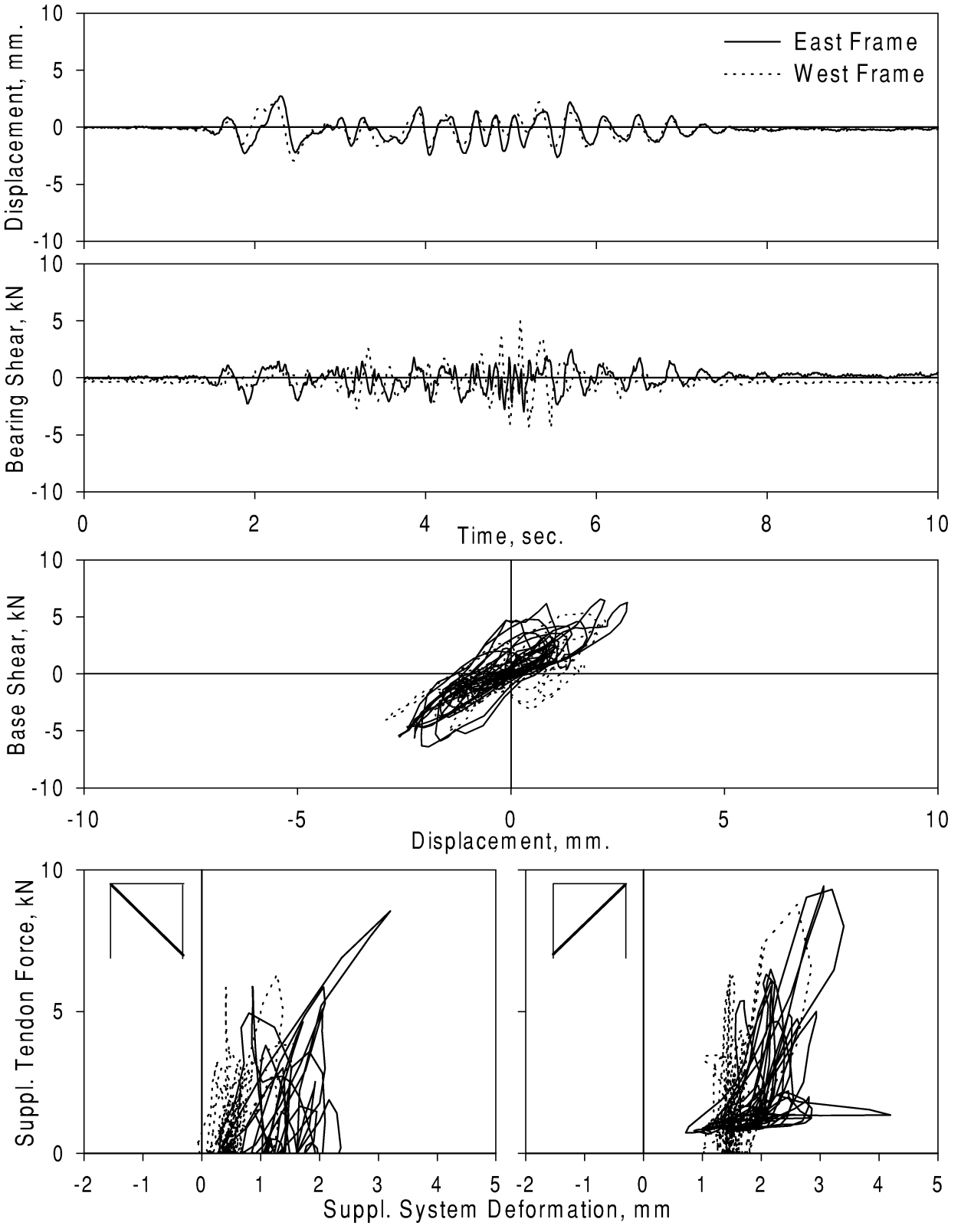

Figure A-19. Experimental Results - PANSFA
Ground Motion: Pacoima Dam (PGA=0.174 g)
Configuration: Retrofitted/Fuse-bars only/Snug

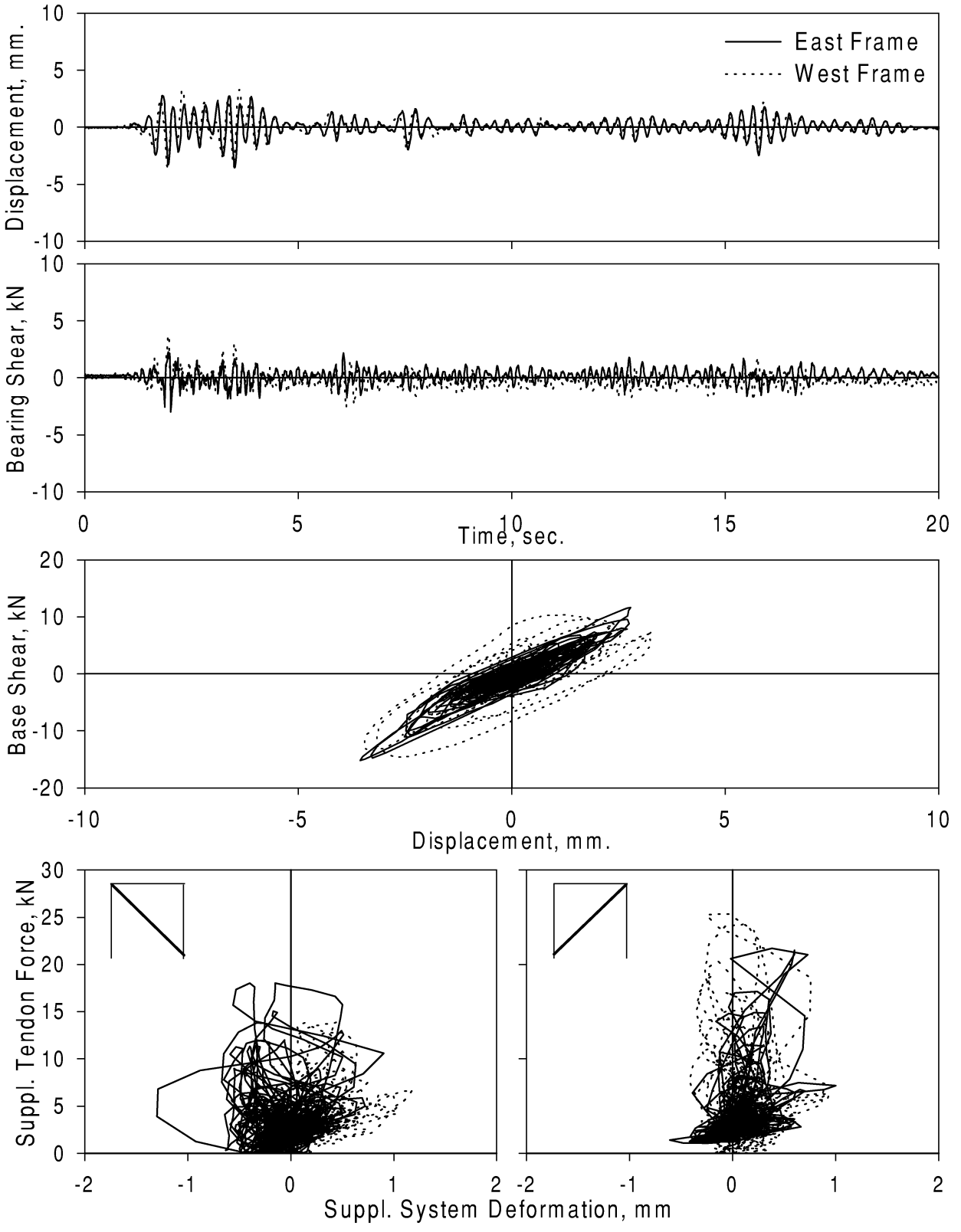

Figure A-20. Experimental Results - ELNDFA
Ground Motion: El Centro (PGA=0.193 g)
Configuration: Retrofitted/Fuse-bars and Damper/Snug

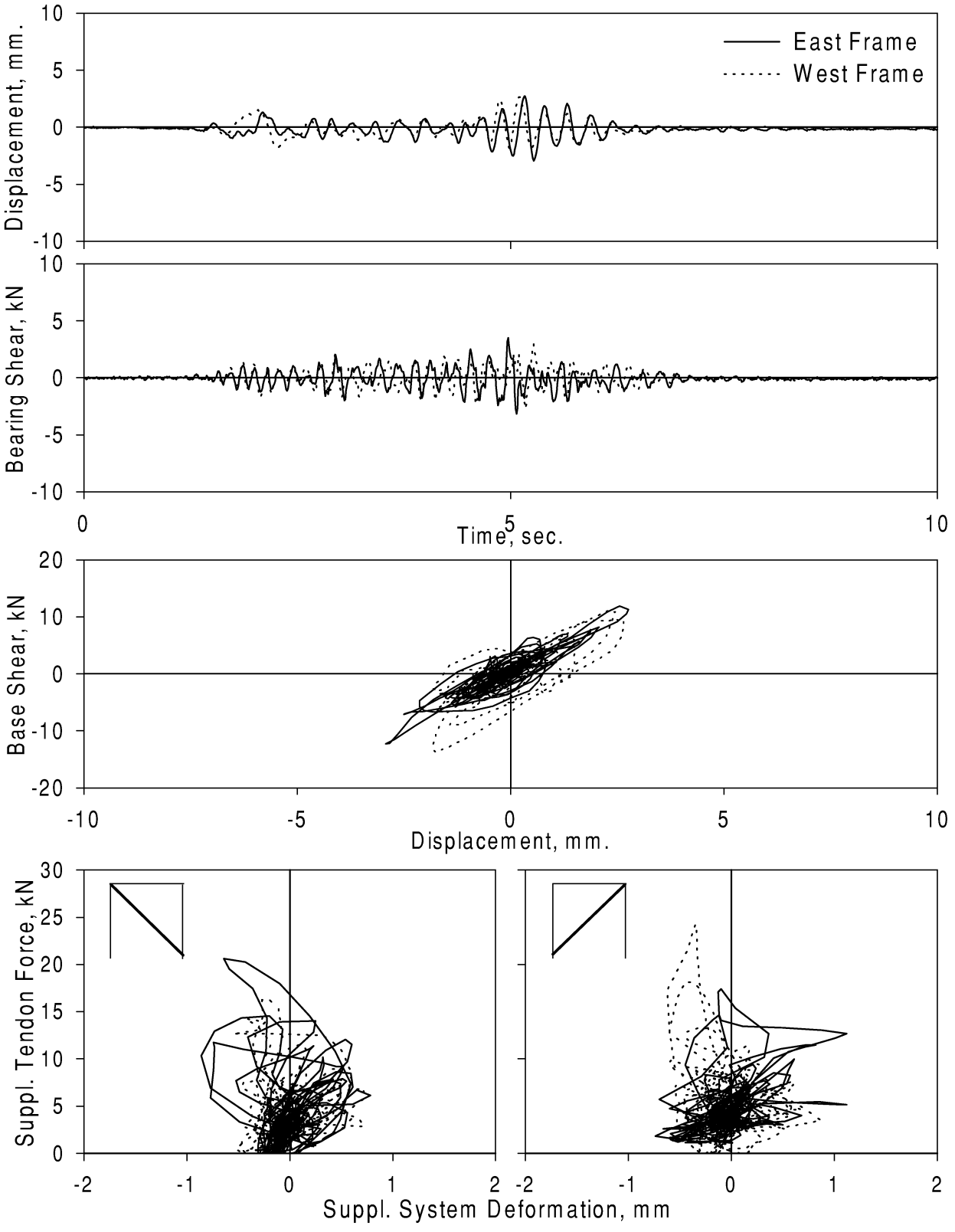

Figure A-21. Experimental Results - PANDFA
Ground Motion: Pacoima Dam (PGA=0.163 g)
Configuration: Retrofitted/Fuse-bars and Damper/Snug

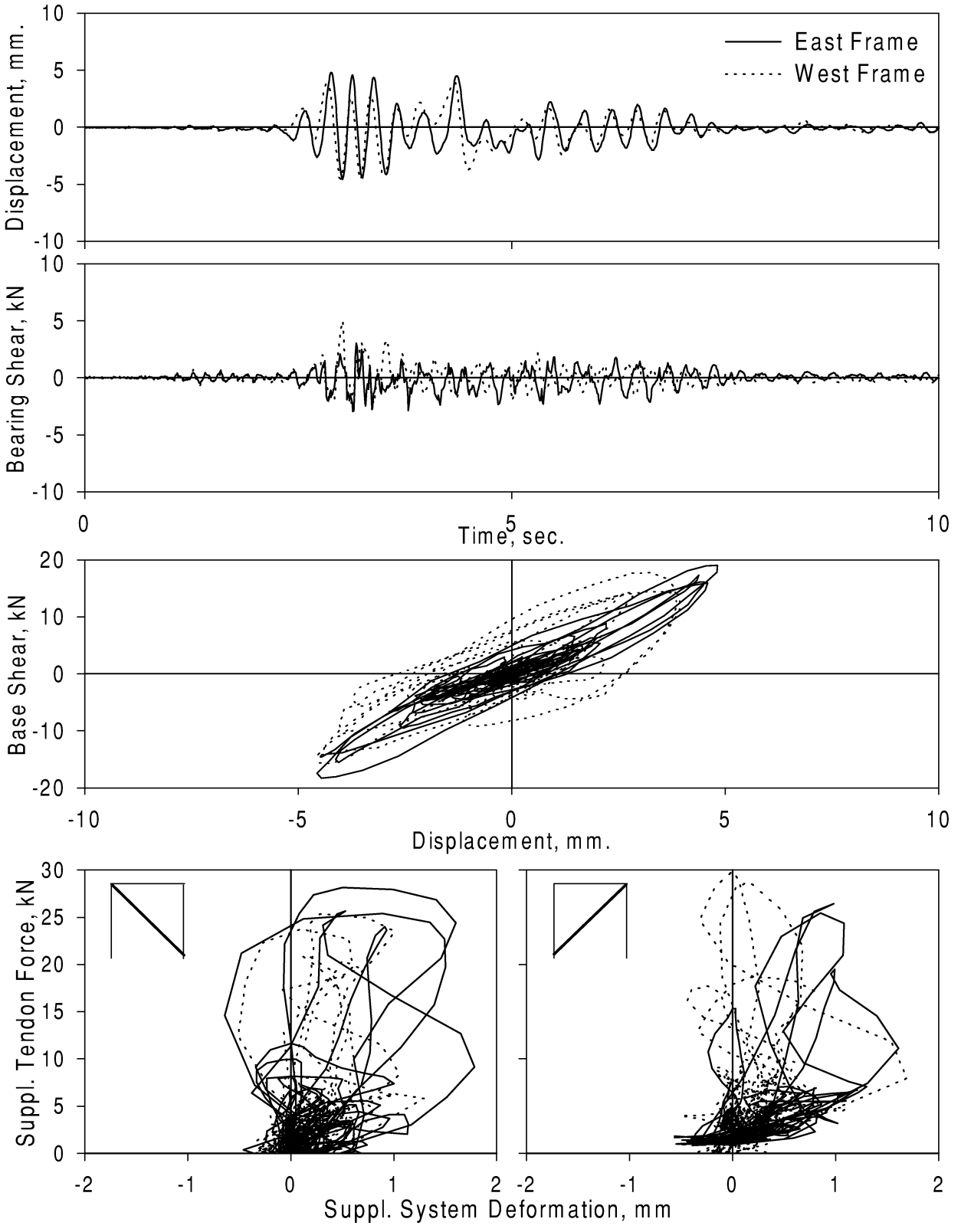

Figure A-22. Experimental Results - SYNDFA
Ground Motion: Sylmar (PGA=0.277 g)
Configuration: Retrofitted/Fuse-bars and Damper/Snug

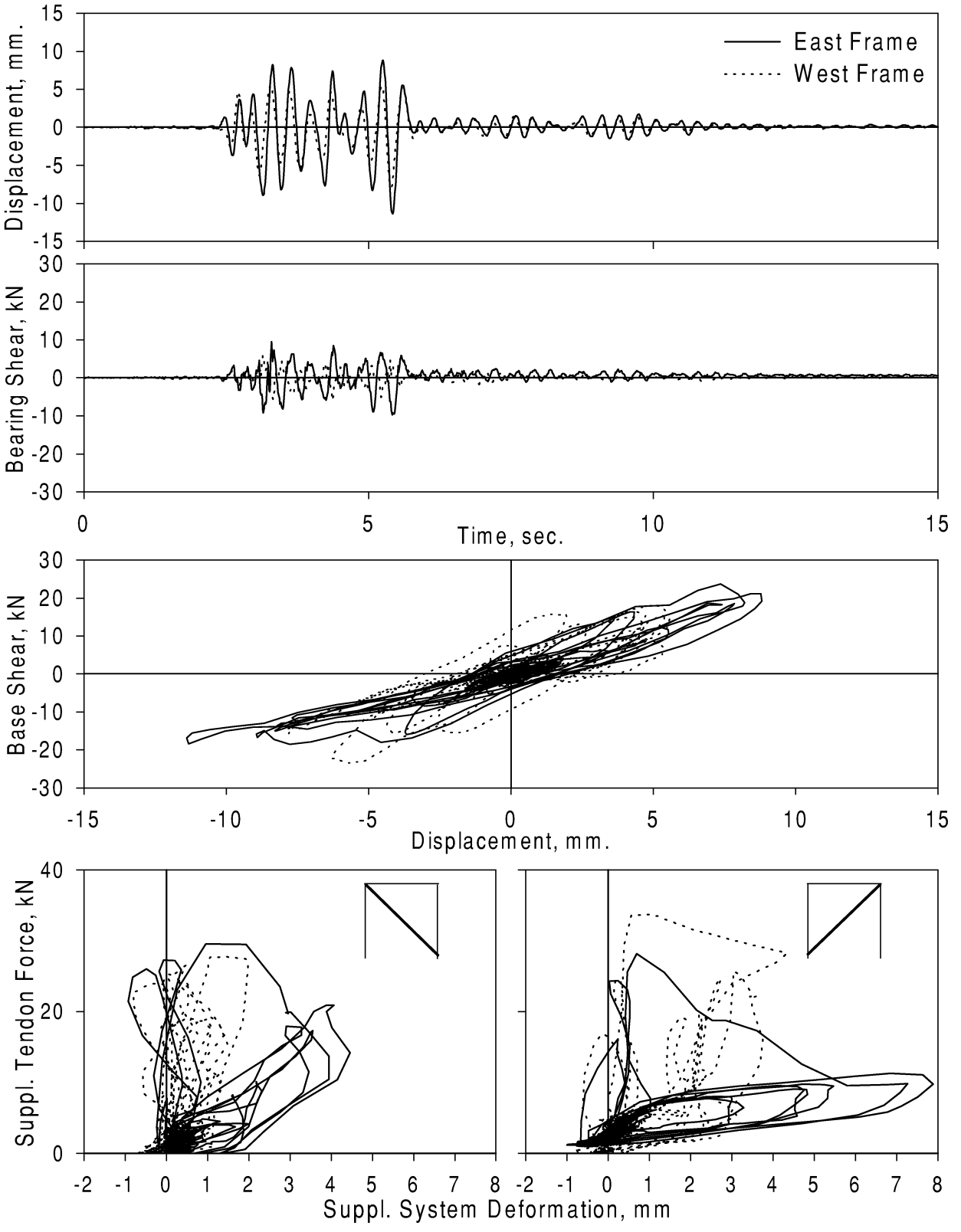

Figure A-23. Experimental Results - KONDFA
Ground Motion: Kobe (PGA=0.268 g)
Configuration: Retrofitted/Fuse-bars and Damper/Snug

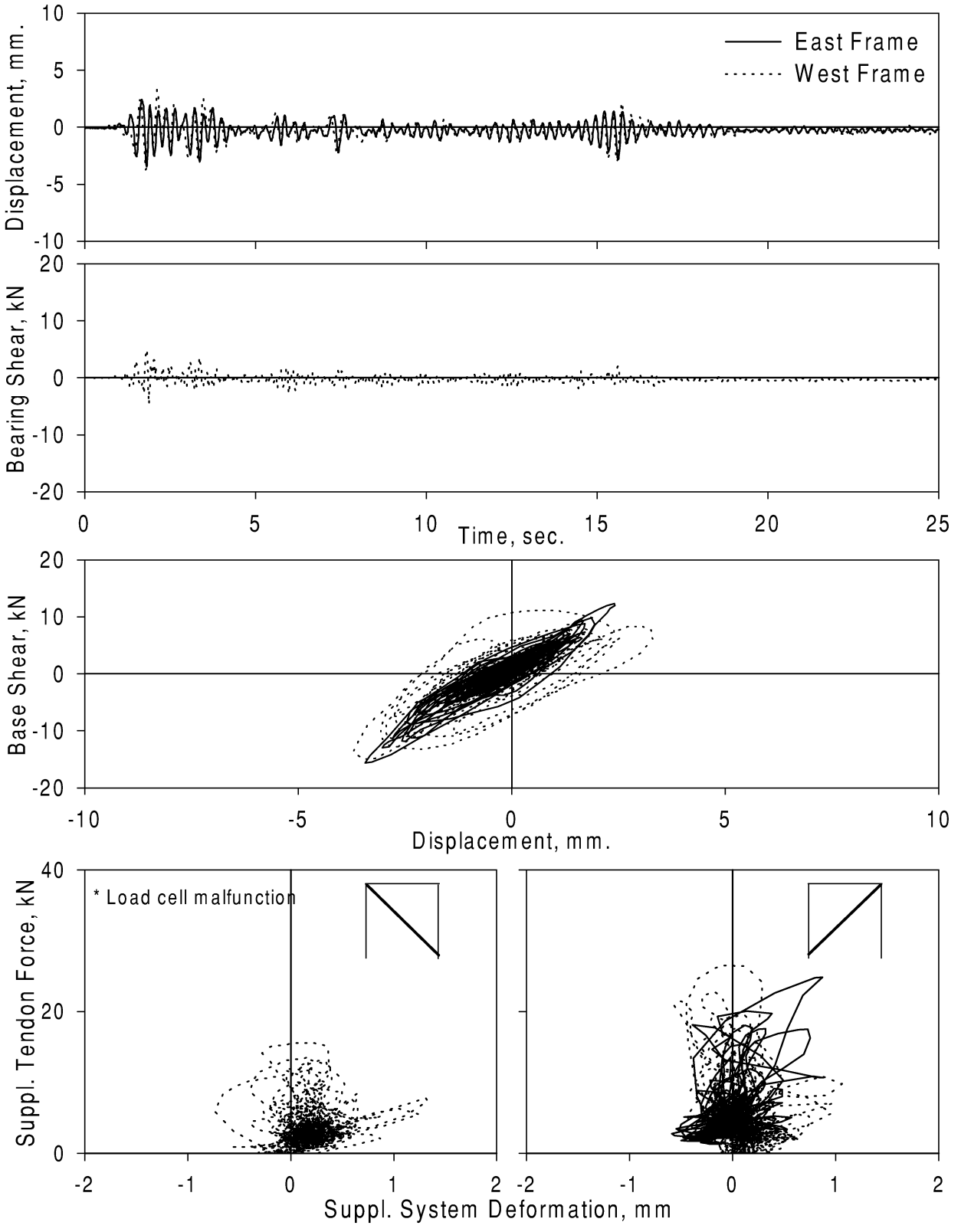

Figure A-24. Experimental Results - ELPDFA
Ground Motion: El Centro (PGA=0.219 g)
Configuration: Retrofitted/Fuse-bars and Damper

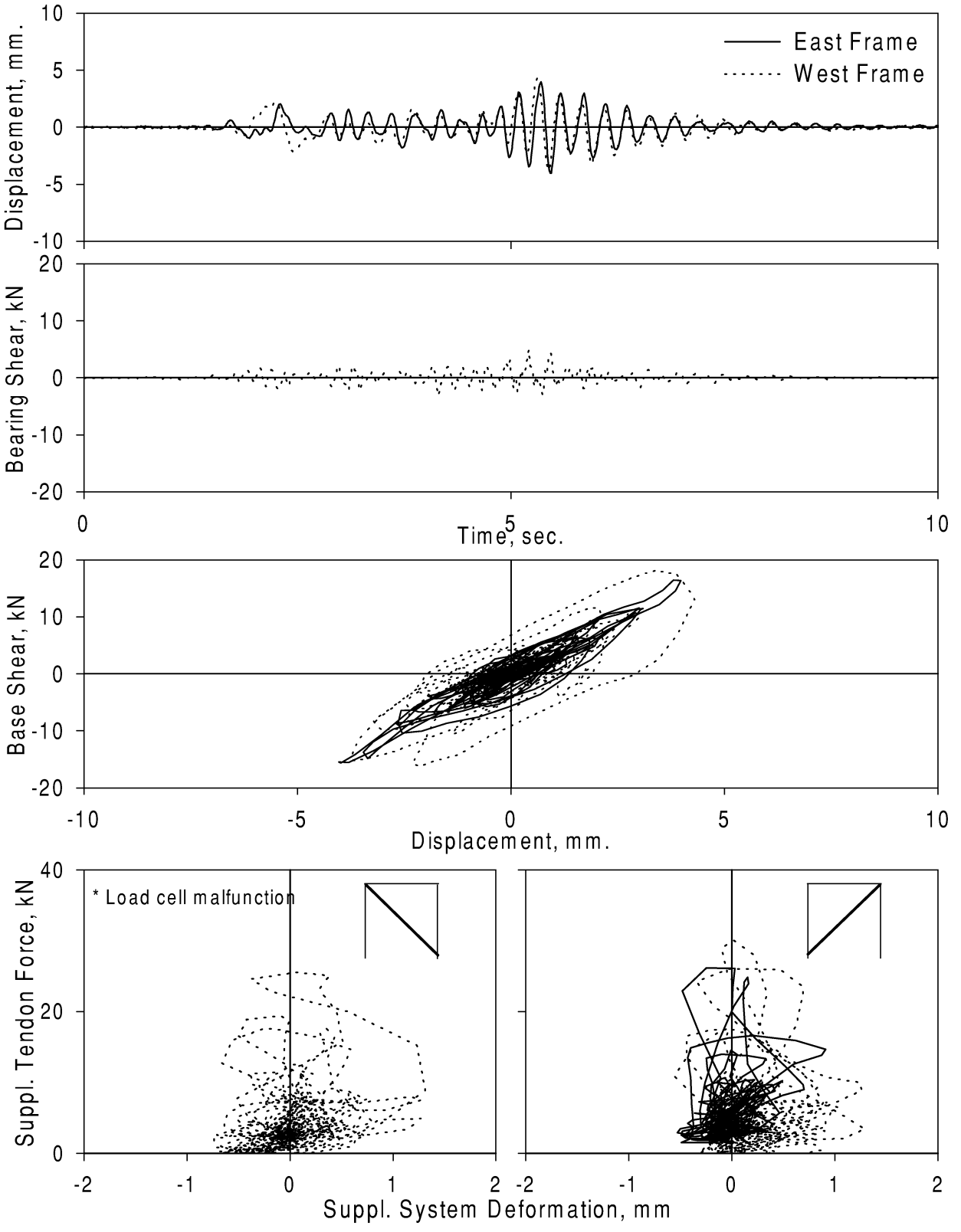

Figure A-25. Experimental Results - PAPDFA
Ground Motion: Pacoima (PGA=0.221 g)
Configuration: Retrofitted/Fuse-bars and Damper

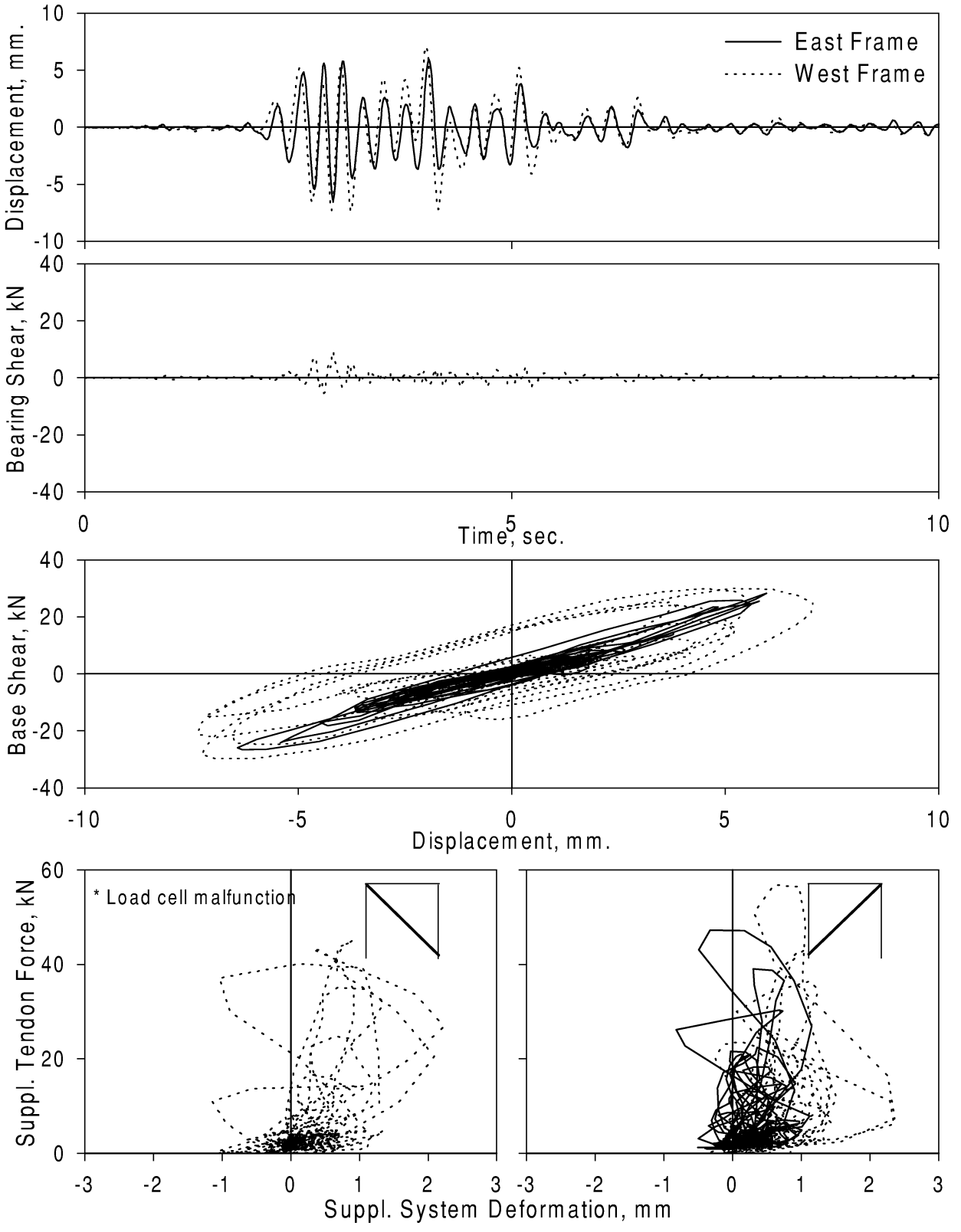

Figure A-26. Experimental Results - SYPDFA
Ground Motion: Sylmar (PGA=0.340 g)
Configuration: Retrofitted/Fuse-bars and Damper

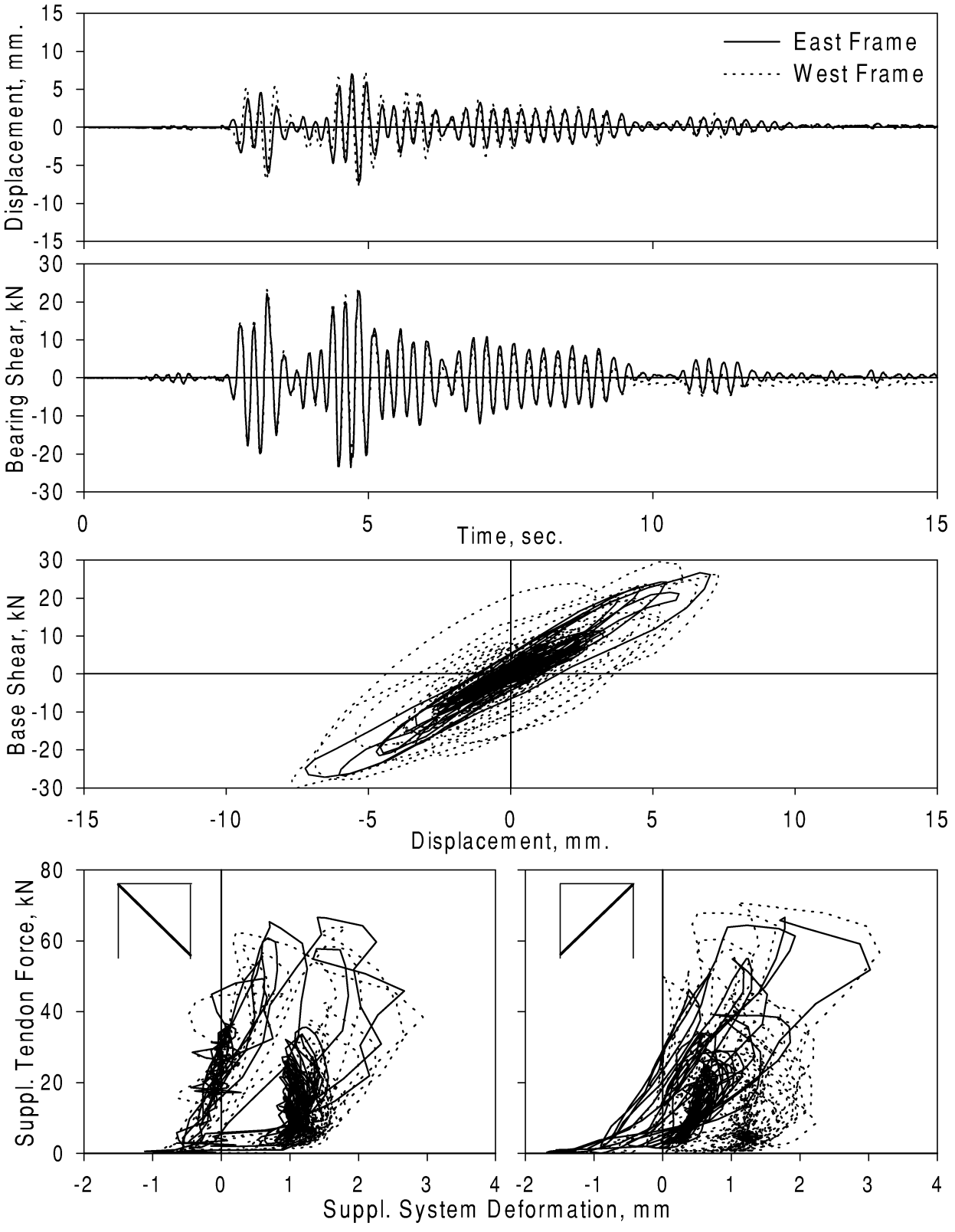

Figure A-27. Experimental Results - KOPDFA
Ground Motion: Kobe (PGA=0.348 g)
Configuration: Retrofitted/Fuse-bars and Damper

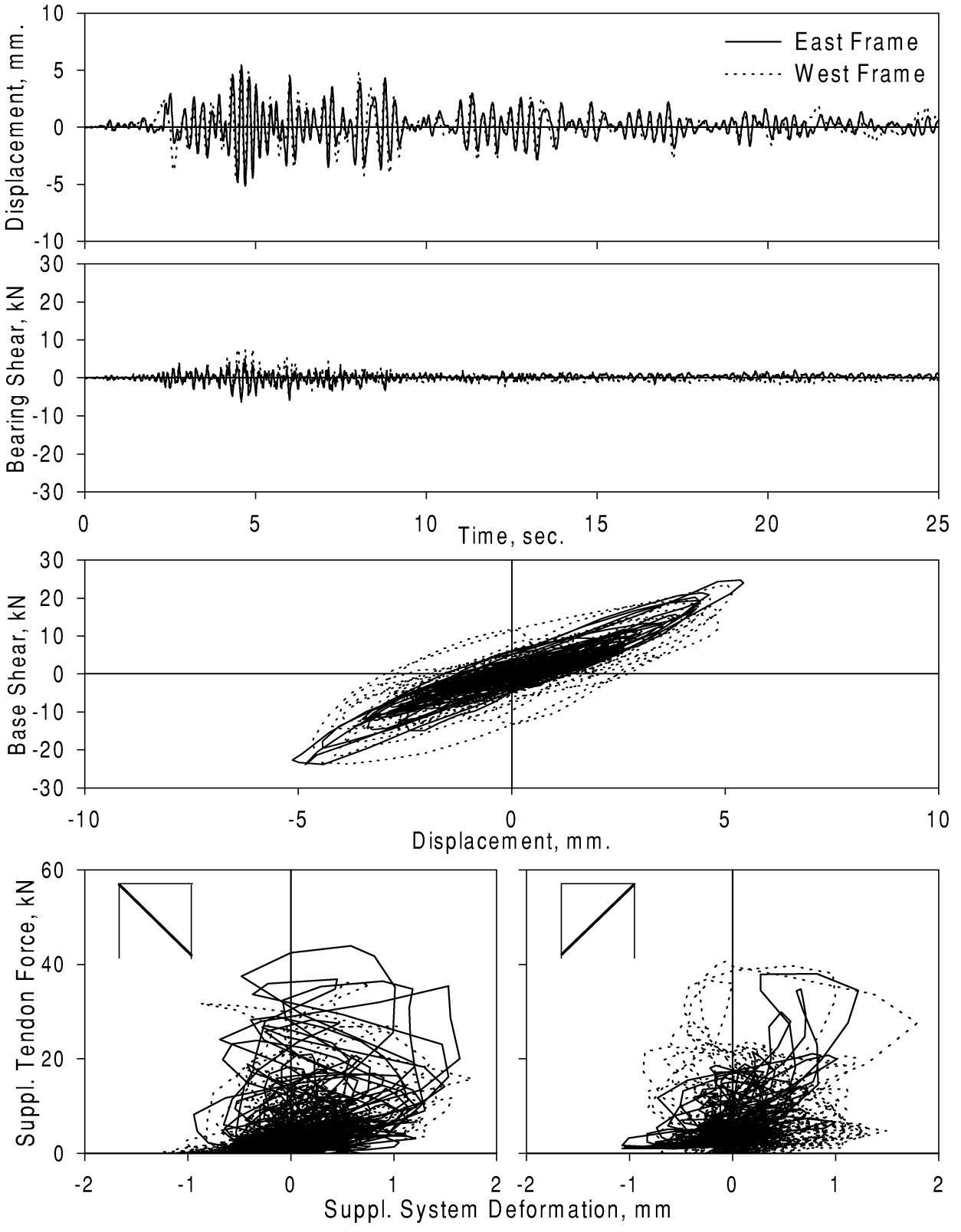

Figure A-28. Experimental Results - TAPDFA
Ground Motion: Taft (PGA=0.293 g)
Configuration: Retrofitted/Fuse-bars and Damper

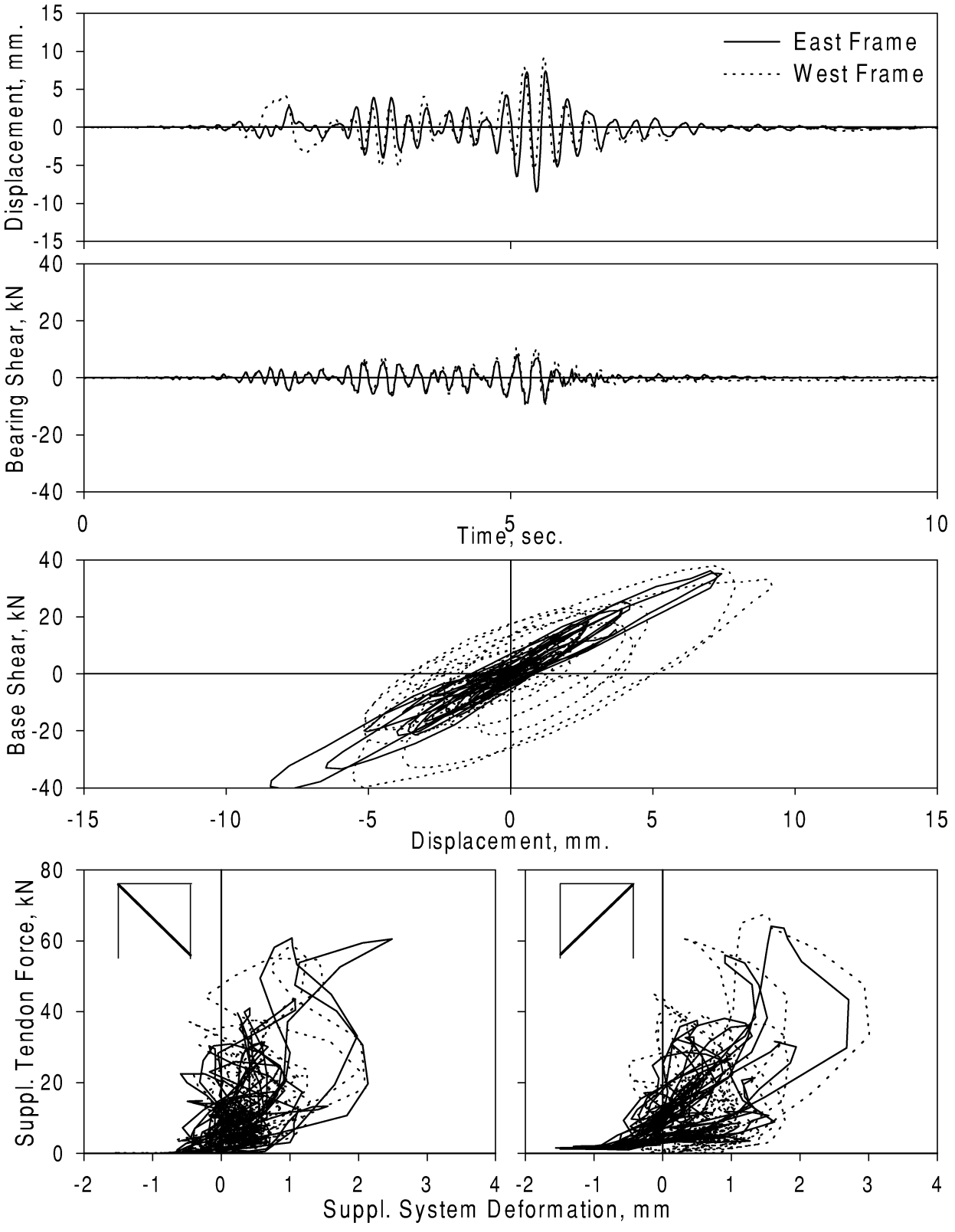

Figure A-29. Experimental Results - PAPDFB
Ground Motion: Pacoima Dam (PGA=0.491 g)
Configuration: Retrofitted/Fuse-bars and Damper

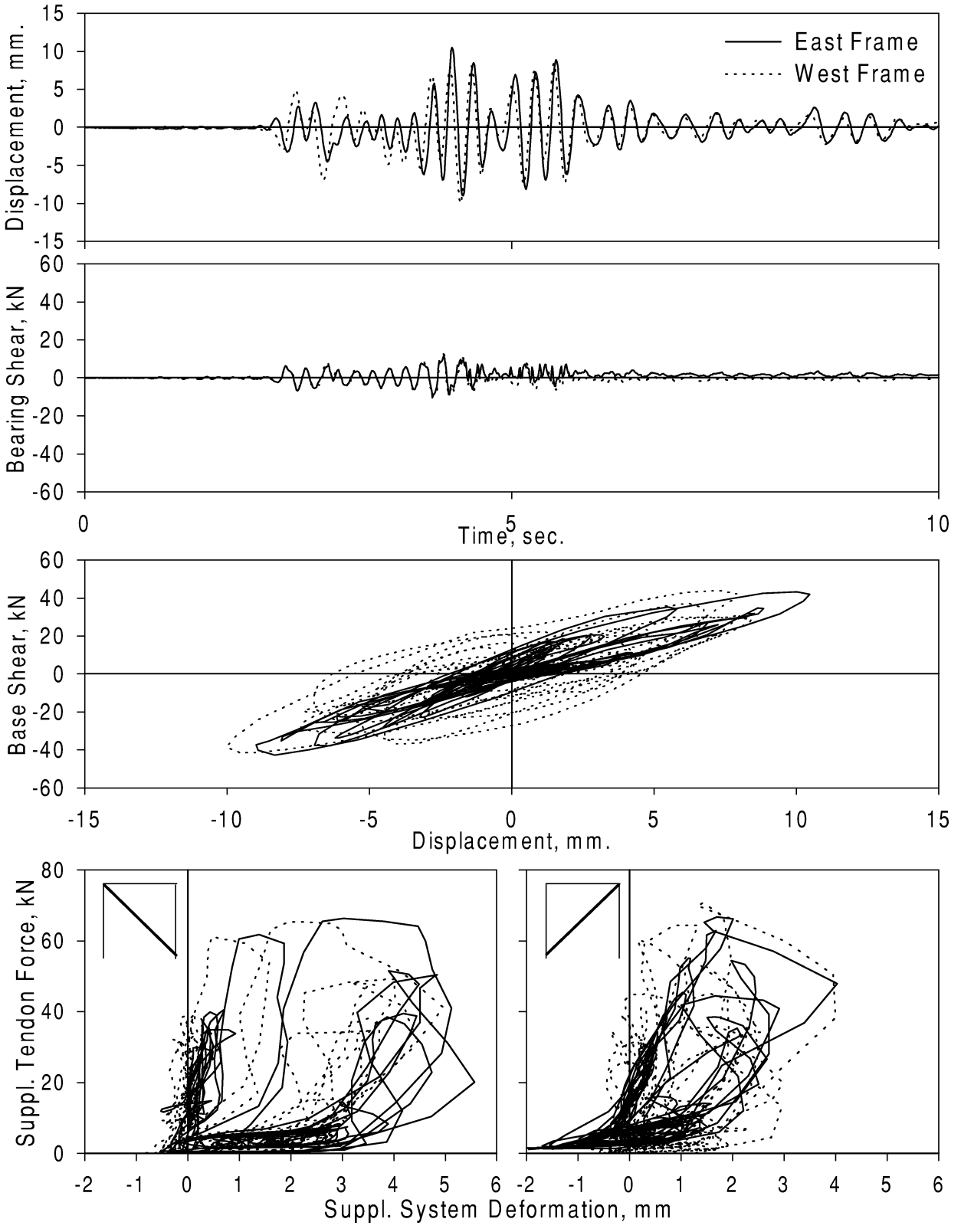

Figure A-30. Experimental Results - KOPDFB
Ground Motion: Kobe (PGA=0.404 g)
Configuration: Retrofitted/Fuse-bars and Damper

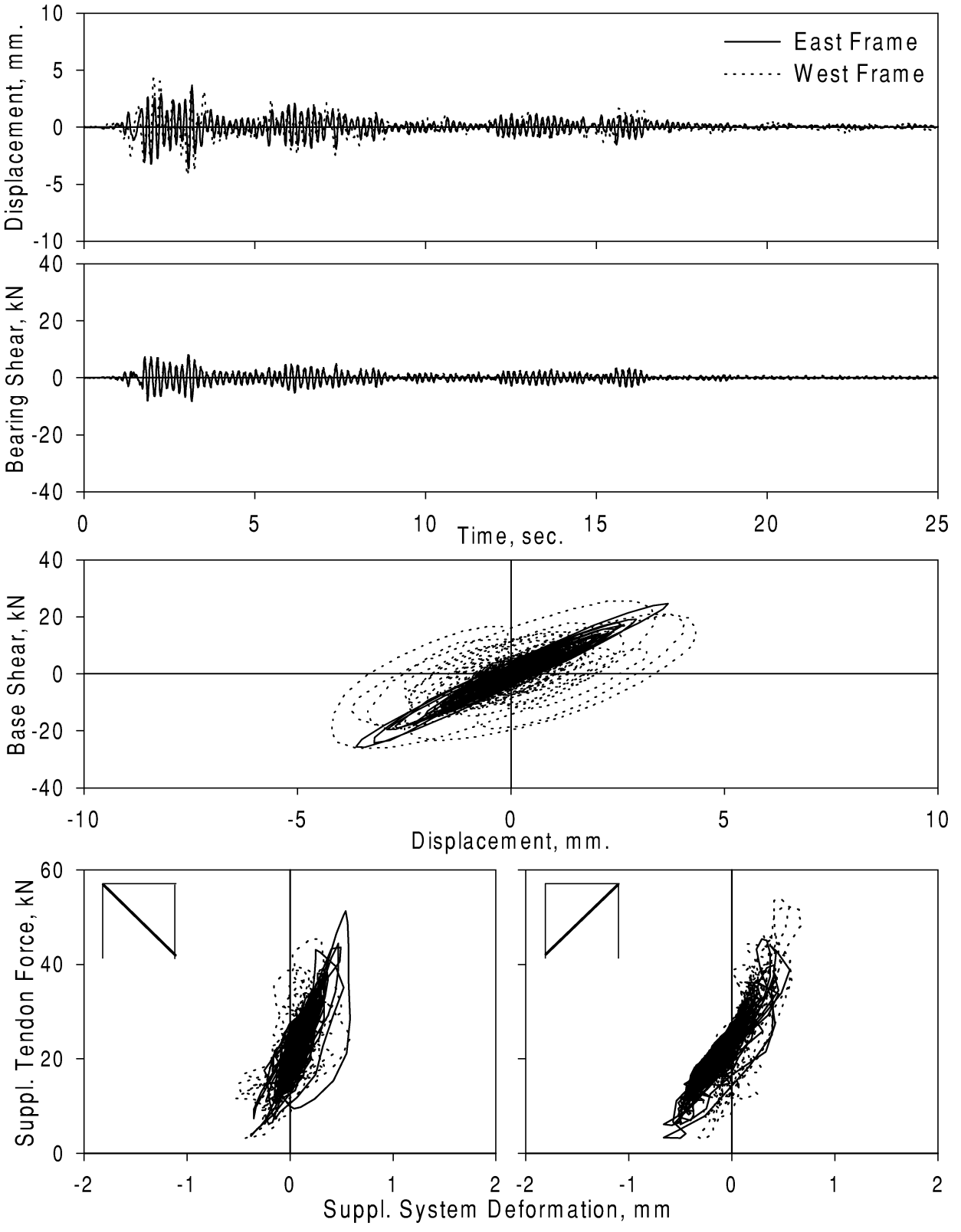

Figure A-31. Experimental Results - ELPDFC
Ground Motion: El Centro (PGA=0.260 g)
Configuration: Retrofitted/Fuse-bars and Damper

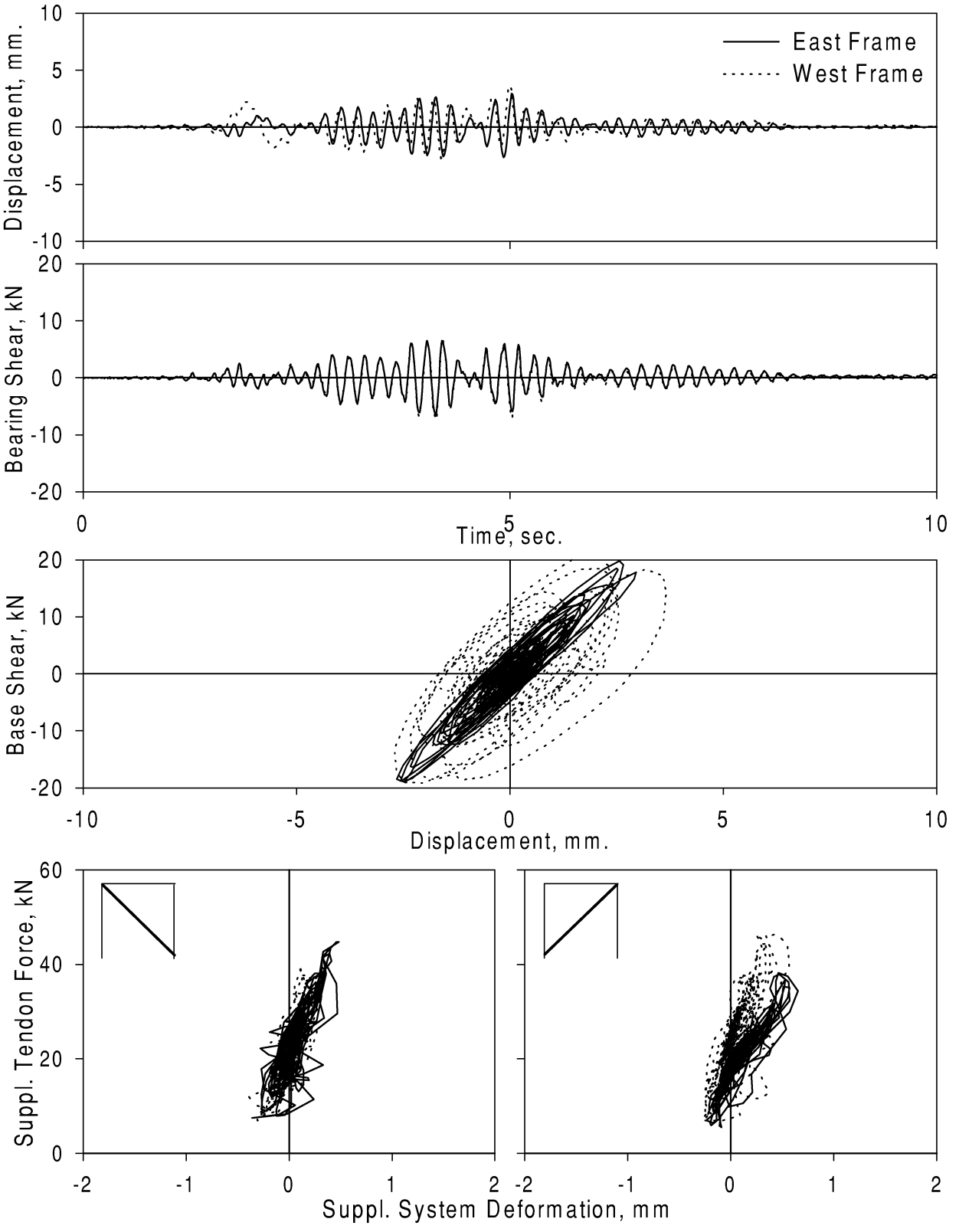

Figure A-32. Experimental Results - PAPDFC
Ground Motion: Pacoima Dam (PGA=0.200 g)
Configuration: Retrofitted/Fuse-bars and Damper

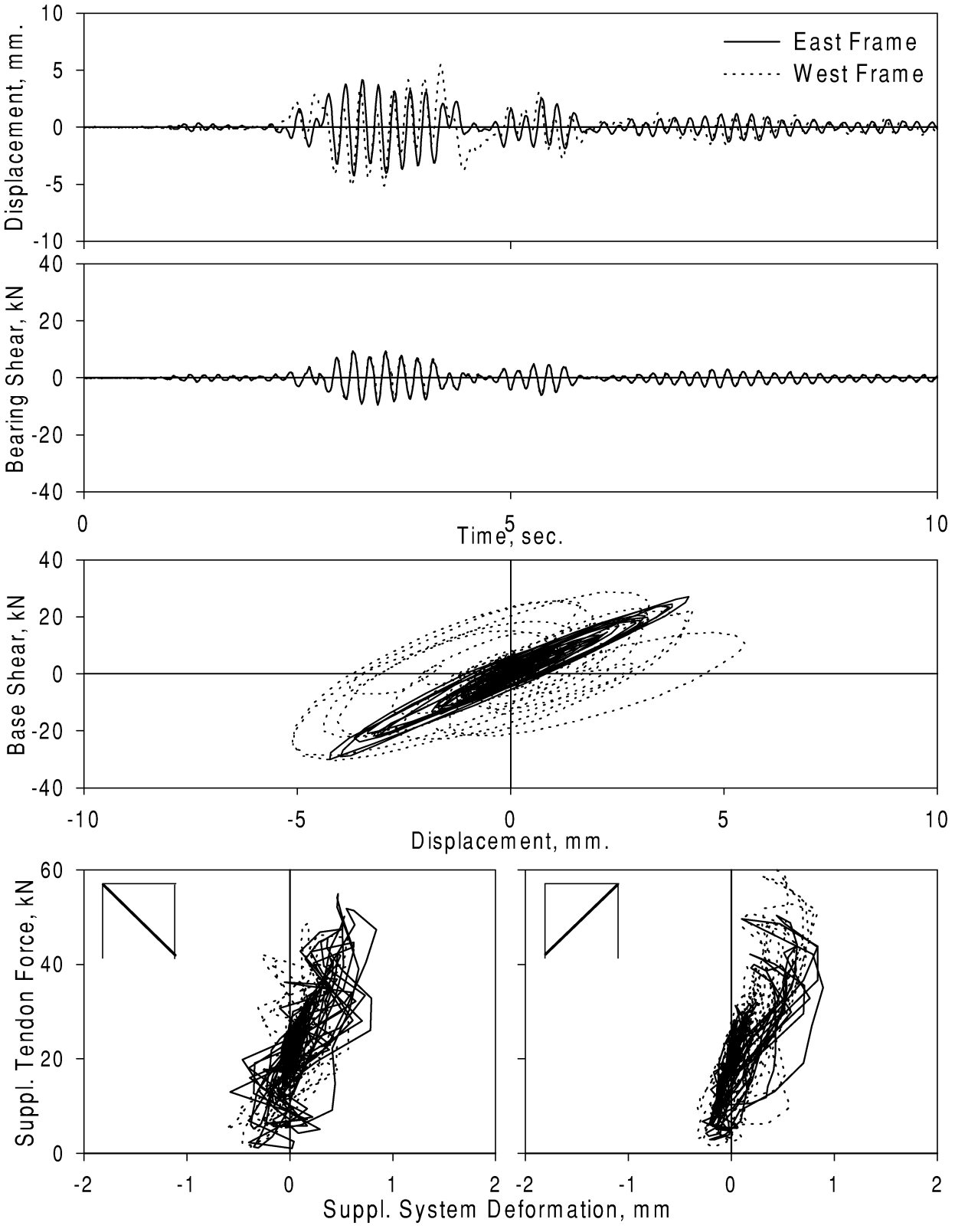

Figure A-33. Experimental Results - SYPDFC
Ground Motion: Sylmar (PGA=0.300 g)
Configuration: Retrofitted/Fuse-bars and Damper

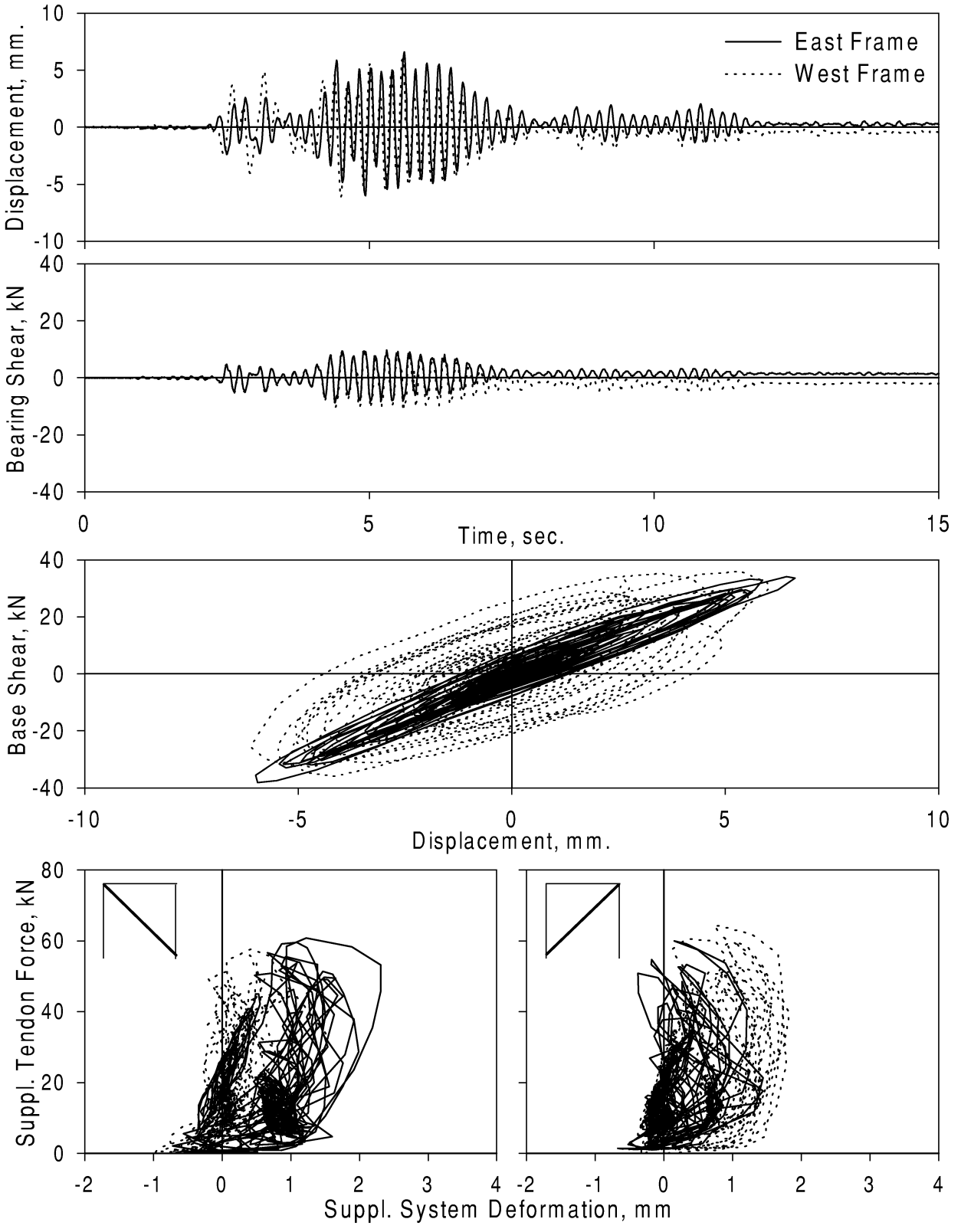

Figure A-34. Experimental Results - KOPDFC
Ground Motion: Kobe (PGA=0.311 g)
Configuration: Retrofitted/Fuse-bars and Damper

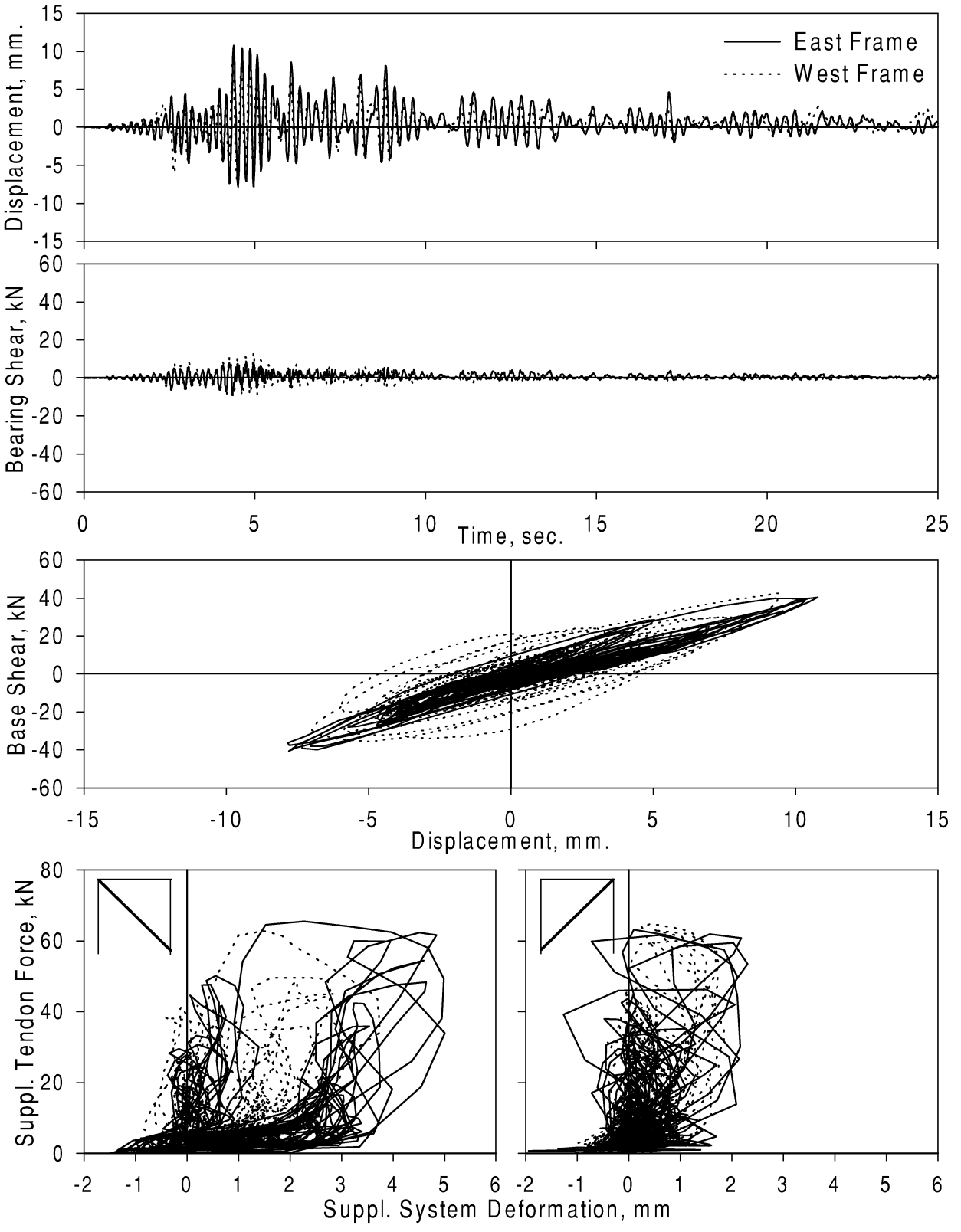

Figure A-35. Experimental Results - TAPDFC
Ground Motion: Taft (PGA=0.450 g)
Configuration: Retrofitted/Fuse-bars and Damper

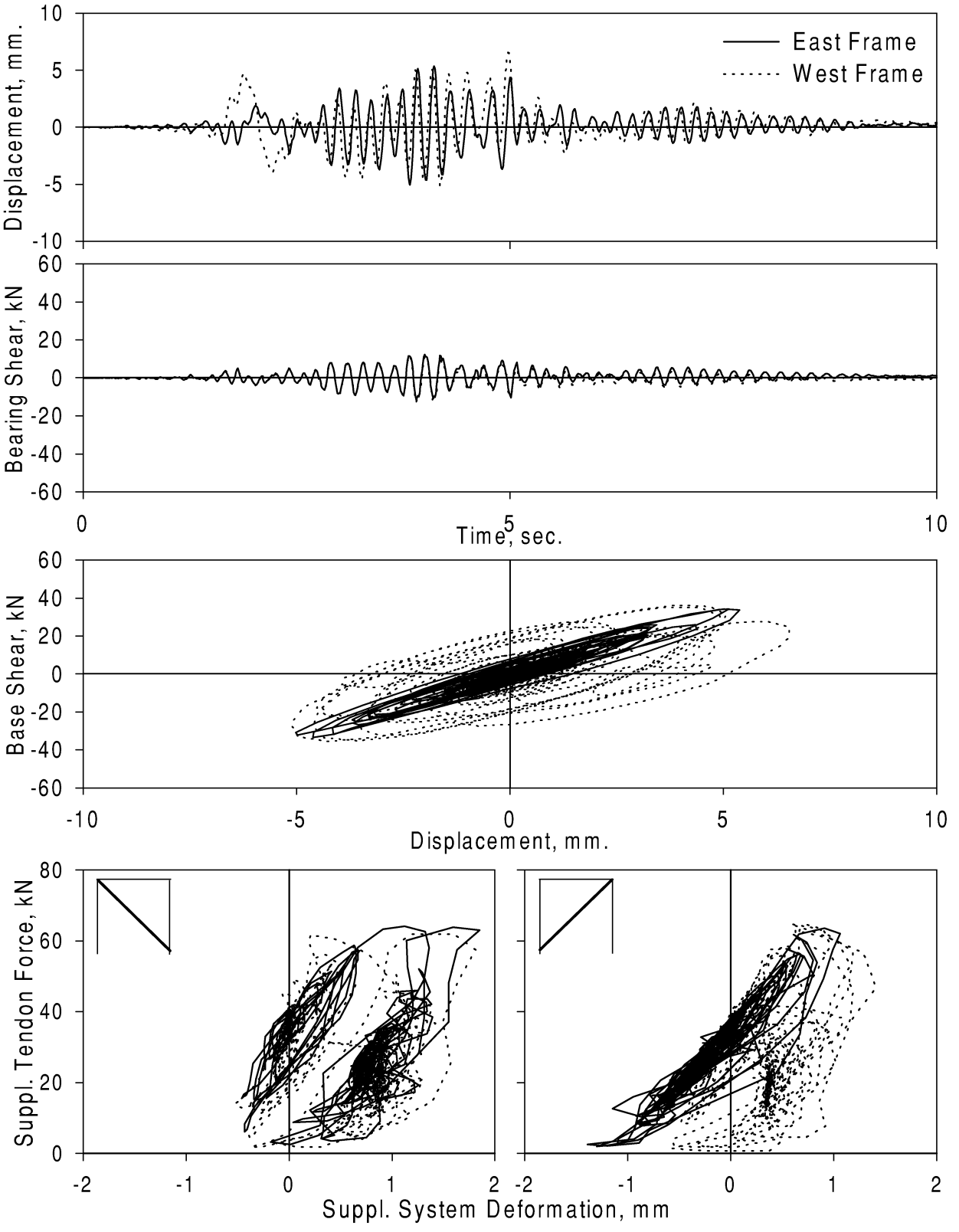

Figure A-36. Experimental Results - PAPDFD
Ground Motion: Pacoima Dam (PGA=0.422 g)
Configuration: Retrofitted/Fuse-bars and Damper

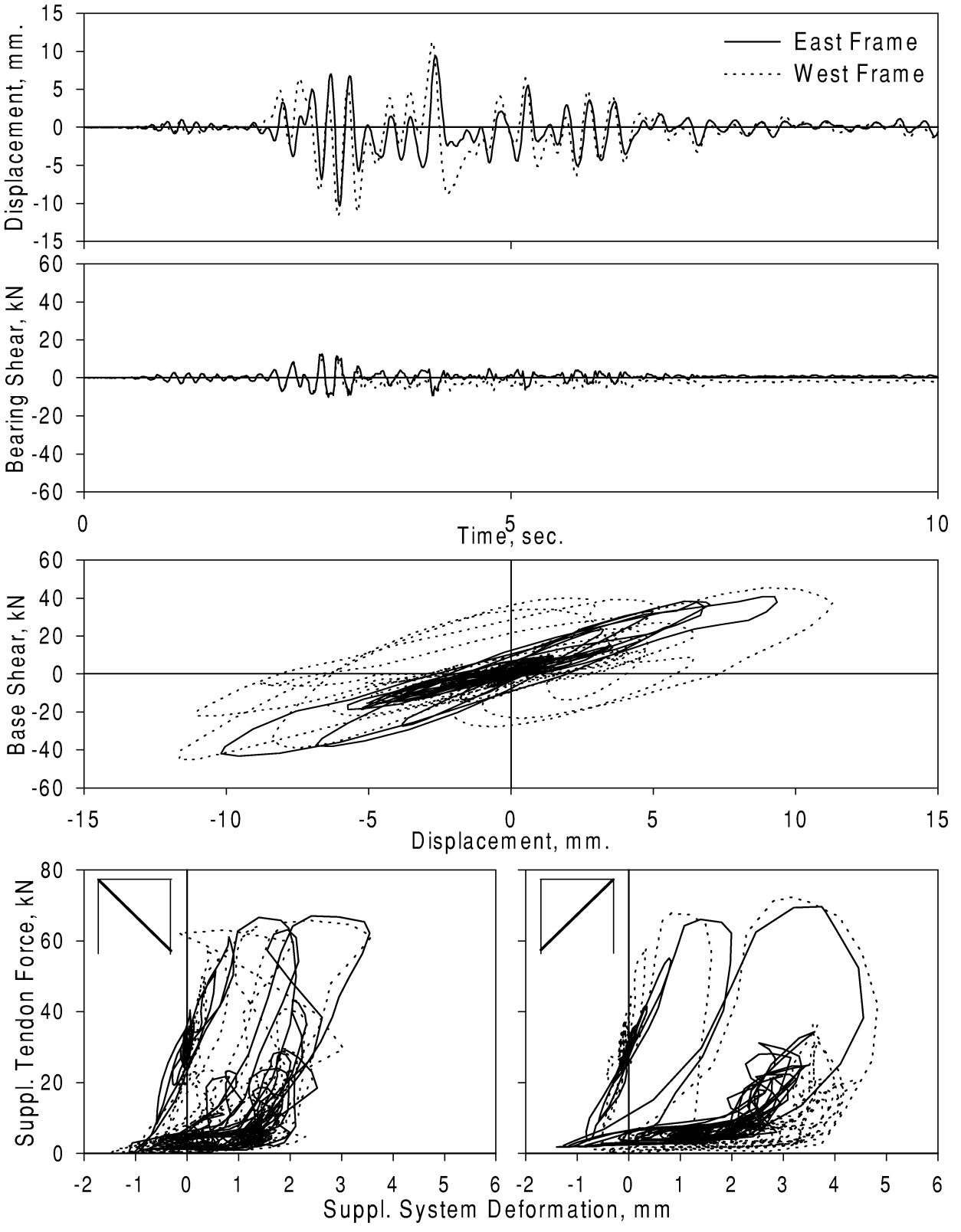

Figure A-37. Experimental Results - SYPDFD
Ground Motion: Sylmar (PGA=0.561 g)
Configuration: Retrofitted/Fuse-bars and Damper

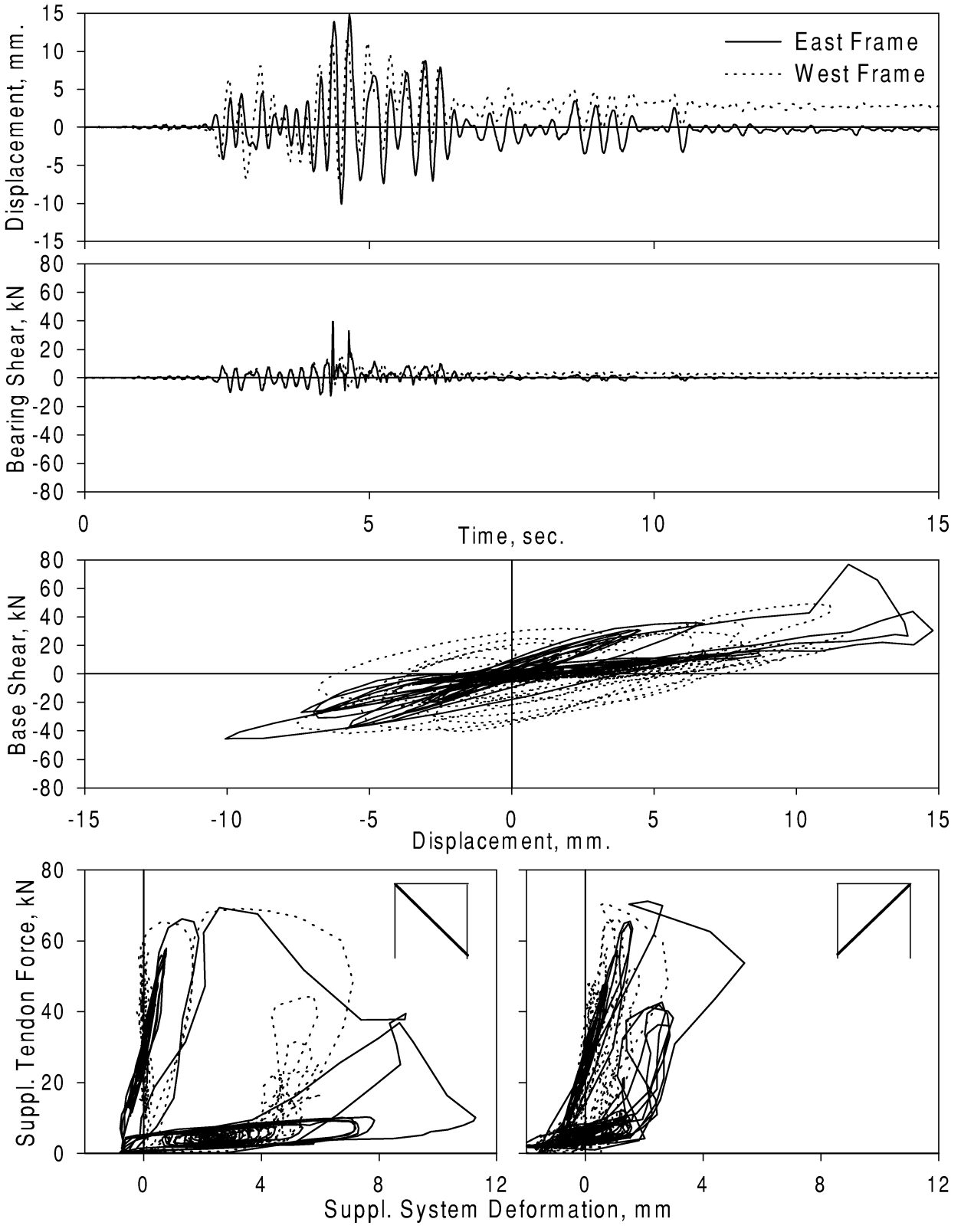

Figure A-38. Experimental Results - KOPDFD
Ground Motion: Kobe (PGA=0.577 g)
Configuration: Retrofitted/Fuse-bars and Damper

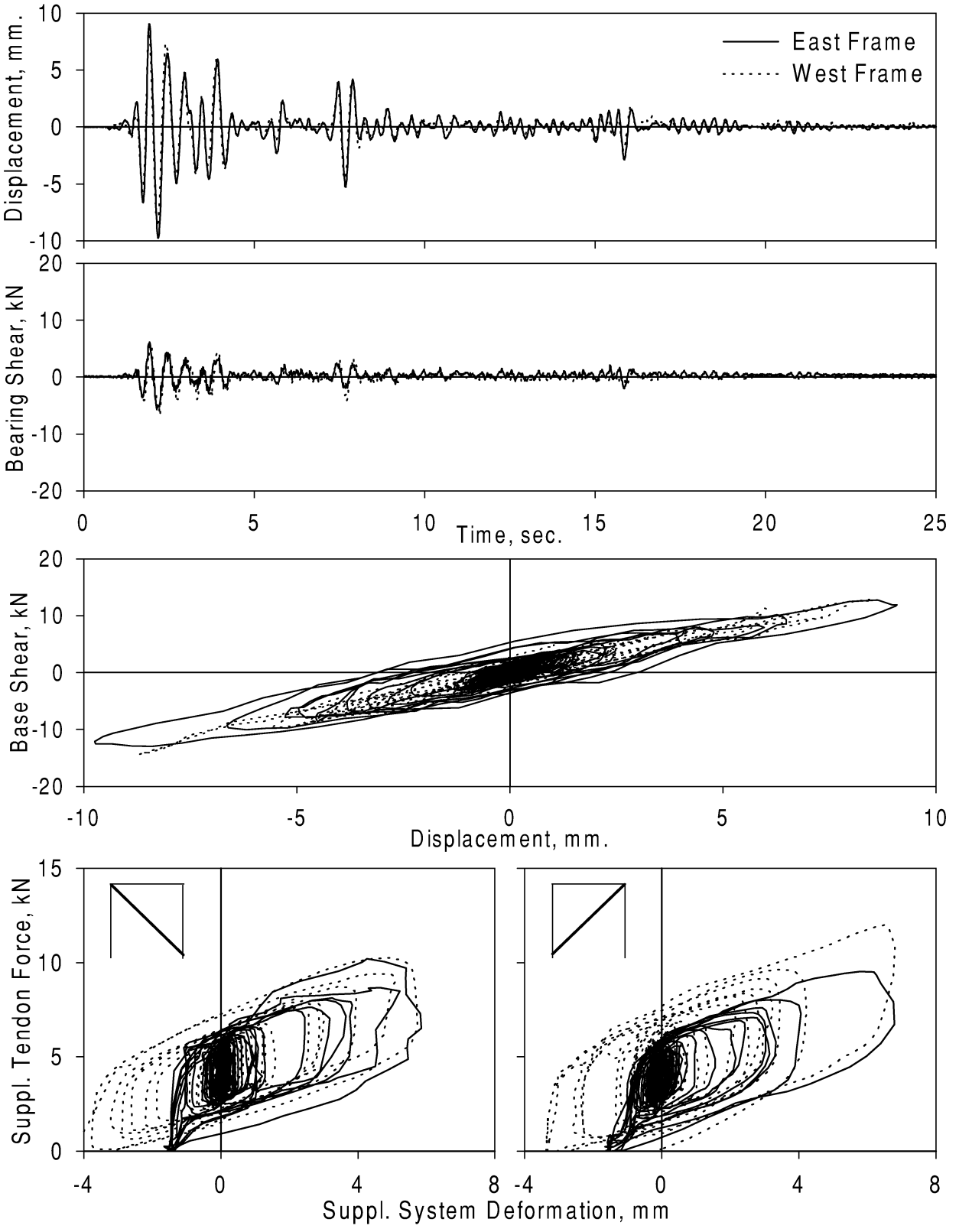

Figure A-39. Experimental Results - E2PRDA
Ground Motion: El Centro (PGA=0.187 g)
Configuration: Retrofitted/Dampers only

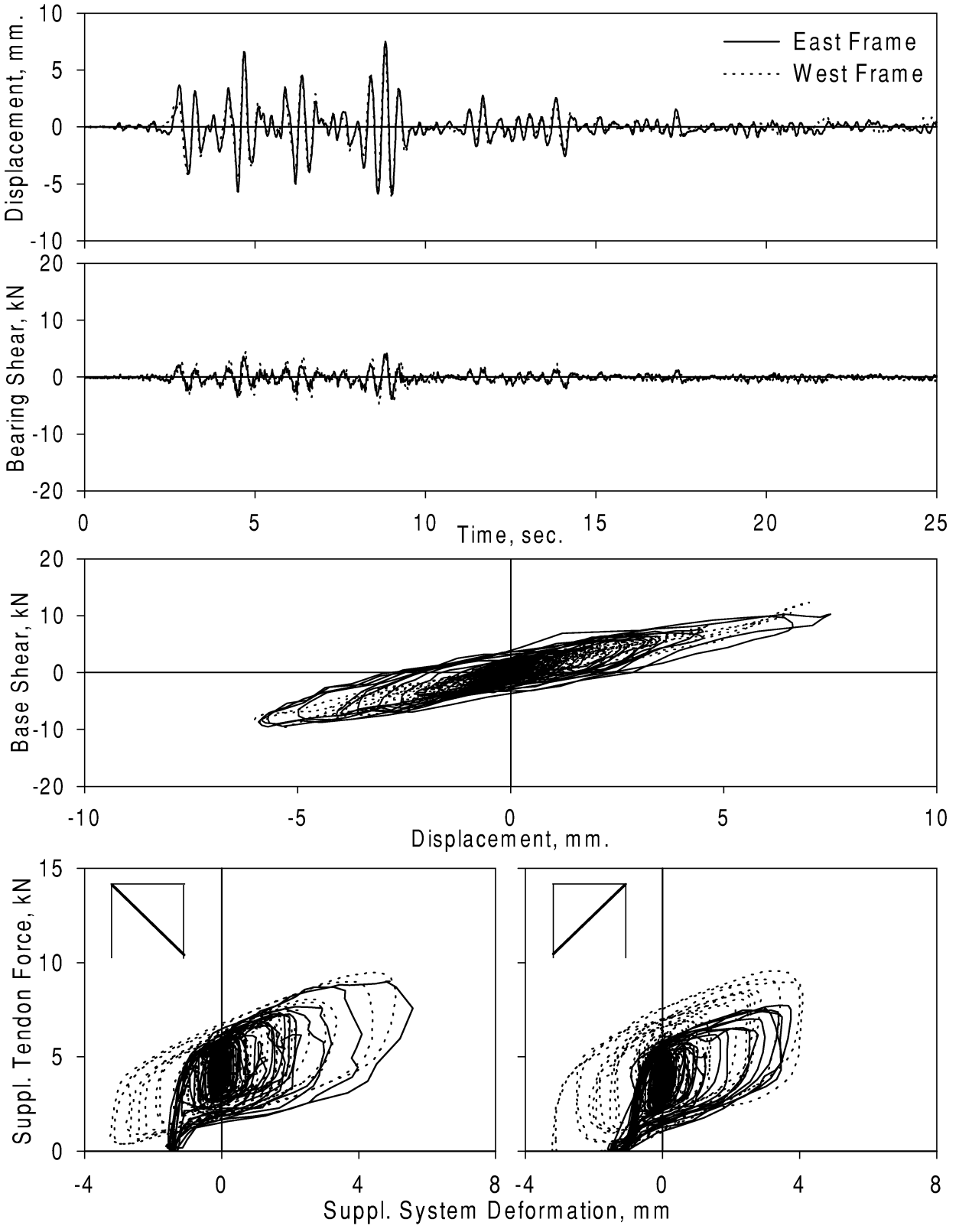

Figure A-40. Experimental Results - T2PRDA
Ground Motion: Taft (PGA=0.151 g)
Configuration: Retrofitted/Dampers only

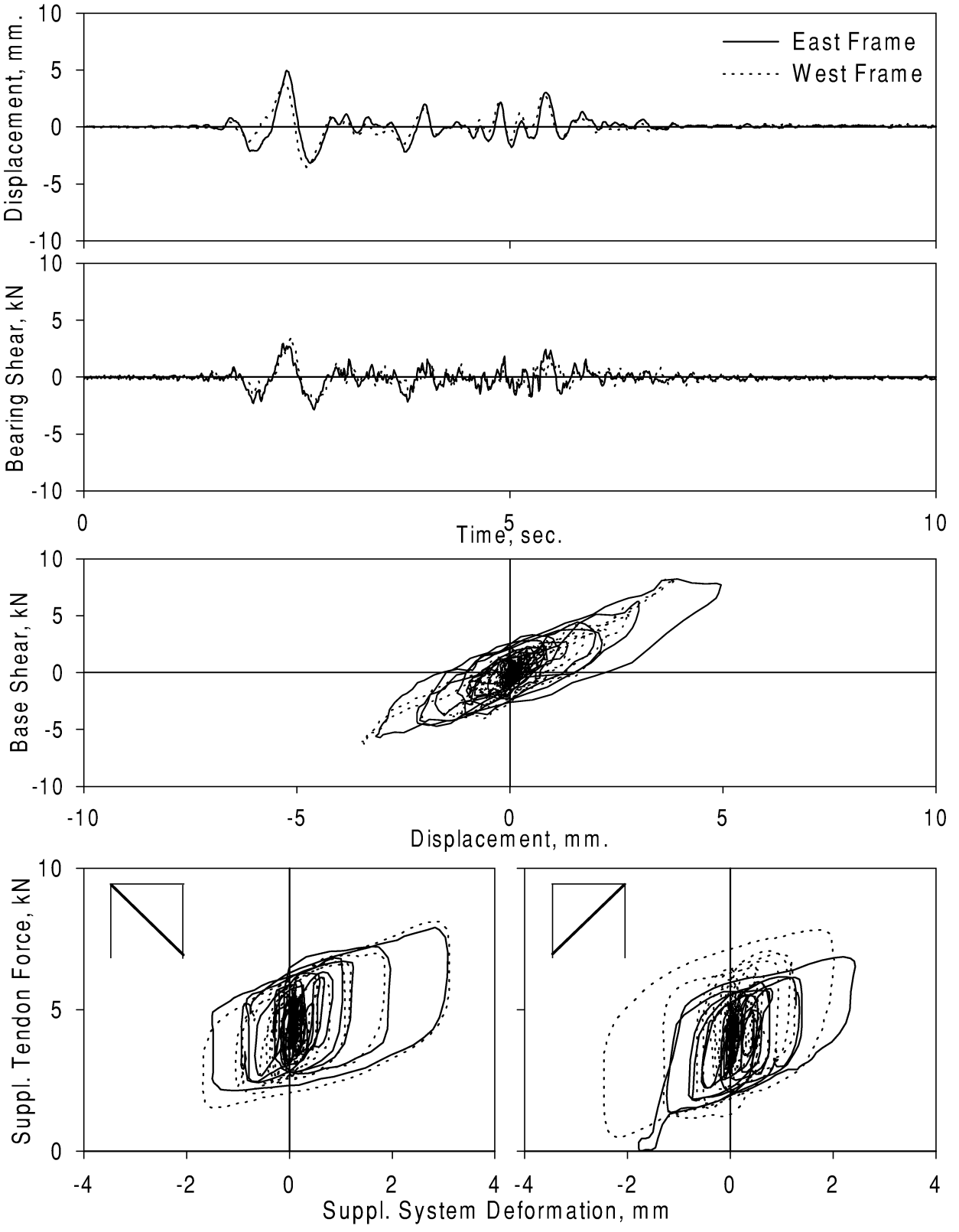

Figure A-41. Experimental Results - P2PRDA
Ground Motion: Pacoima Dam (PGA=0.164 g)
Configuration: Retrofitted/Dampers only

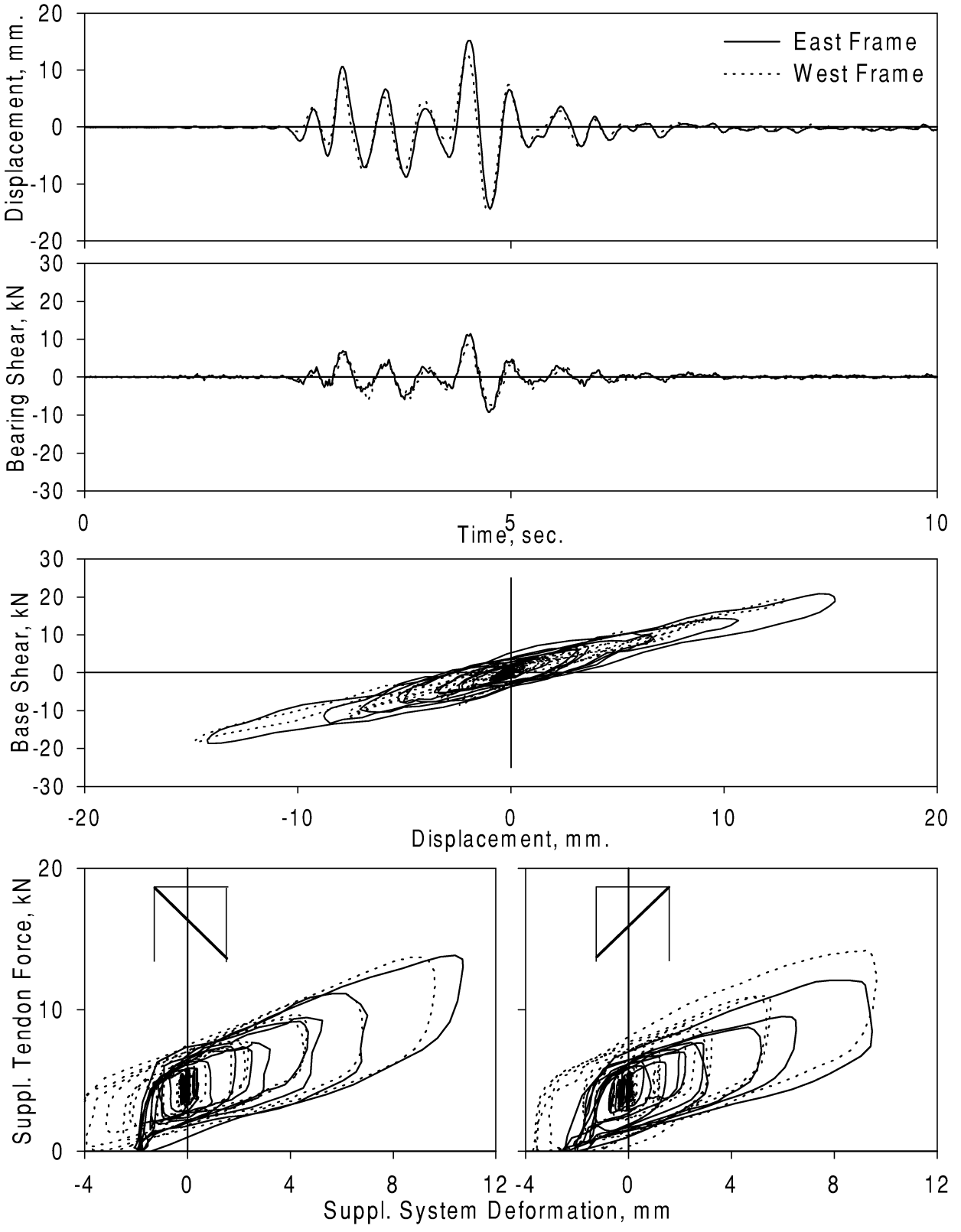

Figure A-42. Experimental Results - S2PRDA
Ground Motion: Sylmar (PGA=0.255 g)
Configuration: Retrofitted/Dampers only

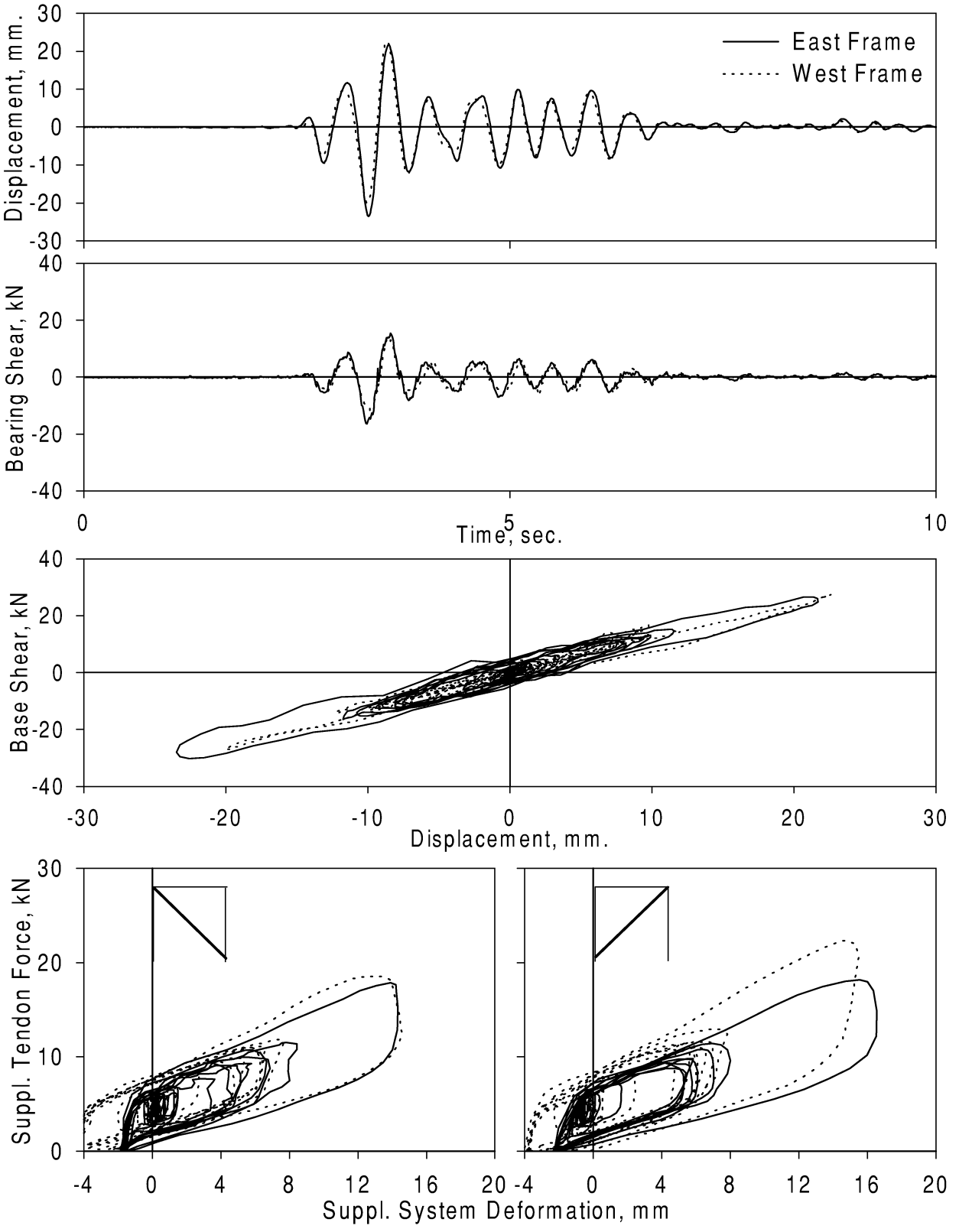

Figure A-43. Experimental Results - K2PRDA
Ground Motion: Kobe (PGA=0.258 g)
Configuration: Retrofitted/Dampers only

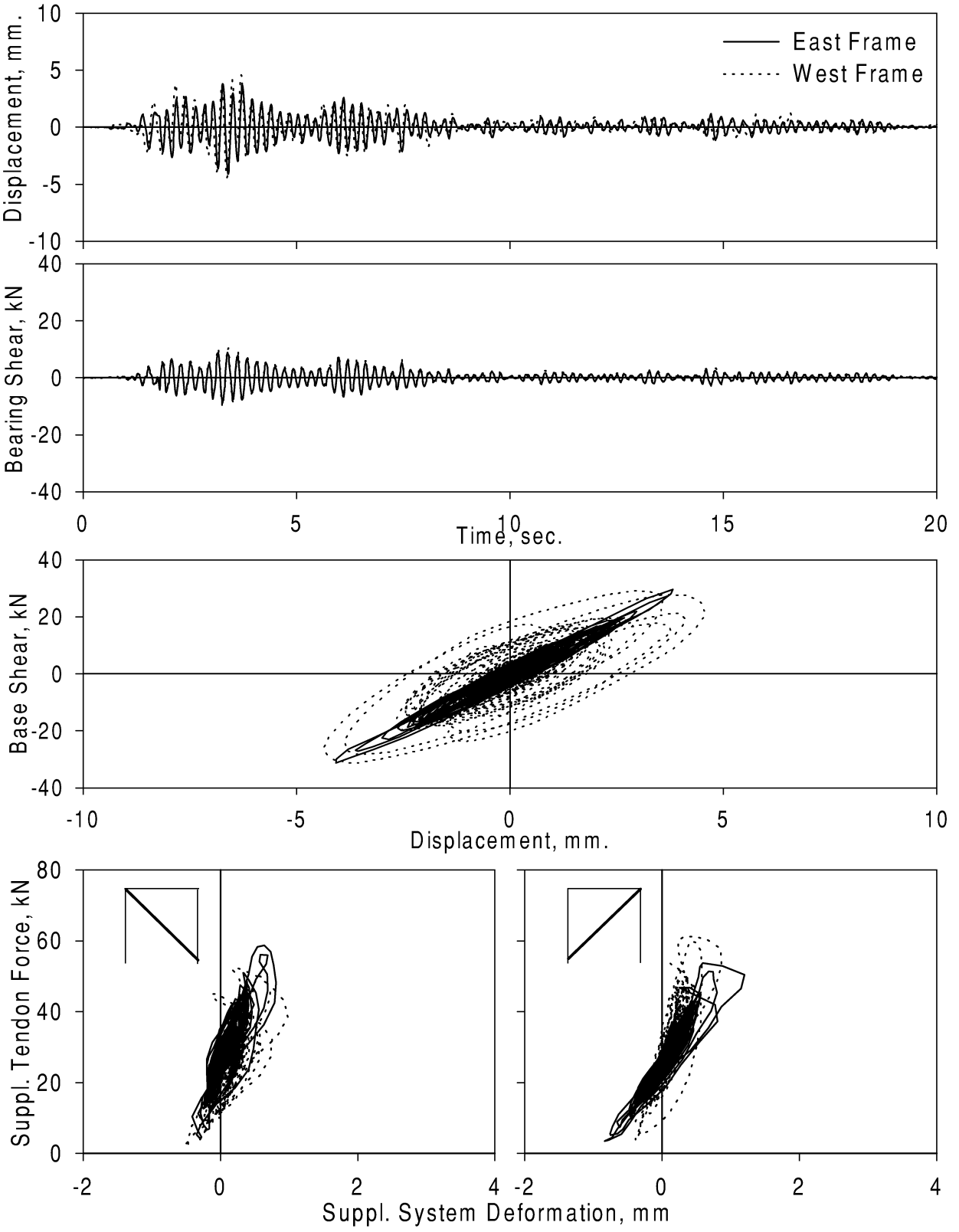

Figure A-44. Experimental Results - E2PDFA
Ground Motion: El Centro (PGA=0.193 g)
Configuration: Retrofitted/Fuse-Bars and Damper

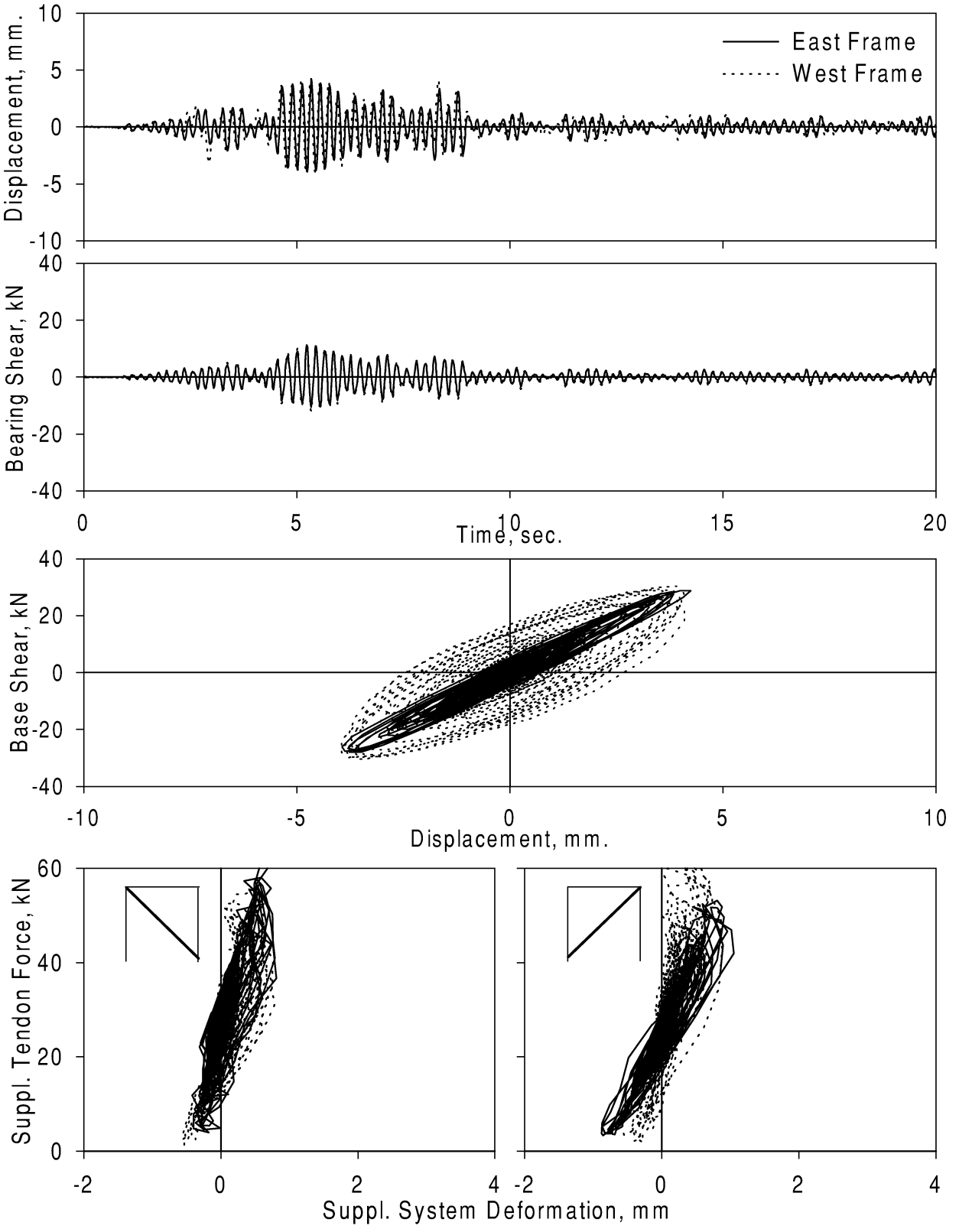

Figure A-45. Experimental Results - T2PDFA
Ground Motion: Taft (PGA=0.160 g)
Configuration: Retrofitted/Fuse-Bars and Damper

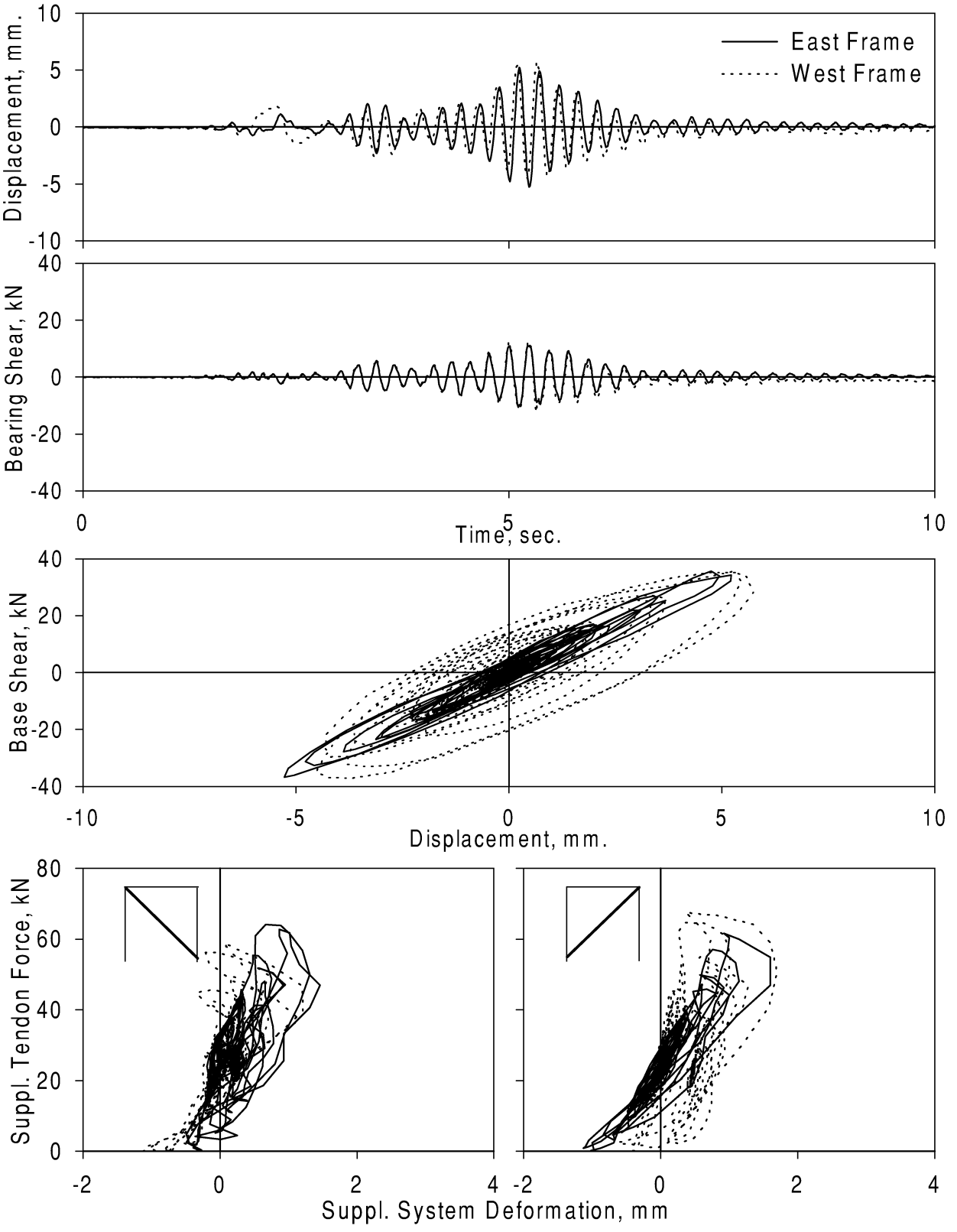

Figure A-46. Experimental Results - P2PDFA
Ground Motion: Pacoima Dam (PGA=0.190 g)
Configuration: Retrofitted/Fuse-Bars and Damper

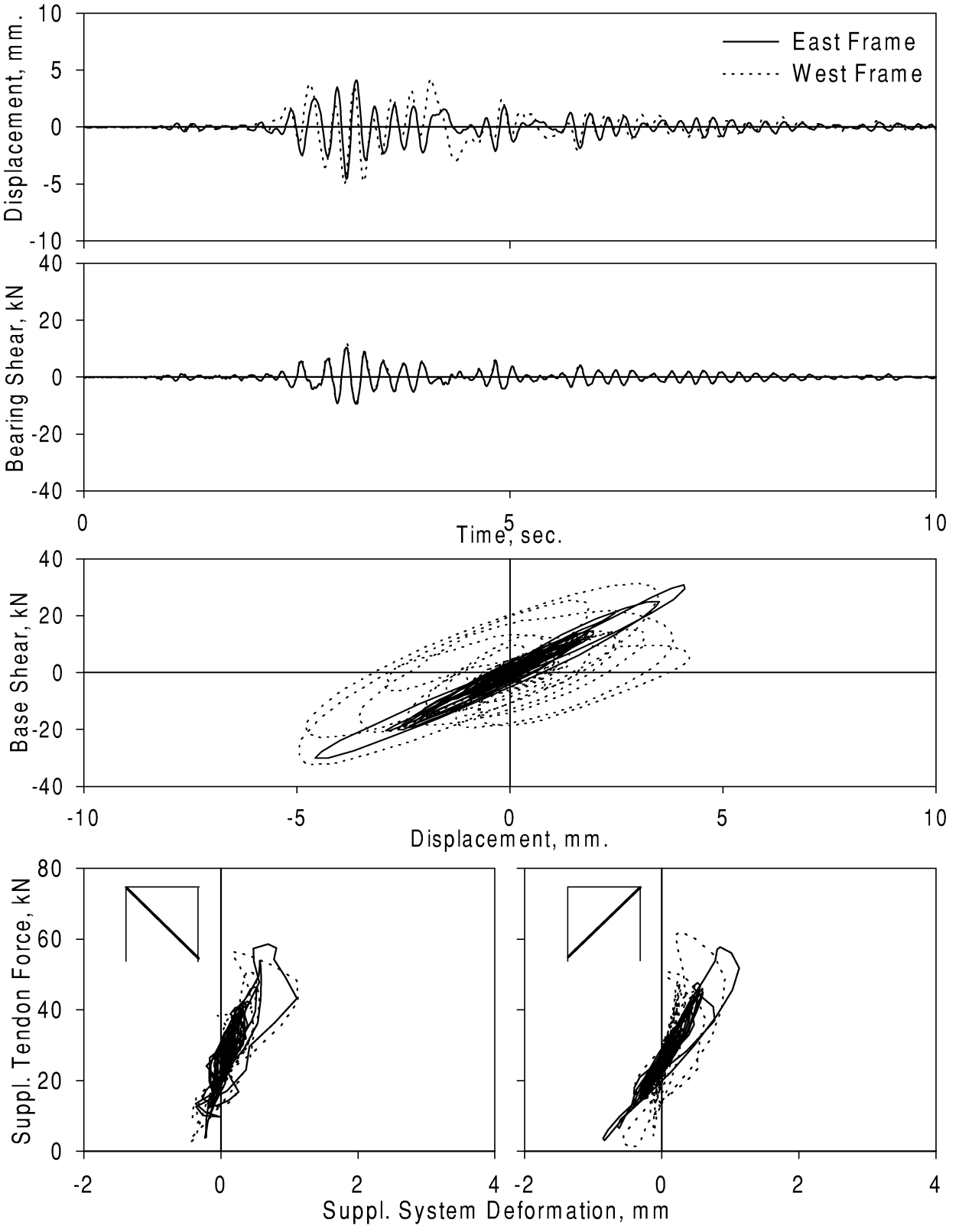

Figure A-47. Experimental Results - S2PDFA
Ground Motion: Sylmar (PGA=0.253 g)
Configuration: Retrofitted/Fuse-Bars and Damper

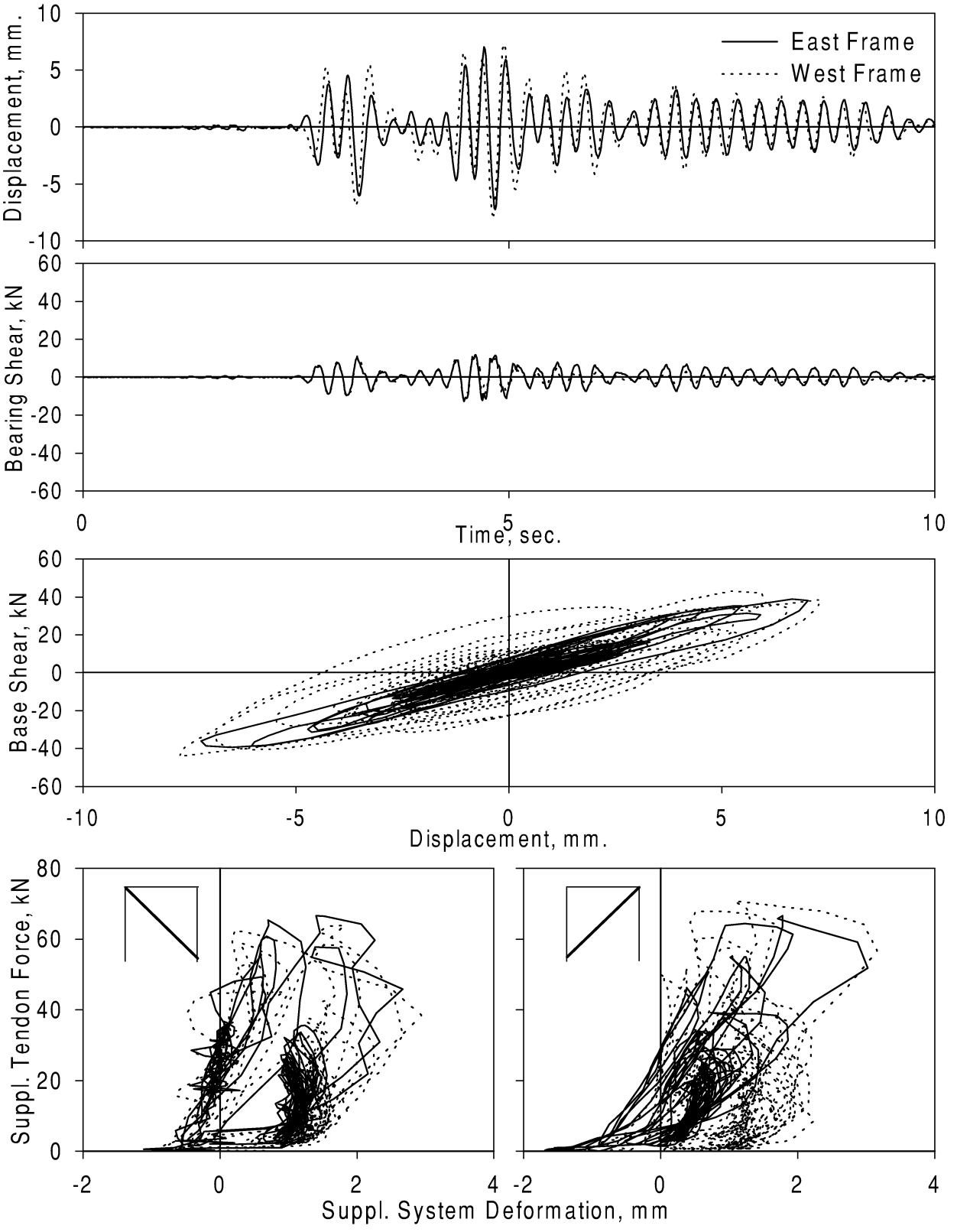

Figure A-48. Experimental Results - K2PDFA
Ground Motion: Kobe (PGA=0.336 g)
Configuration: Retrofitted/Fuse-Bars and Damper

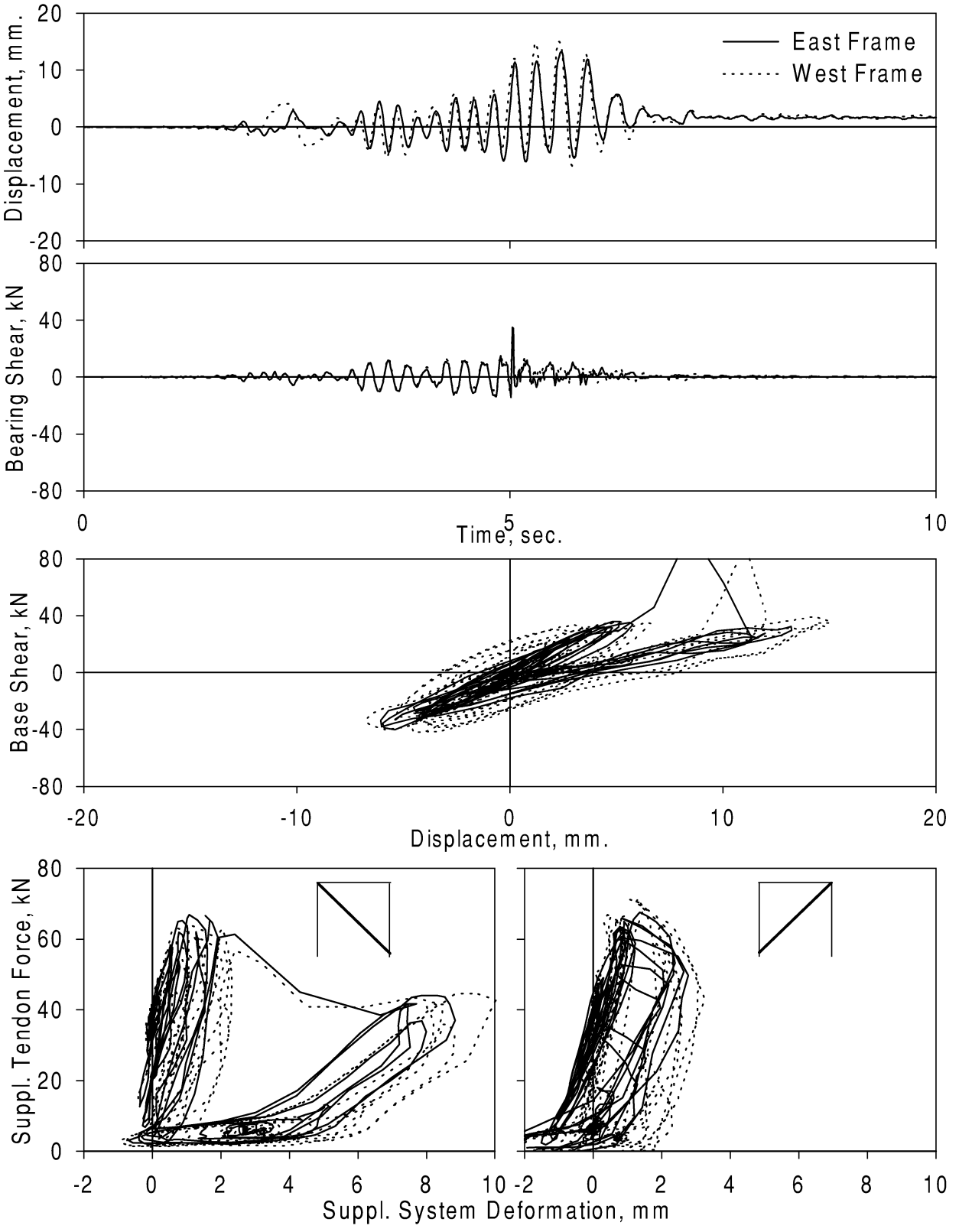

Figure A-49. Experimental Results - P2PDFB
Ground Motion: Pacoima (PGA=0.478 g)
Configuration: Retrofitted/Fuse-Bars and Damper

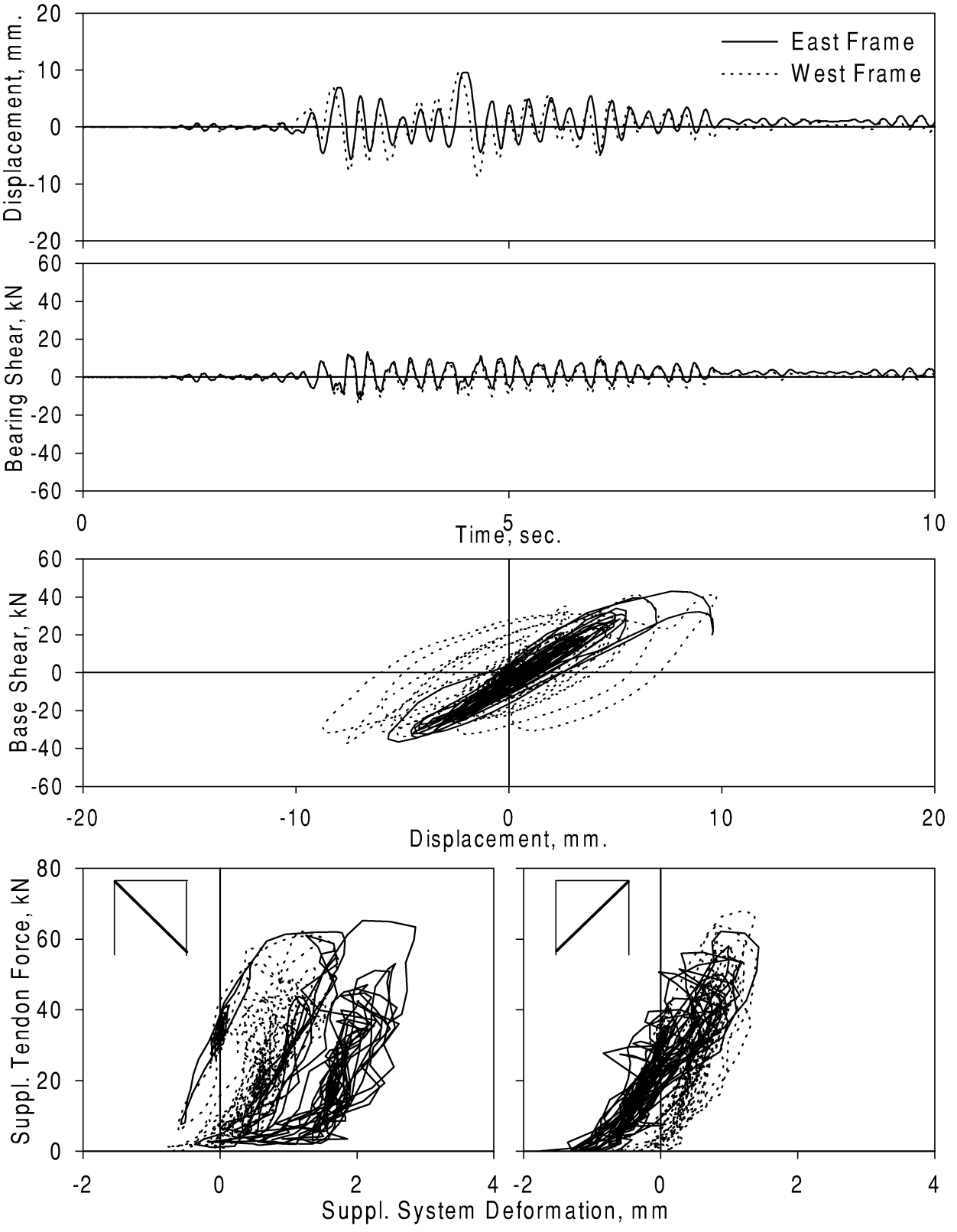

Figure A-50. Experimental Results - S2PDFB
Ground Motion: Sylmar (PGA=0.439 g)
Configuration: Retrofitted/Fuse-Bars and Damper

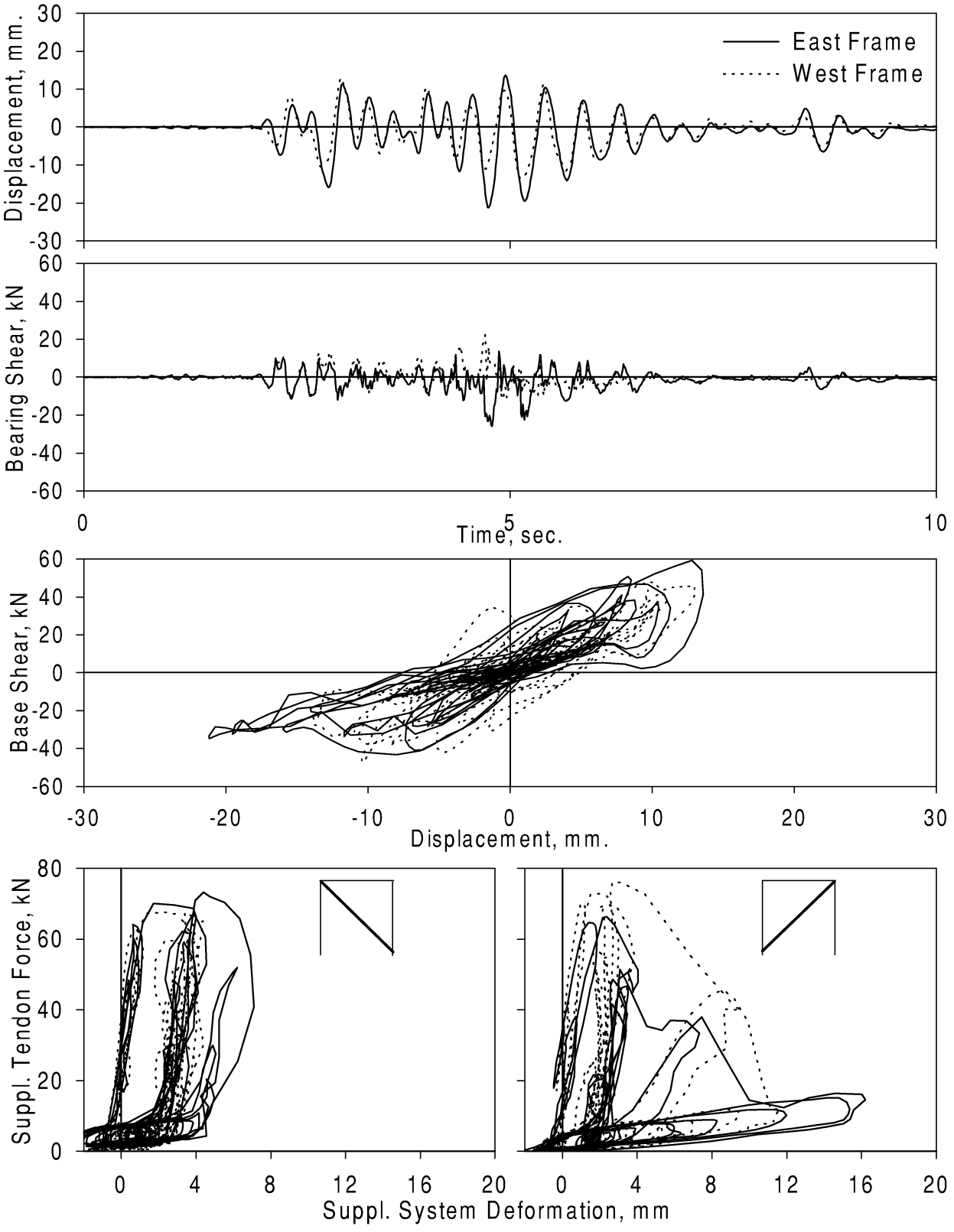

Figure A-51. Experimental Results - K2PDFB
Ground Motion: Kobe (PGA=0.499 g)
Configuration: Retrofitted/Fuse-Bars and Damper

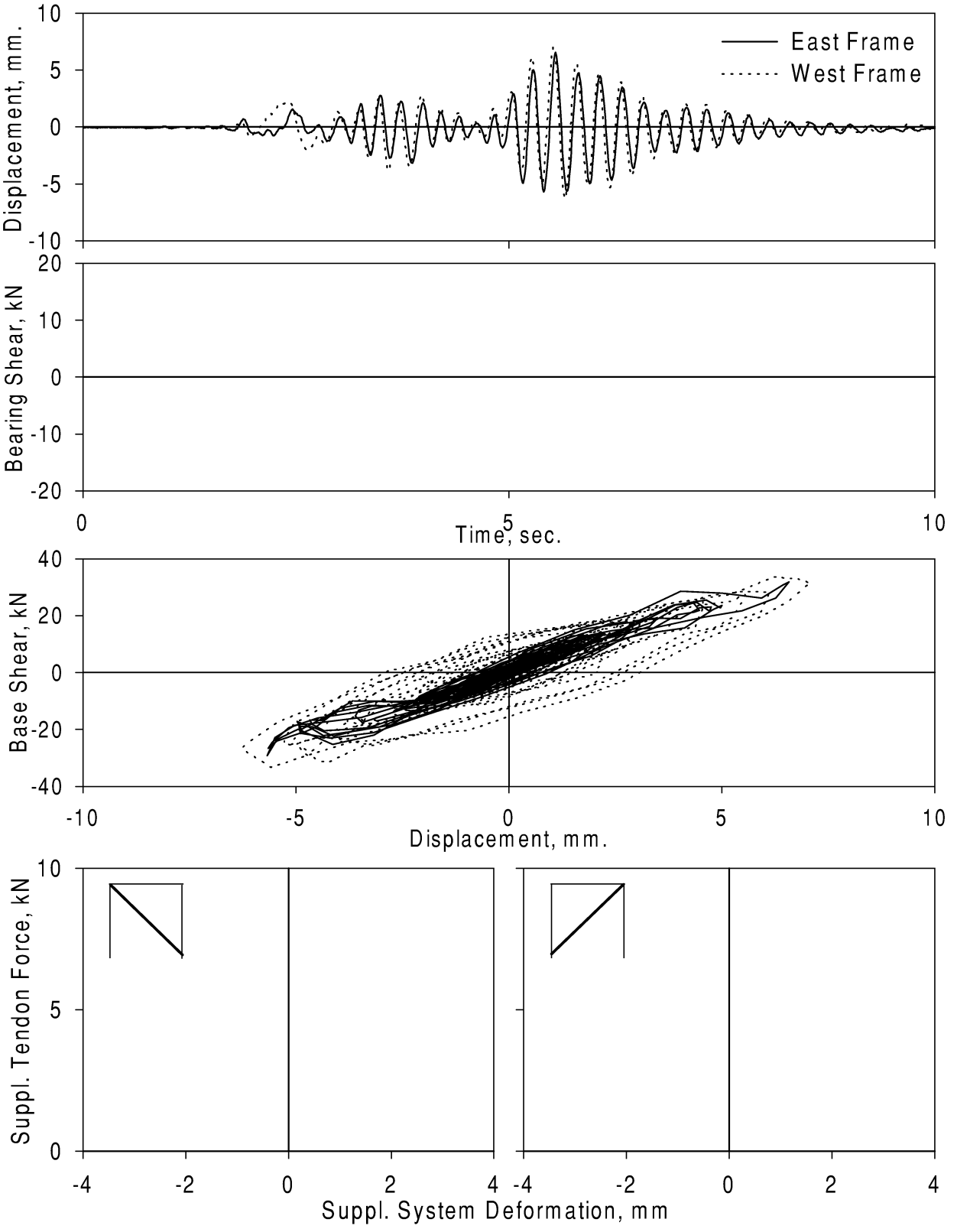

Figure A-52. Experimental Results - P2PRWB
Ground Motion: Pacoima Dam (PGA=0.247 g)
Configuration: w/Tendons (Bracing)

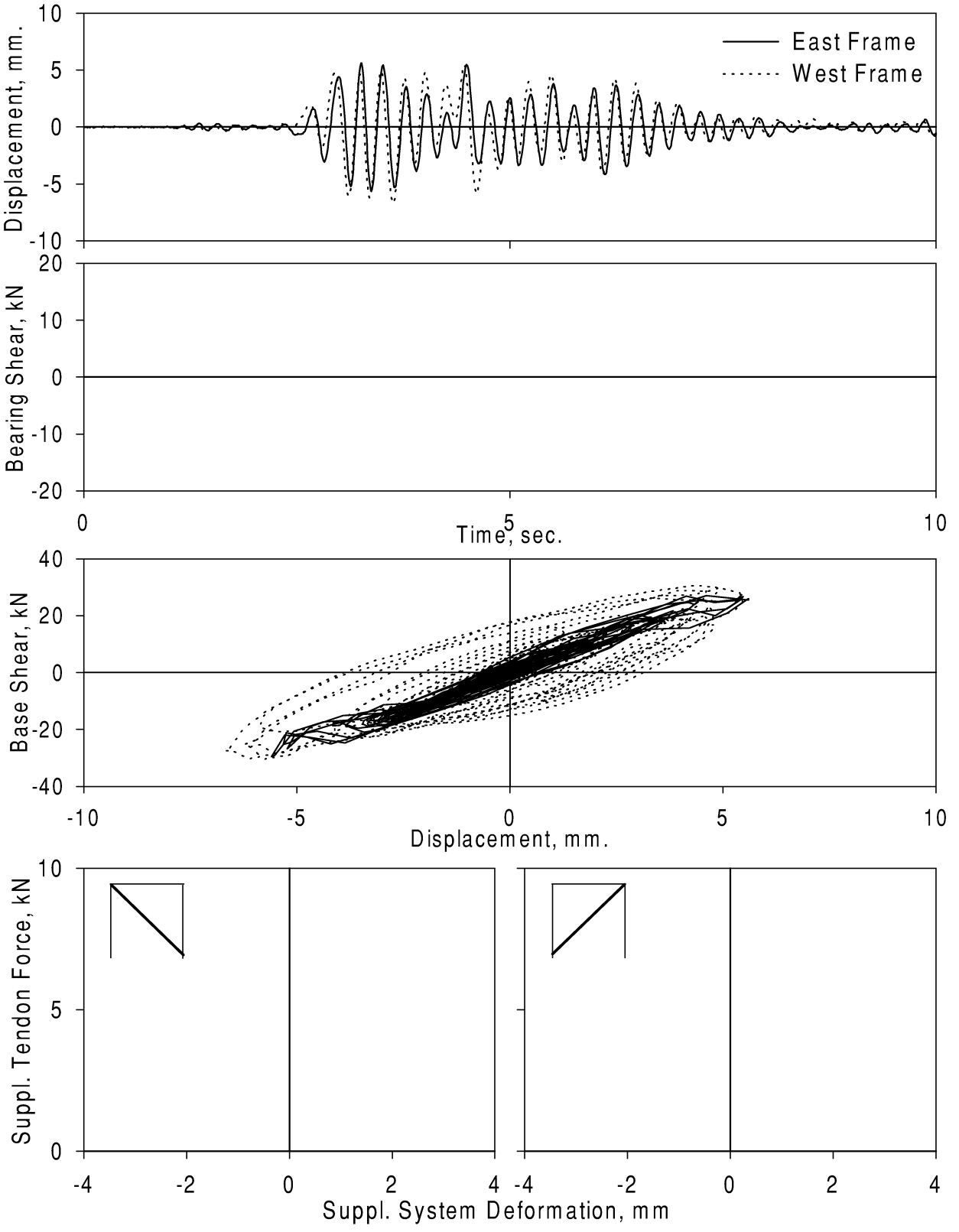

Figure A-53. Experimental Results - S2PRWB
Ground Motion: Sylmar (PGA=0.226 g)
Configuration: w/Tendons (Bracing)

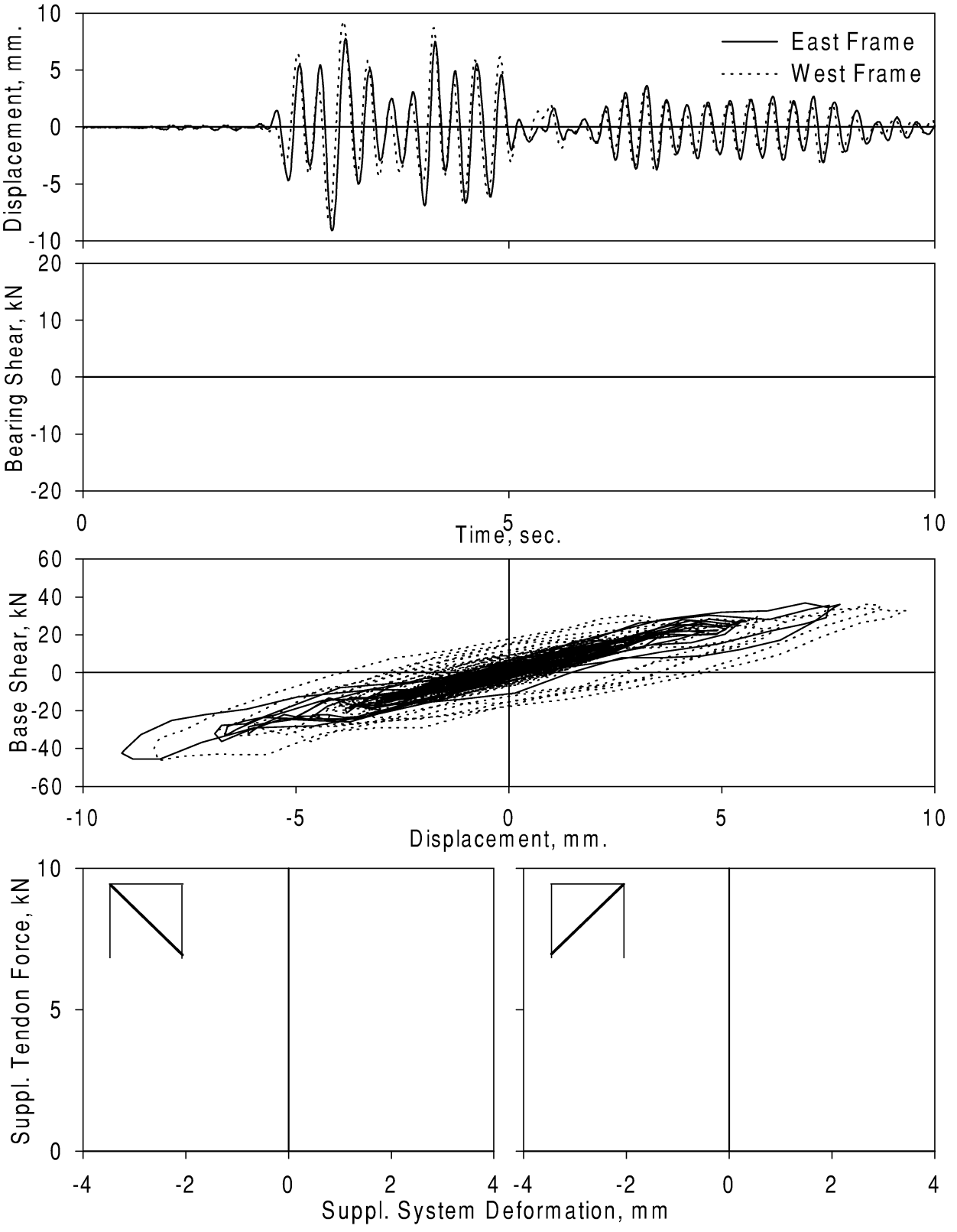

Figure A-54. Experimental Results - K2PRWB
Ground Motion: Kobe (PGA=0.291 g)
Configuration: w/Tendons (Bracing)

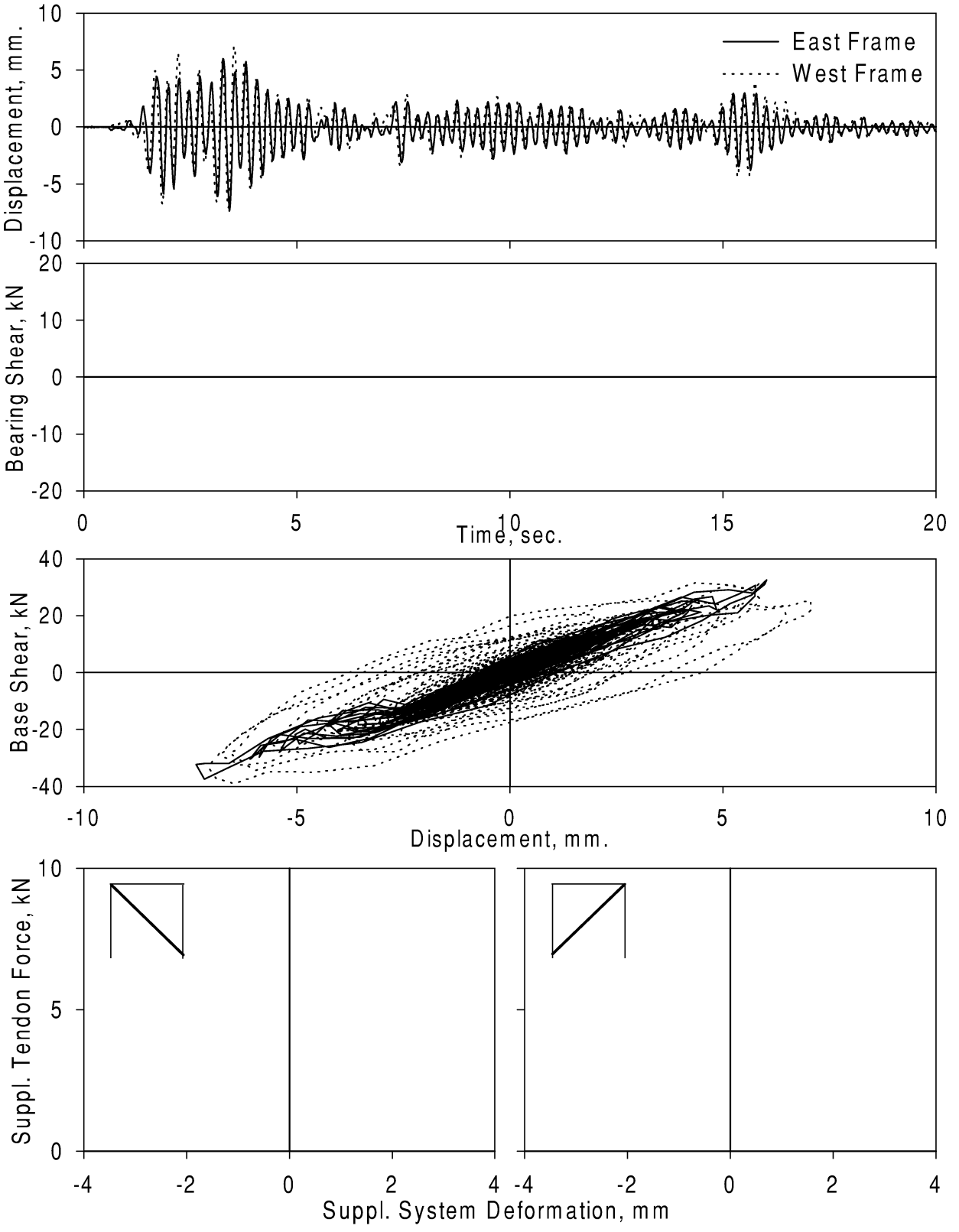

Figure A-55. Experimental Results - E2PRWB
Ground Motion: El Centro (PGA=0.286 g)
Configuration: w/Tendons (Bracing)

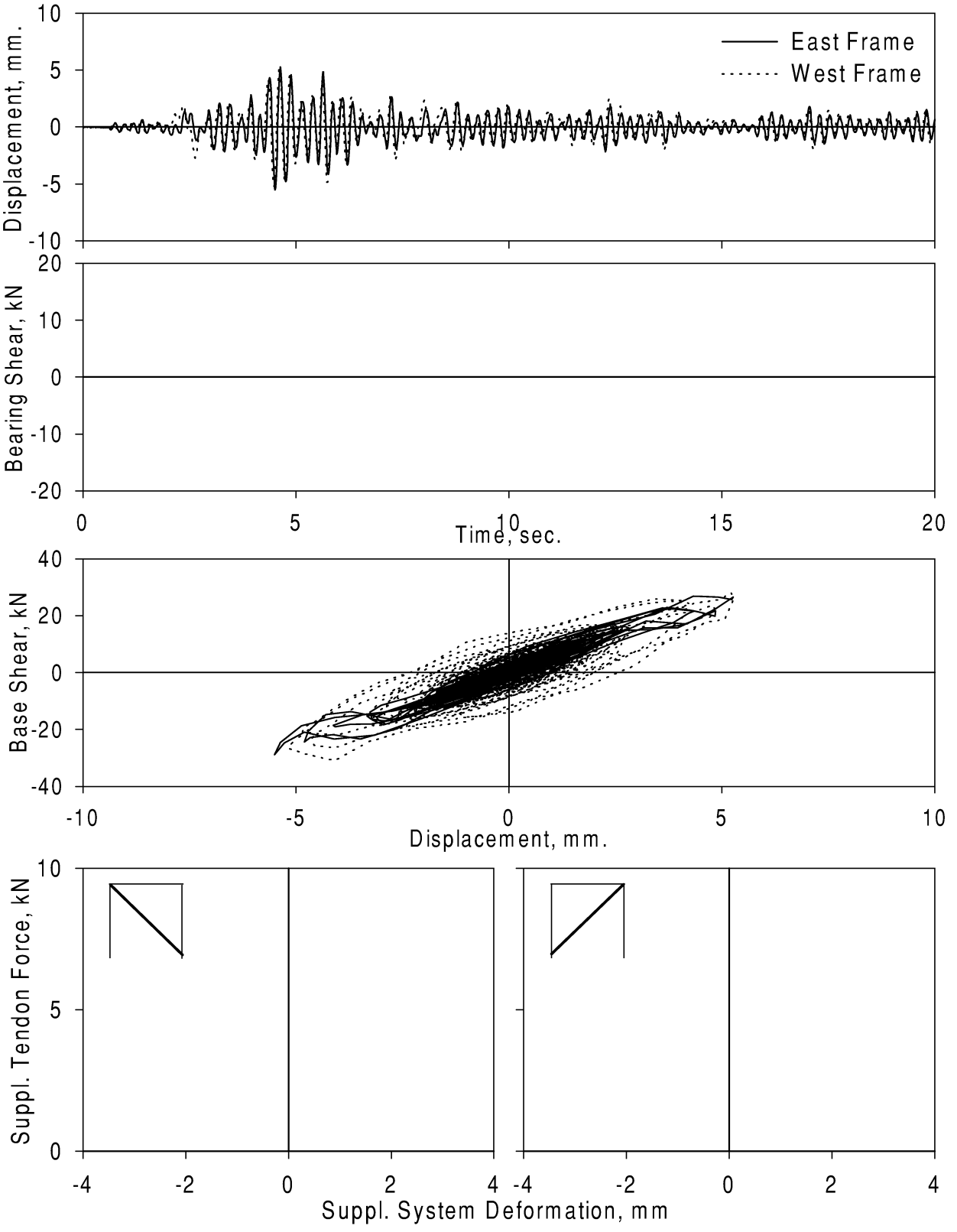

Figure A-56. Experimental Results - T2PRWB
Ground Motion: Taft (PGA=0.169 g)
Configuration: w/Tendons (Bracing)

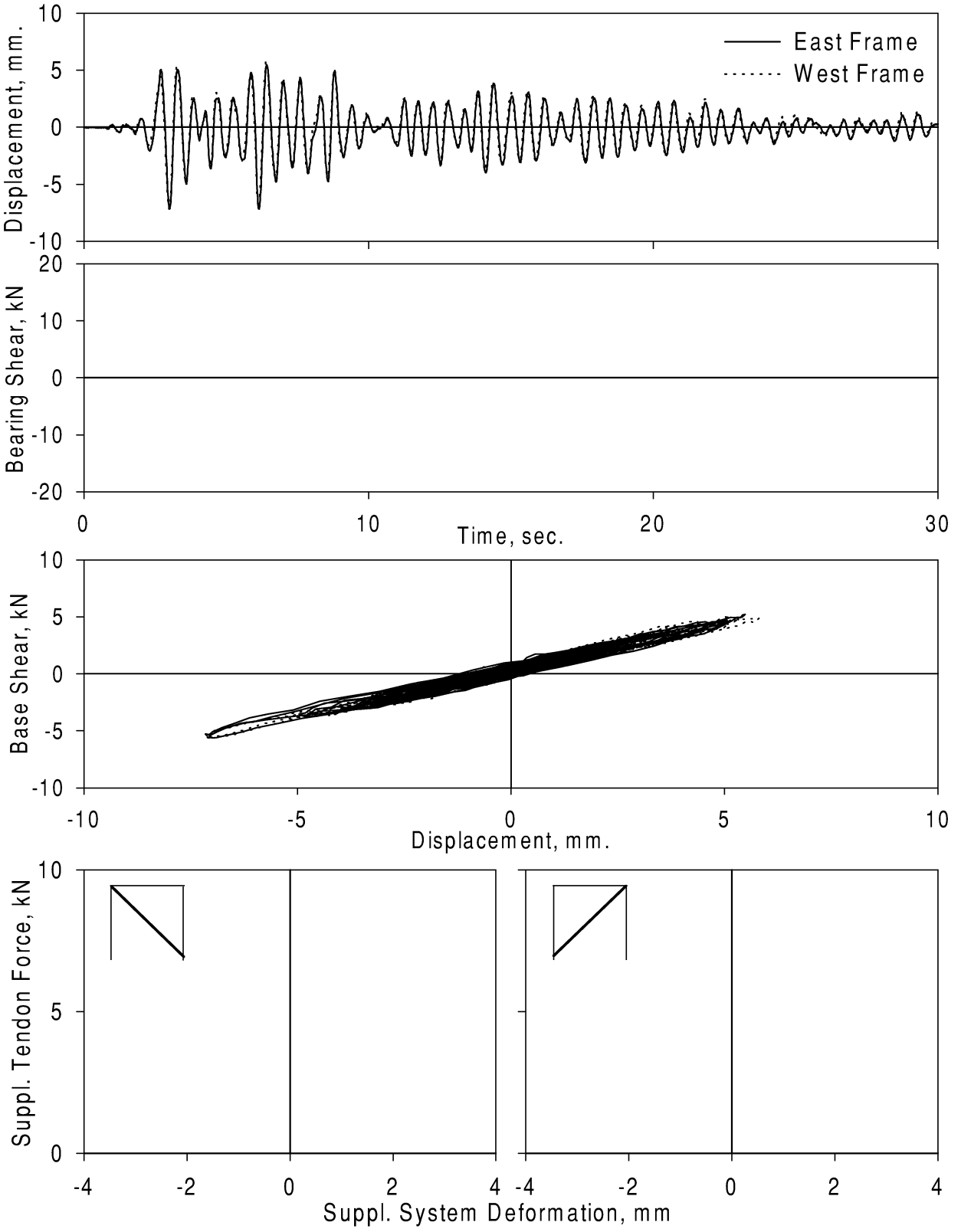

Figure A-57. Experimental Results - TANBXM
Ground Motion: Taft (PGA=0.077 g)
Configuration: Bare Frame w/ extra mass

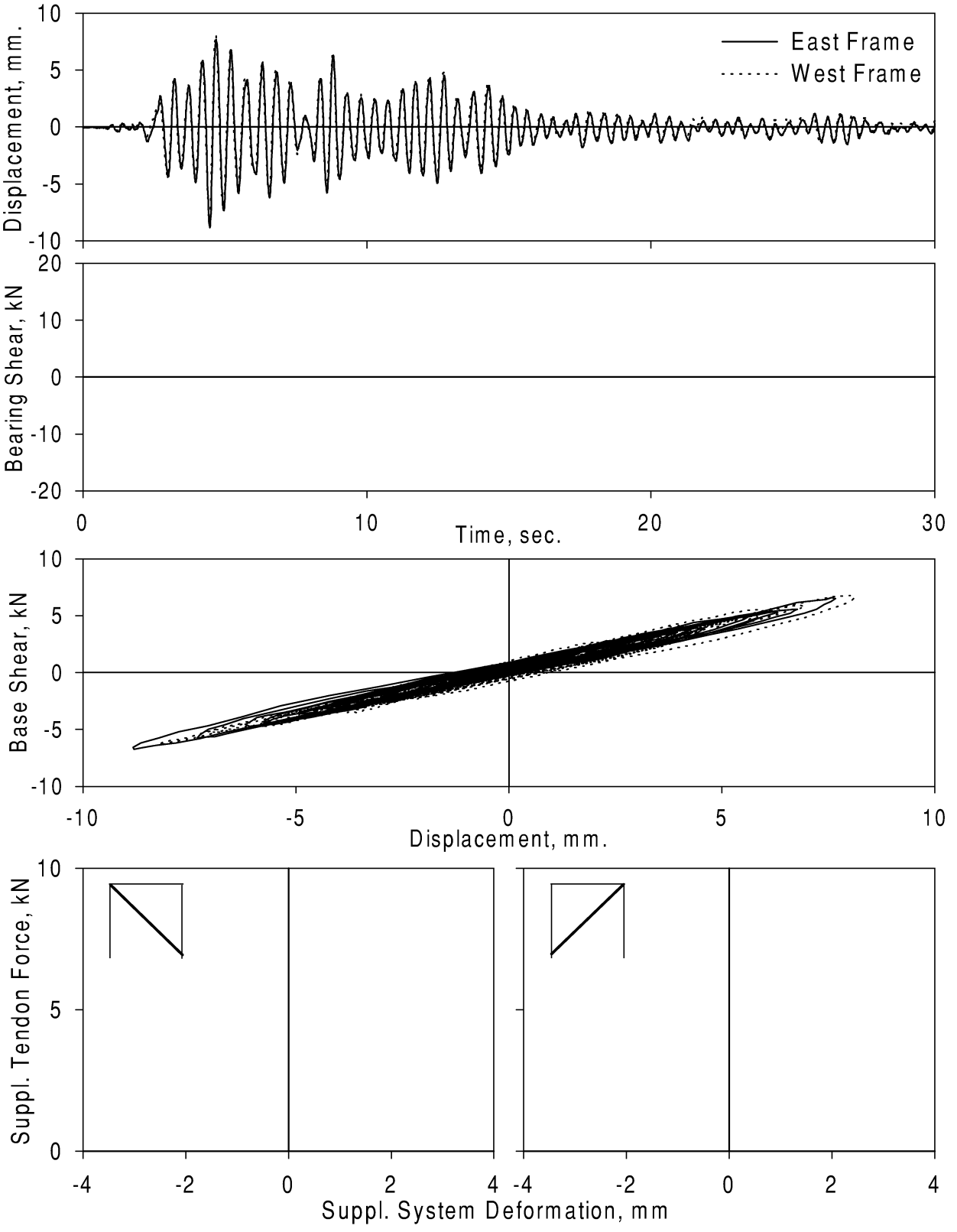

Figure A-58. Experimental Results - TANBNM
Ground Motion: Taft (PGA=0.079 g)
Configuration: Bare Frame

MULTIDISCIPLINARY CENTER FOR EARTHQUAKE ENGINEERING RESEARCH

A National Center of Excellence in Advanced Technology Applications

University at Buffalo, State University of New York
Red Jacket Quadrangle ▪ Buffalo, New York 14261-0025
Phone: 716/645-3391 ▪ Fax: 716/645-3399
E-mail: mceer@acsu.buffalo.edu ▪ WWW Site: http://mceer.buffalo.edu

University at Buffalo *The State University of New York*

ISSN 1520-295X